CONTRACT No. NONR 839 (32) FBM
PROJECT No. NR 064-487

THERMODYNAMICS, THERMAL EFFECTS AND DILATATION OF NATURAL RUBBER

by

MICHEL BOËL AND FREDERICK EIRICH

POLYTECHNIC INSTITUTE OF BROOKLYN

DEPARTMENT
of
AEROSPACE ENGINEERING
and
APPLIED MECHANICS
and
DEPARTMENT OF CHEMISTRY

OCTOBER 1966

PIBAL REPORT No. 931

Contract No. Nonr 839(32)FBM
Project No. NR 064-457

THERMODYNAMICS, THERMAL EFFECTS AND DILATATION OF NATURAL RUBBER

by

Michel Boël and Frederick Eirich

POLYTECHNIC INSTITUTE OF BROOKLYN
DEPARTMENTS OF
AEROSPACE ENGINEERING AND APPLIED MECHANICS
AND
CHEMISTRY

OCTOBER 1966

PIBAL Report No. 931

THIS PIBAL IS TAKEN FROM PART III OF THE

DISSERTATION BY MICHEL BOËL SUBMITTED

IN PARTIAL FULFILLMENT OF THE REQUIREMENTS

FOR THE DEGREE OF

DOCTOR OF PHILOSOPHY (CHEMISTRY)

AT THE

POLYTECHNIC INSTITUTE OF BROOKLYN

INTRODUCTION

A. General and Historical

Vulcanized natural rubber is characterized by an ability to undergo large reversible deformations. In the 19th Century, Gouth [1], Kelvin [2] and Joule [3] studied the peculiar thermodynamic effects which acompanied deformation, e.g., the reversible heat evolution on stretching and the positive temperature coefficient of the force necessary to maintain a given elongation. These properties, as we know now are not unique to natural rubber, but are common to all crosslinked elastomers.

In the classical theory of elasticity, applicable to small strains, the behavior of an isotropic elastic body under any type of deformation can be described completely if two material constants are known, one related to the response to shear, the other to volume change. However, since this theory is based upon the limiting condition of Hooke's law, it is not applicable to rubber-like materials capable of large elastic deformations. A continuum theory, developed in particular by Rivlin [4] seeks to establish in general terms the symmetry relation which governs the behavior of elastic materials under different types of deformation. By comparing the resulting general relation with the experimental stress-strain behavior, one hopes to deduce the equivalent to Hooke's law, in terms of a finite number of material constants.

One might hope also to deduce such a law from our molecular picture of rubbers as an entangled mass of randomly coiled molecules, i.e. deriving energetics from a statistical-mechanical point of view. The complications in this approach are that the picture of rubbers as above is really that of a very complex viscoelastic liquid and that the approximations used to derive an equation of state on a molecular basis must be severe.

It is, of course, also possible to proceed empirically to find an applicable form of Hooke's law by starting from phenomenological observations and casting them into functional-analytical form by observing the necessary conditions of thermodynamics and mechanics. This leads to workable equations, without, however, permitting a mechanistic understanding.

B. Treatment of Network Elasticity in the Gaussian Approximation

By 1932 Meyer, Susich and Valko [5], Mark and Guth [6] and Kuhn [7] had suggested that the elastic retractive force of rubbers arises from the decrease of entropy associated with the smaller number of conformations available when this network of chains is deformed by stretching. The retractive force of a single Gaussian chain can be very easily derived [6], hence most of our present theoretical knowledge concerning rubber-like elasticity stems from treatments invoking the Gaussian chain approximation and extending it to the entire network. Applying this approximation simplifies obtaining the changes in conformational entropy of the network chains, but leaves a number of difficulties associated with the "liquid-like" nature of bulk elastomers unresolved, such as the volume requirements of the molecules themselves, the volume dilation due to the isotropic component of the applied tension, the free energy change accompanying this volume change, and other possible free energy changes which might arise from a change of shape at constant volume. Many of the early treatments assumed simply that all these effects could be neglected in comparison to the contribution from the change in conformational entropy. Recent experimental work, however has prompted a reexamination and modification of earlier theories [8, 9].

The first step in the molecular theory of rubberlike elasticity is the derivation of the statistical properties of a single chain. It is necessary to know the free energy of the molecule quantitatively as a function of its end-to-end distance r and the relation between a given distance and the force necessary to maintain it. Because of the Brownian motion of the chain, the equilibrium distance r must be considered to be an average value and the same must be true for the end-to-end distance during the period of application of a force f. Assuming true randomness of the sequential arrangement of segments, the probability of a given end-to-end vector from r to r + dr in the absence of an external force, W(r), can be approximated by the Gaussian distribution function:

$$W(r)\,dr = (\beta/\sqrt{\pi})^3 \exp(-\beta^2 r^2) \cdot 4\pi r^2\,dr \qquad (1)$$

where the parameter β^2 has the value $3/2\overline{r_o^2}$ ($\overline{r_o^2}$ is the mean-square end-to-end distance of the polymer molecule unperturbed by volume effects). The error incurred by using the Gaussian function in Equation (1) has been found to be negligible provided r is less than one-half of the fully extended chain length [10]. The energetics are introduced by means of statistical thermodynamics, relating W(r) and the Helmholtz free energy of a set of chains. By differentiation with respect to r one arrives at f , the force needed to maintain a specified vectorial length r:

$$f = 3kT\, r / \overline{r_o^2} \qquad (2)$$

The steps of this derivation include considering that the entropy of a chain will decrease upon stretching as the chain assumes various conformations which are characterized by average greater values of r (the entropy must be a maximum at the most average probable value of r) . From the function of the Helmholtz free energy, A, in the form of the conformational integral, the retractive force is derived as the tangent with respect to L as given by Equation (2).

The second step in the theory consists in calculating the elastic free energy, $A_{el.}$, of the network as a function of the macroscopic parameters which characterize the deformation. The network can be considered as an ensemble of chains, each "chain" now being that portion of an original macromolecule which extend from one crosslink to the next. All these chains together will determine the retractive force of the crosslinked sample, and the behavior of this system is assumed to be the sum of the contributions of v chains. Each chain, characterized by $\overline{r_o^2}$ in the undeformed state and by r in the deformed state, contributes according to Equation (2). Since the material is supposed to be initially isotropic, one assumes that the components of the vectorial length of each chain are changed by the external deformation in the same ratio as the corresponding dimensions of the sample. This is known as an "affine" deformation. It is then possible to write the expression for the retractive force in the case of a simple elongation as:

$$f = \frac{\nu k T}{L_i} \cdot \frac{\overline{r_i^2}}{\overline{r_o^2}} \cdot (\lambda - 1/\lambda^2) \qquad (3)$$

where ν: number of chains between crosslinks, k: Boltzmann's constant, L_i : original length of sample, $\lambda = L/L_i$: elongation of sample, L: length of deformed sample, and $\overline{r_i^2} / \overline{r_o^2}$ is the so-called front factor, in which $\overline{r^2}_i$ is the mean-square end-to-end distance in the undeformed isotropic state of a network for all the chains having the same contour length, and $\overline{r_o^2}$ is the corresponding mean-square end-to-end distance for the undeformed chains without crosslinks. Hence, the parameter $(\overline{r_i^2} / \overline{r_o^2})^{1/2}$ represents the geometrical mean of the linear deformation existing in the undeformed network relative to a state where the end-to-end distance for the set of chains coincides with that for the chains unrestricted by the intermolecular links.

For the purpose of this study it will be helpful to reiterate some of the more important assumptions and approximations used in the various derivations:

1. The ν chains of the network are long enough (the degree of crosslinking not excessive) and volume effects negligible in order to assure the validity of the Gaussian distribution.

2. The initial macromolecules are of very high molecular weight in order to assure a negligible percentage of free ends.

3. The contributions by the chains to the total retractive force are additive.

4. The deformation of the chains must be affine to the deformation of the sample, which takes place at constant volume.

As stated these approximations are rather restrictive and tend to over-simplify many features.

Recently, the consequences of one of the major assumptions underlying the simple Gaussian treatment - namely that the chains are volumeless and do not hinder each other - have been reappraised [11]. Taking the volume of the chains into account effects the conformational entropy of the network.

In the unstrained state, the presence of intersegmental obstruction serves only to modify the effective step length of the Brownian motion but does not affect the form of the distribution function. However, when the chains are stretched, the medium is no longer isotropic and the end-to-end distribution for a particular chain becomes affected by its chain volume. Jackson, Shen and McQuarrie [11] take into account the change of conformational entropy by intermolecular obstruction by modifying the end-to-end distribution function in what they call a self-consistent way. If the usual "kinetic-theory" expression can be represented by:

$$f \text{ prop } (\lambda - \lambda^{-2}) \tag{4}$$

then the equation of state for rubber elasticity of these authors can be represented by:

$$f \text{ prop. } (\lambda - \lambda^{-2}) \left[1 - \frac{f_s}{3M(1 - f_s)} (2\lambda^2 + \lambda^{-1}) + \ldots\right] \tag{5}$$

where f and λ have the same meanings as in the previous expression, but where f_s is the fraction of space occupied by polymer molecules, and M is the number of equivalent statistical chain segments. Plotting $f / (\lambda - \lambda^{-2})$ as a function of $(2\lambda^2 + 1/\lambda)$ should give a linear relationship with a constant slope. This was confirmed by using Roe and Krigbaum's data for Viton A [18] Taking a usual value of $M = 100$, f_s, the fractional occupied space turned out to be 0.94 which appears to be reasonable. The authors conclude that "One can at least assert that the volume-exclusion of network chains accounts for part of the C_2 term of the Mooney-Rivlin equation. Other effects, such as chain entanglements, network connectivity, and nonequilibrium states may possibly be the other contributing factors" .

C. Thermodynamics of Rubber Elasticity

Considering a reversible process, application of the first and second laws of thermodynamics gives

$$dE = T\,dS + dW \qquad (6)$$

where E is the internal energy, S the entropy, T the absolute temperature and W is the work done by the surroundings on the system. If P is the external pressure, V the volume and f the force of extension, then

$$dW = f\,dL - p\,dV \qquad (7)$$

Writing the first law

$$dE = T\,dS + f\,dL - p\,dV \qquad (8)$$

and introducing Gibb's free energy, $F = H - TS$ with $H = E + pV$

$$dF = dE + p\,dV + V\,dp - T\,dS - S\,dT \qquad (9)$$

$$dF = -S\,dT + V\,dp + f\,dL \qquad (10)$$

or $$\left(\partial F / \partial L\right)_{p,T} = f \qquad (11)$$

From $F = H - TS$,

$$\left(\partial F / \partial L\right)_{p,T} = \left(\partial H / \partial L\right)_{p,T} - T\left(\partial S / \partial L\right)_{p,T} \qquad (12)$$

and equating Equations (11) and (12),

$$f = \left(\partial H / \partial L\right)_{p,T} - T\left(\partial S / \partial L\right)_{p,T} \qquad (13)$$

Equating further the second partial derivatives of F with respect to T and L,

$$(\partial f/\partial T)_{p,L} = -(\partial S/\partial L)_{p,L} \tag{14}$$

we obtain the thermodynamic equation of state of the rubber,

$$f = (\partial H/\partial L)_{p,T} + T(\partial F/\partial T)_{p,L} \tag{15}$$

These quantities are all at constant pressure and temperature which corresponds to most experimental conditions. However, the quantities of real interest are the partial differential expressions at constant volume and temperature. At constant pressure the positive change in volume of the rubber, referred to as dilation or dilatation(increased molecular separations) gives rise to a change in enthalpy. This change in addition to that of the entropy presents a condition precluded by constant volume.

To obtain the equation of state at constant volume and temperature, again the Helmholtz free energy is applied

$$A = E - TS \tag{16}$$

A derivation analogous to the above, and remembering that

$$T(\partial f/\partial T)_{V,L} = -T(\partial S/\partial L)_{V,L} \tag{17}$$

leads then to:

$$f = (\partial E/\partial L)_{V,T} + T(\partial f/\partial T)_{V,L} \tag{18}$$

The problem can be reformulated by dividing the total retractive force, f into the two components

$$f = f_e + f_s \tag{19}$$

where

f_e : retractive force due to change in internal energy,

f_s : retractive force due to change in entropy

Past authors have frequently neglected the energy contribution to the retractive force [12, 13] at moderate strains. But later work has shown that f_e/f can be an appreciable fraction. For an ideal rubber, for which the internal energy does not depend upon the elongation r/r_i of the chains, the force f is proportional to the absolute temperature T. However, if the internal energy of the chains depends upon r, then not only $\overline{r^2}/\overline{r^2}$ but even $\overline{r^2}_o$ will depend upon the temperature and the force f will no longer be strictly proportional to T.

Having stated that

$$f = f_e + T(\partial f/\partial T)_{V,L} \tag{20}$$

we can write

$$f_e = f - T(\partial f/\partial T)_{V,L} \tag{21}$$

or

$$f_e = -T^2 \left(\frac{\partial [f/T]}{\partial T}\right)_{V,L} \tag{22}$$

from which one can derive that

$$f_e/f = -T \left(\frac{\partial \ln [f/T]}{\partial T}\right)_{V,L} \tag{23}$$

Previously we found that

$$f = \frac{\nu kT}{L_i} \left[\left(\frac{\overline{r_i^2}}{\overline{r_o^2}} \right) (\lambda - \lambda^{-2}) \right] \qquad (3)$$

or $$f/T = \text{function} \left(\overline{r^2}_o \right)^{-1}$$

and therefore, with equation (14), we find:

$$f_e/f = -T \left(\frac{\partial \ln [f/T]}{\partial T} \right)_{V,L} = T \left(\frac{\partial \ln \overline{r^2}_o}{\partial T} \right)_{V,L} \qquad (24)$$

An important advantage of the preceding derivation is that the theory of rubber elasticity offers the possibility of interpreting the energetic component f_e in terms of the molecular properties of the chain.

An important correlation can now be established between the elastic behavior of a crosslinked amorphous polymer and the properties of the same polymer in dilute solution. At the theta-temperature, the intrinsic viscosity of a polymer having a molecular weight of M can be expressed as [27]

$$[\eta]_\theta = \Phi \left(\overline{r^2}_o / M \right)^{3/2} M^{1/2} \qquad (25)$$

where Φ is a constant independent of temperature. Consequently

$$2/3 \left(\partial \ln [\eta]_\theta / \partial T \right) = d \ln \overline{r^2}_o / dt \qquad (26)$$

and from Equations (24) and (26)

$$f_e/f = 2/3 \cdot T \, \partial \ln [\eta]_\theta / \partial T \qquad (27)$$

This equation establishes the interesting possibility to determine the ratio of the energetic to the entropic contribution of rubber elasticity from the variation of the intrinsic viscosity for various solutions of varying theta temperatures or, vice versa, the latter from force-temperature measurements.

The calculation of f_e/f via stress-strain measurements necessitates measurements at constant volume which are difficult to perform. However differentiation and rearrangement of Equation (24), gives [14, 15] :

$$(\partial \ln [f/T] / \partial T)_{p,L} = - (d \ln \overline{r^2}_o / dT) - 3\alpha / (\lambda^3 - 1) \quad (28)$$

and hence

$$f_e/f = - T\left(\frac{\partial \ln [f/T]}{\partial T}\right)_{p,L} - 3\alpha T / (\lambda^3 - 1) \quad (29)$$

where α is the linear expansion coefficient of the polymer.

The sign of f_e will depend upon the sign of $d \ln \overline{r^2}_o / dT$, where the dependence of $\overline{r^2}_o$ upon temperature is determined by the potential associated with internal rotation. For a long chain made up of bonds with uncorrelated rotations which are hindered according to one or another type potentials, the sign of $d \ln \overline{r^2}_o / dT$ is easily predicted. If the potential of internal bond rotation for a given polymer is such that the deepest minimum is near the transposition, then, $\overline{r^2}_o$ will decrease by increasing temperature, f_e will be negative and the stretching process is favored by a decrease of internal energy or by lowering T. If however the rotational minimum is far from the transconformation, $\overline{r^2}_o$ may increase with increasing temperature, since many of the chains which were in conforamtions become longer by increasing the vibrational energy and going to transconformations. Then f_e will be positive and the stretching process will be opposed by an increase in the internal energy. Only in cases where all the possible minima were isoenergetic will $\overline{r^2}_o$ be temperature independent and f_e be equal to zero. A decrease of entropy will always oppose the stretching process.

There are several different methods of calculating f_e/f for a given specimen. If the measurements can be carried out at constant volume then, by application of Equation (17), it would give us an immediate measure of f_e. However direct measurements remain difficult, only a few data exist [9]. If the change in volume were known as a function of elongation, one could calculate f_e via Equation (17), by applying :

$$(\partial f/\partial T)_{V,L} = (\partial f/\partial T)_{p,L} - (\partial V/\partial L)_{p,T} \frac{(\partial V/\partial T)_{p,L}}{(\partial V/\partial p)_{T,L}} \qquad (30)$$

Unfortunately though the cubic thermal expansion coefficient $((\partial V/\partial T)_{p,L})$ and the compressibility $((\partial V/\partial p)_{T,L})$ are readily measured as long as the rubbers are isotropic, the change of volume upon elongation is very small (of the order of 10^{-4} cc/cc) and quite difficult to measure. Holt and McPherson [16], and more recently Hewitt and Anthony [17] reported the only available figures in the field.

The calculation based on Equation (29) supposes that the rubber network obeys Gaussian statistics. Rearranging Equation (29) gives us

$$f_e/f = 1 - \frac{T}{f}\left(\frac{\partial f}{\partial T}\right)_{p,L} - 3\alpha T/(\lambda^3 - 1) \qquad (31)$$

The relationship is exact but is based upon the Gaussian network theory. In contrast, the presence of nonvanishing values of C_2 in the literature indicates considerable deviation of the real network from the simple Gaussian theory, and therefore Equation (31) cannot be strictly justified. Accepting, however, that C_2 arises from mostly failure to attain equilibrium conditions, then only C_1 in Mooney's equation represents an equilibrium property, with the rubber obeying the Gaussian theory

$$f = 2C_1(\lambda - \lambda^{-2}) \qquad (32)$$

from which

$$f_e/f = 1 - T/C_1 \cdot (\partial C_1/\partial T)_p + \alpha T \qquad (33)$$

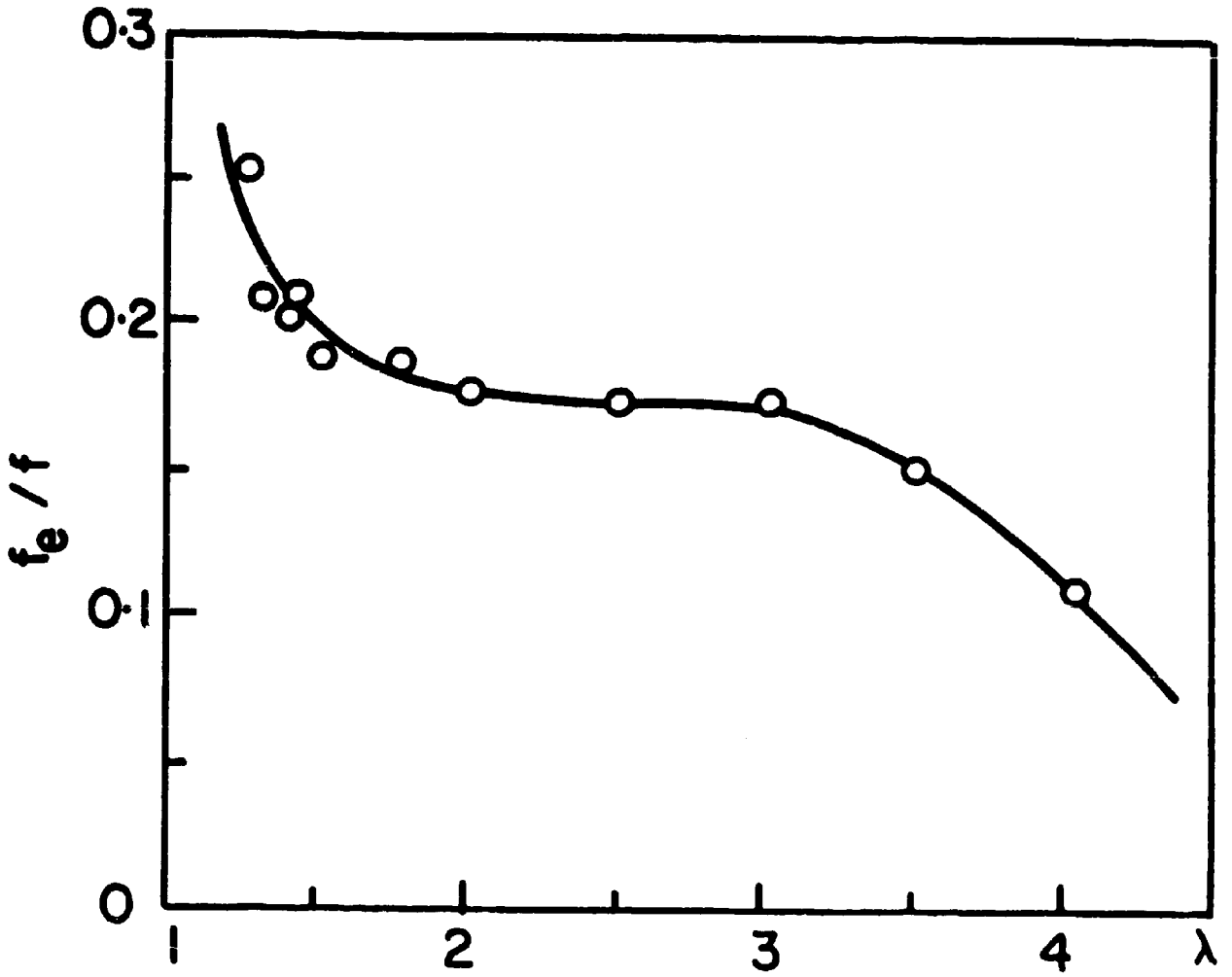

Fig. 1, Ref [8] : Variation with elongation of the fractional contribution of the internal energy to the total tension

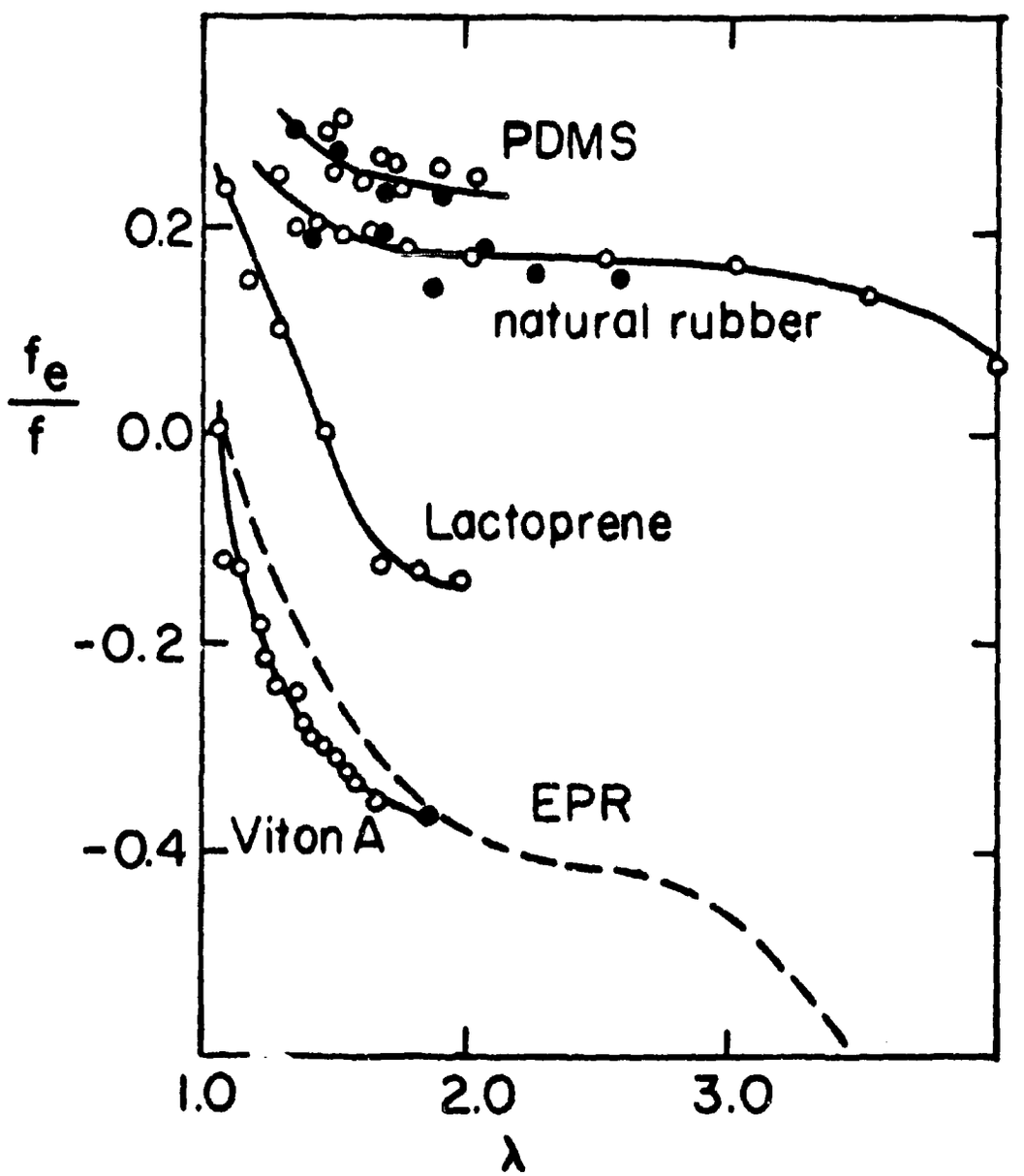

Fig. 2, Ref [18]: Measured values of f_e/f for various polymers shown as a function of elongation

Also in this case the values of f_e/f calculated by application of (31) or (33) should be equal. Checking with literature data, shows that this is not so [8] (Fig. 1). Similarily, forcing the data to comply to Equation (32) by setting $C_2 = 0$, should show f_e/f to be independent of λ, which is not the case.[2] Even more disturbing is the fact that the approximations employed in the Gaussian treatment should become more exact as λ approaches 1, yet it is just in that region that f_e/f varies the most.

Looking closely at f_e/f, [18], (Fig. 2), as a function of λ, one can see that the contribution of internal energy is real, is often quite large, and can be positive or negative. The strong dependence of f_e/f on λ runs counter to the prediction from the Gaussian theory while the drop in f_e/f at large , observed for natural rubber, could be associated with stress induced crystallization by Smith, Greene and Ciferri [19], the rapid variation of f_e/f at very low λ is surprising since, from the nature of the approximations employed, the Gaussian theory would be expected then to be obeyed more exactly. A decrease in f_e/f, which was observed with cis-1, 4 polybutadiene [20], and similar trends can be detected in other systems, appears to be a general phenomenon. There is as yet no satisfactory explanation from a molecular point of view. Most probably, this phenomenon is associated the value of C_2. Further, the sign of C_2 seems to be always positive which appears to correlate with the fact that f_e/f always decreases with λ, irrespective of whether f_e/f is positive or negative. Splitting the C_2 term into its own entropic and energetic components shows that about 50% of the magnitude of C_2 arises from energy effects in natural rubber [8]. Finally, (contributes proportionately more to the total stress at low λ, showing a ain that the deviation from the Gaussian theory is more pronounced.

D. Phenomenological approach to Rubber Elasticity

For this approach one must first understand the nature of the concept of the stored energy function W, which is defined as a function of the strain parameter λ , and of the thermodynamic parameters specifying the enviroment, such as the temperature T or the pressure p. The function W as a form of free energy, represents the total amount of work stored elastically in the body in the process of deforming it into the state of strain represented by λ. W, is furthermore a function of state depending only on the initial and final free energy levels. Theories based on W are, therefore, concerned with equilibria analogous to classical thermodynamics, and complications must arise from non-equilibrium processes when comparing experimental data with the theory.

Since the stored energy does not depend on pure rotation of a body, W is a function of a symmetric matrix, λ' , representing a pure distortion of the shape. A suitable rotation of the coordinate axes reduces this matrix to a diagonal form, whose three elements are the principal extension ratios $(\lambda_i) = (\lambda_1, \lambda_2, \lambda_3)$ as defined earlier. If the body, as assumed, is isotropic in the undeformed state, we may choose as the independent variables for W some functions of the elements of which are invariant with a rotation of the coordinate axes. There are a large number of conceivable strain invariants from which sets of three must be selected which are mutually independent. The simplest choice of such a set is given by

$$I_1 = \lambda_1^2 + \lambda_2^2 + \lambda_3^2 \qquad (34)$$

$$I_2 = \lambda_1^2 \lambda_2^2 + \lambda_1^2 \lambda_3^2 + \lambda_2^2 \lambda_3^2 \qquad (35)$$

$$I_3 = \lambda_1^2 \lambda_2^2 \lambda_3^2 \qquad (36)$$

which are even, symmetric, functions of λ_1, λ_2, and λ_3. Physically, the third invariant I_3 is related to the volume deformation by

$$I_3 = (V/V_o)^2 \tag{37}$$

where V_o and V are the volumes of the body before and after deformation respectively [4].

The stored energy W as a function of the strain invariants can be expressed in terms of a power series [4]:

$$W = \sum_{i,j,k=0}^{\infty} C_{ijk} (I_1 - 3)^i (I_2 - 3)^j (I_3 - 1)^k \tag{38}$$

where the coefficients C_{ijk} are functions of T and p only. An approximation to W can be obtained by retaining only a finite number of low order terms. If only the first term is retained, we have

$$W_1 = C_{100} (I_1 - 3) \tag{39}$$

which is an expression equivalent to that obtained from the statistical theory of rubbers when approximating the rubber chains by Gaussian coils. If the second term of Equation (38) is also retained,

$$W_2 = C_{100} (I_2 - 3) + C_{010} (I_2 - 3) \tag{40}$$

which is identical with the Mooney-Rivlin function for incompressible rubbers [4].

In the case of simple elongation, and assuming incompressibility:

$$\lambda_1 = \lambda = L/L_o \tag{41}$$

where L_o and L are the lengths of the material in the original and stretched state, respectively. Deformation in the lateral direction is then given by

$$\lambda_1 = \lambda_3 = (V/\lambda V_o)^{1/2} \tag{42}$$

The principal stresses, t_i (force acting in the direction of the principal strain λ_i, and measured per unit area of the deformed body), are obtained from W by:

$$t_i = (\lambda_i / I_3^{1/2}) \left(\frac{\partial [W/V_o]}{\partial \lambda_i}\right) + p \tag{43}$$

Replacing values for λ_2 and λ_3, in Equation (43), solving for p and substituting for the value of p in the expression for t, obtained from Equation (43), we have that

$$f = 2\left(\frac{\partial W}{\partial I_1} + 2\frac{\partial W}{\partial I_2} \cdot \frac{1}{\lambda}\right)(\lambda - 1/\lambda^2) \tag{44}$$

f is now the force of elongation per unit cross-sectional area of undeformed material [4].

When the stored energy function is reduced to the first term Equation (39) becomes:

$$f = 2C_{100}\left(\frac{V^{1/3}}{L_o V_o^{1/3}}\right)(\lambda - 1/\lambda^2) \tag{45}$$

comparison of Equation (45) with the results of the statistical theory of Gaussian networks then indicates that Rivlin's constant C_{100} is given by

$$C_{100} = \frac{1}{2} \nu kT \left(\frac{V_o}{V_*}\right)^{2/3} \tag{46}$$

where ν is the number of network chains in the specimen, k is Boltzmann's constant, T is the absolute temperature, and V_* is the reference volume independent of pressure [18]

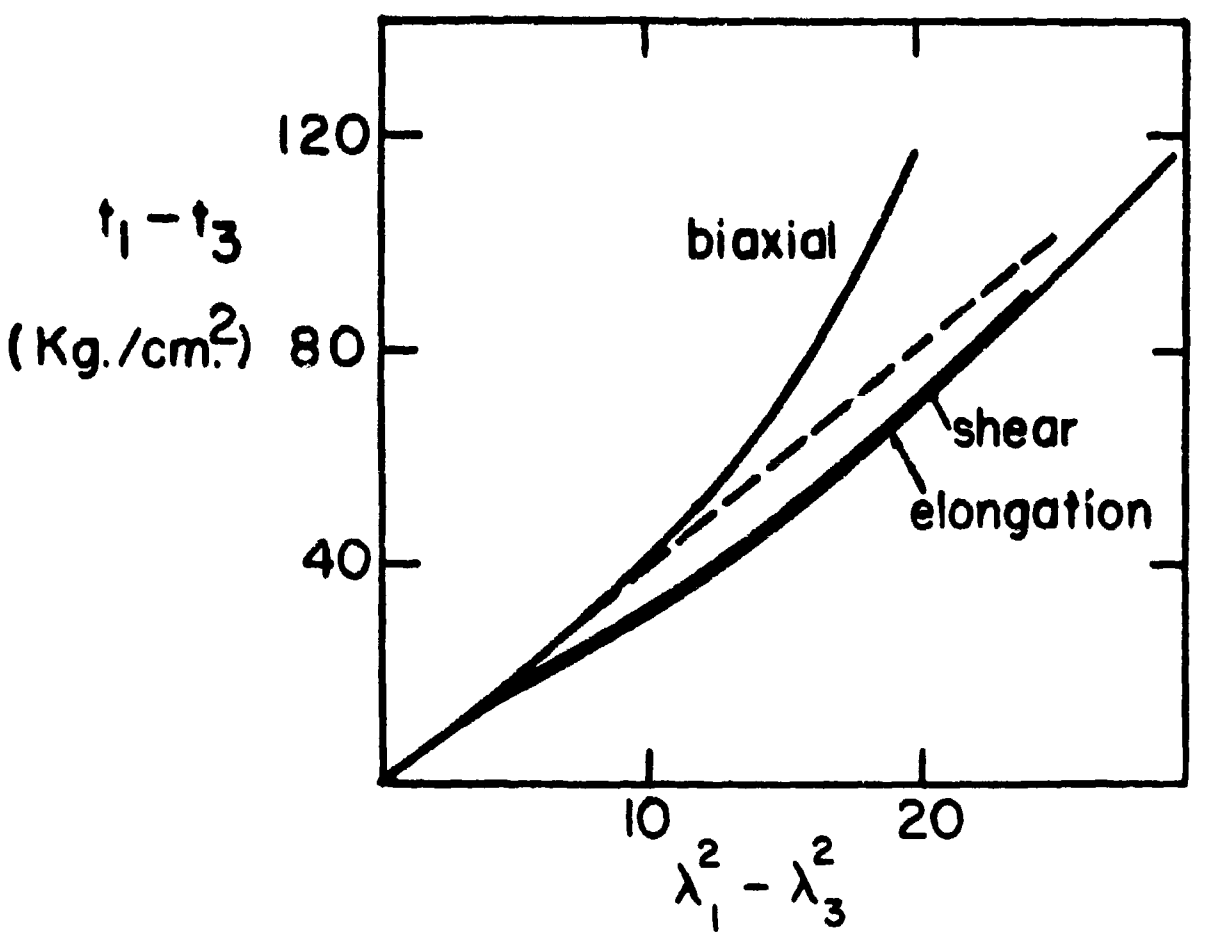

Fig. 3 , Ref [18] : Biaxial stretching, shear and simple elongation (dashed line represents the prediction of Gaussian theory)

Treloar [12] determined the stress-strain relationship for vulcanized natural rubber in simple elongation, uniform biaxial elongation and for strip biaxial stretch. Qualitatively he could recognize two types of deviation from the prediction of the Gaussian theory which requires that $\partial W/\partial I_2 = 0$, (Fig. 3). Firstly, at large strains, the stresses tend to increase much more rapidly than expected from the theory. Secondly, even at moderate strains the curves derived from different types of strain do not coincide with each other, which indicates that $\partial W/\partial I_2 = C_2 \neq 0$. At large strain, the behavior could be expressed only by a large number of terms with arbitrary coefficients for Equation (39).

On the other hand, the upturn in stress at large strains has been successfully explained in terms of the finite extensibility of the network chains [12]. In this region of strain, where an appreciable proportion of the chains becomes highly extended, the Gaussian statistical treatment is no longer valid. We quoted earlier that departures from Gaussian statistics first become important when the vector length of the chain is between one-third to one-half of its fully extended length. [21]. In the case of a network of chains, in which the chain length is related inversely to the degree of cross-linking, this implies that the Gaussian theory becomes increasingly inadequate as the degree of cross-linking is increased. At the limit a , "non-Gaussian" theory becomes essential even under the smallest strains.

E. The Problem of C_2

Behavior at moderate strain strongly suggests that the Mooney-Rivlin function, Equation (44) , is a better approximation than the single-term Gaussian function, Equation (45) . When one is interested in the stress-strain relationship in simple elongation only it is widely recognized that the Mooney-Rivlin function is a very good representation of the data. This holds not only for natural rubber, but also for a wide variety of rubberlike materials such as crosslinked silicones and polyethylene, polyisobutylene, and Vitonfluoro elastomers.

No generally acceptable molecular interpretation of the C_2 term has emerged yet. Gaussian statistics predict a zero value of C_2 , but most experimental work shows the existence of a C_2 term as discussed before. As will be shown later , extremely precise measurements are needed in order to determine the value of C_2 at small strains.

Values of C_2 may be of the same order of magnitude as C_1 . In a few cases C_2 is greater than C_1 , but there are many cases reported where C_2 is very small. There is no clear cut rule by which one could predict the magnitude of C_2 from knowledge of the structure of the material. The situation is different for the behavior of C_1 which increases regularly with increasing crosslink density and with increasing temperature, as follows from the Gaussian theory. Adherence to the latter could, as stated earlier, require that the C_2 term goes to zero at low strains. Van der Hoff's [22] very recent data tends to show that this might in fact be the case.

Experiments on swelling of vulcanized rubbers show that deviations from the Gaussian theory become less noticeable with dilation [23, 24] i. e. with reduced rubber-rubber interactions. In the work of Gumbrell, Mullins, and Rivlin [24] , the effect of various swelling agents on the stress-strain relationship of natural rubber, butadiene-styrene, and butadiene-acrylonitrile copolymers, showed that in all cases that the Mooney-Rivlin 2 term equation was well obeyed and that, if the force per unit cross-sectional area of the unswollen specimen is expressed as :

$$f_u = (\lambda - \lambda^{-2})(2C'_1 + 2C'_2 \lambda)/v_2^{1/3} \qquad (47)$$

(where V_2 is the volume fraction of the rubber.) C'_1 , the equivalent of C_1 for the swollen network,

becomes independent of v_2, while the value of C'_2, the equivalent of C_2 for the swollen network, decreases linearily with decreasing v_2, and becomes zero at $v_2 = 0.25$ irrespective of the nature of the solvent. C'_2 can therefore be represented by

$$C'_2 = \frac{C_2}{3}(4v_2 - 1) \qquad (48)$$

where C_2 is the value of the constant for the unswollen rubber. Other workers have essentially verified these results [25] with crosslinked networks of silicone rubber, butyl rubber, and polymethyl methacrylate.

Another important observation was made by Ciferri and Flory, i. e. that the magnitude of C_2 can be influenced by the time scale of the measurements [25]. Their samples exhibited considerable stress relaxation when held at constant length and the apparent values of C_2 decreased by 10 to 40 percent when the time of relaxation between successive elongations was increased from 15 mins to 10 hours. A similar observation of the effect of time was made by Kraus and Moczvgemba [26].

Thus the values of C_2 may, at least partly, be affected by failure to achieve equilibrium conditions during stress-strain measurements or when insufficient time is allowed for completion of stress relaxation. But as decay of stress in stretched elastomers is often approximately linear with the logarithm of time [24, 27, 28], it is difficult to know when the criterion of equilibrium has been adequately fulfilled. This led Ciferri and Flory [25] to suggest that under ideal equilibrium conditions the values of C_2 might be expected to become negligibly small. Blatz and Ko [29] reported that for polyurethane rubbers which exhibited no detectable relaxation, the value of C_2 was zero.

Other facts, however, lead one to suspect that the equilibrium value of C_2 may not vanish. Swelling the samples with a solvent and then deswelling them improves their approach to equilibrium [29]. When this technique was used by Ciferri and Flory [25] in a butyl rubber vulcanizate, the value of $2C_2$ was found to decrease to 0. 5 kg/cm^2 from the value of 1. 20 kg/cm^2 obtained without the swelling and deswelling cycle, but did not become zero. Roe and Krigbaum [8, 30] studied vulcanizates of natural rubber and Viton floroelastomer by allowing relaxation for at least 24 and 48 hr, and yet the values of $2C_2$

obtained were 0.88 and 2.87 kg/cm^2 , respectively. These values of $2C_2$ are certainly not negligible.

Contradictory results are also reported on the relationship between the magnitude of C_2 and the crosslink density. Gumbrell, Mullins and Rivlin [24] prepared a series of sulfur vulcanizates of natural rubber with $2C_2 \doteq 2.0$ kg/cm^2 , although their values of $2C_1$ ranged from 2.0 to 6.2 kg/cm^2 . Kraus and Moczygemba [26] show that when polybutadiene polymers of different primary molecular weights were crosslinked with controlled amounts of sulfur so as to give approximately the same value of C_1 , the value of C_2 depended on the molecular weight of the original polymer. And Ciferri and Flory [25] noted that in the case of natural rubber, a specimen crosslinked by gamma radiation to give the same value $C_1 \doteq 2.0$ kg/cm^2 as one crosslinked with sulfur with a $2C_2 = 2.0$, exhibited a lower value of $2C_2$, namely, 1.5 kg/cm^2.

Consequently Krigbaum and Roe [18] urged the study of the effect of structural differences on C_2. The distribution of network chain lengths could for example be of some importance. A knowledge of the factors effecting C_2 would help in correlating experimental results such as the energy component of the elastic force obtained by different workers from apparently identical materials [31, 32].

Few studies have been carried out on the temperature dependence of C_2. When C_2 was evaluated from stress-strain data at very short times apparent values of C_2 decreased with increasing temperature, reflecting a faster approach to equilibrium at higher temperatures [28]. Under conditions where relaxation effects could be neglected, the temperature coefficients of C_2 were found to be positive for natural rubber [8] , silicone rubber [28] and nearly zero for butyl rubber [28] . Roe and Krigbaum [8, 30] analyzed stress-strain data with respect to entropy and internal energy contributions to elastic force and found that in the case of natural rubber it is the internal energy effects which are largely responsible for the C_2 term.

Blatz and Ko [29] working with polyurethane foam rubber containing 50% air by volume, found that $2C_1$ was practically negligible and that all of the elastic force arose from the $2C_2$ term. This finding is a good reminder that the existence of the C_2 term is real and that macroscopic as well as microscopic

structural features will determine the relative importance of the C_2 term. In view of the oversimplifications inherent in the statistical theory, one can assume that all the structural features neglected there will come into play such as volume effects, local chain packing or ordering, non-Gaussian segment distribution, free chain ends, crosslink clustering, non equilibrium and thermal effects, and others. In view of these complexities, and of the contradictions so far encountered, an apriori deduction of C_2 seems rather hopeless at this stage, and that efforts should be concentrated on careful measurements of values of C_2 as a function of rubber structure.

F Introduction to Dilatometry

Our knowledge of rubber behavior under simple elongation would not be complete without an insight into the nature of the changes in volume as a function of elongation and time. From a theoretical point of view, the exact function of $(\partial V/\partial L)_{T,P}$ allows one to calculate directly the quantites of thermodynamic interest without having to assume certain approximations as has been the case in previous studies. Following the change in volume at a fixed strain level as a function of time, should permit also the study of ordering or crystallisation kinetics, since at higher levels of order the density of the overall sample must increase. When volume changes have been used to follow the crystallization quantitatively over a range of temperature [33], the final decrease in volume on crystallization was found to lie between 2.0 and 2.7 percent. Experimentally, measurement of ΔV accompanying elongation was first attempted by Holt and McPherson [16], who found no volume change for elongations up to 200%. These authors were specifically interested in effects of crystallization and also worked with filled samples.

At elongations higher than 200% they found that even after 3 or 4 weeks, the volume of the stretched rubber decreased at an approximately uniform rate with the logarithm of time. These decreases were the greater, the higher the elongation, the lower the temperature or the longer the time the rubber was kept stretched. These observations were obviously related to the kinetics of crystallization. In later work [34], Gent followed the crystallization of the sample by measuring decreases in volume and relaxation of the stress. He found that the degree of crystallization as measured by the dilatometer, was proportional to the reduction in stress. In many cases the equilibrium value of stress reached was zero, in some cases the test piece eventually extended, with the additional extension amounting to up to 5% of the unstretched length. We have also observed this phenomena of relaxation by crystallization, but only in the lower temperatures. For the purpose of the thermodynamic studies, our lowest temperature was 30°C and the highest elongation about 200%, so that we were not in the crystallizing region of elongation and temperature. Lately Wolstenholme measured the changes in volume upon elongation of a series of cured gum

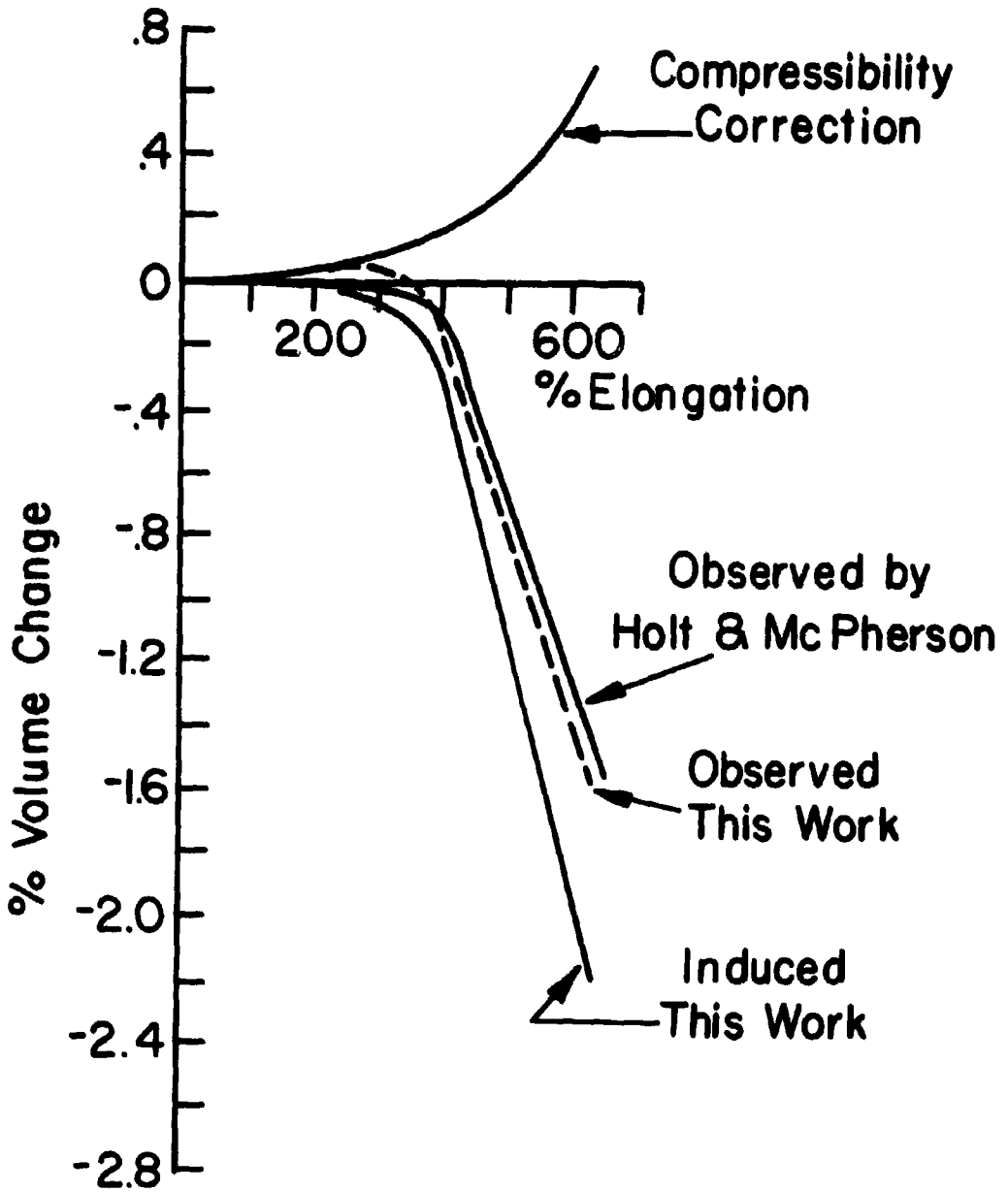

Fig. 4, ref [35] : Volume change measured by Wolstenholme as a function of elongation

elastomers [35]. Using a water-filled dilatometer submerged in a thermostated water bath maintained at ± 0.015 °C, Wolstenholme claims that changes in volume of 10^{-5} cc can readily be determined. He notices that the volume of the sample changes with time after a change in length, which changes were characterized by a rapid drift of the volume in the first half minute after stretching, followed by a very slow change over a longer time. Reproducible results were obtainable when successive elongation changes were made every three minutes. However, water as a confining liquid, presented the additional problem of swelling of the sample which gave rise to a slow transient; these difficulties were minimized by pre-soaking the samples in distilled water at test temperatures for a minimum of 24 hours. This procedure is claimed to decrease subsequent water absorption by the specimen and stabilizes the initial sample volume. Subtracting the volume expansion due to the compressibility of rubber from the total volume change, defines an induced volume change which Wolstenholme attributes to the crystallization of the sample. He tested several commerical elastomer gums, such as Hevea, Neoprene, Butyl, SBR, Paracril B and Paracril C. Elongations applied ranged from 0 to 600%, however no precise data was given for the low elongations. Figure 4 shows the different volume changes of a Hevea sample as a function of stressed length. The compressibility correction is the expansion of the rubber under a given stress, or in other words defines a Poisson ration, ν smaller than the incompressible value of 0.5. In filled samples, he could observe an apparent Poission ratio greater than 0.5 due to vacuole formation [16]. Reduction of the temperature from 35°C to 0°C lowers the elongation at which crystallinity becomes apparent [35]. Finally, cycled dilatometer tests lead to a volume hysteresis that was greatest in crystallizable elastomers and practically zero in non-crystallizable elastomers.

The first people to measure the volume changes in detail at low and moderate strains were Gee, Stern and Treloar [36]. From the earlier data of Holt and McPherson it was obvious that if there were any change in volume upon elongating the sample up to 200%, these changes would have to be less than 0.2% expressed in $\Delta V/V_o$, and Gee [37] had predicted small increases in volume at low strains. For any isotropic compressible body the

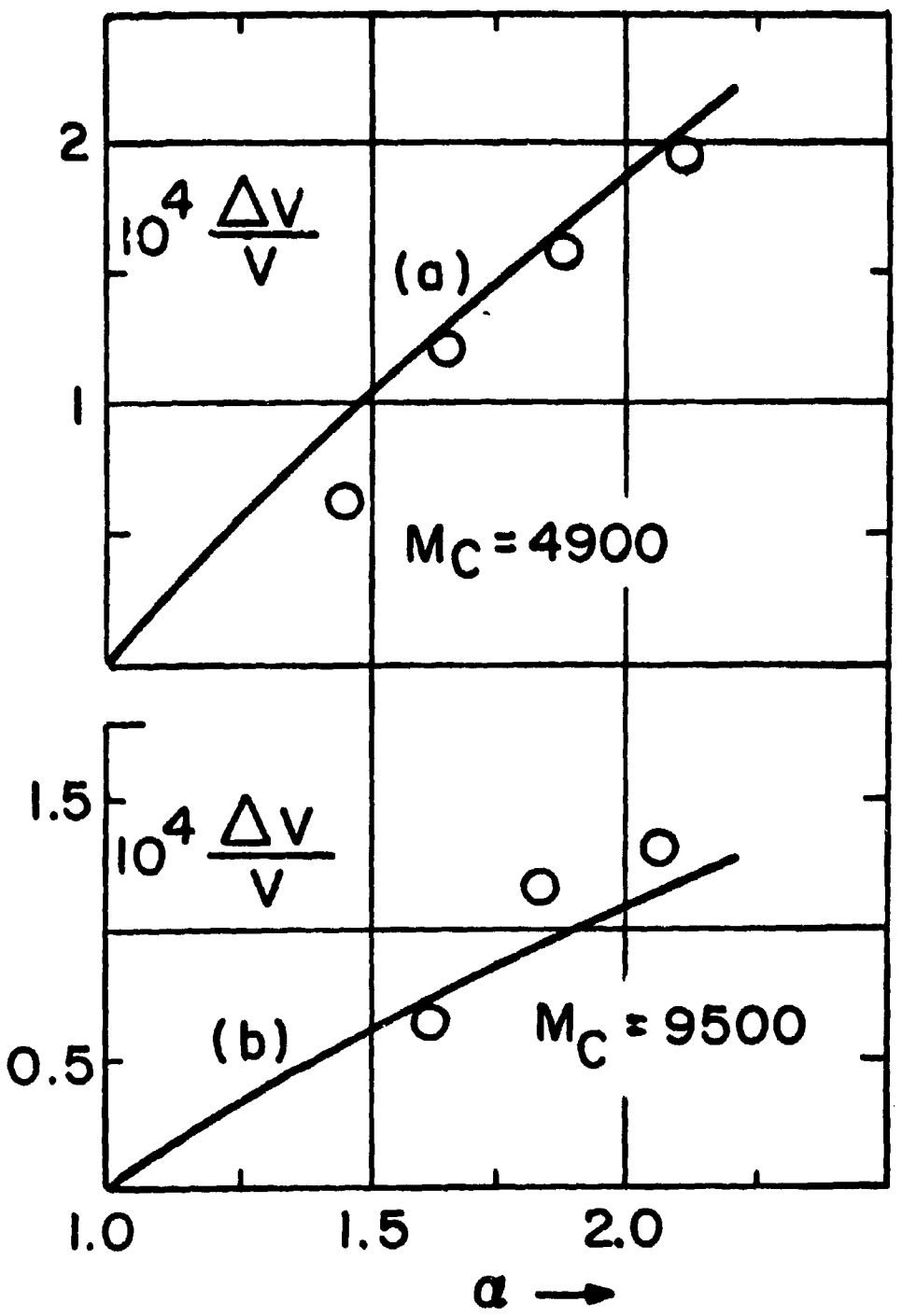

Fig. 5-Ref 36-Fractional increase in volume as a function of Elongation from Gee, Stern and Treloar.

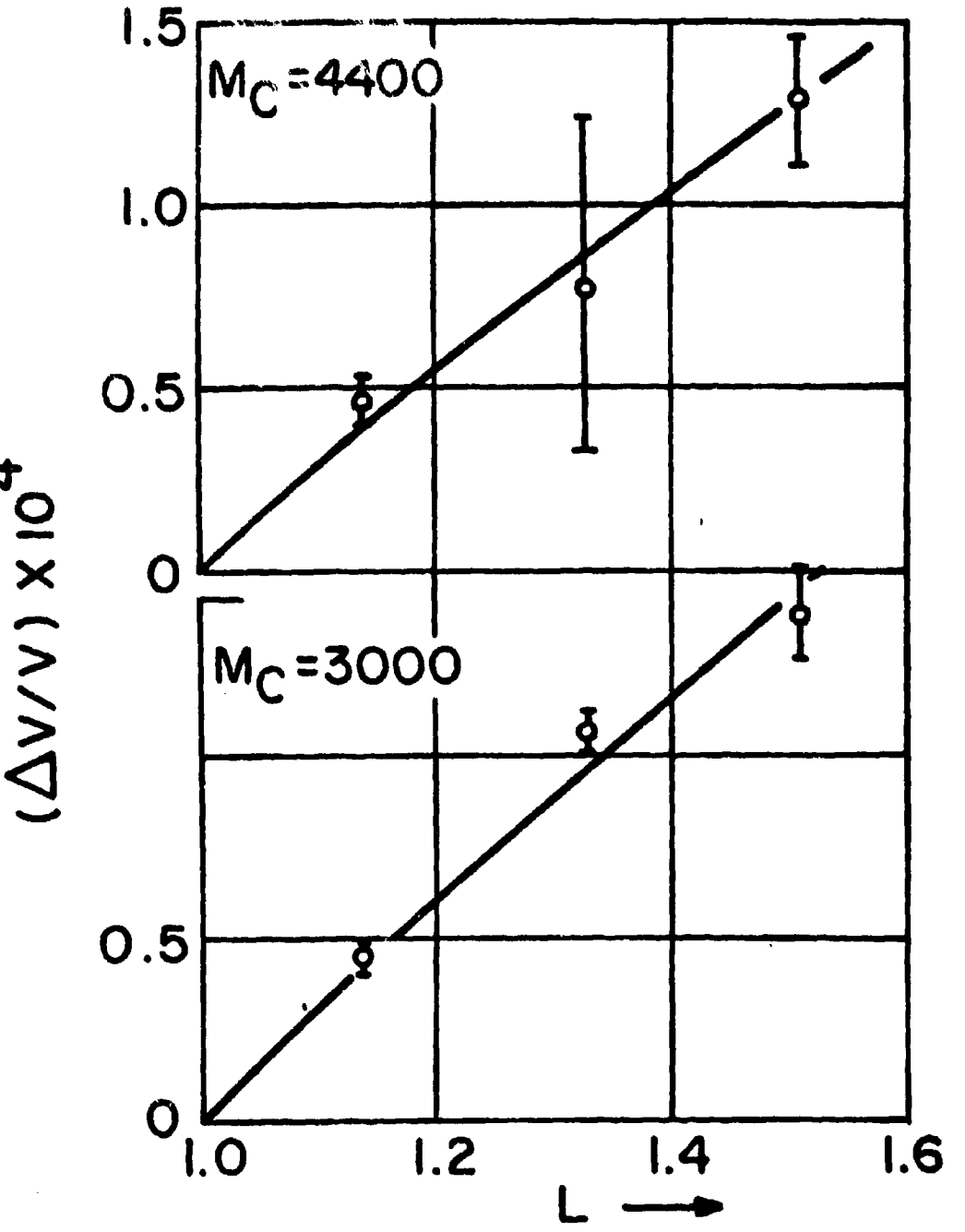

Fig 6- Ref. 17- Fractional increase in volume as a function of Elongation from Hewitt and Anthony .

tensile force may be resolved into shear stresses and an isotropic tension, for a change from L_o to L and a compressibility K, the volume expansion ΔV is given by [37]:

$$\Delta V = \frac{K}{3} \int_{L_o}^{L} L \left(\frac{\partial f}{\partial L}\right)_{p,T} dL \qquad (49)$$

This equation applies so long as the material remains isotropic, and is therefore probably not seriously incorrect for rubber at elongations of up to 100%. By means of Equation (49), it is thus possible to predict values of ΔV from the stress-strain curve, or else one can measure the change in volume directly. Instead of a dilatometer, Gee and co-workers used the method of hydrostatic weighing in water. An accuracy of up to 1 part in 60,000 in volume is claimed. A pure gum rubber containing 2% zinc oxide gave volume changes approximately double of those expected from application of Equation (49). This deviation was explained by postulating the forming of vacuoles around the filler particles, which markedly increase the volume of the sample. Later tests were run on a sample crosslinked by means of di-t-butyl peroxide and showed better the agreement of the results with the theoretical predictions. Figure 5 reproduces Gee and co-workers data, plotted against the predicted curve.

Several years later, Hewitt and Anthony [38], redetermined the change in volume of natural rubber crosslinked by di-t-butyl peroxide. The strains at which they were working were lower than those used by Gee and his group (40% to 110%). Again, to obtain high sensitivity, the experimental technique was that of measuring the buoyancy in water. The temperature control was of the order of 0.005°C as measured with a Beckmann differential thermometer. Figure 6 shows the percent expansion for strains up to $\lambda = 1.6$. Application of Equation (49) results in the theoretical curve as seen in Fig. 6. To evaluate $(\partial f/\partial L)_{p,T}$ these authors used the 1st term of the Mooney-Rivlin equation:

$$f \text{ prop. } (\lambda - 1/\lambda^2) \qquad (50)$$

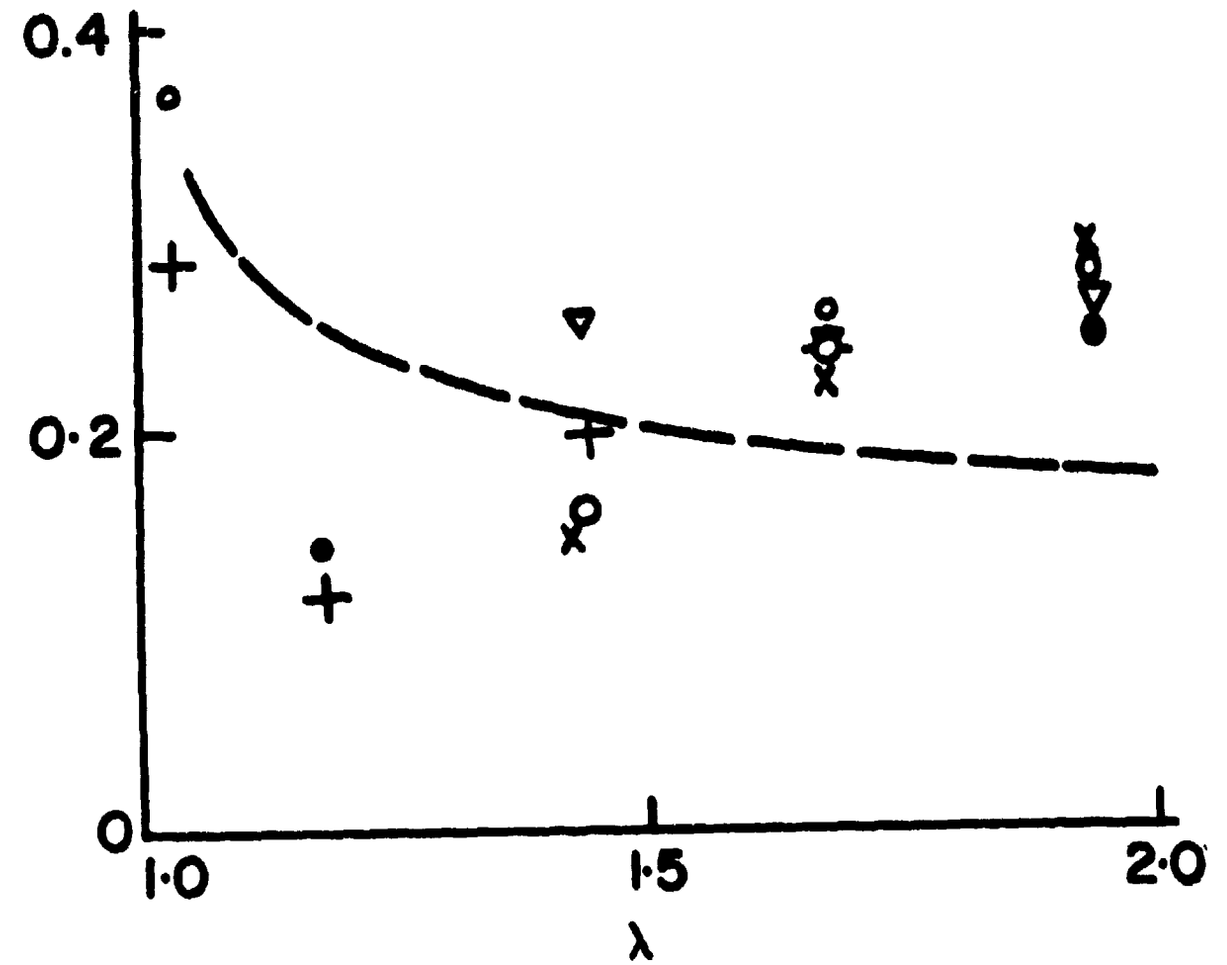

o 27.5 - 32.5°C

+ 30°C

▽ 35 - 40°C

o 45 - 50°C

x 55 - 60°C

Fig. 7, ref [9] : Internal energy contribution from Allen, Bianchi and Price

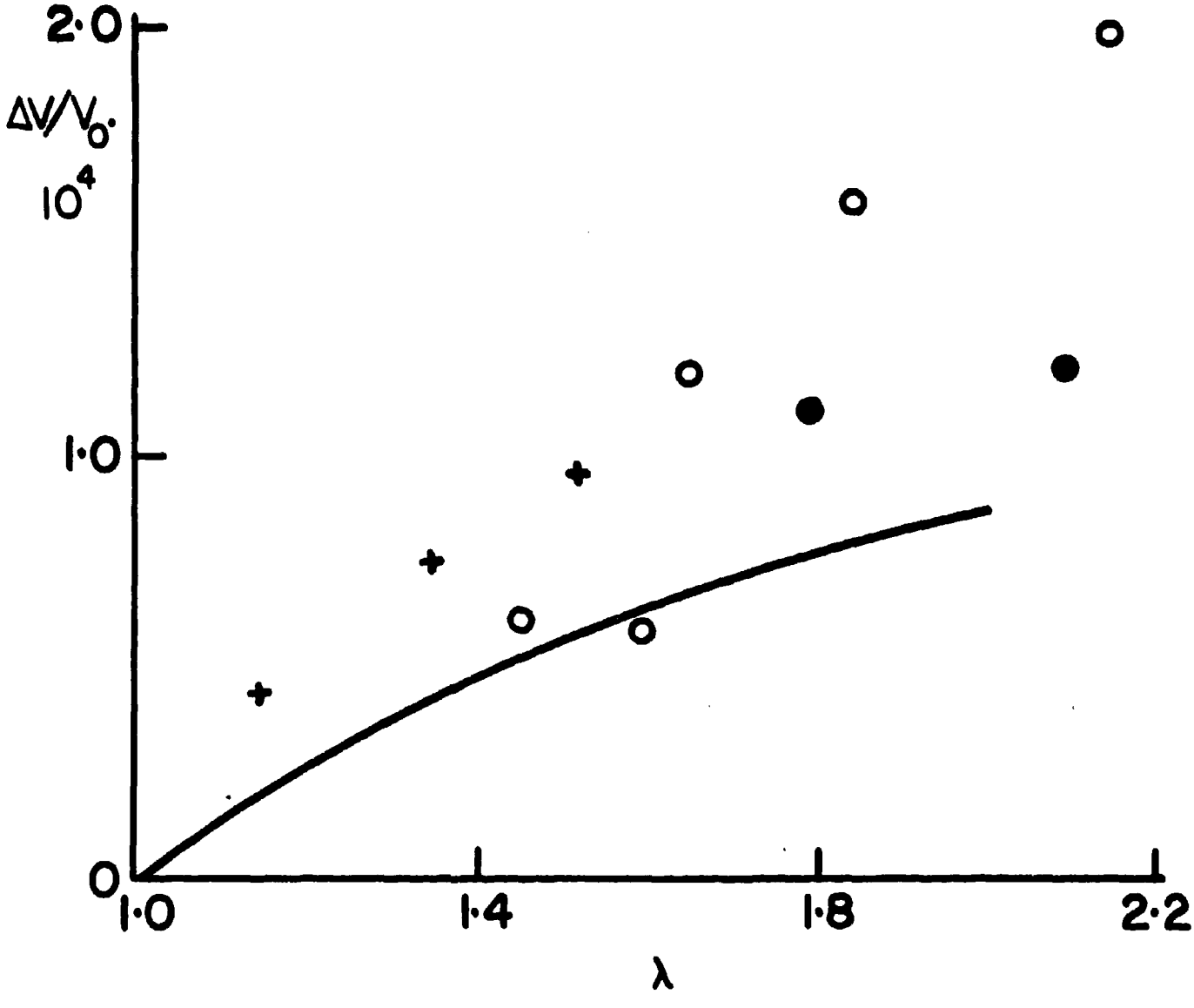

Fig. 8, ref [9] : Dilation of Natural Rubber from Allen, Bianchi and Price

and integrated $(\partial f/\partial L)_{p,T}$ obtained from actual stress-strain measurements. Generally, the agreement between experimental and theoretical results is seen to be good.

Allen, Bianchi and Price, [9] measured the change in volume indirectly by following $(\partial f/\partial p)_{T,L}$ and using one of Maxwell's relationships:

$$(\partial f/\partial p)_{T,L} = (\partial V/\partial L)_{T,p} \qquad (51)$$

Experimentally the problem consists of measuring $(\partial f/\partial T)_{V,L}$ at constant volume, that is to say necessitating a hydrostatic pressure of some 120 atmospheres over a range of 5-10° C. An accurate estimation of $(\partial f/\partial T)_{V,L}$ was obtained by the increase in stress at approximately 1 degree intervals over 5 degrees in all. Indirect measurements of $(\partial f/\partial T)_{V,L}$ were made by measuring $(\partial f/\partial p)_{T,L}$, $(\partial p/\partial T)_{V,L}$ and $(\partial f/\partial T)_{p,L}$.

setting:

$$f_e = f - T(\partial f/\partial T)_{L,V} \qquad (49)$$

These authors obtain f_e/f as a function of elongation (Fig. 7). There is by no means good agreement with the results of other workers who measured f_e/f indirectly. In any case these results confirmed that, at moderate extension ratios, the energetic contribution to the elastic force is approximately 20%. The tests were not at sufficiently low stresses to confirm Roe and Krigbaum's claim that contrary to the behavior of a Gaussian network, there is an energetic contribution to the elastic force which varies with extension ratio at low values of elongation.

Finally in that very broad approach to all aspects of the thermodynamics of rubber-like elasticity, Allen et al. [9] calculate the dilations of their samples as a function of elongation, and compare the results with their data, (Fig. 8). As can be seen, the agreement is not good, but never-the-less the authors

suggest that their indirect method of measuring ΔV via $(\partial f/\partial T)_{V,L}$ would give better results than the direct measurement of dilation, since the latter is so small.

Concerning the use of water as a liquid, we found in preliminary studies that the weight of the samples immersed in water increased markedly as a function of time. Extrapolation to zero time showed that there was an immediate gain in weight upon immersion. The use of swelling or interacting fluids is of course highly questionable because of the introduction of new complexities; thus the choice of a non interacting fluid will be discussed in the experimental section.

Rough estimates even suffice to show that the dilatometer cavity acts as an extremely sensitive thermometer. With a capillary of 0.04 cm diameter, it is possible to detect changes of 0.0001°C using an accurate cathetometer. In view of the work by Wolstenholme, using water as confining liquid, we thought first to set the bath temperature at 3.97°C (maximum density of H_2O) so that, if water were used as the dilatometer fluid since its coefficient of thermal expansion is zero at this temperature there should be no thermometer effect on the dilatometer. Since, subsequent work showed that water should not be used as the confining fluid, this line had to be abandoned.

G. "Fast" Stretching

The temperature rise during adiabatic stretching of rubber has been known for a long time. The first observations were reported by Gough in 1805 [1], but it was Kelvin who first considered the thermodynamic implications and suceeded in showing that the positive stress-temperature coefficient was a necessary thermodynamic consequence of the evolution of heat on extension. A simple application of the second law of thermodynamics to rubber deformation leads, as stated earlier, to

$$dQ_{rev.} = Td\cdot S \qquad (52)$$

Thus, since heat is given off, and the sign of dQ is negative, the entropy must decrease presumably due to the aligning of the chains and thereby there is loss of randomness.

There are three different ways of measuring the heat given off by a rubber during stretching.

(a) direct calorimetric measurement of the heat exchanged when rubber is stretched isothermally; (b) determination of the temperature rise during "adiabatic" stretching, and (c) measurement of the change in heat content between stretched and unstretched rubber.

All work to date has been done by method (b). In the method used by Dart, Anthony and Guth [39], two identical rubber samples were held together by twisting the samples and a thermocouple bead placed between them. The authors found that usually the temperature change on extension was different from that on retraction. Generally, samples which were capable of crystallizing exhibited a marked temperature rise at the onset of crystallinity and there was even less reversibility during the stretching-relaxing process, and the cooling on retraction was generally greater than the heating on extension. The last phenomenon was attributed to a time lag in the crystallization process since as the time during which the rubbers were kept stretched before retraction was increased the differences between the two heats become larger. This was taken to show that crystallization took place before retraction. In this context it is of interest to note that the

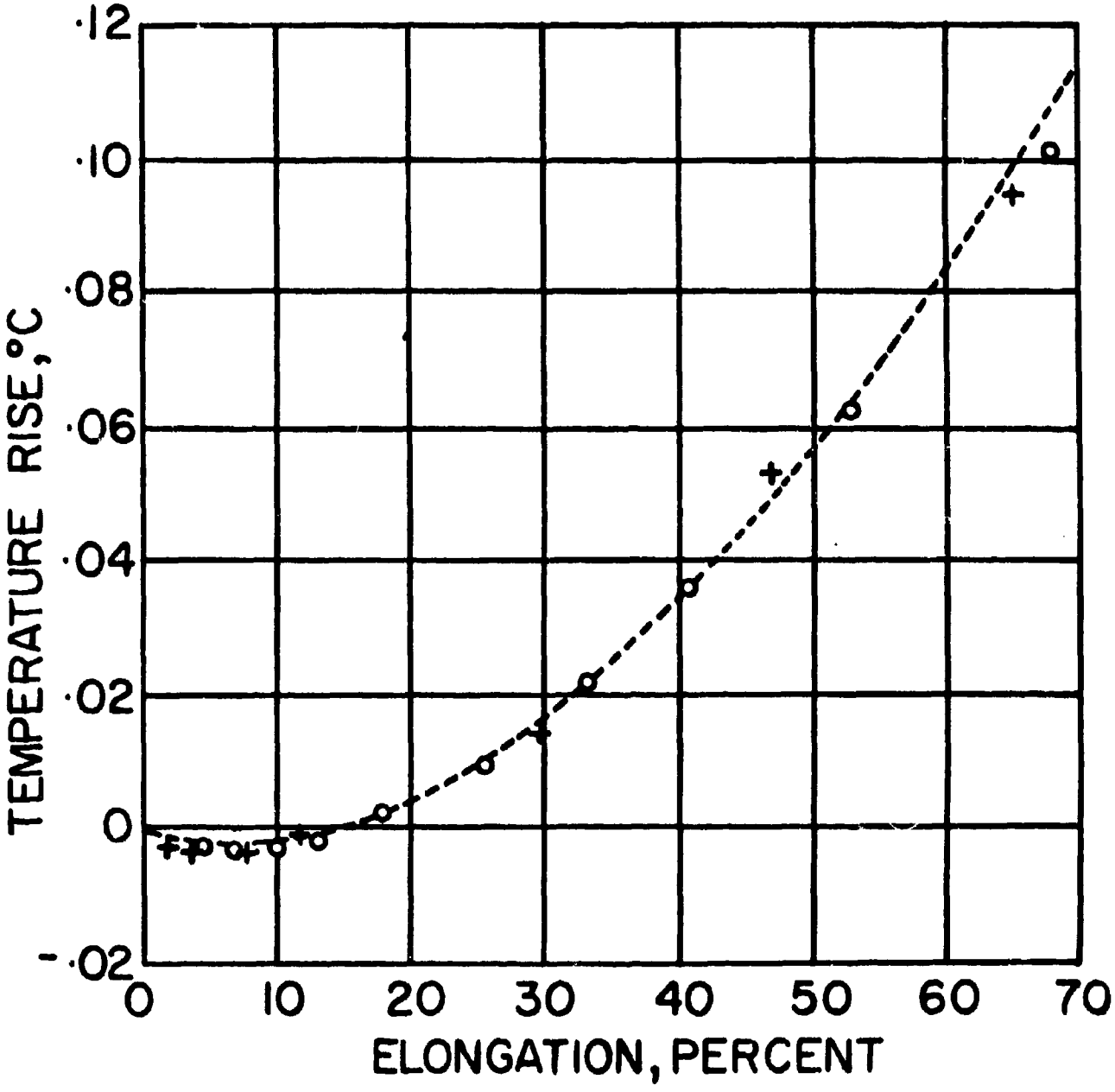

Fig. 9, Ref [12]: Temperature rise in adiabatic extension from Treloar

temperature response was immediate for elongations of less than 300 per cent, but at larger ones there was a lag of the temperature [39] which amounted to as much as 5 seconds for high elongations and could not be due to slowness in the galvonometer of thermocouple response. The authors state: "This implies some process which takes a small amount of time must be going on in the rubber during elongation". One might suppose that there is a diffusion process by which the chains accomodate themselves to the strained positions.

Figure 9 shows the temperature rise in so-called "adiabatic" extension compiled from the earlier measurements undertaken by Joule, James and Guth [12]. The data shows, at small elongations, an initial cooling followed by rapidly rising warming effect as the extension was increased. This course of the thermal changes must be compared to the entropy changes derived from stress-temperature measurements. Thus, the initial cooling corresponds to the initial positive entropy of extension associated with the expansivity of the rubbers and breaking of chain associations while the subsequent heating corresponds to the large negative entropy term from the drop in number of available conformations of the network molecules. At still higher elongations possible crystallization phenomena can introduce further and larger heat effects. It is of interest that rubbers which can not crystalline do not heat as extensively as those that are capable of crystallization. For example, one can obtain differences in temperatures of 14°C in natural rubber at 600% elonation, but only 2°C in a butadiene-acrylic rubber at the same extension. In this connection, fast stretching thermal measurements, which are less accurate than stress-strain measurements, point out in a very direct manner to a necessary consequence of the kinetic theory of elasticity; namely that "the process of deformation of rubber is capable of a reversible transformation of work into heat" [12].

For "fast-stretching", the thermodynamics will be derived as under "adiabatic". In the Discussion it will be shown why these two conditions are hardly strictly equivalent. Under truly adiabatic conditions, the net entropy change molecular ordering plus self-heating is zero, and the change in temperature dT is given by:

$$dT = dH/C_{p,L} \qquad (53)$$

where dH is the amount of heat developed in the process, and $C_{p,L}$ the specific heat at constant length.

The total change in internal energy (adiabatic and at constant pressure) is given by:

$$\Delta E_{tot.} = \int f\,dL + \int T dS - \int p\,dV \qquad (54)$$

which can be written in its differential form

$$\frac{\partial E_{tot.}}{\partial L} = f + T\left(\frac{\partial S}{\partial L}\right)_{p,T} - p\left(\frac{\partial V}{\partial L}\right)_{p,T} \qquad (55)$$

But from the Maxwell relationships, we have seen that

$$\left(\frac{\partial S}{\partial L}\right)_{p,T} = -\left(\frac{\partial f}{\partial T}\right)_{p,L} . \qquad (14)$$

Thus

$$\Delta E_{tot.} = \int f dL - \int T\left(\frac{\partial f}{\partial T}\right)_{p,L} dL - \int p dV \qquad (56)$$

If the rubber is deformed adiabatically, then since $dS = 0$ by definition,

$$\Delta E_1 = f dL - p dV \qquad (57)$$

And now if the system is allowed to transmit the heat developed during the adiabatic stretching process, then

$$\Delta E_2 = -\int_{T_0}^{T_1} C_{V,L}\, dT \qquad (58)$$

But the pathways which lead to the combined energy change $\Delta E_1 + \Delta E_2$ leaves the sample in the same final condition as in the total process associated with ΔE_{tot} Hence $\Delta E_{tot} = \Delta E_1 + \Delta E_2$ and

$$\int f\,dL - T\int \left(\frac{\partial f}{\partial T}\right)_{p,L} dL - \int p\,dV = \int f\,dL - \int p\,dV - \int_{T_2}^{T_1} C_{V,L}\,dT \qquad (59)$$

and we obtain finally,

$$\int_{T_0}^{T_1} C_{V,L}\,dT = T\int \left(\frac{\partial f}{\partial T}\right)_{p,L} dL \qquad (60)$$

If the further assumption is made, that $C_{V,L}$ is independent of T over the range in question, then

$$\Delta_T = \frac{T\int \left(\frac{\partial f}{\partial T}\right)_{p,L} dL}{C_{V,L}} \qquad (61)$$

However, as in most cases when dealing with a liquid or a solid, the difference between the internal energy and the enthalpy, or the work term pdV, is considered negligible. Thus we can write equally well:

$$\Delta T = \frac{T\int \left(\frac{\partial f}{\partial T}\right)_{p,L} dL}{C_{p,L}} \qquad (62)$$

which has been given by Leaderman [40] in the differential form:

$$\left(\frac{\partial T}{\partial L}\right)_{S,p} = \left(\frac{T}{C_L V \rho}\right)\left(\frac{\partial f}{\partial T}\right)_{L,p} \qquad (63)$$

SECTION I

FORCE VERSUS TEMPERATURE MEASUREMENTS

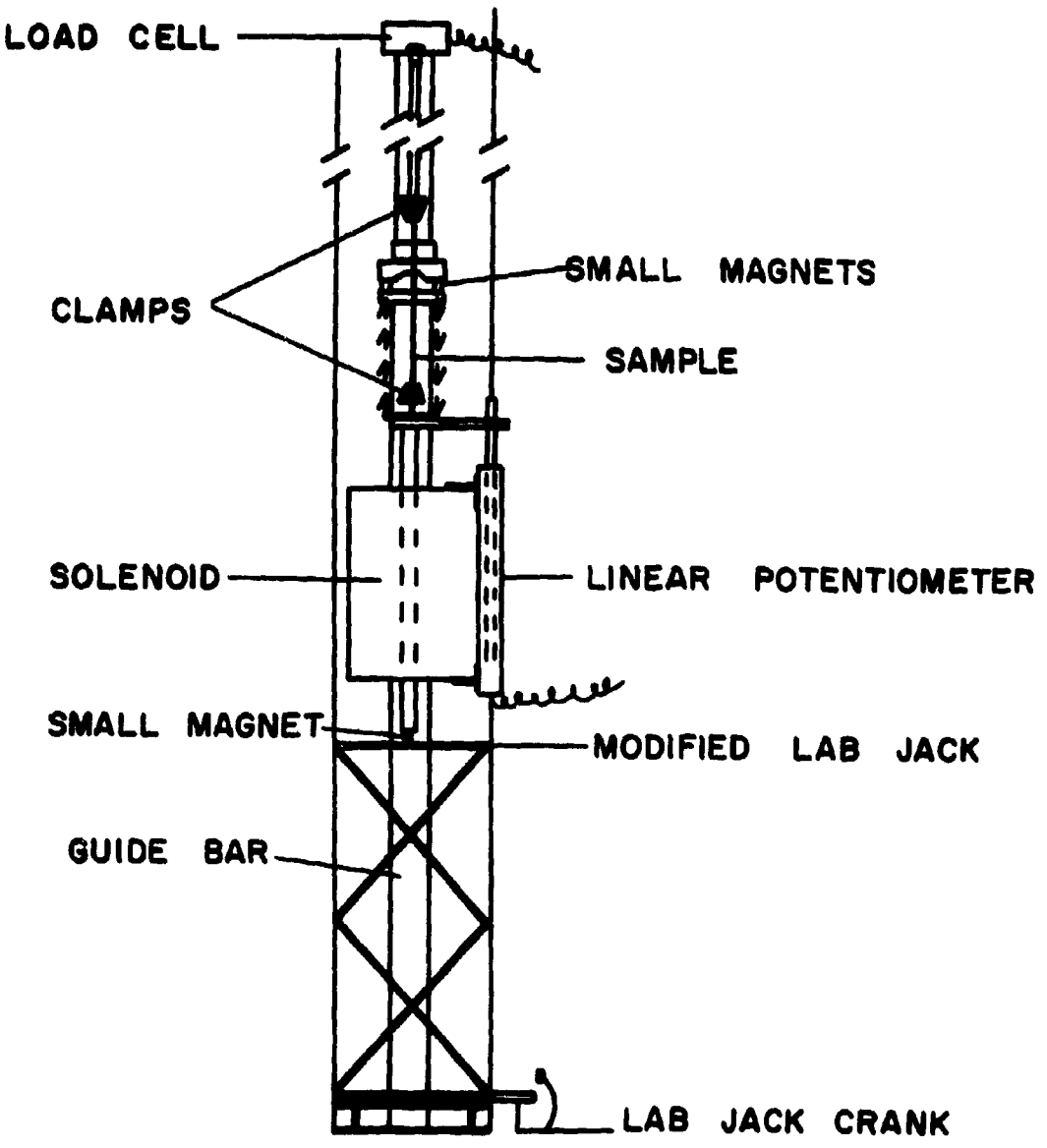

Fig. 10 Loading System

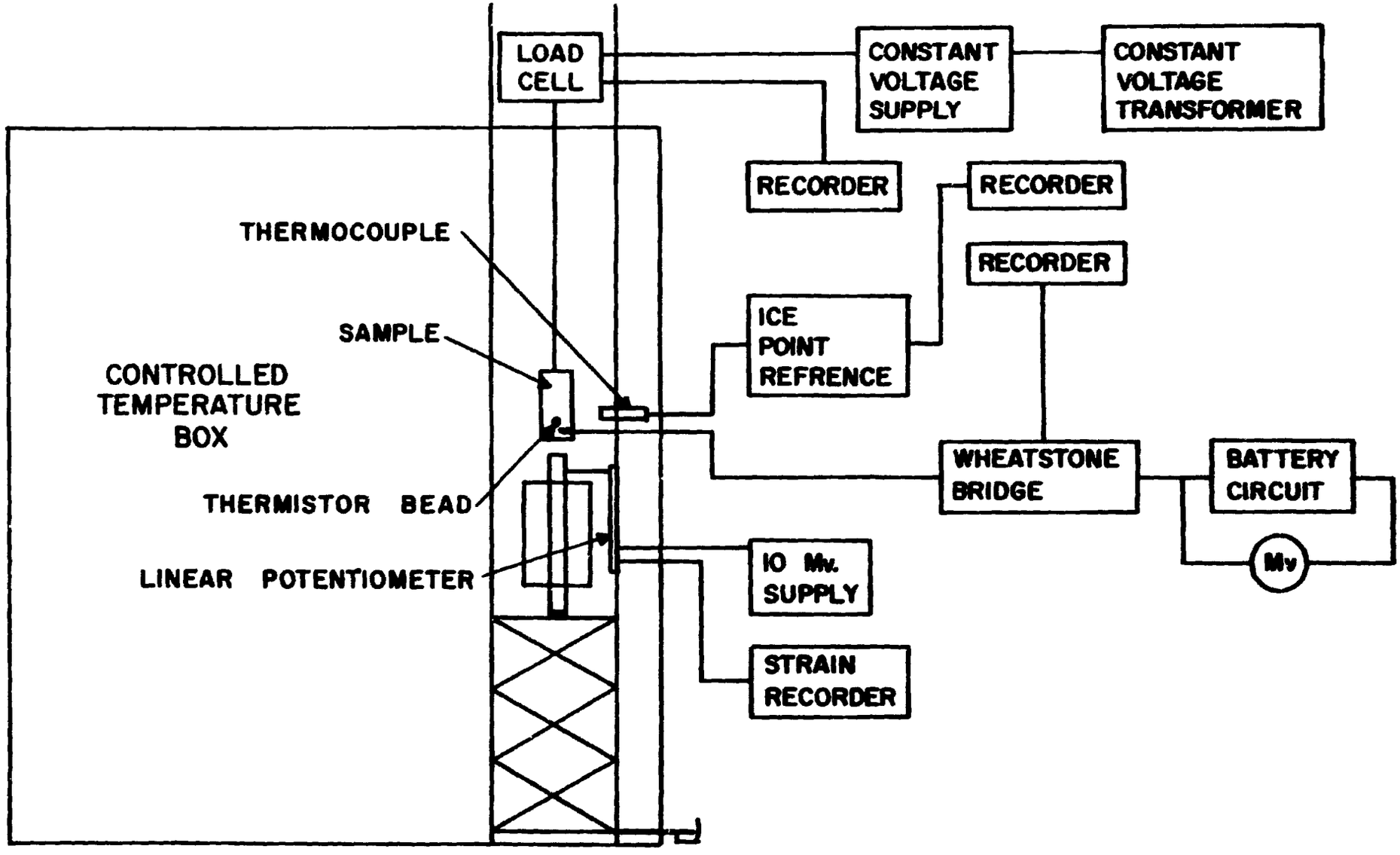

Fig. 11 Overall Experimental Layout for Force versus Temperature and "fast-stretching", experiments for Rubber.

I. EXPERIMENTAL

A. Instrumentation and mechanical devices

In a study of the responses of rubbers to mechanical deformation analysis of the results will require the use of thermodynamic, elastic and rheological equations of state. Consequently it will be necessary to represent the variables in 3-dimensional space where the thermodynamic functions as ordinate will be placed along the z-axis, whilst the x-and y-axis will show the termperature and the extension ratio. Thus the thermodynamic state functions will be treated as dependent variables.

During the force versus temperature measurements, the force is directly measured by a calibrated load cell or more accurately described as a transducer. The instrument used in all the tests was supplied by STATHAM Instruments, Los Angeles 64, model number G1-80-350. The range of load is +- 80 oz. The excitation potential is 15 volts, and the calibration factor is given as 53.08 microvolts (open-circuit) per volt per oz. This unit is not temperature compensated, and therefore shows a thermal zero shift and a thermal sensitivity shift. Since, the transducer should be kept at constant temperature during the experiments, thermal insulation of the transducer was necessary. An Invar drop rod was used, to hook up the sample to the load cell (Fig.10).

The strain sensitive wire elements of the transducer are arranged in the form of a Wheatstone bridge. Direct current was used to excite the transducer. The value of the potential applied must be a constant in time. A HARRISON Laboratories, Berkeley Heights, New Jersey, Model 801 C Power Supply was used in conjunction with a SOLA Electric Company, Chicago, constant voltage transformer, catalogue number 30804. This input potential circuit proved to be remarkably stable (of the order of 1 mv out of 15 v over a period of 3 months).

The force versus temperature measurements being carried out at constant length, both ends of the sample holders are clamped down, and only the force varies as a function of temperature. The sample is contained in a large converted refrigerator (Fig.11) which can either be maintained at constant air-temperature at any point between - 25°C and + 130°C, or can serve as an environmental chamber as the temperature is

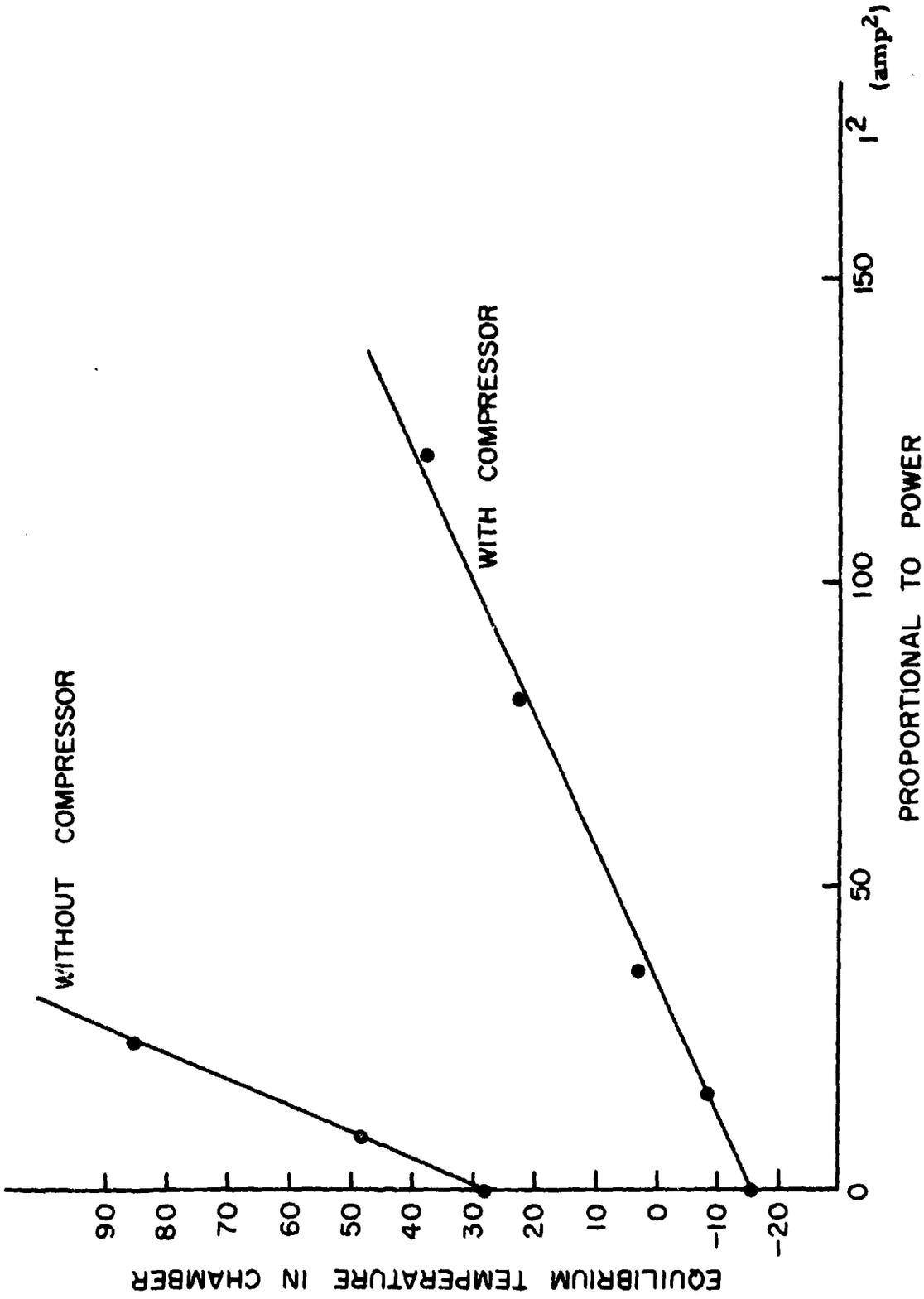

FIG.12 CALIBRATION OF ENVIRONMENTAL CHAMBER

varied. The time-temperature profile is not linear, but as a complete temperature cycle is of the order of 12 hours, thereby thermal equilibrium throughout the sampel is ensured at all times. An added feature is that the atmosphere of the chamber can also be controlled; in most of our tests, nitrogen gas surrounded the sample continuously.

A compressor and a series of strip heaters allow one to reach any temperature in a given range. Most of the force versus temperature experiments were carried out overnight in a time cycle of temperatures from 25° C to 60° C. The heaters are wired to large 15 ampere power-stats , and it is possible to read the amperes of current which are supplied to the various heaters directly. It is also possible to calibrate the temperature of the environmental chamber at equilibrium as a function of the power supplied to the heaters. As expected (Fig.12), these curves are roughly linear, since the heat evolved is proportional to the power which is in turn proportional to the square of the current. These calibrations are extremely useful in obtaining the desired temperature, or range of temperatures. To enable nightime testing, a spring loaded relay w. s installed in the heating circuit; as the temperature rises above a certain predetermined value, the relay opens the heating circuit, and the temperature slowly decreases by losses to the ambient as a function of time. Good thermal insulation ensured the obtention of a long temperature-time cycle and thermal equilibrium within the samples.

A copper-constantan thermocuple from the OMEGA Engineering, Box 47, Springdale, Connecticut was used to measure the temperatures. The reference temperature of 0° C was established by the physical equilibrium of ice and water, sustained by a thermoelectric cooler automatically controlled by a bellows-microswitch sensing mechanism which responds to the relative volumes of ice and water in the hermetic cell. This Ice-Point Thermocouple Reference System is manufactured by the Joseph KAYE and Co., Cambridge 38, Massachusetts; model 1150, and must be specified for correct use of the 1160 interchangeable Thermocouple Probe Assembly, also manufactured by the Joseph KAYE Company.

An x-y Potentiometric Recorder, of the HEWLETT-PACKARD, MOSELEY division, Pasadena, California, model 7001 AM was used to determine the force-temperature characteristics of the rubber. On

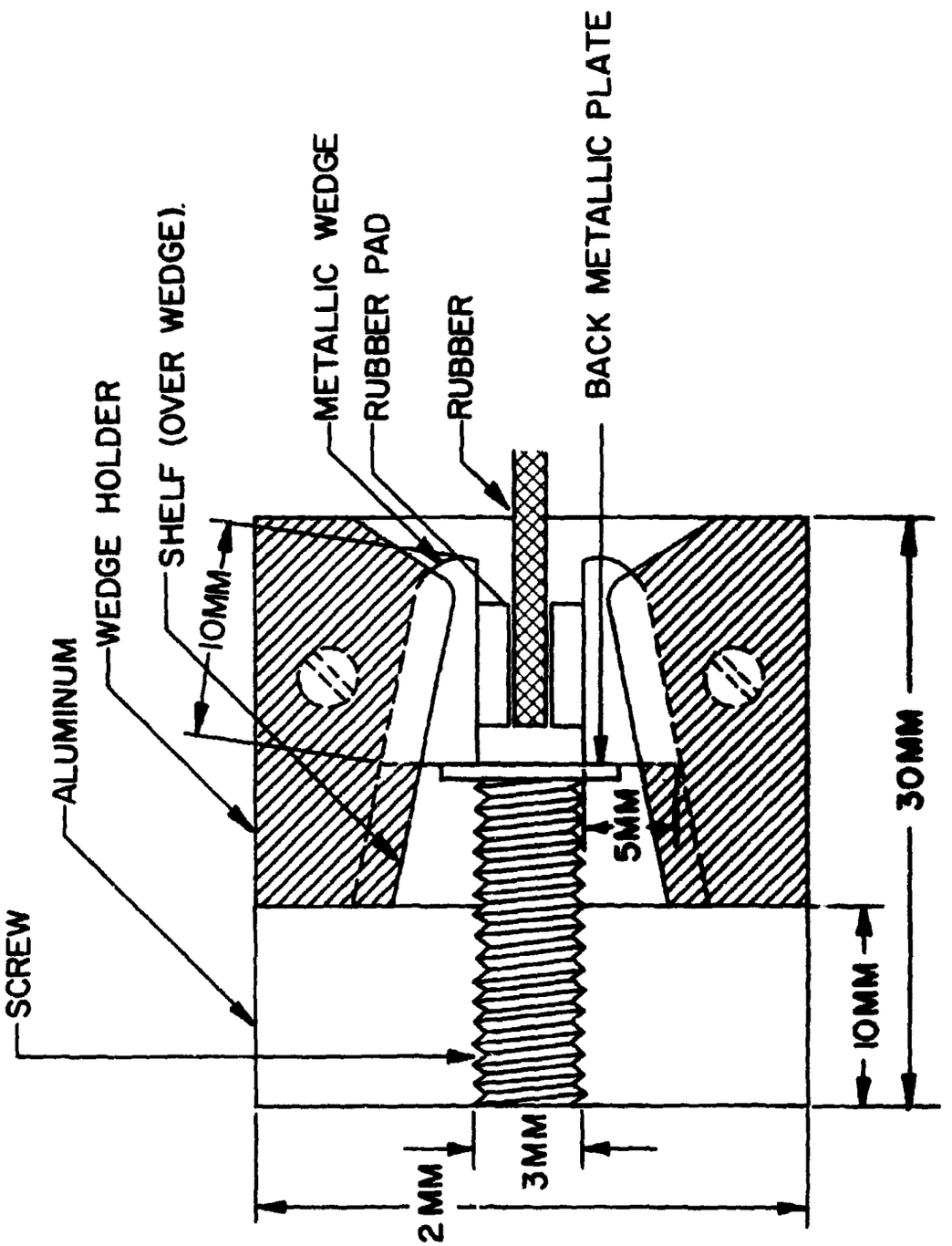

Fig. 13 Sample holder and detail of self-tightening jaws

potentiometric mode, large input resistances are allowable in the most sensitive ranges. Temperature differences of the order of 0.001° C, and differences in stresses of the order of 1% were easily analyzed. The pen system used was a cartridge loader, which after some adjustments, proved to be satisfactory.

A short description of the clamping system follows. Previous very extensive efforts had failed to devise an adhesive bond which would hold at elevated temperatures and elongations [47] Figure13 shows the type of self-tightening end clamps that were finally constructed. The rubber sample is imbedded between two rubber strips tightly held by the self-locking triangular aluminum wedges. As pressure is applied to the wide surfaces of these wedges via the back-pressure screw, the wedges tend to slide forward and lock the sample in its grip. While this method of holding the sample is highly satisfactory at moderate and high levels of strain, the inaccuracies of this system become quite large at very low values of strain ($\lambda < 1.1$, where λ is the extension ratio). This fact will be illustrated further on, in the discussion of the weighting factor to be applied to the Mooney-Rivlin type plot (See Appendix I).

For the measurement of the elongation of the sample, an overall length was measured between the pads of rubber. The rest length was estimated in the same manner. Then after the test, the rubber was taken out and a mark appeared on the rubber at the place of the pads. This total length between pad marks was taken for the zero length, and all other lengths were corrected by the difference in the two initial lengths (these were not appreciably different). A trial run was carried out by marking 6 lines on the rubber with white ink, and measuring the relative distances between the markings with a cathetometer. Plotting the various positions as a function of the initial positions (with the rubber at rest), and applying a least square linear fit to the points so obtained, the slopes of these lines should correspond to the different elongations, measured by taking overall lengths. The "best" elongations obtained by least squares analysis correspond fairly closely to the elongations obtained from an analysis of the overall lengths, however the standard deviations are quite high, being of the order of 5 to 10%. A later section will be devoted to the problems of sample shape and sample holders.

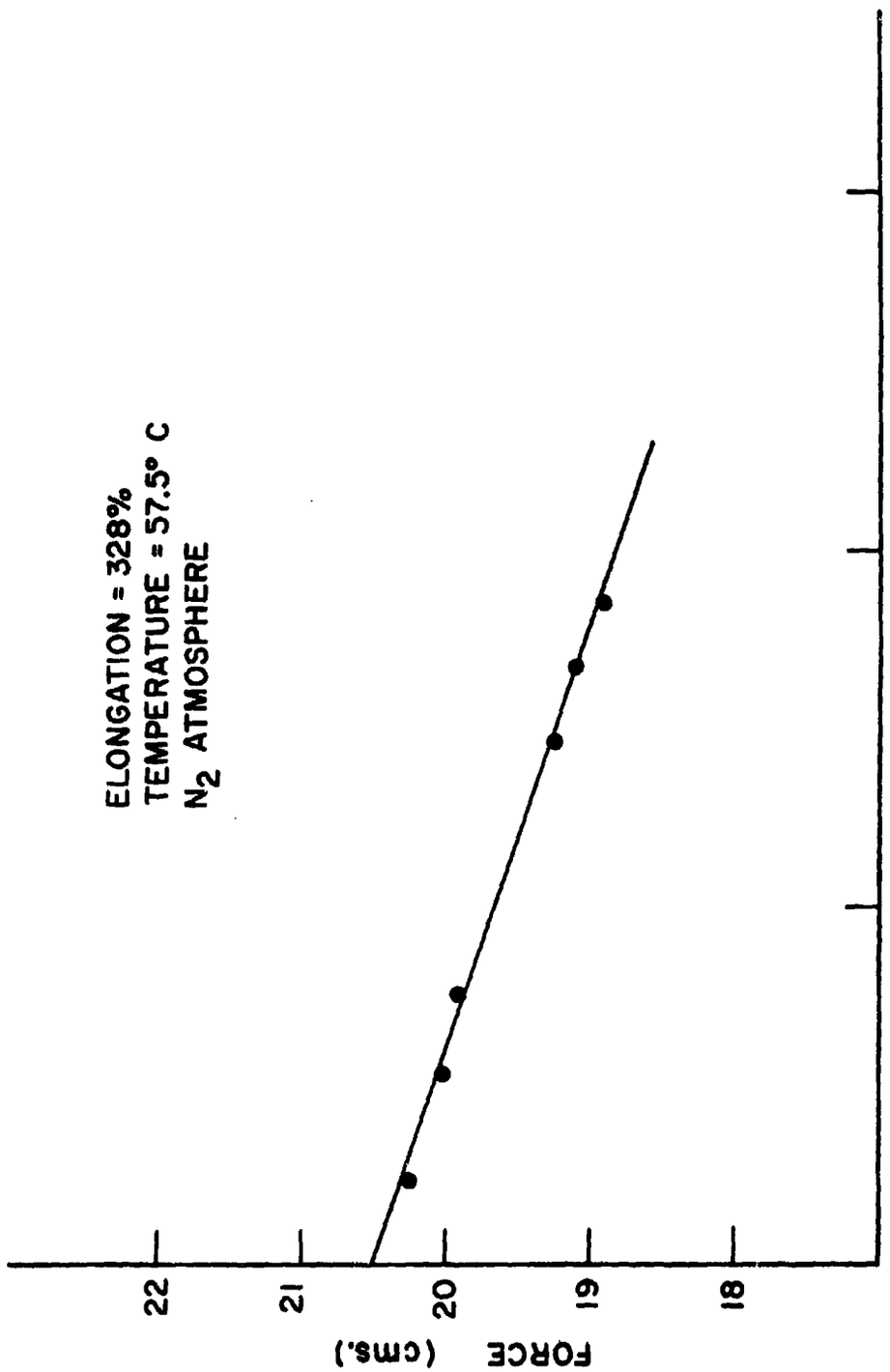

FIG. 14 RELAXATION CURVE FOR DA-14

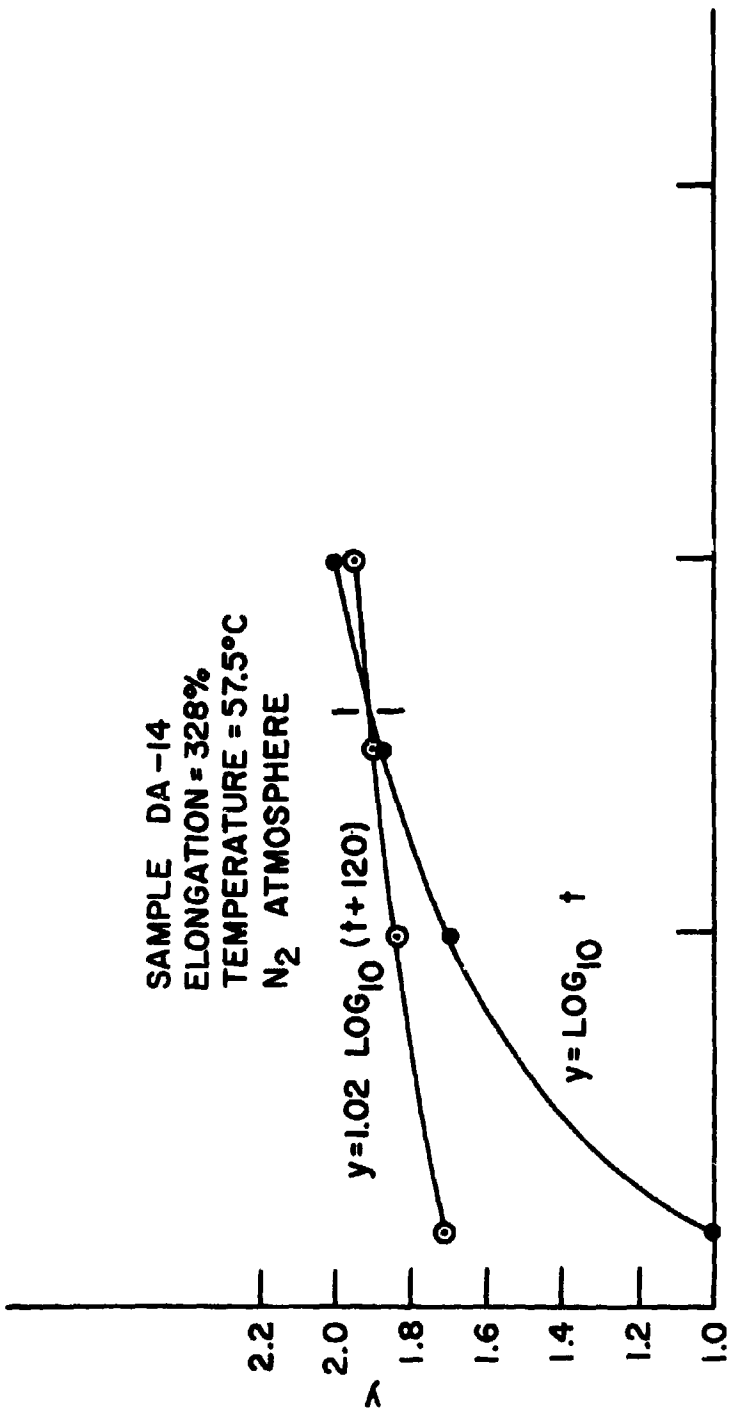

FIG. 15 GRAPHICAL SOLUTION FOR OBTENTION OF TEST TIME

B. Experimental Technique

1. Stress relaxation

Adopting the technique of previous workers [42] , the samples were held for a long period of time at the highest temperature and at the highest elongation to insure minimal relaxation of the stress as a function of time during the actual time-temperature cycles of the tests. A blanket of N_2 gas is kept surrounding the sample at all times to prevent oxidative degradation at the higher temperatures.

The total force on the sample is then read from the xy recorder and plotted as a function of the logarithm of time. There is no claim made as to the mechanism of relaxation, whether it be one of the forms of creep, crystallization or aging. However, if the plot of $F = f(\log_{10} \Delta t)$ where F is the total force is linear, then as can be seen from Fig.14 and Fig.15, it is easy to calculate the time after which testing can commence, allowing a two percent overall relaxation of force at the highest temperature and elongation over the entire period of the tests.

From Fig.14 , the equation of the relaxing specimen is given by:

$$F = A \log_{10} \Delta t + B \qquad (64)$$

where F is the total force, and A and B are the linear coefficients. The coefficients A and B can be read from the plot. Let us now solve for t_1, where $\Delta t = t_2 - t_1$ = amount of time for total test, and where $\varepsilon F = (F_2 - F_1)/F_1 = 0.02$: εF is the relative error on F . From (64)

$$\varepsilon F = \frac{A(\log_{10}(t_1 + \Delta t) - \log_{10} t_1)}{A \log_{10} t_1 + B} \qquad (65)$$

Rearranging (65), $\log_{10} t_1 = \frac{\log(t_1 + \Delta t)}{1 - \varepsilon F} - \frac{B\varepsilon F}{A(1-\varepsilon F)}$ (66)

This equation can be solved graphically, as shown in Fig.15 . Using this technique, it is very easy to know when to start the actual testing. Once the nominal relaxation for the period of testing, is less than two percent at the highest elongation and temperature, then the relaxation is considered sufficiently accomplished, and the temperature is decreased by shutting off the heaters, and the sample is allowed to equilibrate at room temperature and in the environment of N_2. Using the previously

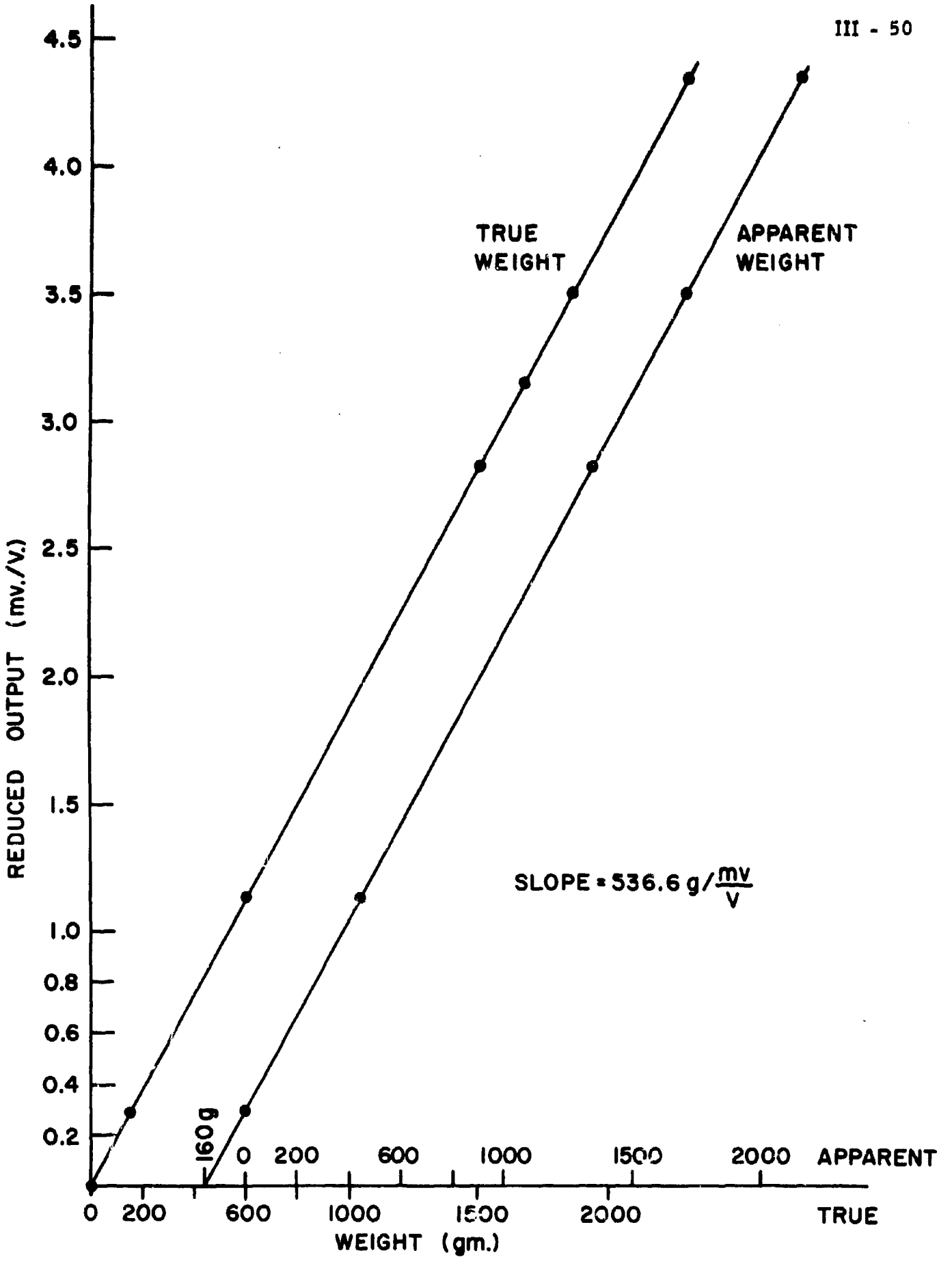

FIG. 16 LOAD CELL CALIBRATION

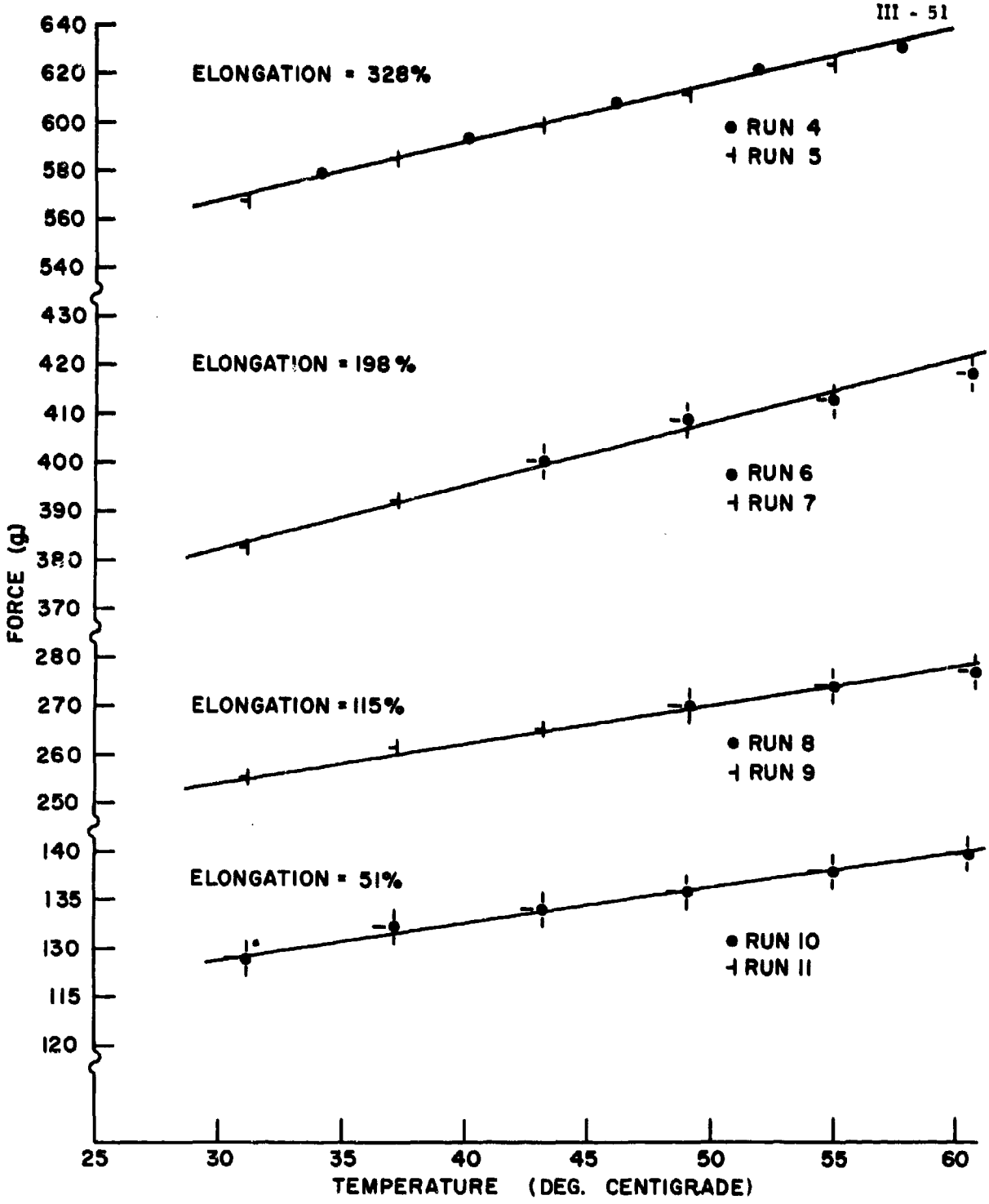

FIG. 17 FORCE–TEMPERATURE CURVES FOR DA–14

described technique of heating and then allowing the sample to cool over a period of approximately 12 hours, a plot of F(force) expressed in millivolts versus T(temperature) also in millivolts is obtained on the xy recorder, as a series of F versus T lines at constant length of the sample. Using thermocouple calibration constants given in the literature[43], the temperature can be expressed in degrees Centigrade or Absolute. The calibration of the load cell is done by hanging known weights on the sample holder, and plotting the reduced output (output divided by potential applied) as a function of the known weights. Plotting the apparent weights at first allows one to extrapolate to the dead weight of the holder and Invar drop rod. The second line of Fig. 16 shows the true calibration curve. A digital voltmeter was used to check from time to time the input potential to the load cell. It was found to be constant to 1mv (out of 15 v applied) over a 3 month period of time.

Knowing all of the calibration constants (thermocouple and load cell), and the zero values and ranges of the x and y axes, a simple computer program (P 31) calculates, for each length, the forces (dynes/cm^2) and temperatures (degrees absolute, degrees centigrade). A listing of the Fortran IV source deck as well as some typical entries and outputs (both written and punched) are discussed in Appendix I..

At each length, two time-temperature cycles were carried out to check upon the reversibility and reproducibility of the data. Fig. 17 shows F versus T for four different elongations. It can be seen that the F-T diagrams are reproducible, and except at the very highest elongations (350%), all runs were completely reversible. In order to save time, subsequent testing would only be carried out on a single cycle per length.

From this point on, all of the raw data has been collected and now only needs to be processed. A series of consecutive computer programs has been written to calculate the various quantities of interest. Each punched output is, with some slight modifications, the input for the next program. Thus a complete analysis of the various parameters at any stage of the study is easy.

From the force-temperature data at constant length, it is possible to calculate the stress-strain curves at constant temperature. But these curves must be corrected for the thermal expansion of the rubber, thus

obtaining corrected stress-strain data. It is possible to then recalculate corrected force-temperature data at constant length. One can also fit the data to a Mooney-Rivlin type plot. It is all of these calculations that are done in the successive computer programs.

2. Sample preparation

The samples under discussion all came from the same supply (1/16") of DUNLOP NATURAL RUBBER with one percent dicumyl peroxide as the crosslinking agent and were obtained by courtesy of Dr. DINGLE. The samples were stored cold in the dark and, as much as possible, all experiments were carried out on specimens from the same slab.

The actual geometrical configuration of the specimens used were rectangular pieces 80 mm x 2 4 mm cut with a die manufactured by the CLEAR CUT STEEL RULE DIE Corp., Plainview, Long Island. Great care had to be taken in the cutting of the samples, in order to avoid nicks or tears which serve as local stress concentration points and initiate rupture of the sample. A small hydraulic press was used in conjunction with a slab of a soft plastic placed between the press and the sample to be cut. The cut sample was then carefully measured at different points with a micrometer from STARRETT Number 1010M as to uniformity of thickness and width. The standard deviations on thickness and width were of the order of three percent. The length of the sample before placing it in its grips was measured with a ruler calibrated in millimeters. A reading could be easily estimated to within 0,5 mm.

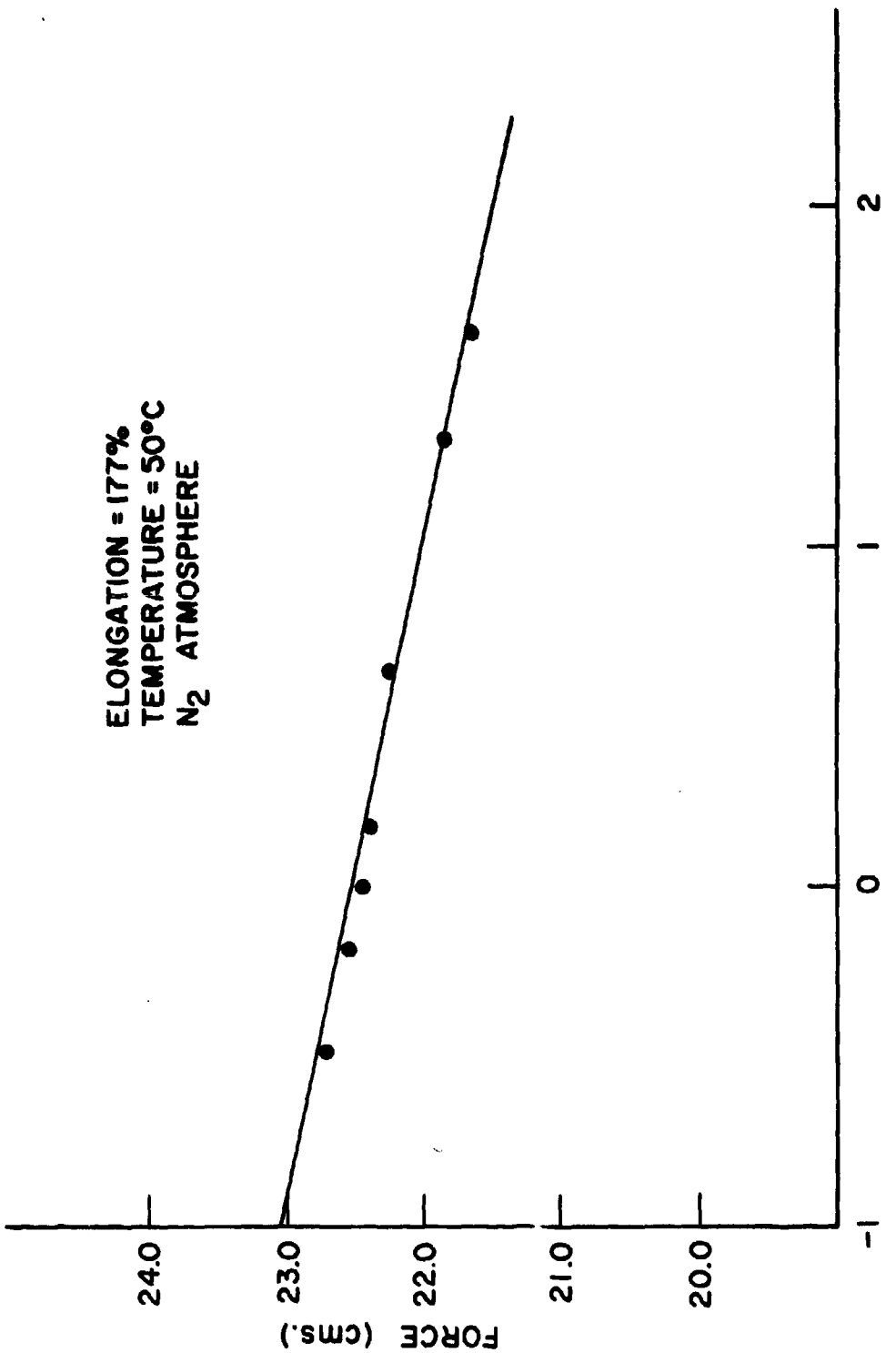

FIG. 18 RELAXATION CURVE FOR DA1-22

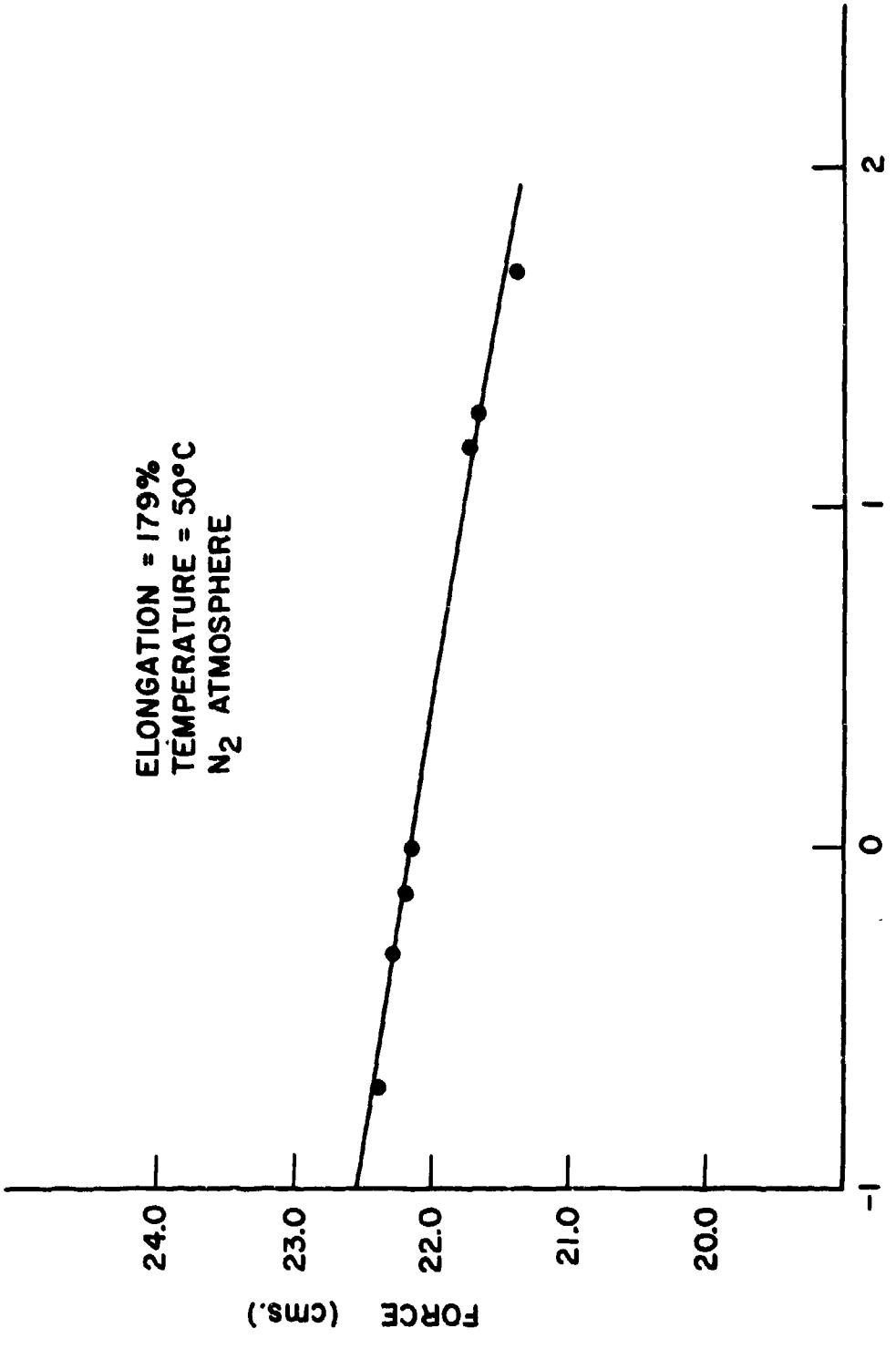

FIG. 19 RELAXATION CURVE FOR DA 1-23

TABLE I

Number of Point	t (hrs)	$\log_{10} t$	net F (cms)
0	0	-	-
1	0.33	-0.478	23.80
2	0.66	-0.181	23.55
3	1	0	23.45
4	1.50	0.176	23.40
5	4.33	0.636	23.75
6	21.12	11.324	22.85
7	43.62	1.639	22.65

Stress Relaxation of DA 1-22 as a function of time

TABLE II

Number of Point	t (hrs)	$\log_{10} t$	net F (cms)
0	0	-	-
1	0.25	-0.699	23.40
2	0.50	-0.301	23.30
3	0.75	-0.125	23.20
4	1.00	0	23.15
5	15.50	1.190	23.70
6	19.33	11.286	22.65
7	49.25	1.692	22.30

Stress Relaxation of DA 1-23 as a function of time

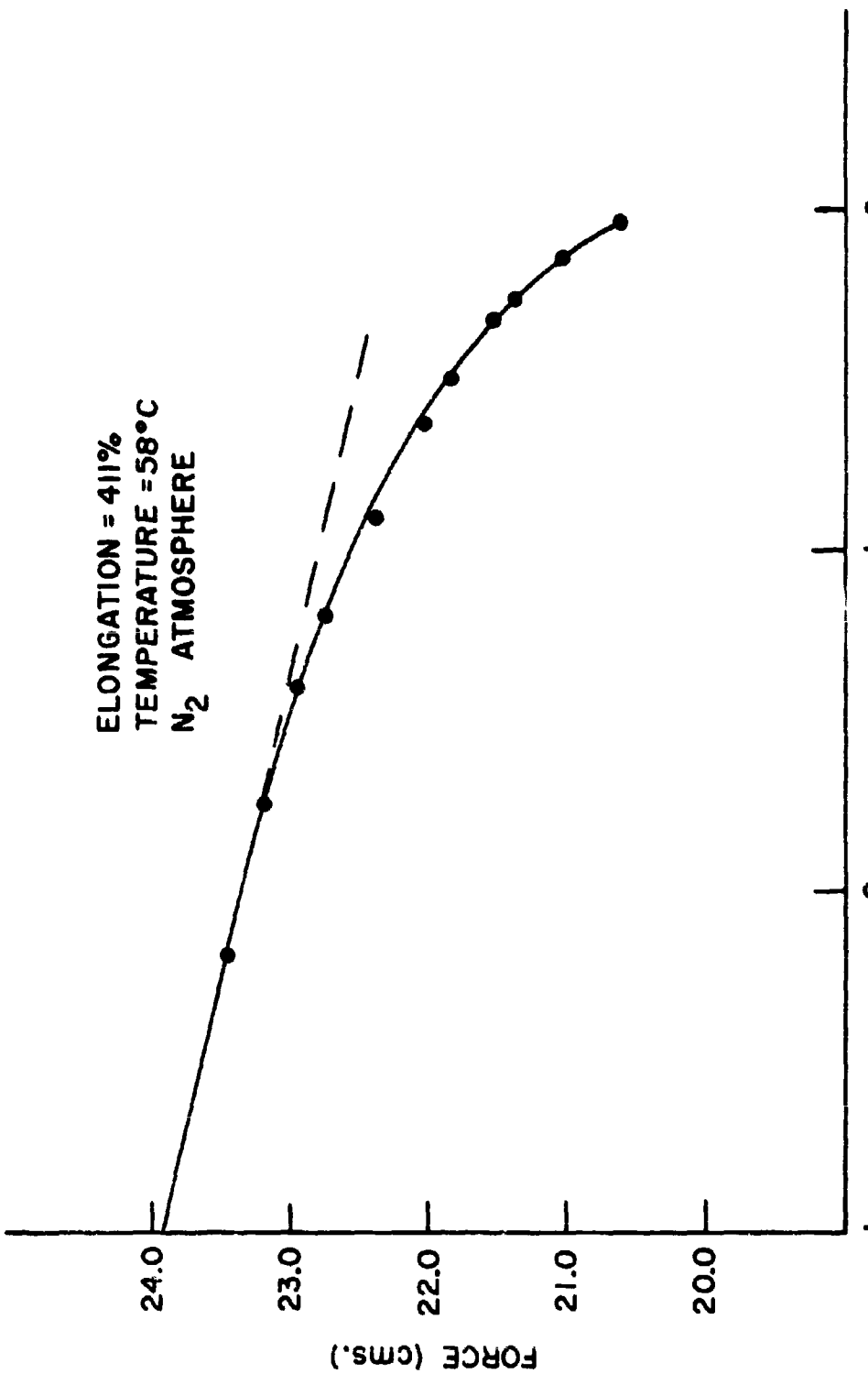

FIG. 20 RELAXATION CURVE FOR DA-15

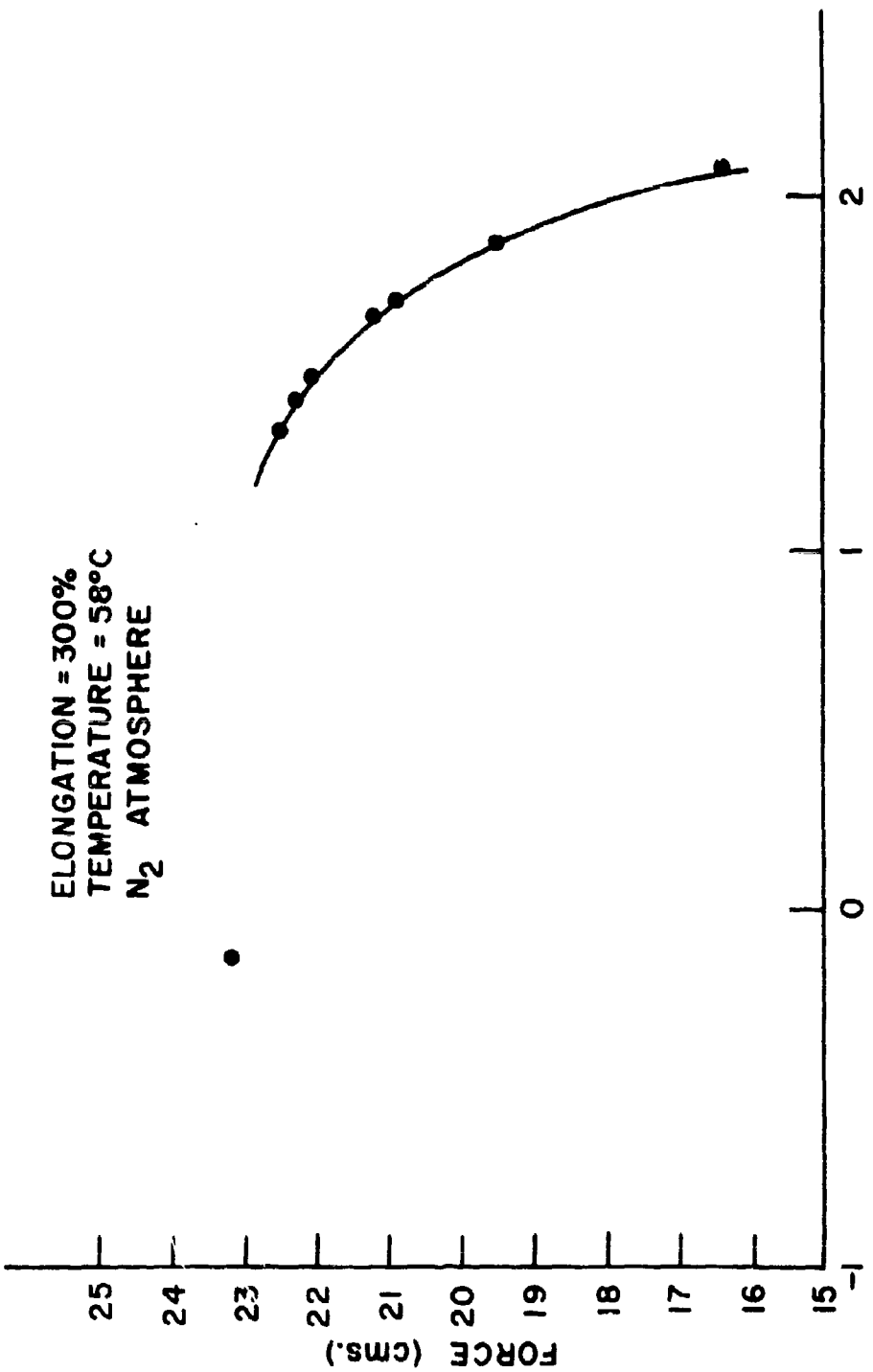

FIG. 21 RELAXATION CURVE FOR DB-2

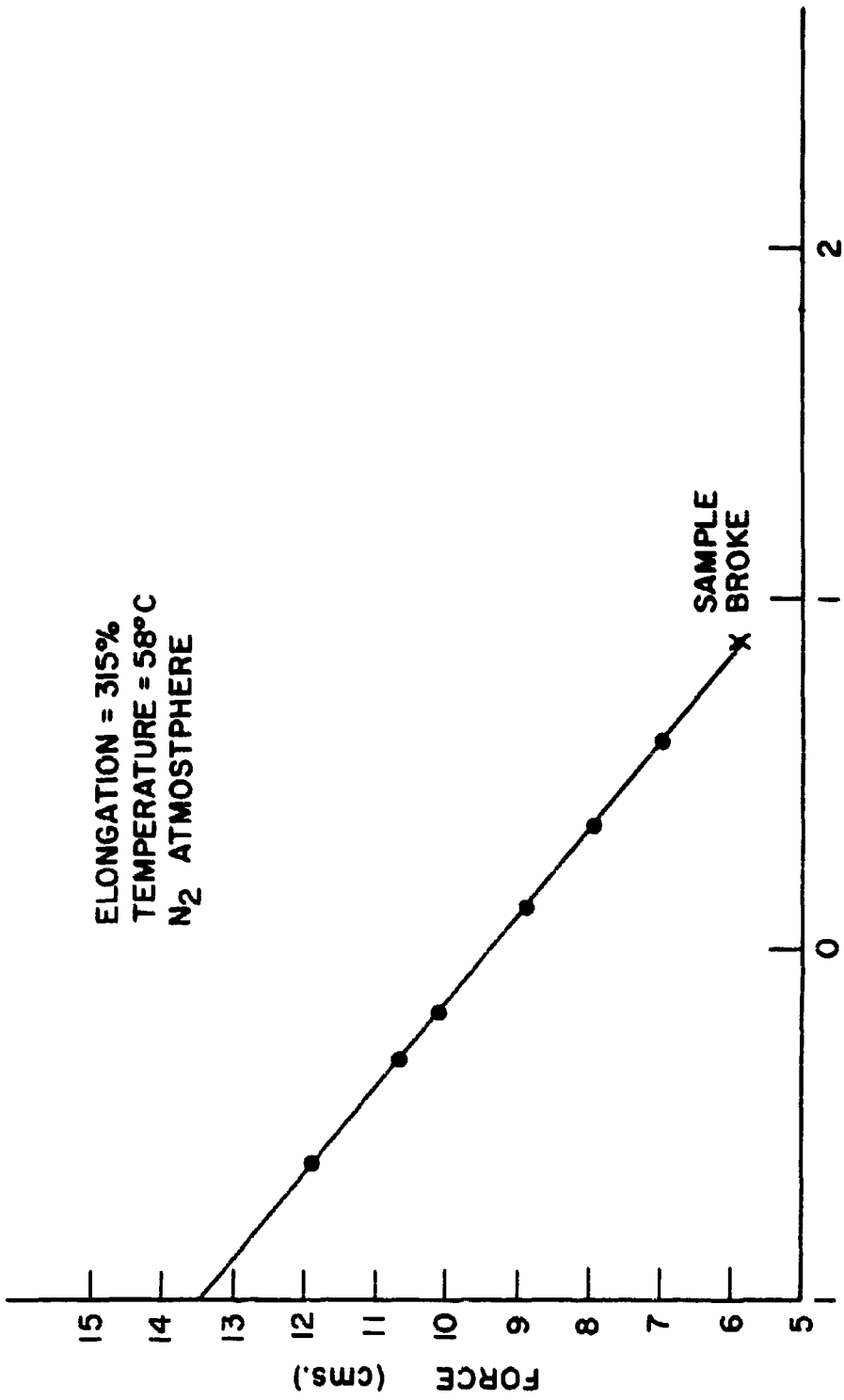

FIG. 22 RELAXATION CURVE FOR S-1

II. RESULTS -

A. Geometry of Samples

Two samples of natural rubber were analyzed exhaustively and these results shall now be presented. The samples examined are numbered DA 1-22 and DA 1-23. All measurements taken after relaxation and consecutive testing cycles. The dimensions are given below:

	Rest length (mm)	Thickness (mm)	Width (mm)	Area (cm^2)
DA 1-22	79	1.89	4.11	$7.603 \cdot 10^{-2}$
DA 1-23	77	1.82	4.06	$7.389 \cdot 10^{-2}$

B. Relaxation of Samples

The samples were each held at about 175% elongation over a period of several days, at the highest temperature of 50°C. The force or total stress on the sample was noted as a function of $\log_{10} t$, where t is the time in hours. From Figures 18, 19 and Tables I, II, it is evident that the relaxation of stress is linear with $\log_{10} t$. It was found on previous samples that either at higher temperatures ($T > 50^{\circ}C$), or at higher elongations ($\lambda > 3.00$), the relaxation curves were initially linear but then the stresses sharply diminished with increasing times (Fig20). Sometimes the samples even broke during the relaxation tests. Higher temperatures would naturally increase relaxation, whether it be creep due to viscoelastic or to chemical relaxation [44] . Higher elongations would of course increase relaxation induced by crystallization, as well as accelerating any crack propagation. We were notably unable to "relax" the synthetic natural rubbers (NATSYN) or the Shell elastomer (Figs.21,22)due to failure after approximately 100 hours. However, probable linear relaxation could be achieved by working at substantially lower elongations and lower temperatures with both of these elastomers.

C. Treatment of data

In this section a brief description of the various calculations carried out upon the raw data by means of a computer program will be given. From there a series of consecutive programs carry out the prescribed algebraic operations. From the F versus T data, as mentioned in the introduction, it is possible to calculate various changes in state

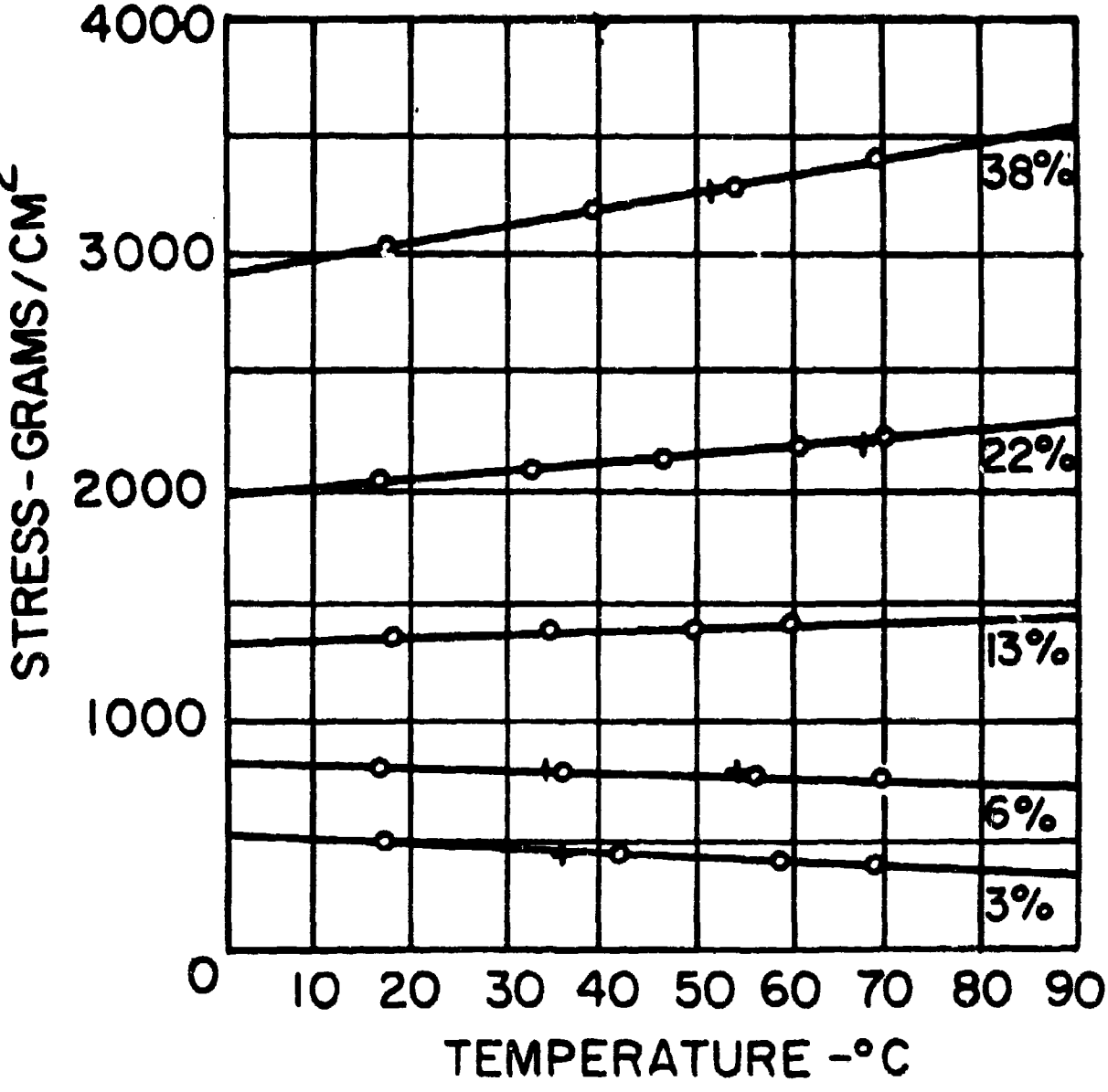

Fig. 23, ref [46] Stress-temperature curves obtained for elongations ranging from 3 per cent to 38 per cent from Anthony, Caston, and Guth

functions. However, it is also possible to present the data in the form prescribed by MOONEY and RIVLIN [45].

It must be remarked at the onset that all of the tests are carried out at constant length. The thermodynamic relationships are a function of ratio of lengths at a given temperature. At elevated temperatures, the normalized length is the total length divided by the rest length at that same temperature. If the slope of the force versus temperature data were to be plotted as a function of length, one would find at very low elongations negative values of the slope (Fig. 23). This is the thermoelastic inversion phenomena, first pointed out by Anthony, Caston and Guth [46]. It is easy to calculate a corrected elongation on the basis of the unstressed length at the temperature in question rather than at room temperature. A set of stress-strain values is obtained at constant length. Each value of strain is then corrected for thermal volume expansion by means of the equation:

$$\lambda_c = \lambda e^{-\bar{\alpha}\Delta T} \tag{67}$$

where $\bar{\alpha}$ is the mean linear temperature coefficient of the unstrained rubber and ΔT is the temperature rise in $^{\circ}C$ above room temperature. Equation (1) is the most general form expressing the temperature dependence of a given parameter. If $\bar{\alpha}$ were to be replaced by $\alpha = \alpha(T)$, then in order to calculate the temperature dependence of the parameter, one would have to integrate Equation(67)overall values of T.

Recently Allen, Bianchi and Price [9] showed that α is independent of elongation and temperature in the intervals $\lambda = 1.0 - 2.2$ and $T = 30^{\circ}C - 70^{\circ}C$. We shall use their value namely $\alpha = 2.196 \times 10^{-4}\ deg^{-1}$. This is the only correction that these or other workers in the field mention. However as pointed out by Blatz[47] there is also a correction for the stresses. These are forces per unit area, and the area is equally temperature dependent. Hence this work comprises also correction terms on the stresses: namely,

$$\sigma_c = \sigma e^{-2\bar{\alpha}\Delta T} \tag{68}$$

However, these corrections are very small and most authors simply neglect them [42]

In essence, the computer programs were written in order to assemble and index the various data, to effect cuts in the implied 3-dimensional surface of F-T-λ perpendicular to the axis, to correct for thermal expansion following Equations (67) and (68) the stress-strain data, and finally to recompute on the one hand the corrected force-temperature data from which the changes in state functions may be derived, and on the other hand to calculate the data in form of the Mooney-Rivlin typeplot. These various programs are described in Appendix I, where a general summary of the programs used is given, as well as a detailed analysis of each one.

It is interesting to note that the least square analysis is a weighted least square, where the weight ascribed to a point is the reciprocal of the variance of that point. But once the original data are considered to be of equal weight, all of the subsequent weights are defined. This allows for much more precise interpretation of the results. In the least squares fitting technique, we assume no error in the independent variables. This is not an essential assumption, but simplifies the computations greatly.

In Appendix I, the explanation, listing and input-output formats will be described. Thus the actual results will be presented in tabular form just as they appear on the computer output sheets

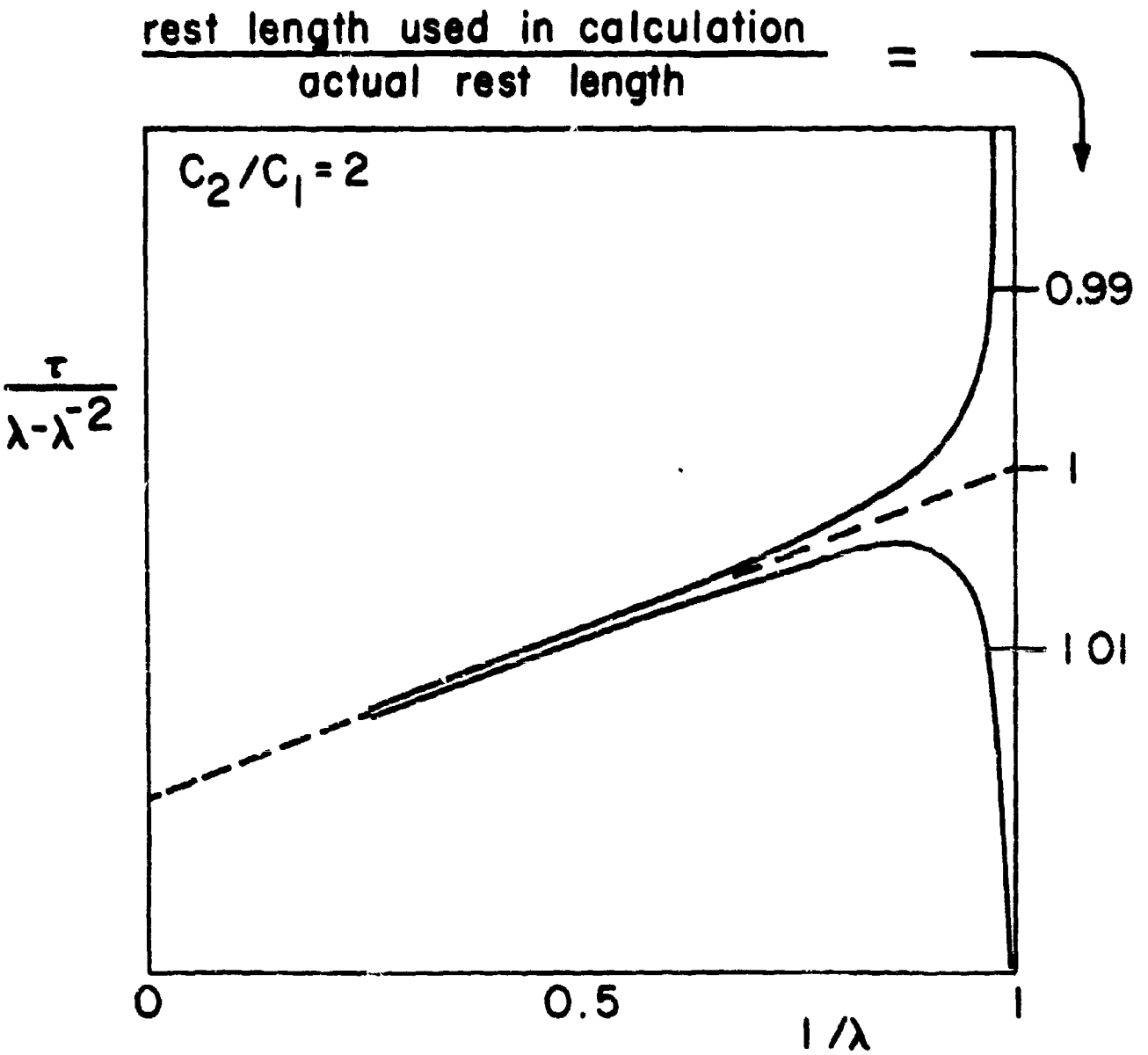

Fig. 24. Ref [22] : Effect of a small change in rest length upon Mooney-Rivlin plot

III. DISCUSSION

Force versus Temperature

Our study of the force-versus-temperature data for the two specimens analyzed brings out a number of interesting points. The first phenomenon of interest are some aspects of the relaxation curves (See figs 18, 19). As already mentioned in the Introduction, [26, 27, 28] where as the classical viscoelastic relaxation is given by a linear plot of log force as a function of time, we find here a linear plot of the decay of force as a function of logarithm time. The same was also found to be the case in a study of the thermodynamic interpretations of the elastic properties of rubbers obtained from Ethylene-Propylene copolymers [49]. Why the relaxation should obey this law is not clear; a further study would be of great interest. It is well established however, that in order to ensure reversibility of the stress temperature runs, the force at a given elongation and temperature must remain constant to within the tolerances of our experimental technique. Few authors specify the cut off point where the relaxation becomes too large so that we endeavoured to set a point arbitrarily. Thus we took a total decrease in force over the entire period of testing, of less than 1% (at the highest level of temperature and elongation) as applicable. A preliminary run of force temperature, carried out after such a relaxation, showed that sucessive runs were undistinguishable. However since the second term of the Mooney-Rivlin equation ($2C_2$) is felt by some authors to arise from the lack of attaining equilibrium, by this criterion however small the relaxation, this procedure could not be used to ascertain the existence of C_2 at true equilibrium. Before a decision is possible, one would have to wait for a molecular understanding of the relaxation phenomenon to give us better insight into the true meaning of the $2C_2$ term, if such a term exists in a true equilibrium state.

In Appendix I it has been shown how very sensitive the function $\sigma/\lambda - \lambda^{-2}$ is when applied to the Mooney-Rivlin plot. Van der Hoff [22] indeed corroborates our findings doing the error analysis of our and his data, by showing the effect of a very small change in rest length upon any fitting to the Mooney-Rivlin plot (Fig. 24). It can be clearly seen that if L_o is not known with great accuracy, the approach of the Mooney-Rivlin plot to $\lambda \to 1$, is meaningless. Van der Hoff

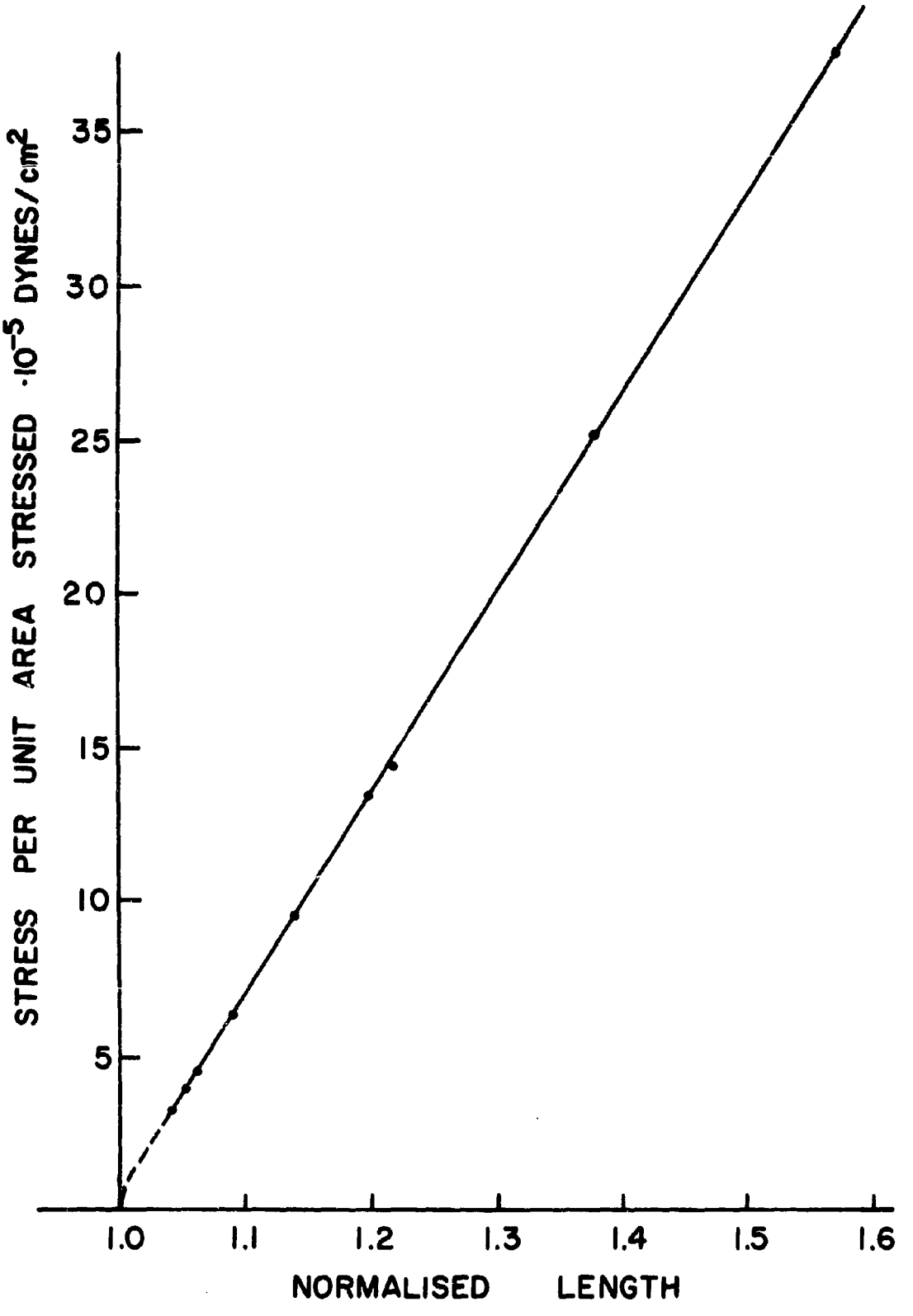

Fig. 25 Stress-Strain Curve - Incompressible - Shen

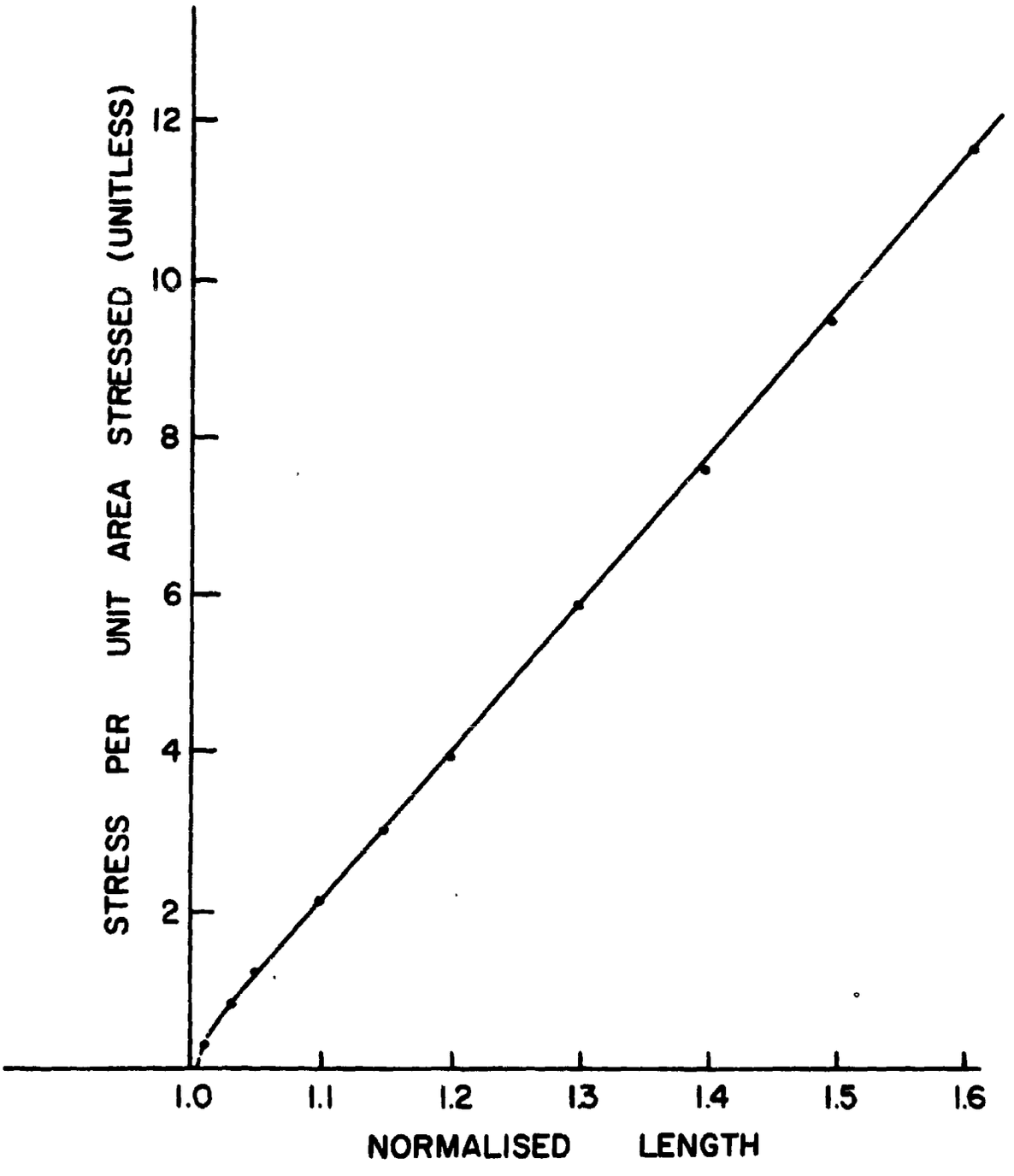

Fig. 26 Stress-Strain Curve - Incompressible - Guth

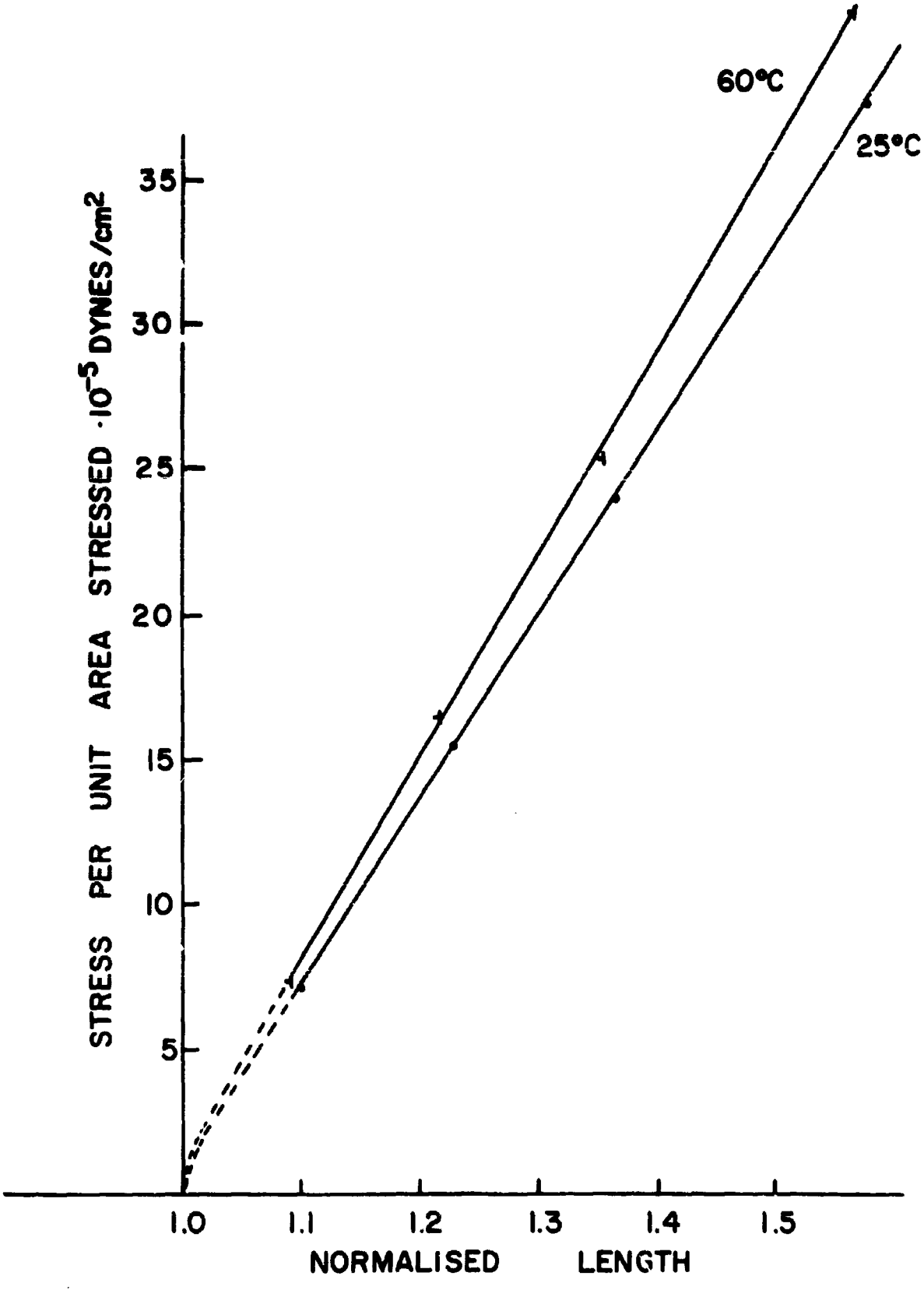

Fig. 27 Stress-Strain Curve - Incompressible - DA1-22

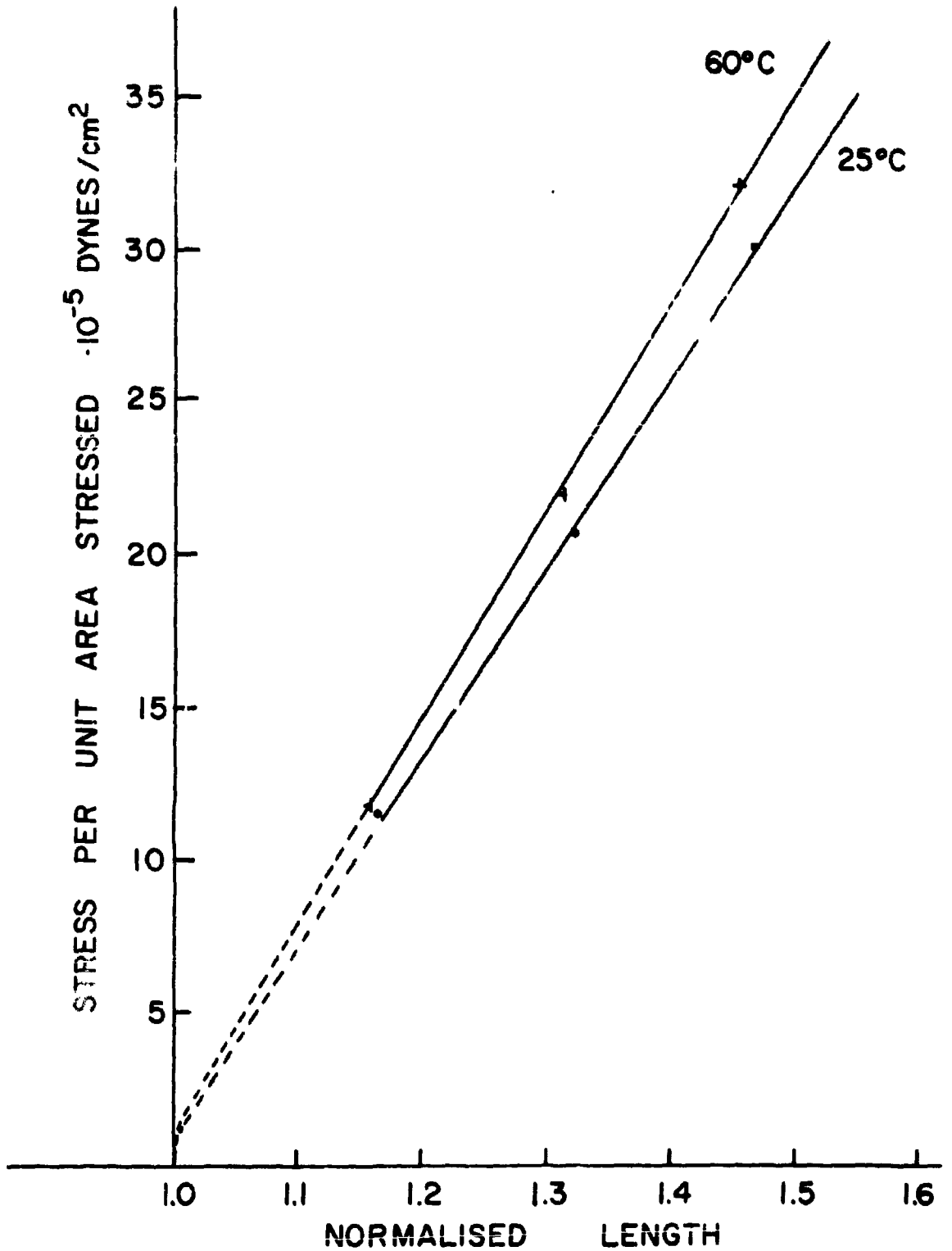

Fig. 28 Stress - Strain Curve - Incompressible - DA1-23

asserts that extremely careful measurements of stress versus strain, and a least squares linear extrapolation to find the rest length, allows one to measure a value of $2C_2 = 0$ when λ is close to unity. We had found a substantial, increasing,departure from linearity close to the rest elongation for both of our samples. This departure was taken to mean that the rest lengths were not accurately known. Consequently in the sensitive range of the Mooney-Riviin plot, the data were effectively discarded by the use of a weighting function as described in Appendix I.

Similarily a careful analysis of the data published or available shows us that Van der Hoff could be quite mistaken. His paper on the extrapolation of his function of true stress versus strain, is based on the "best" least squares linear fit of measured stress at low strains. But several points deserve careful scrutiny of all the known stress versus strain data published for low values of strain (See Figs. 25, 26, 27 and 28). In particular we note several things from these figures.

1. That over a large range of λ(from $\lambda = 1.05$ to $\lambda = 1.60$), the true stress strain curve indicates a neo-Hookeian type behavior, i. e. the stress strain curve is linear. We have fitted these data to a straight line over a range of $\lambda = 1.05$ to $\lambda = 1.80$. The low variances and the variances of the coefficients indicate a good least squares fit.

2. Often it is more important to indicate what a curve does not do, rather than what it does. In all four cases (data collected from Guth, Shen and two in this study) the true stress strain curve does not extrapolate through the origin. Even more interestingly the plots indicate that in all four cases, there would be finite stress at zero strain. Guth's data (Fig. 26) actually shows that at very low strains (1.01) there is actual curvature of the true stress. This curvature is drawn in dotted lines on the other figures, as a trend rather than specific points. It is hardly reasonable to suppose that all three authors estimated their original length with the same sign of error. Rather if there were errors in the determinations of the rest lengths, these errors would be sometimes positive and sometimes negative. This is not the case. All samples even though they are different, show finite intercepts on the stress axis at infinitesimal strains. In

this context it should be noted that in 3 of the analyses, namely that of Guth and our two, the stress strain curves were derived from force temperature data, while Shen's were measured directly. It would be interesting to be able to plot the points obtained by Van der Hoff, before he extrapolates them to $\lambda = 1$.

3. Coming back to Van der Hoff's measurements, he postulates normal stress-strain behavior, fits his experimental points to the various functions, and chooses the function which shows the least fit variance as the best function which he will extrapolate to rest length. This seems to be a dangerous argument since, if the stress-strain behavior is different at very low strains from that at low to moderate strains, it could be incorrect to extrapolate the rest length following the function describing the points at moderate strains. Guth's data (Fig. 26) indeed seem to show that the point corresponding to $\lambda = 1.01$ are not on the linear curve described by the stress - strain relationship at higher strains.

The reason for insisting on this seemingly minor point is that, as was described in our Appendix and in Van der Hoff's paper, the value of the rest length is essential for deriving the behavior of the Mooney-Rivlin plot, and as will be seen later, also the fraction f_e/f (internal energy contribution to the retractive force), at low values of strain; it is there that one would expect the Gaussian approximation to be fulfilled.

4. A last point to be brought up in this connection is the fact that the departure from neo-Hookean behavior is remarkably similar for all four samples. Taking, as the measure for this departure, the value of the intercept of the true stress at $\lambda = 1$ from the least squares line, and $\sigma_{1.00}$ divided by the true stress at some arbitrary value of λ within the linear stress-strain limit of all 4 samples ($\lambda = 1.5$) as a normalizing factor, we obtain

Guth:	$\sigma_{\lambda=1.00}$	= 1.00	/	$\sigma_{\lambda=1.50}$	= 1.50	= 0.0281
Shen:	$\sigma_{\lambda=1.00}$	= 1.00	/	$\sigma_{\lambda=1.50}$	= 1.50	= 0.0152
this study:						
DA1-22	$\sigma_{\lambda=1.00}$	= 1.00	/	$\sigma_{\lambda=1.50}$	= 1.50	= 0.0191
DA1-23	$\sigma_{\lambda=1.00}$	= 1.00	/	$\sigma_{\lambda=1.50}$	= 1.50	= 0.0120

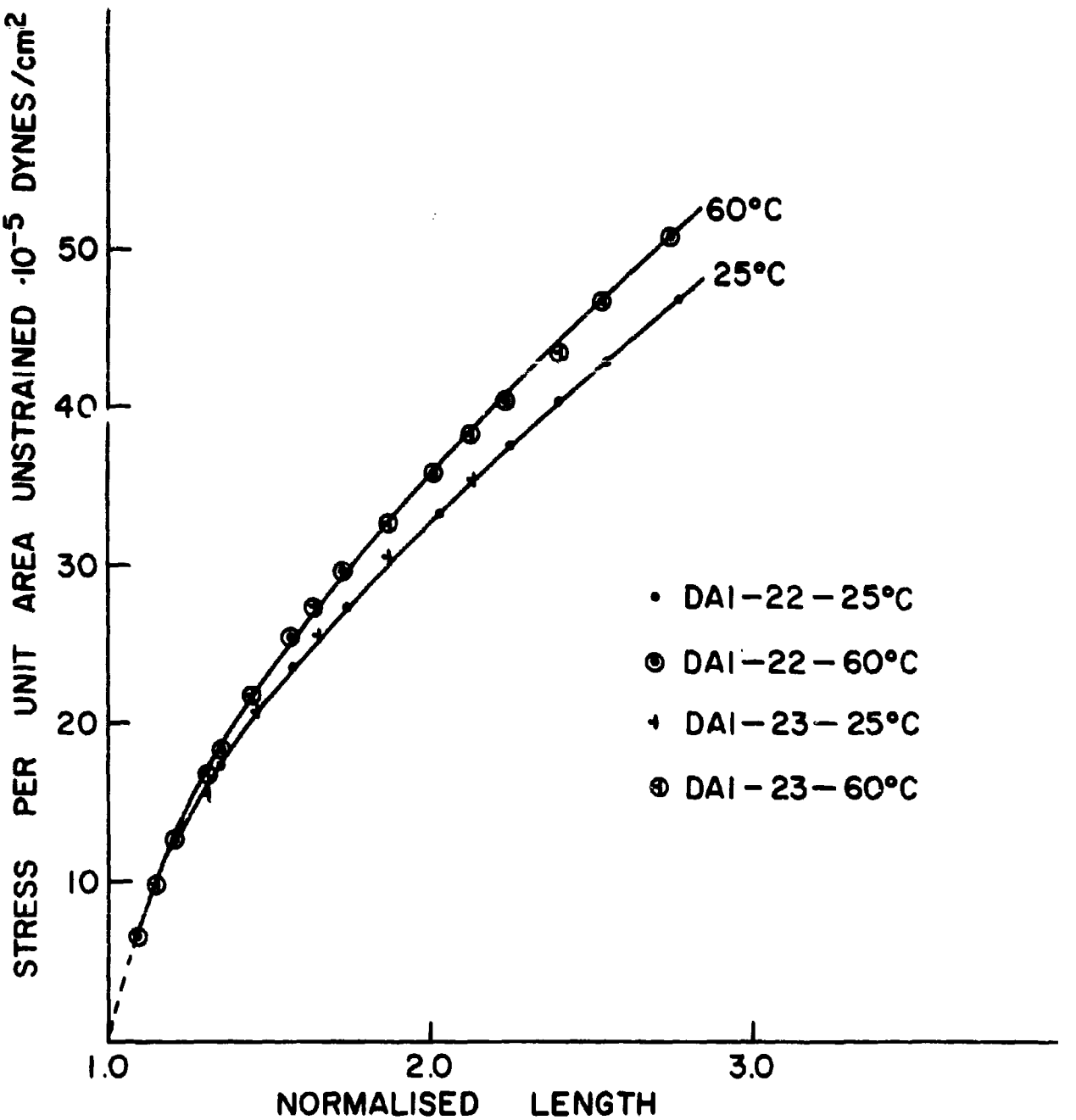

Fig. 29 Stress-Strain Curve -Engineering - DAI-22 , DAI-23

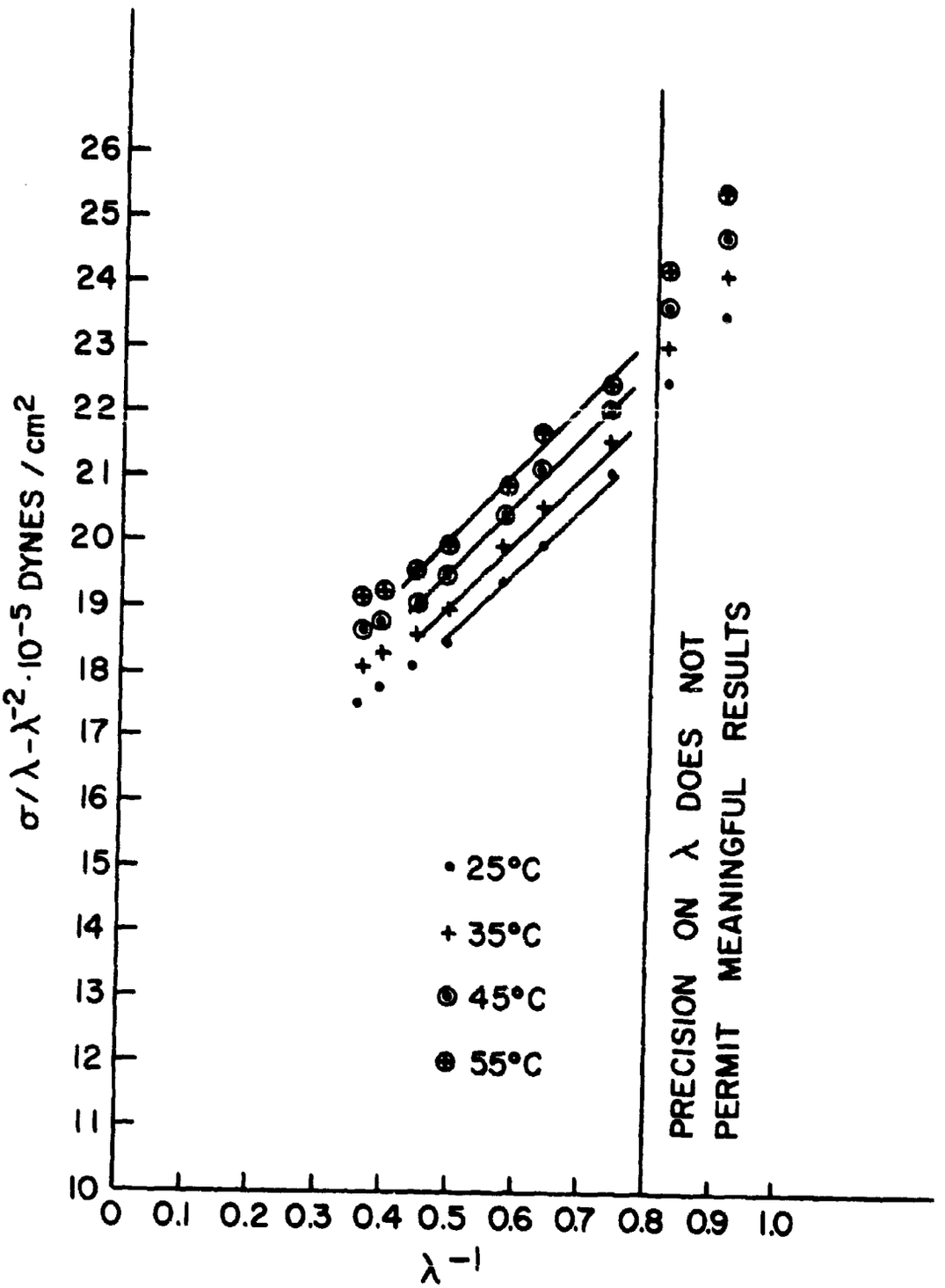

Fig. 30 - Mooney-Rivlin Plot for DA1-22

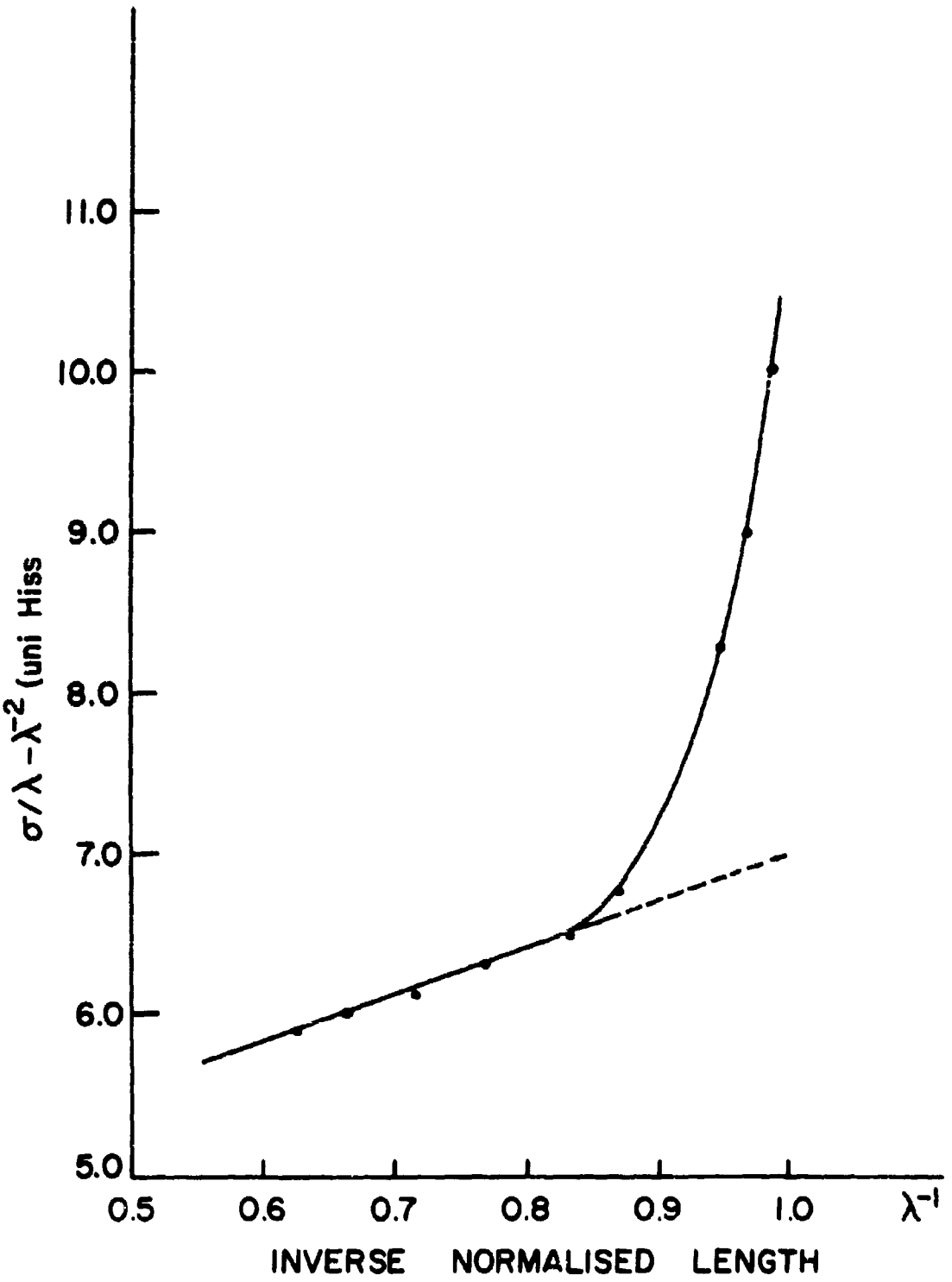

Fig. 31 Mooney-Rivlin Plot of Guth's Data

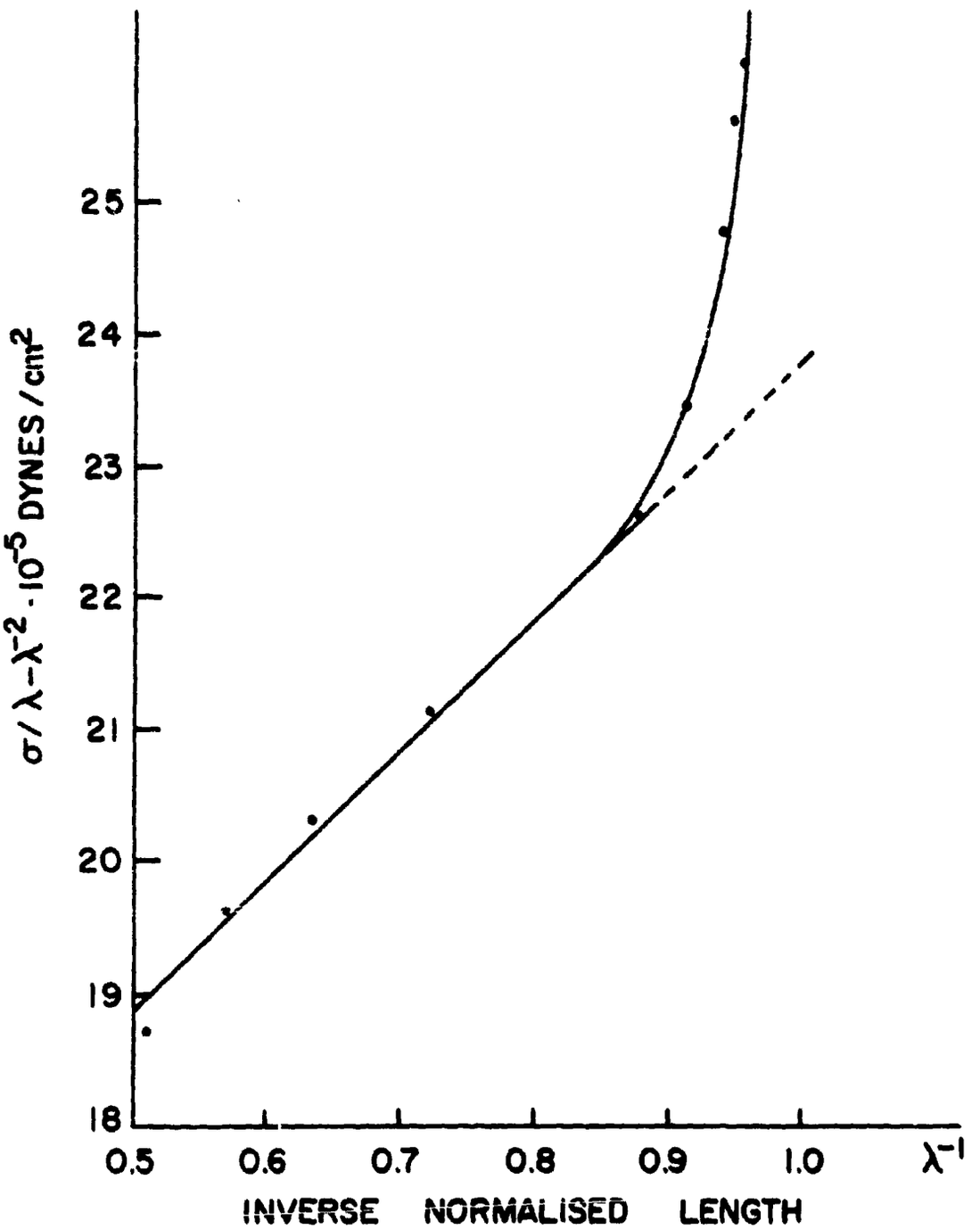

Fig. 32 Mooney-Rivlin Plot of Shen's Data

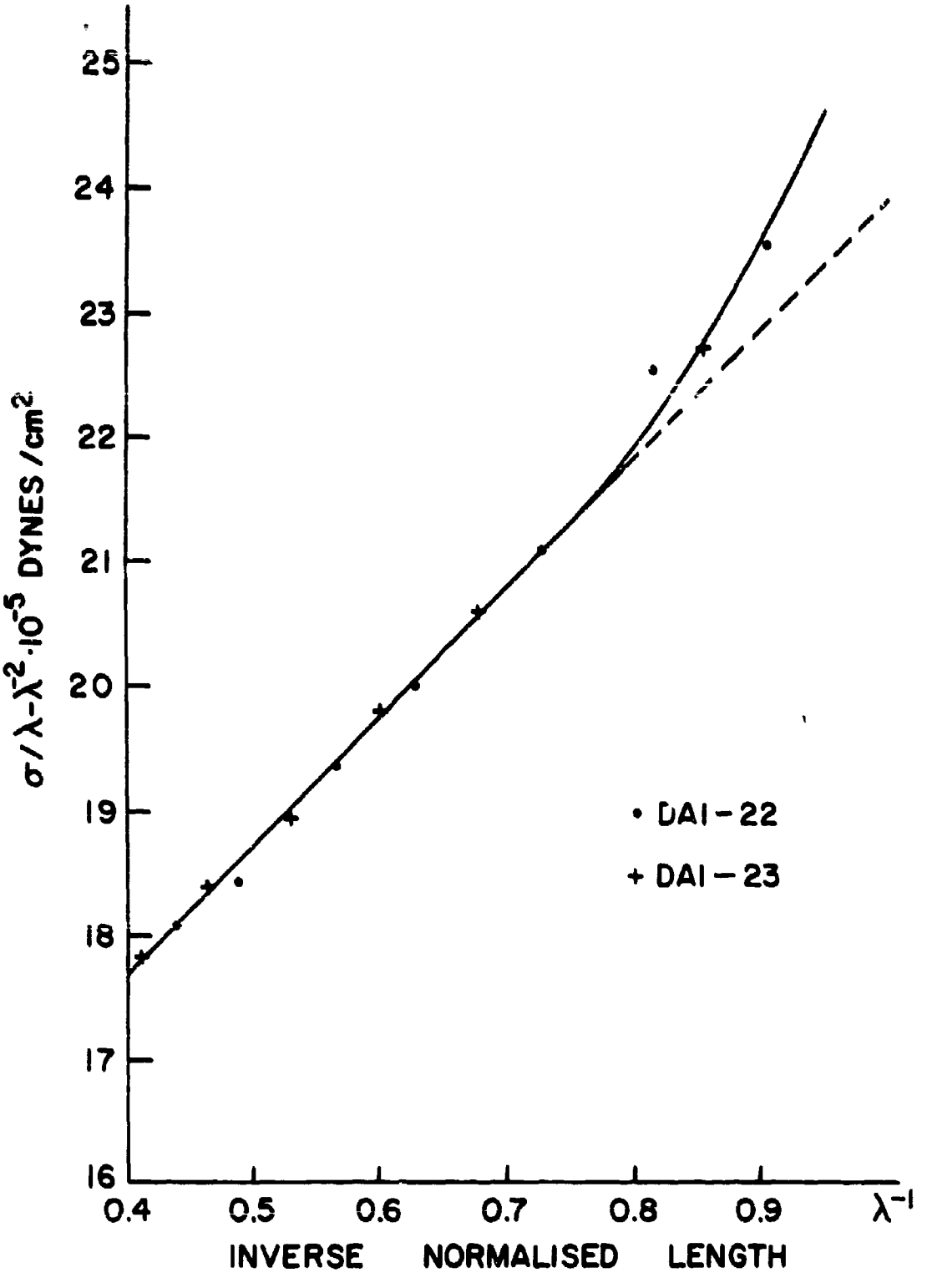

Fig. 33 Mooney-Rivlin Plot of DA1-22, DA1-23

Since the rubbers are different in the three authors' cases, it is not to be expected that the values of $\sigma_{1.00} / \sigma_{1.50}$ should be equivalent, yet they are at least of the same order of magnitude. Such is also the case for the values of negative intercepts on the strain axis, extrapolated along the least square line:

Guth:	$\lambda_{\sigma = 0}$	=	0.986
Shen:	$\lambda_{\sigma = 0}$	=	0.992
this study:			
DA1-22	$\lambda_{\sigma = 0}$	=	0.990
DA1-23	$\lambda_{\sigma = 0}$	=	0.994

Figure 29 shows the engineering stress as a function of strains for both our samples at two different temperatures. Using the computer programs as described previously in Appendix I ,it is possible to calculate the stress-strain behavior and any of the derived plots for as many temperatures as desired. Figure 30 shows the Mooney-Rivlin plot for sample DA1-22 and for various temperatures. A detailed discussion of the constants $2C_1$ and $2C_2$ will be undertaken in a later paragraph.

Comparing now the Mooney-Rivlin plots of the data taken from Guth (Fig. 31), Shen (Fig. 32) and this work (Fig. 33), we see that in all four cases, the Mooney-Rivlin plot shows an upward departure from linearity as the sample approaches its rest length. Even though many precise determinations of the stress-strain curve at very low elongations would be necessary, we do not necessarily believe Van der Hoff's assertion that at low elongations the value of $2C_2$ vanishes. However we recognize our own data taken around $\lambda = 1$, is not sufficiently precise to enable us to positively reject this aspect of Van der Hoff's work. Returning to the Mooney-Rivlin plots of our data (Fig. 30, 33) (samples DA1-22, DA1-23) the weighting function as described in the Appendix I is applied to the weighted least squares linear fit for the purpose of measuring $2C_1$ and $2C_2$. The linear portions of the Mooney-Rivlin plots are roughly parallel as can be

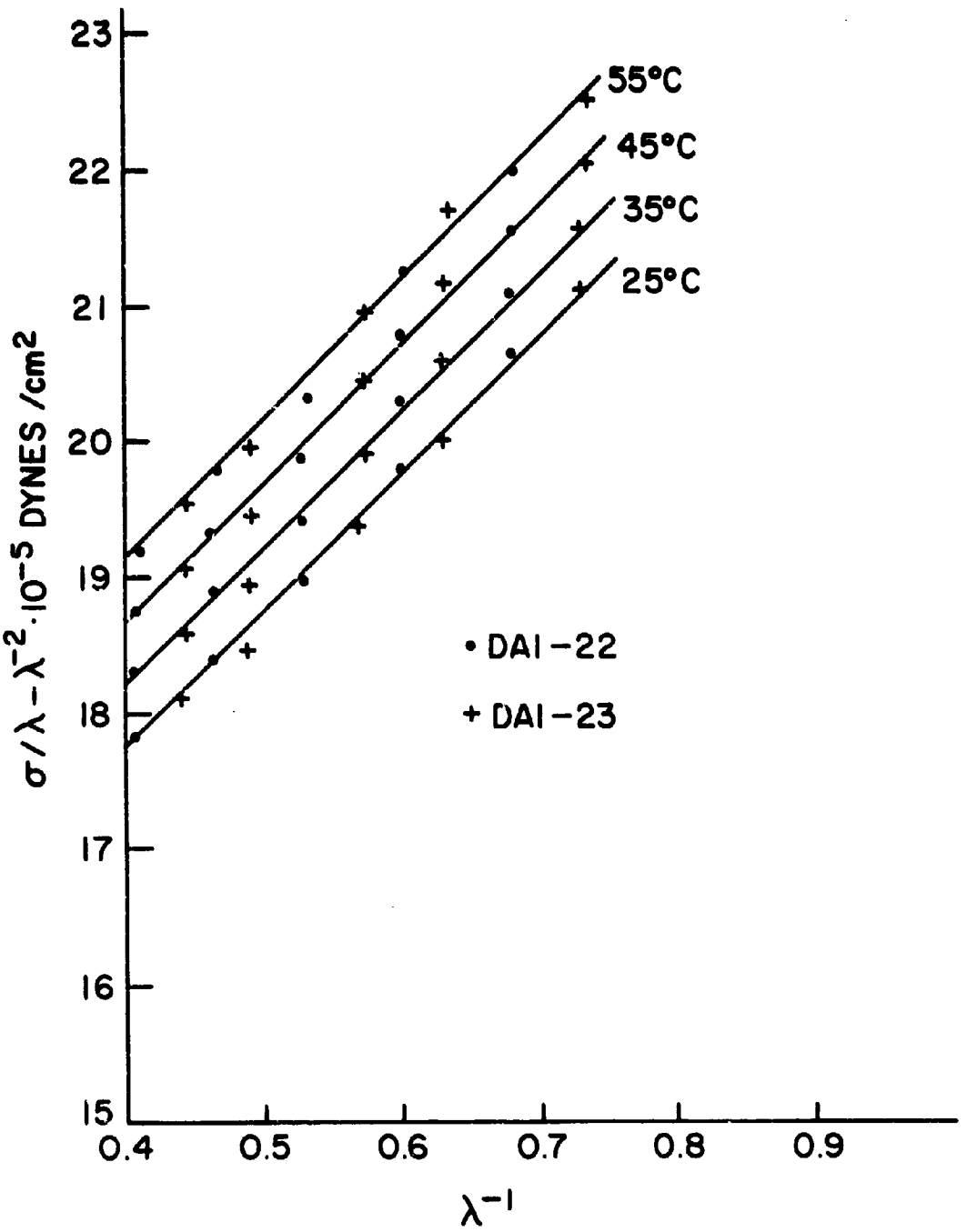

Fig. 34 Mooney-Rivlin Plot for DA1-22 and DA1-23 at various temperatures

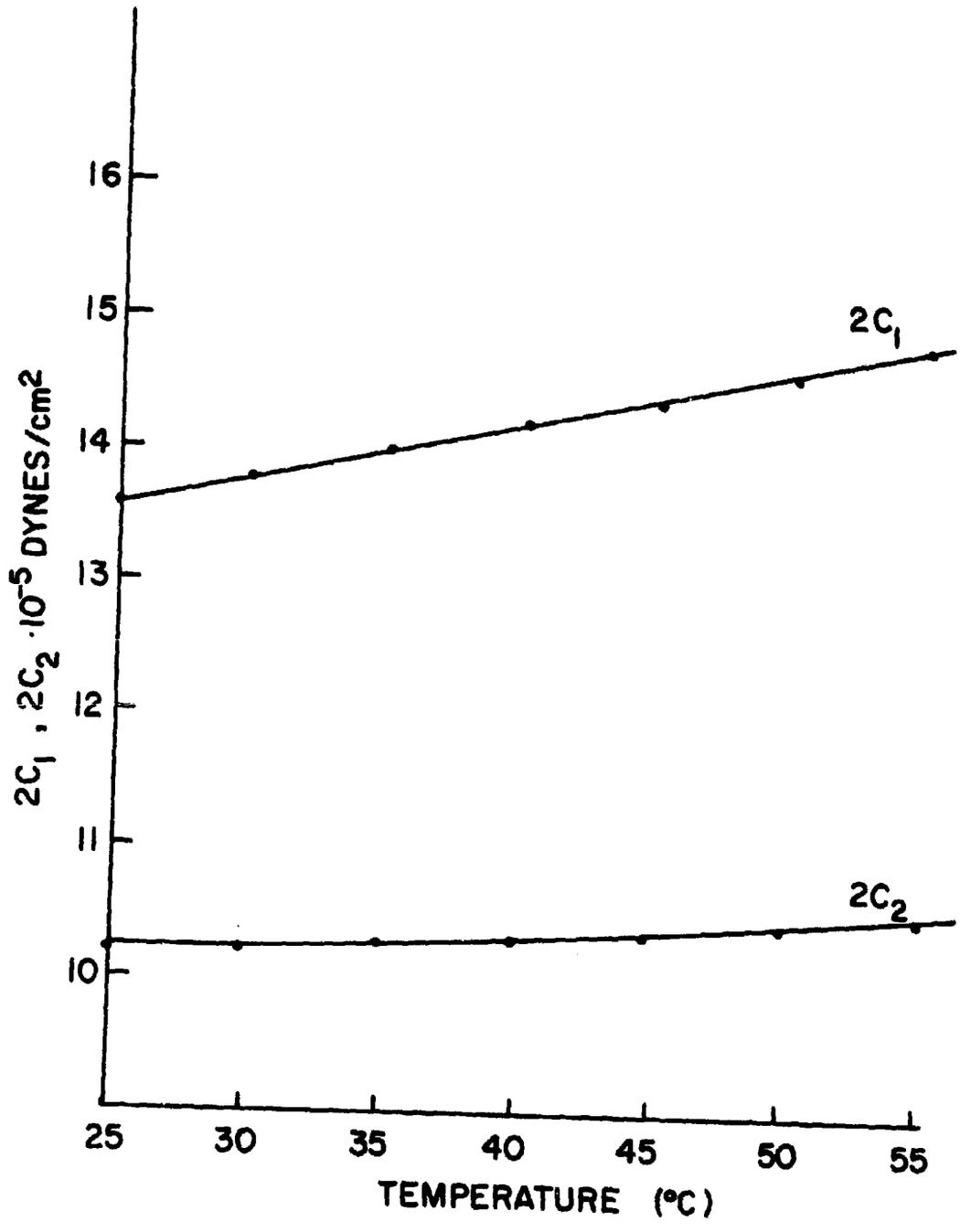

Fig. 35 Temperature dependence of $2C_1$ and $2C_2$ for combined samples DA1-22, DA1-23

seen from Fig. 34. The points for both DA1-22 and DA1-23 are statistically equivalent and are given for various temperatures. At 25°C, the values of $2C_1$ and $2C_2$ are respectively, $13.57 \cdot 10^5$ dynes/cm^2 (1.38 kg/cm^2) and $10.24 \cdot 10^5$ dynes/cm^2 (1.05 kg/cm^2). The value of $2C_2$ is often less than that of $2C_1$ as was mentioned in the Introduction. In our case, however there was a finite non zero value of $2C_2$ calculated for intermediate values of strain.

The temperature dependence of these coefficients is given below and graphed in Figure 35.

Temp °C	$2C_1$ · 10^{-5} dynes/cm^2	$2C_2$ 10^{-5} dynes/cm^2
25	13.57	10.24
30	13.77	10.27
35	14.00	10.32
40	14.21	10.36
45	14.42	10.41
50	14.63	10.46
55	14.83	10.51
60	15.04	10.57

TABLE III : Temperature dependence of $2C_1$ and $2C_2$

$2C_1$ is a linear function of absolute temperature. Comparing this table with the data obtained by Roe and Krigbaum [8] and T. L. Smith [28], we see that $2C_1$ is appreciably temperature dependent, but that $2C_2$ is practically temperature independent. For a better view, the values of $2C_1$ and $2C_2$ of Table III, normalized to 30° C are compared to the corresponding values of $2C_1$ and $2C_2$ at 30° C of Roe and Krigbaum, and are listed in the next table.

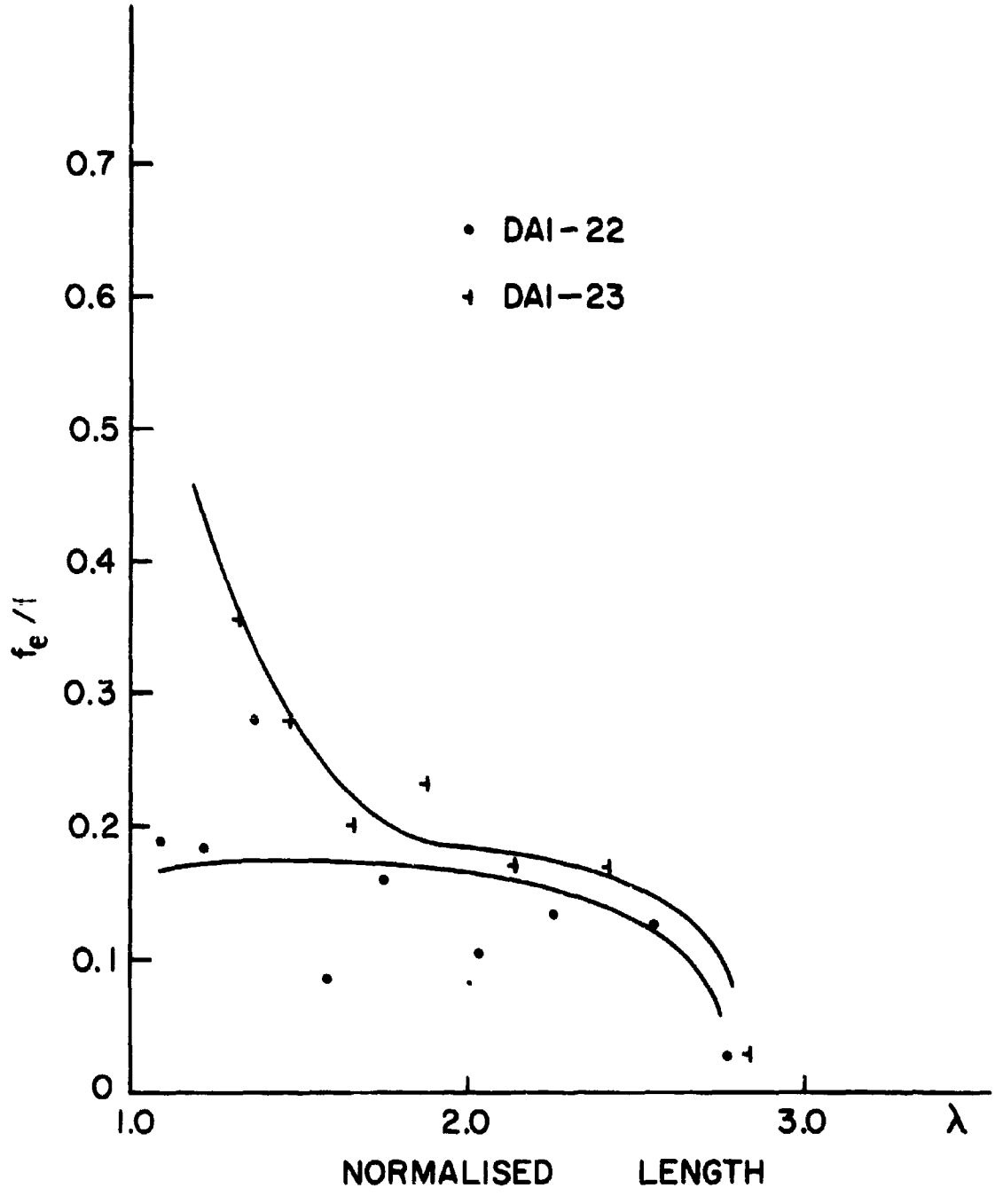

Fig. 36 Internal Energy Contribution to Retractive Force, DA1-22, DA1-23

T°C	This work $2C_1/2C_1$ at 30°C	Roe and Krigbaum $2C_1/2C_1$ at 30°C	This work $2C_2/2C_2$ at 30°C	Roe Krigbaum $2C_2/2C_2$ at 30°C
30	1.000	1.000	1.000	1.000
40	1.035	1.032	1.010	1.009
50	1.065	1.062	1.019	1.028
60	1.094	1.093	1.028	1.042

TABLE IV : Comparaison of C_1 and C_2 with literature values

Thus the temperature dependence of $2C_1$ is the same as that of Roe and Krigbaum. The temperature dependence of $2C_2$, still small, seems to be lar ,er in their case. Ours resembles more closely the behavior of T. L. Smith's data [28].

One of the very important questions in the theory of rubber elasticity is the question of the contribution of the internal energy to the total elastic retractive force. Up to recently it was thought that most of the retractive force at moderate elongations came from the decrease in entropy due to the redistribution of $\overline{r^2}$ towards higher values, and possibly to some chain alignment. However lately, it has been shown that in the case of natural rubber, something like 20% of the force is due to the internal energy even at small strains. By application of Equation (31) it is possible to calculate f_e/f knowing $(\partial f/\partial T)_{p,L}$ and f vs. λ at different values of the temperature. Figure 36 shows the values of f_e/f for both our samples. There is so much scatter in the data due to the uncertainty in $(\partial f/\partial T)_{p,L}$, that little can be said about the value of f_e/f for low strains except that there does seem to be an energetic contribution to the total retractive force at low strains , which shows a decrease at higher strains, in accordance with the literature.

The only available figures on the dependency of f_e/f on λ at low values of strain come from a paper to be published by Shen, McQuarrie and Jackson [50].

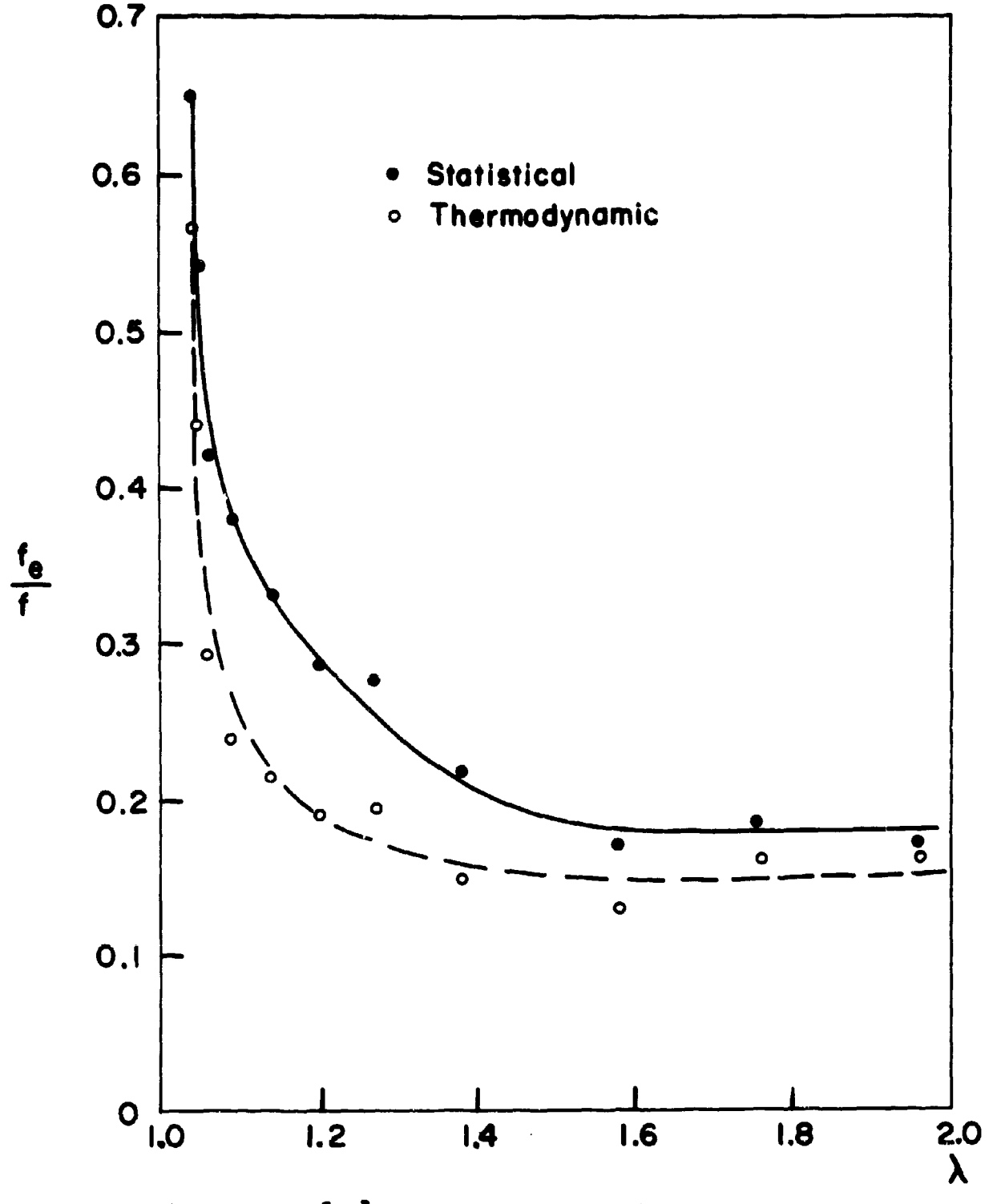

Fig. 37, Ref [50] : Dependence of f_e/f upon elongation at low elongations, from Shen, McQuarrie and Jackson

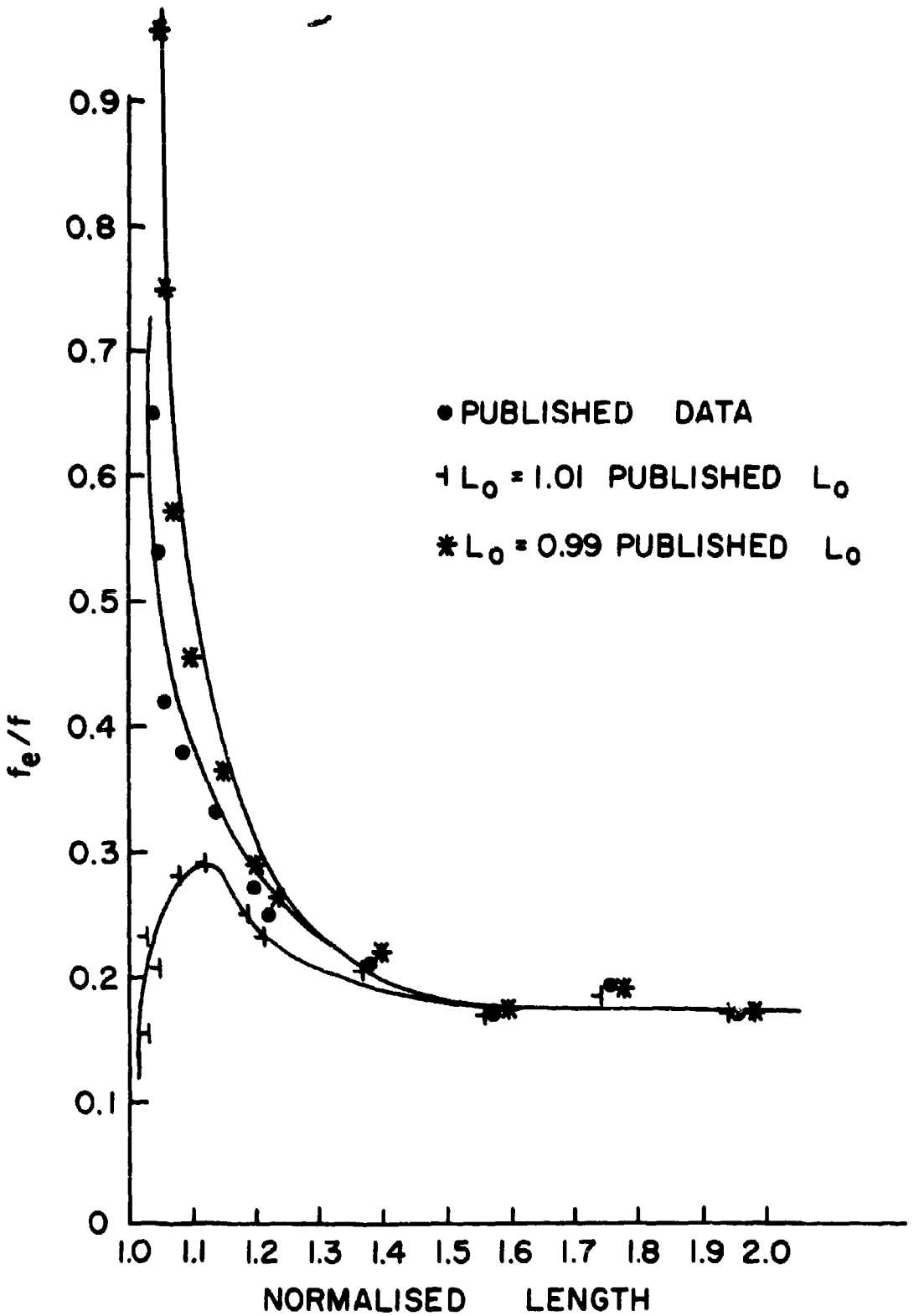

Fig. 38 Internal Energy Contribution from Shen's Data

Figure 37 shows their values. While, for higher strains, all the values in recent publications, seem to agree, Shen and co-workers at their low strains show a very strong dependance of f_e/f on λ. A glance at Equation (31) shows us that here again we have a particularly sensitive function of λ, since $\lambda^3 - 1$ goes to 0 as $\lambda \to 1$.

In the following, we give an analysis of the data presented in tabular form by Shen and co-workers. Just as Van der Hoff showed the effect of a small change of L_o (the rest length) on the Mooney-Rivlin plot, we can show now the effect of a small change of L_o on the f_e/f plot. Knowing a given change in L_o for example, $\pm$ 0.01 L_o, we can recalculate their values of f_e/f, and plot them as in Figure 38. This figure shows very emphatically, as did the earlier one corresponding to the Mooney-Rivlin plot, the effect of very small (1%) changes in rest length on the plot of f_e/f. Thus once more we would have to know the rest length with extreme accuracy to learn the true energetic contribution at very low strains.

We can, now summarize this topic of f_e/f by saying that, at low to moderate strains, ($\lambda \to 1.2$ to 2.5) the contribution to the total retractive force of the internal energy is of the order of 15 to 20%. At higher elongations, ($\lambda > 2.5$) there is a loss of internal energy (f_e/f becomes negative) due to alignment of the chains that are about to crystallize. At very low elongations ($\lambda < 1.2$) the picture is not at all clear. While, the Gaussian approximation should be best observed experimentally, according to the data of Shen and co-workers the internal energy contribution rises sharply while $\lambda \to 1$.

Taking the data of Shen for a Mooney-Rivlin plot, ($2C_1 + 2C_2$) shows an upturn at low strain which Van der Hoff asserts does not exist if the initial length is very carefully determined. However one must doubt Van der Hoff's assertion of Hookean behavior (straight line extending from the origin into the moderate strain region) as discussed above. It remains then to find a better explanation of the stress pattern at very low strains, especially the positive intercept on the stress axis. Combining the evidence of Shen's finding of high internal energy contributions at low strains with the downward curvature towards the origin of the stress-strain plot we can postulate the existence of a type of superstructure

in the rubber that imposes some long range order at the very lowest strain, this superstructure holds; it must be broken up for the rubber to assume true through going random behavior at larger strains. This is the same as saying that, at very low strains energy must be supplied to distort the superstructure. Once the latter has been broken down, then the entropic, or cooperative rotational, changes of conformation take over. More data at these low strains would help clarify and corroborate the picture.

A final paragraph may be devoted to the problem of equilibrium versus non-equilibrium results. Ever since Ciferri and Flory [25] showed the magnitude of C_2 was influenced by the time scale of the measurements, much debate has been going on as to the nature of C_2. Unfortunately, since the relaxation of force is linear with log t, no true equilibrium values have been reported and therefore the interpretation of C_2 as an equilibrium phenomenon has to be postponed. In view of this, one must also doubt that Van der Hoff's measurements were at true equilibrium. Thus the whole question of C_2 is still very much unresolved.

IV. APPENDIX I

General outline of programs:

A. P. 31. This program indexes and computes the raw data as it is read off the xy recorder, as force and temperature. There follows a listing of the program written in FORTRAN IV, as well as an example of the listed output. In general each program will have two types of output, one punched that serves as part of the input to the next program and the other written as a permanent record of the calculations.

```
$IBFTC P31
      DIMENSION LENGN(20),XZERCM(20),YZERCM(20),RANGE(20),YRANGE(20)
      DIMENSION XDWTCM(20),AREA25(20)
      DIMENSION XCM(20,20),YCM(20,20),XEMFM(20,20),YEMFM(20,20)
      DIMENSION FORCEX(20,20),THPTCY(20,20),FORCED(20,20),THPTK(20,20)
      REAL LENGN
      READ(5,102)
      WRITE(6,102)
      READ(5,100)CLOCEL,VLOCEL,A1THPT,A2THPT
      READ(5,101)II
      DO 10 I=1,II
      READ(5,106)
      WRITE(6,106)
      WRITE(7,106)
      READ(5,103)JJ,LENGN(I),AREA25(I),XZERCM(I),ZZERCM(I),XRANGE(I),YRA
     1NGE(I),XDWTCM(I)
      WRITE(6,152)LENGN(I),AREA25(I)
      WRITE(7,153)LENGN(I),AREA25(I)
      WRITE(6,154)
      DO 11 J=1,JJ
      READ(5,105)XCM(I,J),YCM(I,J)
      XEMFM(I,J)=(XCM(I,J)-XZERCM(I)-XDWTCM(I))*XRANGE(I)
      YEMFM(I,J)=(YCM(I,J)-YZERCM(I))*YRANGE(I)
      FORCEX(I,J)=CLOCEL*XEMFM(I,J)/VLOCEL
      THPTCY(I,J)=(-A1THPT+(A1THPT**2+4.*YCM(I,J)*A2THPT)**0.5)/(2.*A
     1 2THPT)
      FORCED(I,J)=FORCEX(I,J)*0.9836665E+0
      THPTK(I,J)=THPTCY(I,J)+0.2731
      WRITE(7,151)THPTK(I,J),FORCED(I,J)
      WRITE(6,151)J,THPTCY(I,J),FORCED(I,J)
   11 CONTINUE
   10 CONTINUE
  100 FORMAT(1X,4(E12.5,2X))
  101 FORMAT(1X,I2)
  102 FORMAT(1H1,80H
     1                                                              )
  106 FORMAT(1H1,80H
     1                                                              )
  103 FORMAT(1X,I2,1X,2(E12.5,1X),4(F9.2,1X),E12.3)
  105 FORMAT(2(E12.5,2X))
  150 FORMAT(1X,2(E12.5,2X))
  151 FORMAT(1X,I2,2X,2(E12.5,2X))
  152 FORMAT(9HLENGN = ,E12.5,14H AREA25 = ,E12.5)
  153 FORMAT(1X,21H  =  ,E12.5,6X,E12.5,2X)
  154 FORMAT(33H  J    THPTCY(I,J)    FORCED(I,J)  )
      CALL EXIT
      END
```

P31-BK 2,F 36-DAI-22-LENGTH=21.9CM,NORMALISED LENGTH=2.777-RUN 1

LENGTH = 2.277[illegible]E 01 AREA25 = 0.767[illegible]E-01

J	IMPICY(I,J)	FORCE(I,J)
1	0.30[illegible]44E 02	[illegible].357835 06
2	0.312578 02	[illegible].359596 06
3	[illegible].324684E 02	[illegible].361345 06
4	0.336756 02	[illegible].3631[illegible]E 06
5	[illegible].348807E 02	[illegible].36397E 06
6	[illegible].360[illegible]82E 02	[illegible].366[illegible]E 06
7	0.372816 02	[illegible].367485 06
8	0.384[illegible]AE 02	[illegible].369235 06
9	[illegible].396716 02	[illegible].37[illegible]11E 06
10	[illegible].408626 02	[illegible].371516 06
11	0.420[illegible]E 02	[illegible].372746 06
12	[illegible].432[illegible]E 02	[illegible].373626 06
13	[illegible].444196 02	[illegible].375376 06
14	0.455[illegible]E 02	[illegible].376256 06
15	[illegible].467766 02	[illegible].377136 06
16	[illegible].479516 02	[illegible].378536 06

B. P 391. This program normalizes the data, calculates the normalized lengths, calculates the various types of stresses and fits the data by linear least squares analysis. The input to this program is but a slight modification of the punched output from P 31.

The various types of stresses used we defined as follows:

$$\sigma \text{ (engineering)} = F/\text{Area of unstressed sample}$$

$$\sigma \text{(incompressible)} = F/\text{Area of stressed sample}$$

where by incompressible we assume that there is no volume change upon linear extension. If such is the case, then where F is the total force, from its geometry, it is easy to calculate the area at any given stress or strain.

$$\text{AREA } (\lambda) = \text{AREA } (1)/\lambda$$

The program also fits the stress (both engineering and incompressible) as a function of the temperature. Both the written and the punched output list the least squares coefficients, their variances and covariances. A listing of the subroutines is given in this section. There is a plot option, which allows the checking of any mispunched data very quickly. The output from P 391 is the linear least squares fit of the force-temperature data. Up to this point no thermal expansion corrections have been taken into consideration.

```
$IBFTC P99102
C   INDEXING AND NORMALISING OF DATA- FORCE VERSUS TEMPERATURE- CALCULATION OF
C   NORMALISED LENGTH-
C   DIMENSION STATEMENTS
      DIMENSION ALENG(20),JNI(20),NLENG(20),AREAL(  ),TMPTK1(20),STRES1(
     1 20),STRIS1(20),A(20),A(20),B(20),AEFT0(20),VA_FT0(20),AEFT1(20),VA
     2 EFT1(20),AIFT0(20),VAIFT0(20),AIFT1(20),VAIFT1(20),COVE21(20),COVI
     3 21(20)
      DIMENSION TMPTK(20,20),FORCED(20,20),TMPTC(20,20),STRES2(20,20),ST
     1 RIS2(20,20),COV(2),20)
C   TYPE STATEMENTS
      REAL NLENG
      READ(5,100)
  100 FORMAT(80H
     1                                                                )
      WRITE(6,100)
      READ(5,101)
  101 FORMAT(80H
     1                                                                )
      WRITE(6,101)
      READ(5,102)IN,AMULTP,RLENG,AREA25,INCSTR
      WRITE(6,106)RLENG
  106 FORMAT(9HORLENG = ,E12.5)
  102 FORMAT(1X,I2,2X,3(E12.5,2X),I2,2X)
      DO 15 I=1,IN
      READ(5,103)
  103 FORMAT(80H
     1                                                                )
      READ(5,104)ALENG(I),JNI(I)
  104 FORMAT(1X,E12.5,2X,I2)
      WRITE(6,105)
      NLENG(I)=ALENG(I)/RLENG
      WRITE(6,150)NLENG(I)
  150 FORMAT(21H NORMALISED LENGTH = ,F12.5)
      WRITE(6,151)
  151 FORMAT(43H TEMPERATURE   ENG.STRESS       INC.STRESS )
      WRITE(6,152)
  152 FORMAT(43H DEGREES       DYNES PER SQC. DYNES PER SQC.)
      JM=JNI(I)
      DO 11 J=1,JM
      READ(5,1.5)TMPTK(I,J),FORCED(I,J)
  1 5 FORMAT(1X,2(E12.5,2X))
      STRES2(I,J)=FORCED(I,J)*AMULTP/AREA25
      TMPTC(I,J)=TMPTK(I,J)-.27315E+03
      AREAL(I)=AREA25/NLENG(I)
      STRIS2(I,J)=FORCED(I,J)*AMULTP/AREAL(I)
      WRITE(6,153)TMPTC(I,J),STRES2(I,J),STRI 2(I,J)
  153 FORMAT(1X,3(E12.5,2X))
   11 CONTINUE
   10 CONTINUE
      READ(5,2  )
  2   FORMAT(8
     1
      WRITE(6,2  )
      READ(5,201)
  201 FORMAT(8CH
     1
      READ(5,2 2)
```

```
202   FORMAT(80H
      :
      READ(5,203)TKMIN,TKMAX
203   FORMAT(1X,2(E12.5,2X))
      DO 2" I=1,IN
      WRITE(7,154)NLENG(I),JNI(I)
154   FORMAT(1X,E12.5,2X,I2,2X)
      JN=JNI(I)
      DO 21 J=1,JN
      TKPTK1(J)=TKPTK(I,J)
      STRES1(J)=STRES2(I,J)
      STRIS1(J)=STRIS2(I,J)
      W(J)=1.
21    CONTINUE
      WRITE(6,2"1)
      WRITE(6,15.)NLENG(I)
      CALL BIMEA(JN,2,TKPTK1,STRES1,,A,B,COV,C,3)
      CALL PLOTPR(JN,TKPTK1,STRES1,A,2,TKMIN,TKMAX)
      AEFT(I)=A(1)
      VAEFT(I)=B(1)
      AEFT1(I)=A(2)
      VAEFT1(I)=B(2)
      COVF21(I)=COV(2,1)
      WRITE(7,21) AEFT (I),VAEFT (I),AEFT1(I),VAEFT1(I),COVF21(I)
21"   FORMAT(1X,E15.8,4(1X,E15.8))
      IF(INCSTR,NE.1)GO TO 22
      WRITE(6,202)
      WRITE(6,15.)NLENG(I)
      CALL BIMEA(JN,2,TKPTK1,STRIS1,,A,B,COV,C,3)
      CALL PLOTPR(JN,TKPTK1,STRIS1,A,2,TKMIN,TKMAX)
      AIFT(I)=A(1)
      VAIFT(I)=B(1)
      AIFT1(I)=A(2)
      VAIFT1(I)=B(2)
      COVI21(I)=COV(2,1)
      WRITE(7,21.)AIFT (I),VAIFT(I),AIFT1(I),VAIFT1(I),COVI21(I)
22    CONTINUE
23    CONTINUE
      CALL EXIT
      END
```

P381-LENGTH=21.9CM,RUN 1
NORMALISED LENGTH = 0.27722E 01

TEMPERATURE DEGREES	ENG.STRESS DYNES PER SQCM	INC.STRESS DYNES PER SQCM
[illegible]30040E 02	0.47061E 02	0.13046E 03
[illegible]31260E 02	0.47293E 02	0.13110E 03
[illegible]32470E 02	0.47523E 02	[illegible].13174E 03
0.33680E 02	0.47754E 02	0.13238E 03
[illegible].34890E 02	0.47869E 02	0.13270E 03
0.36080E 02	0.48219E 02	0.13366E 03
0.37290E 02	0.48330E 02	0.13398E 03
0.38490E 02	0.48561E 02	0.13462E 03
[illegible].39670E 02	0.48676E 02	[illegible].13494E 03
0.40860E 02	0.48860E 02	0.13545E 03
[illegible].42050E 02	0.49022E 02	[illegible].13590E 03
0.43240E 02	0.49138E 02	0.13622E 03
0.44420E 02	0.49368E 02	0.13686E 03
0.45600E 02	0.49484E 02	0.13718E 03
0.46780E 02	0.49600E 02	[illegible].13750E 03
[illegible].47950E 02	0.49784E 02	0.13801E 03

P381-LENGTH=20.2CM,RUN 2
NORMALISED LENGTH = 0.25570E 01

TEMPERATURE DEGREES	ENG.STRESS DYNES PER SQCM	INC.STRESS DYNES PER SQCM
[illegible].28030E 02	0.43139E 02	[illegible].11031E 03
0.30040E 02	0.43371E 02	0.11090E 03
[illegible].31240E 02	0.43601E 02	0.11149E 03
[illegible].32470E 02	0.43832E 02	0.11208E 03
[illegible].33680E 02	0.43947E 02	[illegible].11237E 03
[illegible].34880E 02	0.44063E 02	0.11267E 03
0.36080E 02	0.44178E 02	0.11296E 03
[illegible].37280E 02	0.44293E 02	0.11325E 03
[illegible].38480E 02	0.44524E 02	0.11385E 03
0.39670E 02	0.44684E 02	0.11424E 03
0.40860E 02	0.44870E 02	0.11473E 03
0.42050E 02	0.45054E 02	0.11520E 03
[illegible].43240E 02	0.45170E 02	0.11550E 03
0.44420E 02	0.45332E 02	0.11591E 03
0.45600E 02	0.45444E 02	0.11620E 03
0.46780E 02	0.45562E 02	0.11650E 03
[illegible].47950E 02	0.45678E 02	0.11680E 03
0.49120E 02	0.45746E 02	[illegible].11697E 03
0.50290E 02	0.45859E 02	0.11721E 03
[illegible].51460E 02	0.45980E 02	0.11736E 03

P381-LENGTH=17.8CM,RUN 3
NORMALISED LENGTH = 0.22532E 01

TEMPERATURE DEGREES	ENG.STRESS DYNES PER SQCM	INC.STRESS DYNES PER SQCM
[illegible].28030E 02	0.37604E 02	0.84727E 02
0.30040E 02	0.37710E 02	0.84985E 02
0.31260E 02	0.37834E 02	0.85244E 02
0.32470E 02	0.37996E 02	0.85618E 02
0.33680E 02	0.38110E 02	0.85868E 02
0.34880E 02	0.38296E 02	0.86286E 02
0.36080E 02	0.38410E 02	0.86544E 02
0.37280E 02	0.38526E 02	0.86805E 02
0.38480E 02	0.38641E 02	[illegible].87065E 02
0.39670E 02	0.38826E 02	0.87480E 02
0.40860E 02	0.38910E 02	0.87680E 02
0.42050E 02	0.39057E 02	0.88002E 02
0.43240E 02	0.39217E 02	0.88363E 02
0.44420E 02	0.39388E 02	0.88624E 02

0.45600E 02	0.39449E 02	0.88885E 02
0.46780E 02	0.39517E 02	0.89039E 02
0.47950E 02	0.39611E 02	0.89249E 02
0.49120E 02	0.39679E 02	0.89404E 02
0.50290E 02	0.39841E 02	0.89768E 02
0.51460E 02	0.39911E 02	0.89925E 02

P381-LENGTH=16.1CM,RUN 4
NORMALISED LENGTH = 0.20380E 01

TEMPERATURE DEGREES	ENG.STRESS DYNES PER SQCM	INC.STRESS DYNES PER SQCM
.28830E 02	0.33450E 02	0.68171E 02
0.30040E 02	0.33566E 02	0.68407E 02
0.31260E 02	0.33682E 02	0.68643E 02
.32470E 02	0.33796E 02	0.68876E 02
.33680E 02	0.33982E 02	0.69254E 02
.34880E 02	0.34120E 02	0.69535E 02
0.36080E 02	0.34258E 02	0.69817E 02
.37280E 02	0.34374E 02	0.70053E 02
..38480E 02	0.34489E 02	0.70288E 02
0.39670E 02	0.34650E 02	0.70615E 02
0.40860E 02	0.34720E 02	0.70758E 02
.42050E 02	0.34904E 02	0.71133E 02
.43240E 02	0.34996E 02	0.71320E 02
0.44420E 02	0.35111E 02	0.71556E 02
0.45600E 02	0.35181E 02	0.71698E 02
.46780E 02	0.35250E 02	0.71838E 02
.47950E 02	0.35365E 02	0.72074E 02
0.49120E 02	0.35411E 02	0.72167E 02
0.50290E 02	0.35481E 02	0.72309E 02
..51460E 02	0.35527E 02	0.72403E 02

P381-LENGTH=13.8CM,RUN 5
NORMALISED LENGTH = 0.17468E 01

TEMPERATURE DEGREES	ENG.STRESS DYNES PER SQCM	INC.STRESS DYNES PER SQCM
.28830E 02	0.27729E 02	0.48439E 02
.30040E 02	0.27845E 02	0.48641E 02
.31260E 02	0.27983E 02	0.48882E 02
0.32470E 02	0.28145E 02	0.49165E 02
.33680E 02	0.28261E 02	0.49367E 02
.34880E 02	0.28307E 02	0.49447E 02
.36080E 02	0.28421E 02	0.49647E 02
.37280E 02	0.28537E 02	0.49849E 02
.38480E 02	0.28583E 02	0.49930E 02
.39670E 02	0.28675E 02	0.50090E 02
.40860E 02	0.28767E 02	0.50251E 02
.42050E 02	0.28883E 02	0.50453E 02
0.43240E 02	0.28929E 02	0.50534E 02
0.44420E 02	0.28998E 02	0.50656E 02
0.45600E 02	0.29114E 02	0.50858E 02
.46780E 02	0.29160E 02	0.50938E 02
.47950E 02	0.29229E 02	0.51058E 02
.49120E 02	0.29275E 02	0.51138E 02
0.49240E 02	0.29321E 02	0.51218E 02
0.51460E 02	0.29390E 02	0.51340E 02

P381-LENGTH=12.5CM,RUN 6
NORMALISED LENGTH = 0.15823E 01

TEMPERATURE DEGREES	ENG.STRESS DYNES PER SQCM	INC.STRESS DYNES PER SQCM
0.28830E 02	0.23923E 02	0.37853E 02
.30040E 02	0.23969E 02	0.37926E 02
.31260E 02	0.24039E 02	0.38036E 02
..32470E 02	0.24131E 02	.38182E 02
0.33680E 02	0.24245E 02	0.38363E 02

0.34880E 02	0.24339E 02	0.38511E 02
0.36080E 02	0.24410E 02	0.38623E 02
0.37280E 02	0.24523E 02	0.38802E 02
0.38480E 02	0.24615E 02	0.38948E 02
0.39670E 02	0.24685E 02	0.39058E 02
0.40860E 02	0.24799E 02	0.39239E 02
0.42050E 02	0.24869E 02	0.39349E 02
0.43240E 02	0.24961E 02	0.39495E 02
0.44420E 02	0.25007E 02	0.39568E 02
0.45600E 02	0.25053E 02	0.39641E 02
0.46780E 02	0.25123E 02	0.39751E 02
0.47950E 02	0.25192E 02	0.39861E 02
0.49120E 02	0.25261E 02	0.39970E 02
0.50290E 02	0.25284E 02	0.40007E 02
0.51460E 02	0.25353E 02	0.40115E 02

P381-LENGTH=10.8CM,RUN7
NORMALISED LENGTH = 0.13671E 01

TEMPERATURE DEGREES	ENG.STRESS DYNES PER SQCM	INC.STRESS DYNES PER SQCM
0.31260E 02	0.17787E 02	0.24316E 02
0.32470E 02	0.17833E 02	0.24379E 02
0.33680E 02	0.17856E 02	0.24411E 02
0.34880E 02	0.17902E 02	0.24474E 02
0.36080E 02	0.17940E 02	0.24537E 02
0.37280E 02	0.17971E 02	0.24567E 02
0.38480E 02	0.18040E 02	0.24663E 02
0.39670E 02	0.18086E 02	0.24726E 02
0.40860E 02	0.18132E 02	0.24789E 02
0.42050E 02	0.18178E 02	0.24852E 02
0.43240E 02	0.18202E 02	0.24884E 02
0.44420E 02	0.18271E 02	0.24977E 02
0.45600E 02	0.18317E 02	0.25040E 02
0.46780E 02	0.18340E 02	0.25073E 02
0.47950E 02	0.18386E 02	0.25136E 02
0.49120E 02	0.18410E 02	0.25168E 02
0.50290E 02	0.18410E 02	0.25168E 02
0.51460E 02	0.18432E 02	0.25199E 02

P381-LENGTH=9.7CM,RUN 8
NORMALISED LENGTH = 0.12278E 01

TEMPERATURE DEGREES	ENG.STRESS DYNES PER SQCM	INC.STRESS DYNES PER SQCM
0.28830E 02	0.12780E 02	0.15692E 02
0.30140E 02	0.12804E 02	0.15721E 02
0.31260E 02	0.12827E 02	0.15749E 02
0.32470E 02	0.12896E 02	0.15834E 02
0.33680E 02	0.12942E 02	0.15891E 02
0.34880E 02	0.12988E 02	0.15947E 02
0.36080E 02	0.13011E 02	0.15976E 02
0.37280E 02	0.13057E 02	0.16032E 02
0.38480E 02	0.13080E 02	0.16061E 02
0.39670E 02	0.13103E 02	0.16089E 02
0.40860E 02	0.13126E 02	0.16117E 02
0.42050E 02	0.13150E 02	0.16146E 02
0.43240E 02	0.13173E 02	0.16174E 02
0.44420E 02	0.13219E 02	0.16231E 02
0.45600E 02	0.13265E 02	0.16287E 02
0.46780E 02	0.13265E 02	0.16287E 02
0.47950E 02	0.13265E 02	0.16287E 02
0.49120E 02	0.13311E 02	0.16344E 02
0.50290E 02	0.13311E 02	0.16344E 02
0.51460E 02	0.13311E 02	0.16344E 02

P381-LENGTH=9.7CM,RUN 9
NORMALISED LENGTH AT0.11013E 01

TEMPERATURE DEGREES	INC. STRESS DYNES PER SQCM	INC. STRESS DYNES PER SQCM
0.32470E 02	0.65287E 01	0.71898E 01
0.33480E 02	0.65517E 01	0.72152E 01
0.34880E 02	0.65517E 01	0.72152E 01
0.36080E 02	0.65747E 01	0.72405E 01
0.37280E 02	0.65979E 01	0.72660E 01
0.38480E 02	0.65979E 01	0.72660E 01
0.39670E 02	0.65979E 01	0.72660E 01
0.40860E 02	0.66209E 01	0.72914E 01
0.42050E 02	0.66209E 01	0.72914E 01
0.43240E 02	0.66209E 01	0.72914E 01
0.44420E 02	0.66209E 01	0.72914E 01
0.45600E 02	0.66209E 01	0.72914E 01
0.46780E 02	0.66209E 01	0.72914E 01
0.47950E 02	0.66209E 01	0.72914E 01
0.49120E 02	0.66209E 01	0.72914E 01
0.50290E 02	0.66209E 01	0.72914E 01

P581-ENGINEERING STRESS VERSUS ABSOLUTE TEMPERATURE
NORMALIZED LENGTH = 0.27722E 01
TABLE OF INPUT DATA X,Y,W AND RESIDUALS

3.0819000 E 02	4.7061221 E 01	1.0000000 E 00	-1.2351751 E-01
3.0441000 E 02	4.7292694 E 01	1.0000000 E 00	-7.4759960 E-02
3.0962000 E 02	4.7522850 E 01	1.0000000 E 00	-2.5820255 E-02
3.0683000 E 02	4.7754323 E 01	1.0000000 E 00	2.4435043 E-02
3.0803000 E 02	4.7868744 E 01	1.0000000 E 00	-4.0842560 E-02
3.0929000 E 02	4.8214637 E 01	1.0000000 E 00	1.2931137 E-01
3.1043000 E 02	4.8330373 E 01	1.0000000 E 00	6.1328411 E-02
3.1163000 E 02	4.8560530 E 01	1.0000000 E 00	1.1176586 E-01
3.1282000 E 02	4.8676267 E 01	1.0000000 E 00	4.9281120 E-02
3.1401000 E 02	4.8860392 E 01	1.0000000 E 00	5.5184841 E-02
3.1520000 E 02	4.9022160 E 01	1.0000000 E 00	3.8730621 E-02
3.1639000 E 02	4.9137896 E 01	1.0000000 E 00	-2.3754120 E-02
3.1757000 E 02	4.9368054 E 01	1.0000000 E 00	2.9679298 E-02
3.1875000 E 02	4.9483790 E 01	1.0000000 E 00	-3.1308651 E-02
3.1993000 E 02	4.9599526 E 01	1.0000000 E 00	-9.2296124 E-02
3.2110000 E 02	4.9783652 E 01	1.0000000 E 00	-8.3396912 E-02

VARIANCE OF THE FIT= 5.7577855 E-03
LEAST SQUARES COEFFICIENTS AND THEIR VARIANCES

0.17771809E 01 X** 0	0.11581971E 01
0.14976602E 00 X** 1	0.11879336E-04

TABLE OF COVARIANCES
-3.7086841 E-03 2 1

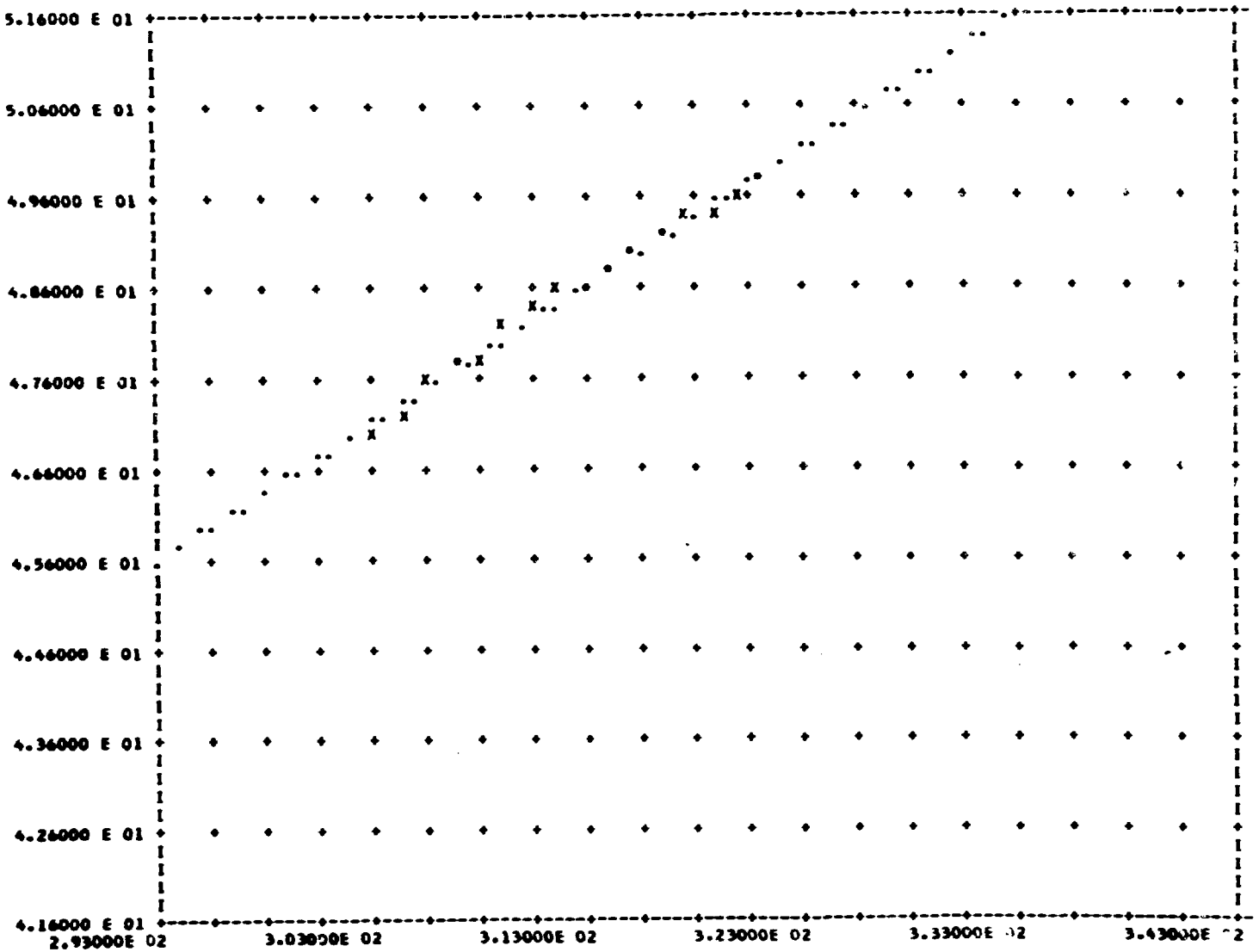
5.16000 E 01
5.06000 E 01
4.96000 E 01
4.86000 E 01
4.76000 E 01
4.66000 E 01
4.56000 E 01
4.46000 E 01
4.36000 E 01
4.26000 E 01
4.16000 E 01
2.93000E 02
3.03000E 02
3.13000E 02
3.23000E 02
3.33000E 02

```
P381-INCOMPRESSIBLE STRESS VERSUS ABSOLUTE TEMPERATURE
NORMALISED LENGTH =  0.27722E 01
TABLE OF INPUT DATA X,Y,W AND RESIDUALS
     3.0319000 E 02      1.3046086 E 02      1.0000000 E 00     -3.4266854 E-01
     3.0441000 E 02      1.3110253 E 02      1.0000000 E 00     -2.0747185 E-01
     3.0562000 E 02      1.3174056 E 02      1.0000000 E 00     -7.1765900 E-02
     3.0683000 E 02      1.3238224 E 02      1.0000000 E 00      6.7583084 E-02
     3.0803000 E 02      1.3269943 E 02      1.0000000 E 00     -1.1339760 E-01


     3.0923000 E 02      1.3365830 E 02      1.0000000 E 00      3.4729767 E-01
     3.1043000 E 02      1.3397914 E 02      1.0000000 E 00      1.6996002 E-01
     3.1163000 E 02      1.3461717 E 02      1.0000000 E 00      3.0981636 E-01
     3.1282000 E 02      1.3493801 E 02      1.0000000 E 00      1.3663292 E-01
     3.1401000 E 02      1.3544843 E 02      1.0000000 E 00      1.5303421 E-01


     3.1520000 E 02      1.3589687 E 02      1.0000000 E 00      1.0745430 E-01
     3.1639000 E 02      1.3621771 E 02      1.0000000 E 00     -6.5729141 E-02
     3.1757000 E 02      1.3685575 E 02      1.0000000 E 00      8.2429886 E-02
     3.1875000 E 02      1.3717658 E 02      1.0000000 E 00     -8.6625072 E-02
     3.1993000 E 02      1.3749742 E 02      1.0000000 E 00     -2.5563813 E-01


     3.2110000 E 02      1.3800785 E 02      1.0000000 E 00     -2.3693033 E-01
VARIANCE OF THE FIT=      4.4247207 E-02
LEAST SQUARES COEFFICIENTS AND THEIR VARIANCES
     2.49355906E 01 X** 0      0.89C05917E 01
     0.41514541E 00 X** 1      0.91291133E-04
TABLE OF COVARIANCES
    -2.8500748 E-02  2  1
```

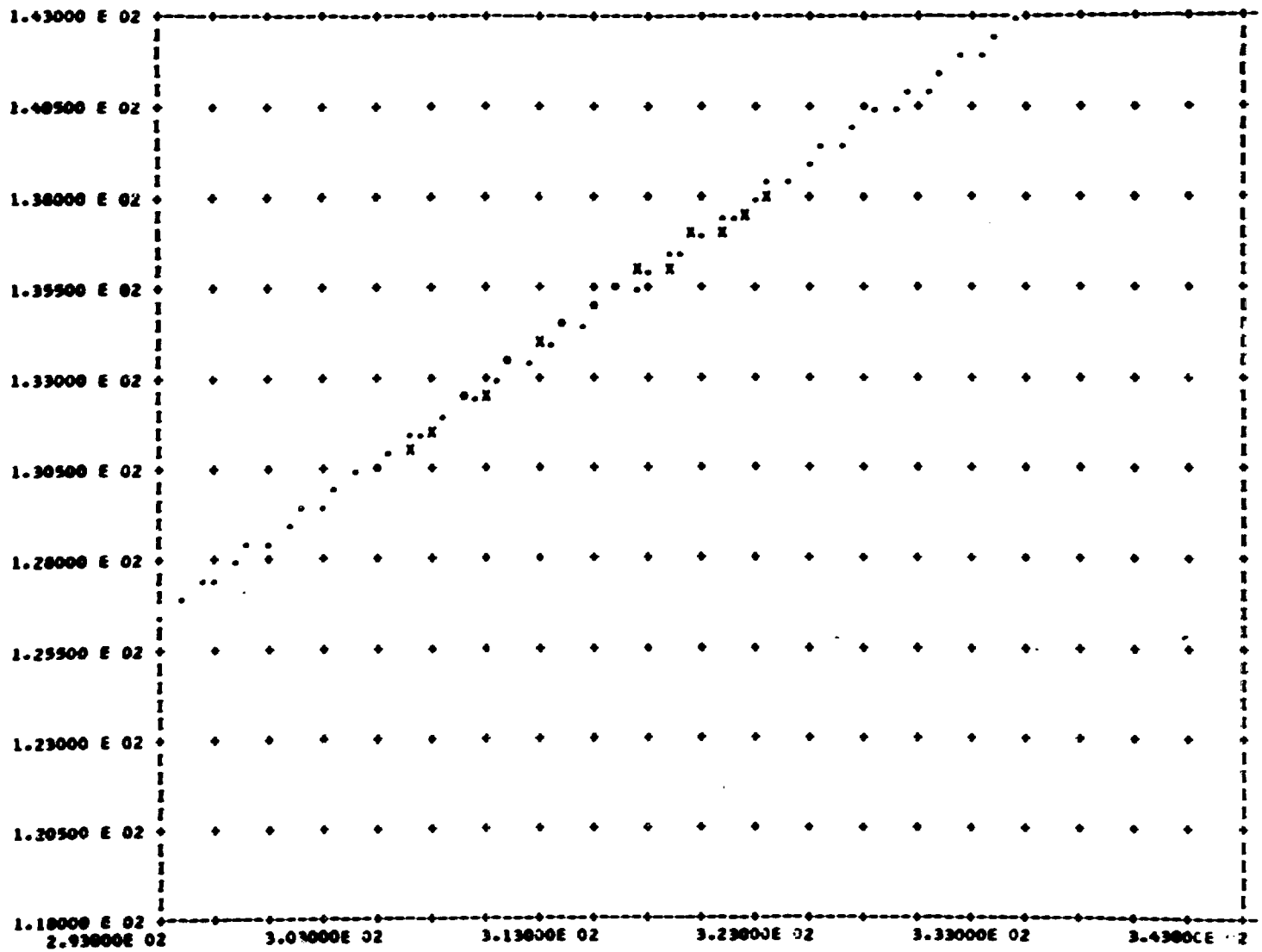
1.43000 E 02
1.40500 E 02
1.38000 E 02
1.35500 E 02
1.33000 E 02
1.30500 E 02
1.28000 E 02
1.25500 E 02
1.23000 E 02
1.20500 E 02
1.18000 E 02
2.93000E 02
3.03000E 02
3.13000E 02
3.23000E 02
3.33000E 02
3.43000E 02

C. P. 392. This program calculates the stress-strain curves at constant temperature from the previous force-temperature curves at constant lengths. With this program added, one now has a complete 3-dimensional picture of the stresses as a function of strain and temperature.

Some sort of decision must be reached as to the order of the fitting polynomial. When a testing program was written, two important conclusions became evident. Firstly, as the order of the polynomial increased, the variance decreased markedly; there is a point however, where, as the order of the fitting polynomial keeps on increasing, the variance increases abruptly. This is to be expected since, as the fit gets better, the residues get smaller, while raising the residues to a high power can give number sufficiently small for the computer to compound them with a zero value (underflow).

Degress of Polynomial	Variance
0	$2.14 \cdot 10^{4}$
1	$7.35 \cdot 10^{2}$
2	$1.97 \cdot 10^{2}$
3	$3.22 \cdot 10^{1}$
4	$1.06 \cdot 10^{1}$
5	$3.86 \cdot 10^{3}$

Secondly it was found that both the x's and the y's to be fitted should be of the same magnitude. Or, as the magnitude's change with respect to one another, the coefficients should change by the same ratio. In the case of the higher order polynomials, the coefficients were found to change by a much larger order of magnitude. In this present work, it was decided to use fourth order polynomials to fit the stress-strain data. and also to multiply the data by a constant such that x and y were of the same order of magnitude.

Once the stress-strain curves are stored in memory, one can proceed to the thermal expansion corrections of stress and strain. These corrections are small as was mentioned previously but should still be taken into account.

Finally the program fits by least squares the corrected stress-strain data. It is important to note that the weights given to the points

are the reciprocal of the variances. The propagation of variance, or mean square error, is described in DEMING's, Statistical Adjustment of Data[48]. In general if

$$y = ax + b \qquad \text{(App. I:1)}$$

then

$$dy = x\,da + db \qquad \text{(App. I:2)}$$

and

$$dy^2 = x^2\,da^2 + db^2 + 2x\,da\,db \qquad \text{(App. I:3)}$$

where

$dy^2 = \sigma y$ variance of y

da^2, $db^2 = \sigma a$, σb variance of a and b

$da\,db = \sigma\,ab$ covariance of a and b

We are assuming no error on x . Equation (App. I:3)allows one to calculate the variance on y (dependent variable) knowing the elements of the reciprocal matrix and assuming the independent variable to be error free.

```
$IBFTC P39202
C     LEAST SQUARES FITTING OF STRESS-STRAIN DATA FROM FORCE-TEMPERATURE DATA
C     CORRECTION OF STRESS AND NORMALISED LENGTH FOR CUBICAL THERMAL EXPANSION OF
C     RUBBER- LEAST SQUARES FITTING OF CORRECTED STRESS-STRAIN DATA
C     CORRECTED MOONEY RIVLIN ERROR ANALYSIS
C     DIMENSION STATEMENTS
      DIMENSION NLENG(20),JNI(20),AEFT0(20),VAEFT0(20),AEFT1(20),VAEFT1(
     1 20),AIFT0(20),VAIFT0(20),AIFT1(20),VAIFT1(20),TMPTKC(20),TMPTKK(20
     2 ),YE1(20),AESS1(20),YEC1(20),NLENGC(20),II(20),AISS1(20),IC1(20)
     3 ,W(20),A(20),B(20),COVE21(20),COV121(20),COV21(20),COV31(20),COV41
     4 (20),COV51(20),COV32(20),COV42(20),COV52(20),COV43(20),COV53(20),
     5 COV54(20)
      DIMENSION YEC2(20,20),NLENC2(20,20),IC2(20,20),AESS(20,20),VAESS(
     1 20,20),AISS(20,20),VAISS(20,20),E2(20,20),COV(20,20)
C     TYPE STATEMENTS
      REAL NLENG,NLENC2,NLENGC
      READ(5,300)
  300 FORMAT(80H
     1                                                                   )
      READ(5,301)
  301 FORMAT(80H
     1                                                                   )
      READ(5,302)IN,KN,ALPHA,INCSTR
  302 FORMAT(1X,I2,2X,I2,2X,E12.5,2X,I2)
      READ(5,303)
  303 FORMAT(80H
     1                                                                   )
      READ(5,304)
  304 FORMAT(80H
     1                                                                   )
      READ(5,305)
  305 FORMAT(80H
     1                                                                   )
      READ(5,306)
  306 FORMAT(80H
     1                                                                   )
      READ(5,307)
  307 FORMAT(80H
     1                                                                   )
      DO 30 I=1,IN
      READ(5,310)NLENG(I),JNI(I)
  310 FORMAT(1X,E12.5,2X,I2,2X)
      READ(5,311)AEFT0(I),VAEFT0(I),AEFT1(I),VAEFT1(I),COVE21(I)
  311 FORMAT(1X,E15.8,4(1X,E15.8))
      IF(INCSTR.NE.1)GO TO 31
      READ(5,311)AIFT0(I),VAIFT0(I),AIFT1(I),VAIFT1(I),COV121(I)
   31 CONTINUE
   30 CONTINUE
      READ(5,312)(TMPTKC(K),K=1,KN)
  312 FORMAT(5(F12.5,2X))
      READ(5,313)SMIN,SMAX
  313 FORMAT(1X,2(E12.5,2X))
      DO 32 K=1,KN
      DO 33 I=1,IN
      TMPTKK(K)=TMPTKC(K)+0.27315E+03
      YE1(I)=AEFT1(I)*TMPTKK(K)+AEFT0(I)
      AESS1(I)=1./(TMPTKK(K)**2*VAEFT1(I)+VAEFT0(I)+2.*TMPTKK(K)*COVE21(
     1 I))
```

```
      YEC1(I)=YE1(I)*(1.-2.*ALPHA*(TMPTKK(K)-0.29815E+03))
      NLENGC(I)=NLENG(I)*(1.-ALPHA*(TMPTKK(K)-0.29815E+03))
      YEC2(K,I)=YEC1(I)
      NLENC2(K,I)=NLENGC(I)
      XESS2(K,I)=XESS1(I)
      WRITE(7,351)YEC2(K,I),NLENC2(K,I),XESS2(K,I)
351   FORMAT(1X,3(F12.5,2X))
      IF(INCSTR.NE.1)GO TO 34
      YII(I)=AIFT(I)*TMPTKK(K)+AIFT0(I)
      WISS(I)=1./(TMPTKK(K)**2*VAIFT2(I)+VAIFT1(I)+2.*COVIZ1(
     1 I))
      YIC1(I)=YII(I)*(1.-2.*ALPHA*(TMPTKK(K)-0.29815E+03))
      YIC2(K,I)=YIC1(I)
34    CONTINUE
33    CONTINUE
      WRITE(6,300)
      WRITE(6,301)
      WRITE(6,303)
      WRITE(6,350)TMPTKC(K)
350   FORMAT(15H TEMPERATURE = ,E12.5)
      CALL BINNEA(IN,5,NLENG,YE1,XESS1,A,B,COV,C,3)
      CALL PLOTPN(IN,NLENG,YE1,A,5,...,AX)
      IF(INCSTR.NE.1)GO TO 35
      WRITE(6,301)
      WRITE(6,304)
      WRITE(6,350)TMPTKC(K)
      CALL BINNEA(IN,5,NLENG,YII,...,A,B,COV,C,3)
      CALL PLOTPN(IN,NLENG,YII,A,5,...,AX)
35    CONTINUE
      WRITE(6,305)
      WRITE(6,306)
      WRITE(6,350)TMPTKC(K)
      CALL BINNEA(IN,5,NLENGC,YEC1,XESS1,A,B,COV,C,3)
      CALL PLOTPN(IN,NLENGC,YEC1,A,5,...,AX)
      DO 37 J=1,5
      JEXP=J-1
      JIND=J
      AESS(K,JI)=A(J)
      VAESS(K,J)=B(J)
      WRITE(7,352)AESS(K,J),VAESS(K,J)
352   FORMAT(1X,2(E15.8,2X))
37    CONTINUE
      COV21(K)=COV(2,1)
      COV31(K)=COV(3,1)
      COV41(K)=COV(4,1)
      COV51(K)=COV(5,1)
      COV32(K)=COV(3,2)
      COV42(K)=COV(4,2)
      COV52(K)=COV(5,2)
      COV43(K)=COV(4,3)
      COV53(K)=COV(5,3)
      COV54(K)=COV(5,4)
      WRITE(7,353)COV21(K),COV31(K),COV41(K),COV51(K),COV32(K)
      WRITE(7,353)COV42(K),COV52(K),COV43(K),COV53(K),COV54(K)
353   FORMAT(1X,E15.8,4(1X,E15.8))
      IF(INCSTR.NE.1)GO TO 36
      WRITE(6,305)
      WRITE(6,307)
```

```
      WRITE(6,350)TMPTKC(K)
      CALL BINNEA(IN,5,NLENGC,YIC1,...,A,B,COV,C,3)
      CALL PLOTPR(IN,NLENGC,YIC1,A,5,SMIN,SMAX)
      DO 38 J=1,5
      JEXP=J-1
      JIND=J
      ATSS(K,J)=A(J)
      VATSS(K,J)=B(J)
   38 CONTINUE
   36 CONTINUE
   32 CONTINUE
      CALL EXIT
      END
```

P389-OBTENTION OF STRESS-STRAIN DATA FROM FORCE-TEMPERATURE DA1-22-BK2,P36

P392-ENGINEERING STRESS AS A FUNCTION OF NORMALISED LENGTH

TEMPERATURE = 0.30000E 02

TABLE OF INPUT DATA X,Y,W AND RESIDUALS

2.1722000 E 00	4.7178750 E 01	7.5075920 E 02	1.1545992 E-01
2.5570000 E 00	4.3451837 E 01	7.6085421 E 02	-1.9870996 E-01
2.2532000 E 00	3.7724969 E 01	2.5380847 E 03	-2.3677826 E-02
2.0380000 E 00	3.3632562 E 01	1.0214750 E 03	8.8579655 E-02
1.7468000 E 00	2.7935015 E 01	1.7660227 E 03	2.0698643 E-01
1.5823000 E 00	2.4011336 E 01	2.9516890 E 03	-7.2472095 E-03
1.3671000 E 00	1.7745544 E 01	7.7930486 E 03	-1.6095781 E-01
1.2278000 E 00	1.2841786 E 01	6.9897786 E 03	1.8897402 E-01
1.1013000 E 00	6.5453108 E 00	1.1542632 E 04	-3.2635331 E-02

VARIANCE OF THE FIT= 1.4727776 E 02

LEAST SQUARES COEFFICIENTS AND THEIR VARIANCES

-0.16905654E 03 X** 0	0.34763833E 03
0.32740388E 03 X** 1	0.19704736E 04
-0.21668976E 03 X** 2	0.14628668E 04
0.67577157E 02 X** 3	0.19946331E 03
-0.78755230E 01 X** 4	0.35697192E 01

TABLE OF COVARIANCES

-8.2649116 E 02	2	1
7.0923458 E 02	3	1
-1.6954565 E 03	3	2
-2.6022759 E 02	4	1
6.2363743 E 02	4	2
-5.3946995 E 02	4	3
3.4526522 E 01	5	1
-8.2929607 E 01	5	2
7.1908072 E 01	5	3
-2.6651486 E 01	5	4

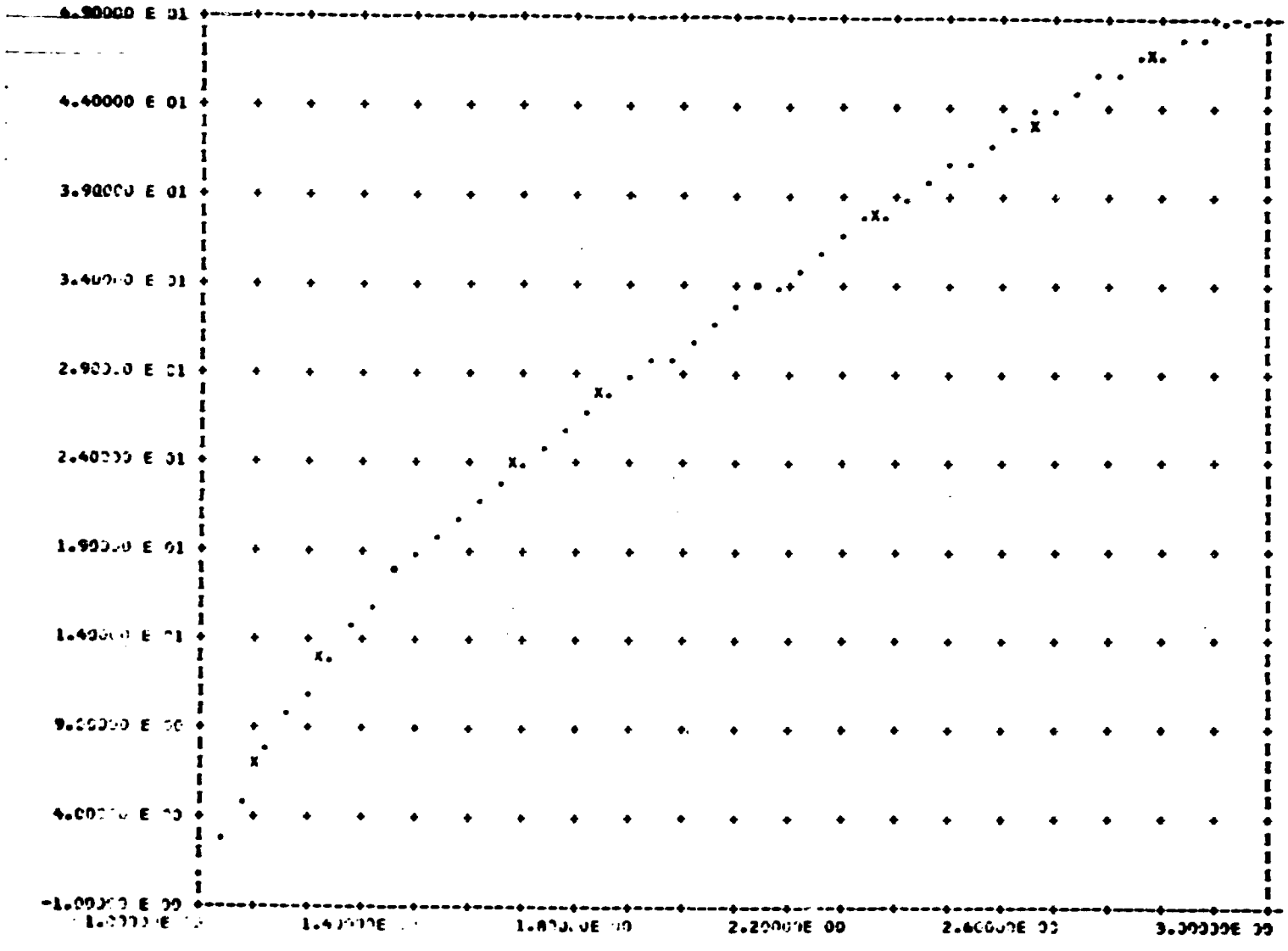
4.40000 E 01
3.90000 E 01
2.40000 E 01
1.40000 E 01
2.20000E 00
2.60000E 00
3.00000E 00

P389-OBTENTION OF STRESS-STRAIN DATA FROM FORCE-TEMPERATURE DA1-22-8K2.P36

P392-INCOMPRESSIBLE STRESS AS A FUNCTION OF NORMALISED LENGTH
TEMPERATURE = 0.3000 E 02
TABLE OF INPUT DATA X,Y,W AND RESIDUALS

2.7722000 E 00	1.3078692 E 02	9.7694173 E 01	-3.3010483 E-02
2.5570000 E 00	1.1113469 E 02	1.1637106 E 02	1.6838074 E-01
2.2532000 E 00	8.5067893 E 01	4.9992449 E 02	-7.7263832 E-02
2.0380000 E 00	6.8542413 E 01	2.4594614 E 02	-1.2777996 E-01
1.7468000 E 00	4.8797929 E 01	5.7873423 E 02	2.7969122 E-01
1.5823000 E 00	3.7992634 E 01	1.1789618 E 03	6.2101364 E-02
1.3671000 E 00	2.4259742 E 01	4.1699359 E 03	-1.7458224 E-01
1.2278000 E 00	1.5767777 E 01	4.6365112 E 03	1.7832327 E-01
1.1013000 E 00	7.2081609 E 00	9.5175534 E 03	-2.9443979 E-02

VARIANCE OF THE FIT= 8.5752320 E 01
LEAST SQUARES COEFFICIENTS AND THEIR VARIANCES

-0.11812768E 03	X** 0	0.48144184E 03
0.19323394E 03	X** 1	0.28469991E 04
-0.10725223E 03	X** 2	0.22391790E 04
0.36332816E 02	X** 3	0.31515461E 03
-0.40051849E 01	X** 4	0.59019797E 01

TABLE OF COVARIANCES

-1.1691249 E 03	2	1
1.0253835 E 03	3	1
-2.5041289 E 03	3	2
-3.8440326 E 02	4	1
9.4141052 E 02	4	2
-8.3307198 E 02	4	3
5.2056547 E 01	5	1
-1.2782977 E 02	5	2
1.1345553 E 02	5	3
-4.3957864 E 01	5	4

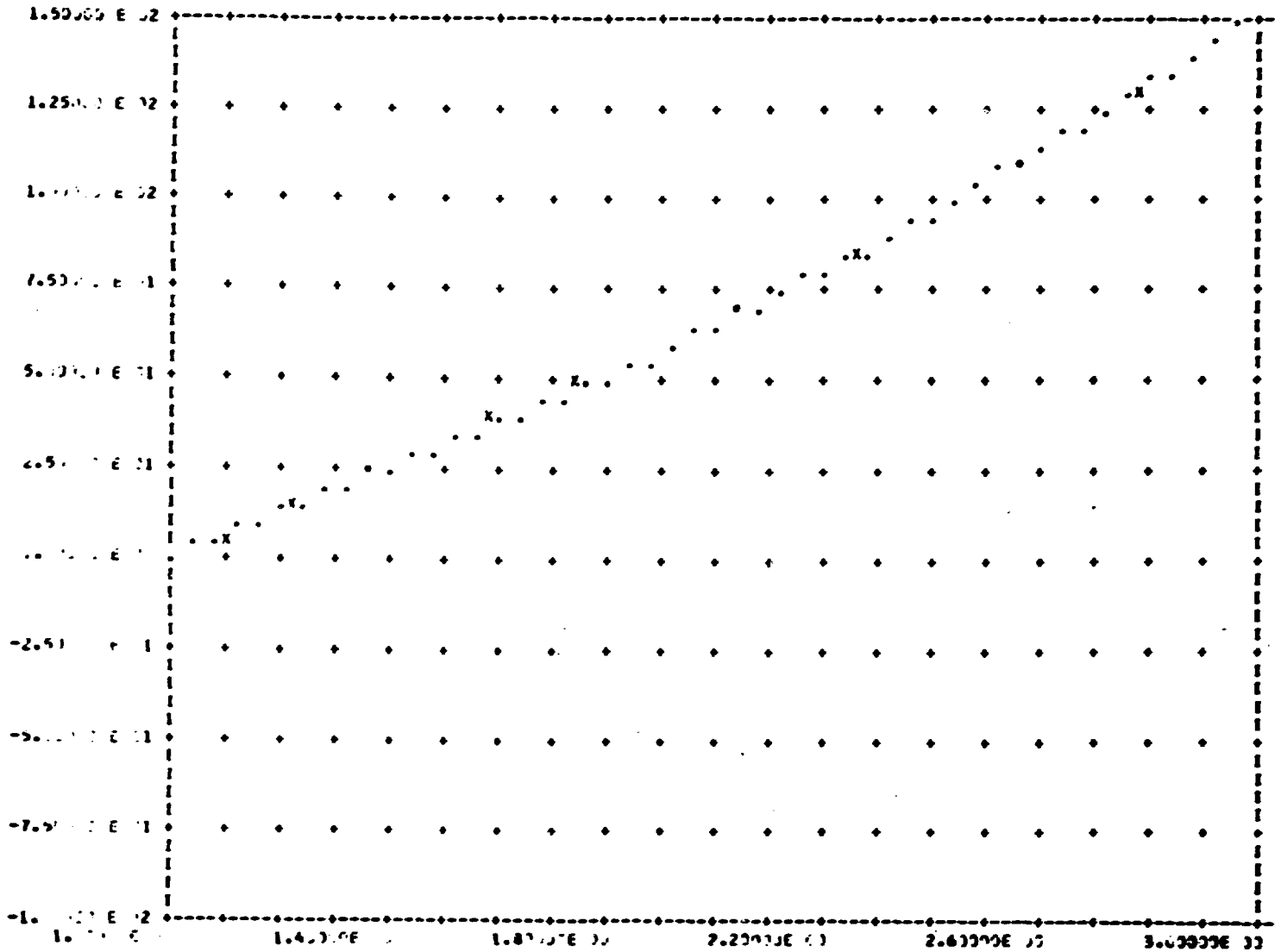

P392-CORRECTION OF STRESS AND STRAIN FOR CUBICAL THERMAL EXPANSION OR RUBBER

P392-CORRECTED ENGINEERING STRESS AS A FUNCTION OF CORRECTED NORMALISED LENGTH
TEMPERATURE = [illegible]E 02
TABLE OF INPUT DATA X,Y,W AND RESIDUALS

2.7691993 E [illegible]	4.7075116 E 01	7.5075920 E 02	6.2119484 E-02
2.5541916 E [illegible]	4.3356391 E 01	7.6085421 E 02	-1.2638998 E-01
2.25[illegible]7253 E [illegible]	3.7672036 E 01	2.5380847 E 03	-1.1725426 E-03
2.[illegible]357617 E [illegible]	3.3558683 E [illegible]	1.0214751 E 03	4.9429893 E-02
1.7448815 E [illegible]	2.7873653 E 01	1.7660227 E 03	1.5042973 E-01
1.58[illegible]5621 E [illegible]	2.3958593 E 01	2.9516893 E 03	-3.4765482 E-02
1.3699985 E [illegible]	1.7706564 E 01	7.7930486 E 03	-1.4116979 E-01
1.2264515 E [illegible]	1.2813577 E 01	6.9897786 E 03	2.1324944 E-01
1.10[illegible]934 E [illegible]	6.93[illegible]9334 E 00	1.1542632 E 04	-4.7769547 E-02

VARIANCE OF THE FIT= 1.4[illegible]14761 E 02
LEAST SQUARES COEFFICIENTS AND THEIR VARIANCES

-[illegible].161931[illegible]E [illegible]	X** 0	0.3[illegible]4846[illegible]E 03
[illegible].3[illegible]960972E 03	X** 1	[illegible].17301903E 04
-[illegible].291067[illegible]E [illegible]	X** 2	[illegible].12867363E 04
[illegible].6187760[illegible]E 02	X** 3	[illegible].17583458E 03
-[illegible].712186[illegible]E 01	X** 4	[illegible].3155[illegible]672E 01

TABLE OF COVARIANCES

-7.2518606 E [illegible]2	2	1
6.2260512 E [illegible]2	3	1
-1.4099297 E [illegible]3	3	2
-2.2860228 E [illegible]2	4	1
5.4848483 E [illegible]2	4	2
-4.75[illegible]1229 E [illegible]2	4	3
[illegible].[illegible]344993 E [illegible]1	5	1
-7.2997915 E [illegible]1	5	2
6.3382307 E [illegible]1	5	3
-2.3523731 E [illegible]1	5	4

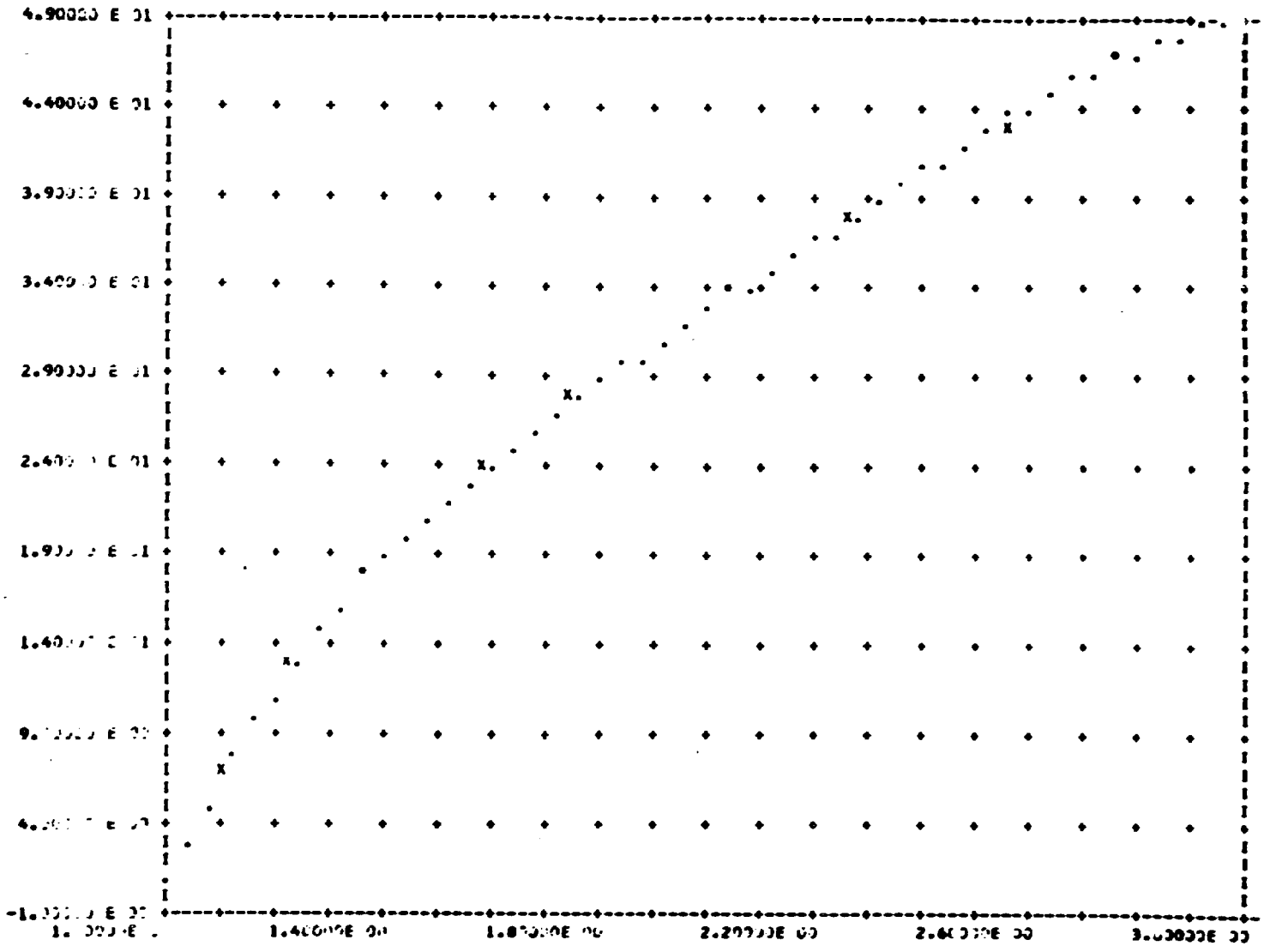
4.90000 E 01
4.40000 E 01
3.90000 E 01
3.40000 E 01
2.90000 E 01
2.40000 E 01
1.90000 E 01
1.40000 E 01
9.00000 E 00
4.00000 E 00
-1.00000 E 00
1.40000E 00
1.80000E 00
2.20000E 00
2.60000E 00
3.00000E 00

P392-CORRECTION OF STRESS AND STRAIN FOR CUBICAL THERMAL EXPANSION OR RUBBER

P392-CORRECTED INCOMPRESSIBLE STRESS AS A FUNCTION OF CORRECTED NORMALISED LENG
TEMPERATURE = [illegible]
TABLE OF INPUT DATA X,Y,W AND RESIDUALS

2.7691553 E [illegible]	1.3949763 E 02	9.7694173 E 01	3.2342911 E-02
2.5541916 E [illegible]	1.1[illegible]6763 E 02	1.1637106 E 02	1.1577988 E-01
2.2[illegible]7253 E [illegible]	8.4881029 E 01	4.9992449 E 02	-1.6815334 E-01
2.[illegible]357617 E [illegible]	6.8391852 E 01	2.4594614 E 02	-1.1217022 E-01
1.7449815 E [illegible]	4.869[illegible]739 E 01	5.7873423 E 02	3.1766224 E-01
1.5[illegible]5621 E [illegible]	3.79[illegible]9179 E 01	1.1789618 E 03	8.6098194 E-02
1.3655985 E [illegible]	2.42[illegible]6453 E 01	4.1699359 E 03	-1.8091917 E-01
1.2264515 E [illegible]	1.5733141 E [illegible]1	4.6365112 E 03	1.6377008 E-01
1.1[illegible]904 E [illegible]	[illegible]7.1923275 E [illegible]0	9.5175534 E [illegible]3	-2.3666918 E-02

VARIANCE OF THE FIT= 8.59795[illegible]6 E 01
LEAST SQUARES COEFFICIENTS AND THEIR VARIANCES

-[illegible].12277391E 03 X** [illegible]	[illegible].5202638 E 03
[illegible].20500972E 03 X** 1	[illegible].30852774E 04
-[illegible].11783564E 03 X** 2	[illegible].23999303E 04
[illegible].40366715E 02 X** 3	[illegible].34305460E 03
-[illegible].45583713E [illegible]1 X** 4	[illegible].64344143E [illegible]1

TABLE OF COVARIANCES

-1.2653103 E 03	2	1
1.1114481 E 03	3	1
-2.7173036 E 03	3	2
-4.1731142 E 02	4	1
1.0229272 E 03	4	2
-9.3601608 E 02	4	3
5.6599773 E 01	5	1
-1.3908423 E 02	5	2
1.2352784 E 02	5	3
-4.6911274 E 01	5	4

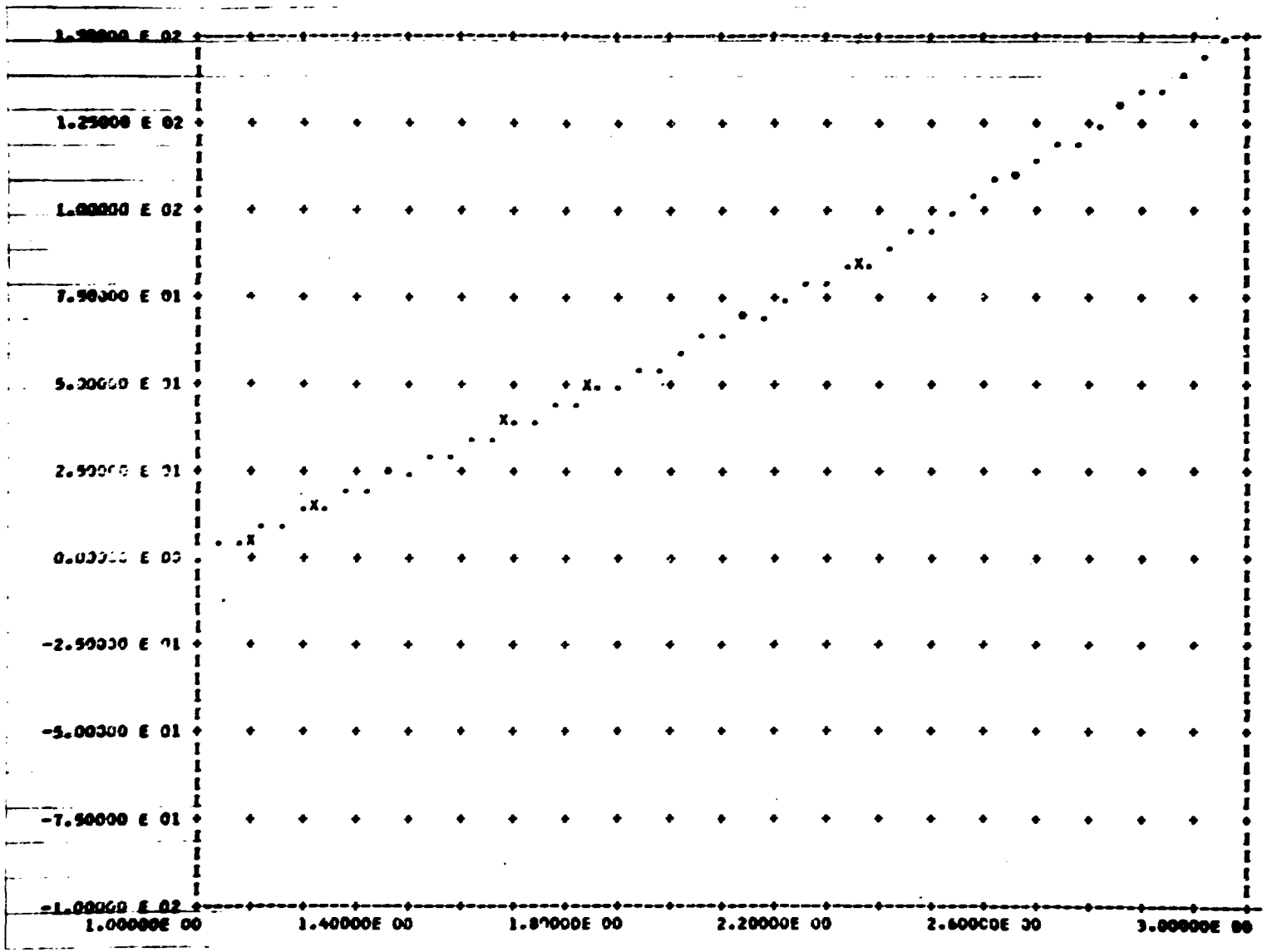
1.25000 E 02
1.00000 E 02
7.50000 E 01
5.00000 E 01
2.50000 E 01
0.00000 E 00
-2.50000 E 01
-5.00000 E 01
-7.50000 E 01
-1.00000 E 02
1.00000E 00
1.40000E 00
1.80000E 00
2.20000E 00
2.60000E 00
3.00000E 00

D. P 393. From the previous program, it is now possible to calculate the Mooney-Rivlin fit of the data. From [4] :

$$\frac{\sigma}{\lambda - \lambda^{-2}} = 2C_1 + 2C_2 \cdot \frac{1}{\lambda} \qquad \text{(App. I:4)}$$

The form of this equation and the importance of the coefficients $2C_1$ and $2C_2$ are discussed in the main text. However, it need not be obvious that any measurements at low strains ($\lambda \rightarrow 1$) must be carried out with extreme accuracy. The following sections will be devoted to the sensitivity of the ordinate ($\sigma/\lambda - \lambda^{-2}$) and to the weight to be given to it any any given value of the abcissa.

If $$y = \frac{\sigma}{\lambda - \lambda^{-2}} \qquad \text{(App. I:5)}$$

and

$$x = \frac{1}{\lambda} \qquad \text{(App. I:6)}$$

Then the Mooney-Rivlin equation can be written as

$$y = 2C_1 + 2C_2 x$$

The variance of y as a function of the variances of (stress) and of l_o (the unstressed length) can be derived as follows: From Equation (App. I:5)

$$dy = \frac{d\sigma}{\lambda - \lambda^{-2}} - \frac{\sigma(1 + 2\lambda^{-3})}{(\lambda - \lambda^{-2})^2} d\lambda \qquad \text{(App. I:7)}$$

but if

$$\lambda = \frac{l}{l_o} \qquad \text{(App. I:8)}$$

then $$d\lambda = \frac{dl}{l_o} - \frac{l dl_o}{l_o^2} \qquad \text{(App. I:9)}$$

We can assume that the variance of l_o (the unstressed length) and of l (the stressed length) are equal.

Thus

$$d\lambda^2 = \frac{dl_o^2}{l_o^2} + \frac{l^2}{l_o} dl_o^2$$

$$d\lambda^2 = \frac{dl_o^2}{l_o^2} (\lambda^2 + 1) \qquad \text{(App. I:10)}$$

Replacing the value of $d\lambda^2$ from Equation (App I:10) into Equation (App I:7), we obtain

$$dy^2 = \frac{d\sigma^2}{(\lambda - \lambda^{-2})^2} + \frac{\sigma^2(1+2\lambda^{-3})^2}{(\lambda - \lambda^{-2})^4}(\lambda^2 + 1)\frac{dl_o^2}{l_o^2} \qquad \text{(App. I:11)}$$

This may be written as

$$dy^2 = B_1\, d\sigma^2 + B_2\sigma^2 \frac{dl_o^2}{l_o^2} \qquad \text{(App. I:12)}$$

where B_1 and B_2 are functions only of λ. There are therefore two contributions to the total variance on y, the first from the variance of the stress and the second from the variance of the unstressed length. It will be seen in Appendix I that the larger effect comes from the second term. As previously, the weight given to each point in this plot is equal to the reciprocal of the total variance of that point.

A careful scrutiny of B_1 and B_2 show immediately that by far the most important factor is the variation of the denominator as a function of λ. Clearly, as $\lambda \rightarrow 1$, both denominators approach zero, hence the variance of y approaches infinite as λ approaches unity. The important conclusion of this study is therefore that as the elongation goes to unity, or in other words when the sample is close to its unstressed length, the uncertainty of the corresponding Mooney-Rivlin stresses tends towards infinity.

```
$IBFTC P39303
C     LEST SQUARES MOONEY RIVLIN ANALYSIS
C     CORRECTED ERROR ANALYSIS
      DIMENSION TMPTKC(2_),LNGMR(20),DENOMR(20),YDEMR(20),XDEMR(20),
     1 VYDEMR(20),WYDEMR(20),SEMR1(20),VSEMR1(20),DEAEMR(20),YEMR1(20),
     2 XEMR1(20),VYEMR1(2 ),XYEMR1(20),A(20),B(20),A1D(20),B2D(20),A2D(20),A1D(20
     3 ),A2D(20),B1(20),B2(20),A1(20),A2(20),VDEMR(20),COV21(20),COV31(20
     4 ),COV41(20),COV51(20),COV32(20),COV42(20),COV52(20),COV43(20),COV53
     5 3(20),COV54(20)
      DIMENSION YEC2(20,20),NLENC2(20,20),ALOG(20,20),AL 1(20,20),ALOG
     1 (20,2 ),COV(20,20)
      REAL LNGMR,NLENC2,MPIN,MPMAX
      READ(5,402)
  402 FORMAT(8H
     1                                                              )
      READ(5,401)
  401 FORMAT(8H
     1                                                              )
      READ(5,402)
  402 FORMAT(80H
     1                                                              )
      READ(5,403)
  403 FORMAT(6H
     1                                                              )
      READ(5,41 )(_,I=1,I  ),VLA  ,  I=1, MAX
  41  FORMAT(1X,8(I2,2X),8(E12.5,2X))
      READ(  ,41)(TMPTKC(K),K=1,KK)
  411 FORMAT(5(F12.0,2X))
      READ(  ,412)(LNGMR(I),I=1,IMR)
  412 FORMAT(8(E12.0,2X))
      DO   K=1,KK
      DO   I=1,IMR
      READ(5,413)YEC2(K,I),NLENC2(K,I),WES32(K,I)
  413 FORMAT(3E12.0,2X)
      DENOMR(I)=NLENC2(K,I)-NLENC2(K,I)**(-2)
      YDEMR(I)=YEC2(K,I)/DENOMR(I)
      XDEMR(I)=1./NLENC2(K,I)
      1D(I)=DENOMR(I)**(-2)
      B2D(I)=DENOMR(I)**(-4)*(1.+2.*NLENC2(K,I)**(-3))**2*I1.+NLENC2(K,I
     1 )**2)
      A1D(I)=A1D(I)/WES32(K,I)
      A2D(I)=YEC2(K,I)**2*A2D(I)*VLAMDA
      VYDEMR(I)=A1D(I)+A2D(I)
      WYDEMR(I)=1./VYDEMR(I)
  41  CONTINUE
      WRITE(6,402)
      WRITE(6,411)
      WRITE(6,415)(NLENC2(K,I),A1D(I),A2D(I),VYDEMR(I),I=1,IMR)
  415 FORMAT(15HNLENC2(K,I) = ,E15.8,1OH A1D(I) = ,E15.8,1OH A2D(I) = ,
     1 E15.8,13H VYDEMR(I) = ,E15.8)
      WRITE(6,412)
      WRITE(6,450)TMPTKC(K)
  450 FORMAT(15H TEMPERATURE = ,F15.8)
      CALL BINVEA(IMR2,XDEMR,YDEMR,A,B,COV,C,3)
      CALL PLOTPN(IMR,XDEMR,YDEMR,A,2,MPMIN,MPMAX)
      READ(5,414)(AESS(K,J),VAESS(K,J),J=1,5)
  414 FORMAT(1X,E15.8,2X,E15.8,2X)
      READ(5,417)COV21(K),COV31(K),COV41(K),COV51(K),COV32(K)
```

```
      READ(5,417)COV42(K),COV52(K),COV43(K),COV53(K),COV54(K)
  417 FORMAT(1X,E15.8,4(1X,E15.8))
      DO 47 I=1,IMR
      SEMR1(I)=0.
      VSEMR1(I)=0.
      DO 44 J=1,5
      JEXP=J-1
      JIND=J
      SEMR1(I)=SEMR1(I)+AESS1K,JIND)*LNGMR(I)**JEXP
      VSEMR1(I)=VSEMR1(I)+VAESS(K,JIND)*LNGMR(I)**(2*JEXP)
   44 CONTINUE
      VSEMR1(I)=VSEMR1(I)+2.*(COV21(K)*LNGMR(I)+COV31(K)*LNGMR(I)**2
     1 +COV41(K)*LNGMR(I)**3+COV51(K)*LNGMR(I)**4+COV32(K)*LNGMR(I)**3
     2 +COV42(K)*LNGMR(I)**4+COV52(K)*LNGMR(I)**5+COV43(K)*LNGMR(I)**5
     3 +COV53(K)*LNGMR(I)**6+COV54(K)*LNGMR(I)**7)
      DENEMR(I)=LNGMR(I)-LNGMR(I)**(-2)
      YEMR1(I)=SEMR1(I)/DENEMR(I)
      XEMR1(I)=1./LNGMR(I)
      B1(I)=DENEMR(I)**(-2)
      B2(I)=DENEMR(I)**4*(1.+2.*LNGMR(I)**(-3))**2*(1.+LNGMR(I)**2)
      A1(I)=B1(I)*VSEMR(I)
      A2(I)=SEMR1(I)**2*B2(I)*VL/ DA
      VYEMR1(I)=A1(I)+A2(I)
      WYEMR1(I)=1./VYEMR1(I)
   47 CONTINUE
      WRITE(6,401)
      WRITE(6,403)
      WRITE(6,416)(LNGMR(I),A1(I),A2(I),VYEMR1(I),I=1,IMR)
  416 FORMAT(1ZHOLNGMR(I) = ,E15.8,9H A1(I) = ,E15.8,9H A2(I) = ,E15.8,
     1 13H VYEMR (I) = ,E15.8)
      WRITE(6,450)TMPTKCTK)
      CALL BINNEA(IMR,2,XEMR1,YEMR1,WYEMR1,A,b,COV,C,3)
      CALL PLOTPR(IMR,XEMR1,YEMR1,A,2,MRMIN,MRMAX)
   60 CONTINUE
      CALL EXIT
      END
```

P393-ENGINEERING STRESS-ACTUAL POINTS
TEMPERATURE = 0.2500000E 02
TABLE OF INPUT DATA X,Y,W AND RESIDUALS

3.6072434 E-01	1.7573289 E 01	1.0961749 E 02	1.0508418 E-01
3.9108330 E-01	1.7817821 E 01	9.7268550 E 01	6.8571568 E-02
4.4381325 E-01	1.8126926 E 01	7.9814626 E 01	-1.3046340 E-01
4.9067714 E-01	1.8446104 E 01	6.1267658 E 01	-2.2512197 E-01
5.7267538 E-01	1.9428191 E 01	3.5962891 E 01	-2.7179718 E-04
6.5199140 E-01	2.0018821 E 01	2.2923963 E 01	3.9397001 E-02
7.3167938 E-01	2.1120283 E 01	8.9312664 E 00	2.1990013 E-01
8.1446490 E-01	2.2531791 E 01	3.0353795 E 00	8.6314344 E-01
9.0801779 E-01	2.3560742 E 01	5.2581020 E-01	1.0260410 E 00

VARIANCE OF THE FIT= 1.3440289 E 00
LEAST SQUARES COEFFICIENTS AND THEIR VARIANCES

0.14128048E 02 X** 0	0.73447596E-01
0.92573457E 01 X** 1	0.35087558E 00

TABLE OF COVARIANCES
-1.5498957 E-01 2 1

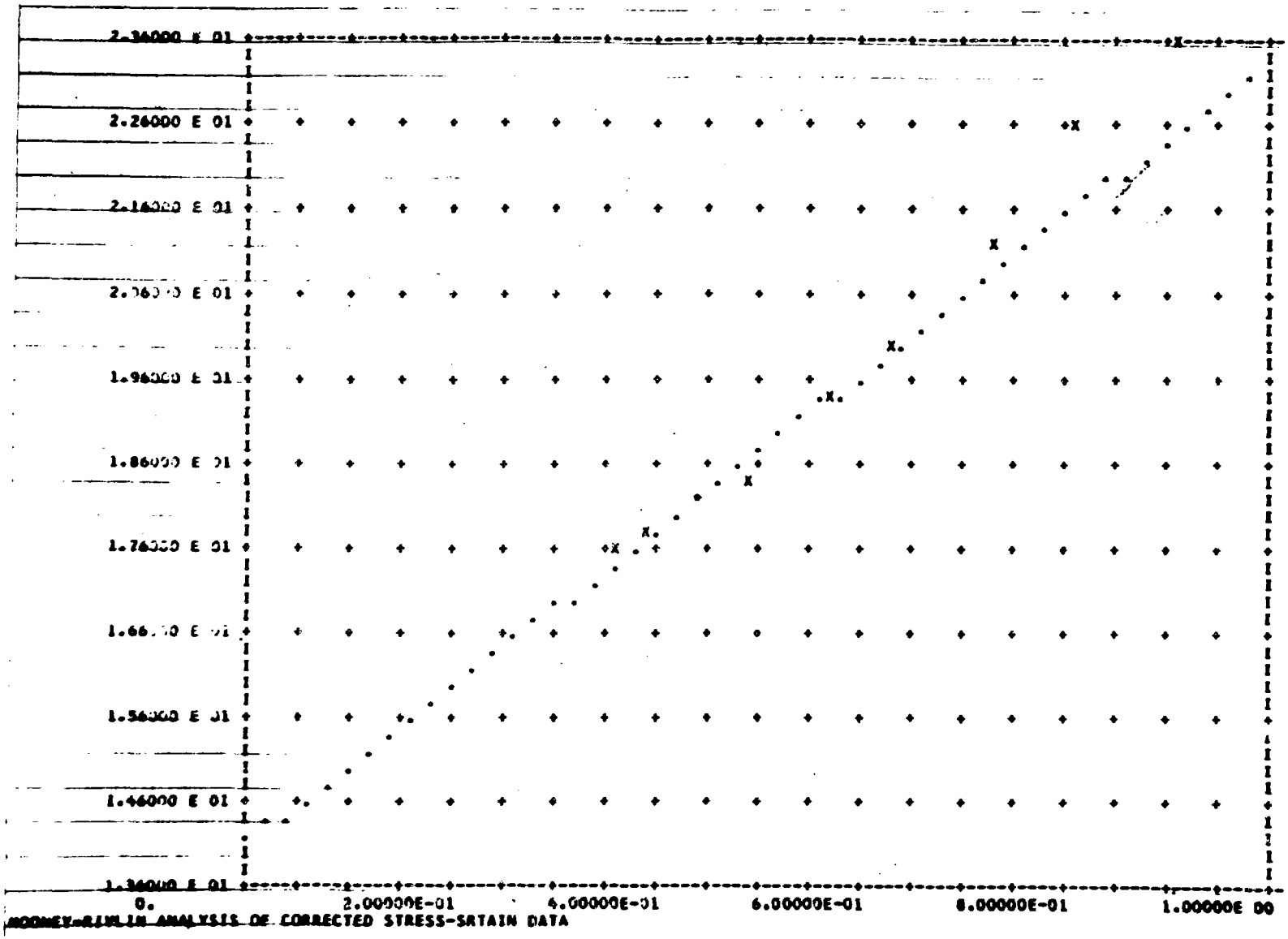

MOONEY-RIVLIN ANALYSIS OF CORRECTED STRESS-SRTAIN DATA

E. P 394. From the punched output of P 392, it is now possible to reconstruct the corrected force-temperature curves. It suffices to interpolate the corrected stresses as is the case of P 392, as a function of temperature, keeping the strain a constant. A least squares linear fit gives the slope and intercept of the force-temperature lines, which are of thermodynamic importance.

```
      PROGRAM P39402
C     LEAST SQUARES LINEAR ANALYSIS OF CORRECTED FORCE-TEMPERATURE DATA OBTAINED
C     FROM P39202=INTEGRATION OF (DF/DT)P,T=F(L) AND (F)P,T=F(L)
C     DIMENSUON STATEMENNTS
      DIMENSION TMPTKC(20),NLENG(20),
      DIMENSION AESS(20,20),VAESS(20,20)
      DIMENSION COV21(20),COV31(20),COV41(20),COV51(20),COV32(20),
     1 COV43(20),COV53(20),COV54(20),COV42(20),COV52(20)
      DIMENSION YEC2(20,20),VSEMR2(20,20),VSERR(20,20),TMPTKK(20),YEC1K(
     1 20),WYEC1K(20),DFDT(20),EXTFT(20),A(20),B(20),COV(20),VDFDT(20),
     2  VEXTFT(20),ADFDT(20),INTFT(20),YEC11(20),          WLFT(20),WEX
     3 IFT(20),INTYEC(20,20),          FE F(20,20),NLENG1(19),FE F1(19,1
     4 9),WFE FT(20),WFE F1(19)
C     TYPE STATEMENTS
      REAL NLENG,NLMIN,NLMAX,INTFT,INTYEC,NLENG1
      EQUIVALENCE (NLENG(2),NLENG1(1))
      EQUIVALENCE (FE F(2),FE F1(1))
      EQUIVALENCE (WFE F(2),WFE F1(1))
      READ(5,100)
  100 FORMAT(80H
     1                                                              )
      READ(5,101)
  101 FORMAT(80H
     1                                                              )
      READ(5,102)KK,IN,TMIN,TMAX,NLMIN,NLMAX,ALPHA
  102 FORMAT(1X,2(I2,2X),5(E12.5,2X))
      READ(5,103)(TMPTKC(K),K=1,KK)
  103 FORMAT(E12.5,4E14.5)
      READ(5,104)(NLENG(I),I=1,IN)
  104 FORMAT(E12.5,4E14.5)
      WRITE(6,105)
      WRITE(6,101)
      DO 13 K=1,KK
      READ(5,105)(AESS(K,J),VAESS(K,J),J=1,5)
  105 FORMAT(1X,E15.8,2X,E15.8,2X)
   13 CONTINUE
      DO 12 I=1,IR
      DO 10 K=1,KK
      YEC2(K,I)=0.
      IF(I.EQ.1)GO TO 14
      DO 11 J=1,5
      JJ=J-1
      YEC2(K,I)=YEC2(K,I)+AESS(K,J)*NLENG(I)**JJ
   11 CONTINUE
   14 CONTINUE
   10 CONTINUE
   12 CONTINUE
      DO 20 I=2,IN
      DO 21 K=1,KK
      TMPTKK(K)=TMPTKC(K)+273.15
      YEC1K(K)=YEC2(K,I)
      WYEC1K(K)=1.
   21 CONTINUE
      WRITE(6,252)NLENG(I)
  252 FORMAT(1H1,12H NLENG(I) = ,E12.5)
      CALL BINREA(KK,2,TMPTKK,YEC1K,WYEC1K,A,B,COV,C,3)
      CALL PLOTPR(KK,TMPTKK,YEC1K,A,2,TMIN,TMAX)
      DFDT(I)=A(2)
```

```
      EXTFT(I)=A(I)
      WDFDT(I)=1.
      WEXTFT(I)=1.
   20 CONTINUE
      BEXTFT(1)=5.0
      EXTFT(1)=0.0
      WDFDT(1)=0.0
      WEXTFT(1)=0.0
      CALL BINREAIN(5,NLENG,DFDT,WDFDT,A,G,COV,C,3)
      CALL PLOTPN(IN,NLENG,DFDT,A,5,NLMIN,...,MAX)
      DO 22 J=1,5
      ADFDT(J)=A(J)
   22 CONTINUE
      WRITE(6,251)
  251 FORMAT(2CHINTEGRATION OF DFDT)
      DO 23 I=1,IN
      IF(I.EQ.1)GO TO 25
      INTFT(I)=0.
      DO 24 J=1,5
      JJ=J
      AJ=J
      INTFT(I)=INTFT(I)+(ADFDT(J)/AJ)*(NLENG(I)**JJ-1.)
   24 CONTINUE
      IF(I.NE.1)GO TO 26
   25 INTFT(I)=0.
   26 CONTINUE
      WRITE(6,250)NLENG(I),INTFT(I)
  250 FORMAT(12H NLENG(I) = ,F15.8,12H INTFT(I) = ,E15.8)
   23 CONTINUE
      DO 30 K=1,KN
      WRITE(6,351)
  351 FORMAT(20HIINTEGRATION OF F-L )
      THPTKC(K)=THPTKK(K)-273.15
      WRITE(6,352)THPTKC(K)
  352 FORMAT(13HCTHPTKC(K) = ,E15.8)
      DO 31 I=1,IN
      IF(I.EQ.1)GO TO 32
      INTYEC(K,I)=0.
      DO 33 J=1,5
      AJ=J
      JJ=J
      INTYEC(K,I)=INTYEC(K,I)+(AESS(K,J)/AJ)*(NLENG(I)**JJ-1.)
      INTYEC(K,I)=INTYEC(K,I)+AESST(K,J)*NLENG(I)**JJT/AJ
   33 CONTINUE
      IF(I.NE.1)GO TO 34
   32 INTYEC(K,I)=0.0
   34 CONTINUE
      WRITE(6,350)NLENG(I),INTYEC(K,I)
  350 FORMAT(12H NLENG(I) = ,E15.8,15H INTYEC(K,I) = ,E15.8)
   31 CONTINUE
   30 CONTINUE
      CALL EXIT
      END
```

```
 NLENG(1) =  0.3[illegible]CE 01
TABLE OF INPUT DATA X,Y,& AND RESIDUALS
     2.9815000 E 02       4.8922446 E 01       1.0000000[illegible] E 00      -3.4800053 E-02
     3.0315000 E 02       4.9226226 E 01       1.0000000[illegible] E 00      -1.9467831 E-01
     3.0815000 E 02       5.0379796 E 01       1.0000000[illegible] E 00      -2.0876894 E-01
     3.1315000 E 02       5.1617487 E 01       1.0000000[illegible] E 00       4.5326519 E-01
     3.1815000 E 02       5.2716209 E 01       1.0000000[illegible] E 00       1.5632912 E-01

     3.2315000 E 02       5.2424667 E 01       1.0000000[illegible] E 00      -2.6104212 E-01
     3.2815000 E 02       5.4325901 E 01       1.0000000[illegible] E 00       5.7479369 E-01
     3.3315000 E 02       5.4091842 E 01       1.0000000[illegible] E 00      -5.2501345 E-01
VARIANCE OF THE FIT=      1.6679253 E-01
LEAST SQUARES COEFFICIENTS AND THEIR VARIANCES
    -9.3[illegible]197[illegible]E 01 X** 0       5.1582476[illegible]8F 02
     6.1731317[illegible] X** 1       6.1582467[illegible]E-03
TABLE OF COVARIANCES
    -5.2142343 E-02  2  1
```

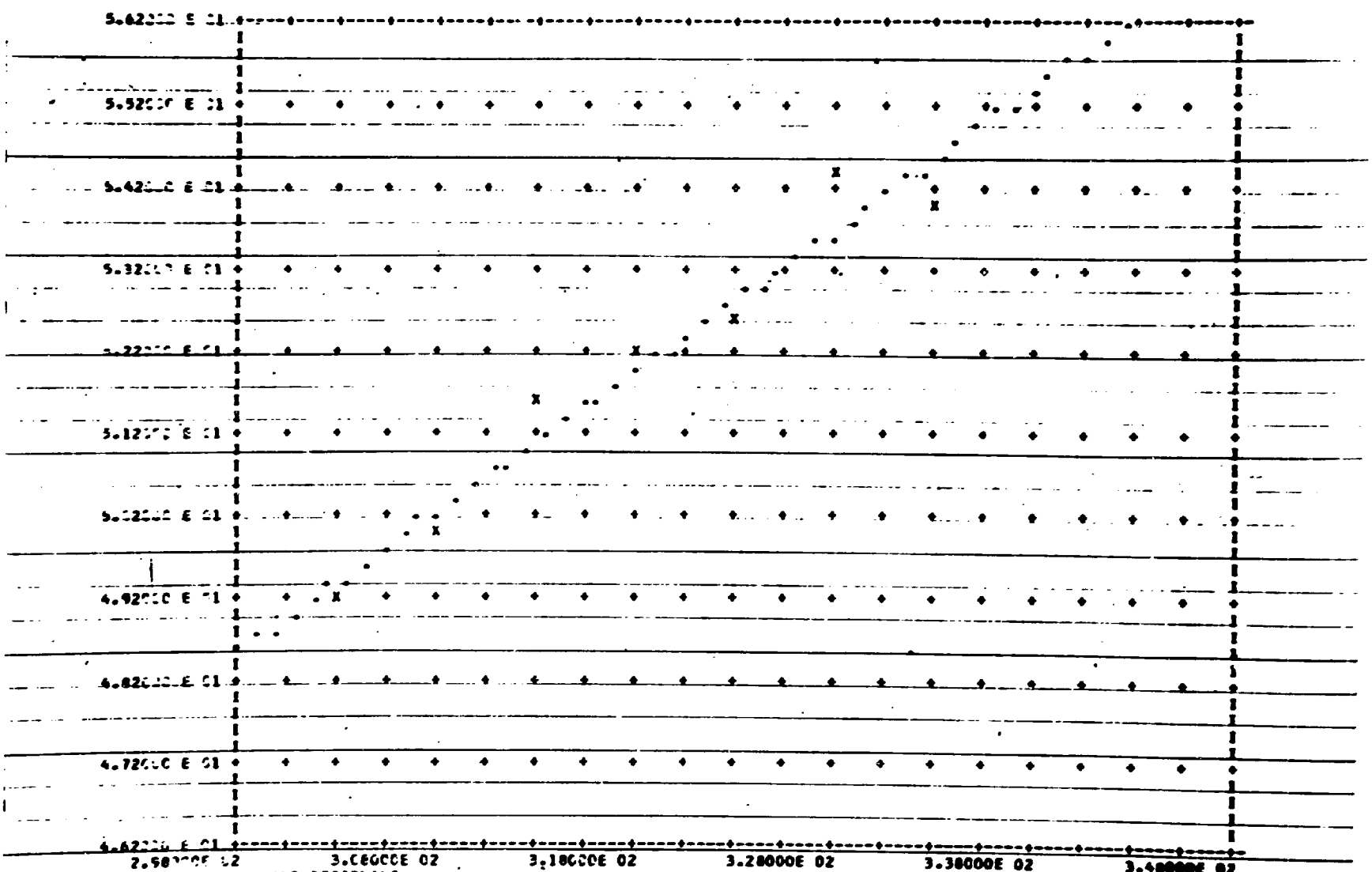

TABLE OF INPUT DATA X,Y,W AND RESIDUALS

1.0000000 E 00	0.	0.	-6.9659908 E-03
1.0100000 E 00	7.7654644 E-03	1.0000000 E 00	1.2133678 E-05
1.0500000 E 00	1.1327231 E-02	1.0000000 E 00	3.7003774 E-06
1.1000000 E 00	1.5253567 E-02	1.0000000 E 00	-3.8039871 E-06
1.2000000 E 00	2.4260458 E-02	1.0000000 E 00	-1.1154450 E-05
1.3000000 E 00	3.3475626 E-02	1.0000000 E 00	-1.1661558 E-05
1.5000000 E 00	5.1383648 E-02	1.0000000 E 00	7.2084367 E-07
2.0000000 E 00	8.5561817 E-02	1.0000000 E 00	2.4240464 E-05

P021 IIT-

SECTION II

"FAST-STRETCHING" of NATURAL RUBBER

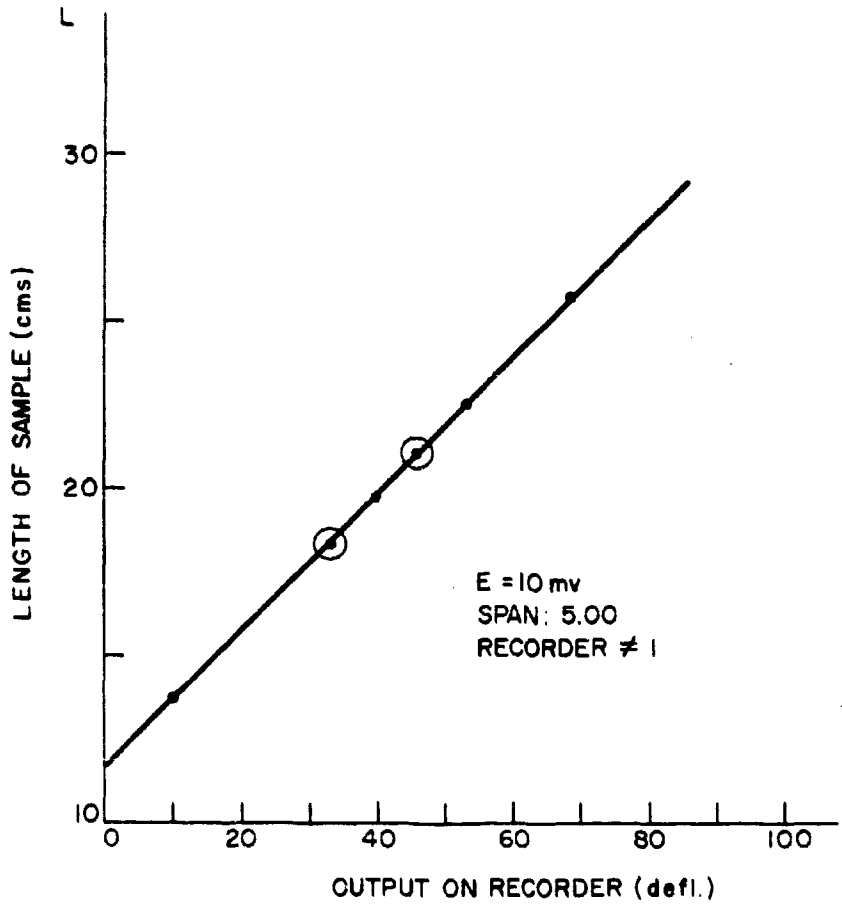

Fig. 39 : Calibration of Linear Potentiometer

III. EXPERIMENTAL

For the purpose of determining the temperature rise in the sample upon elongation, it was necessary to embed a small temperature measuring device. This "thermometer" must have a large thermal response, since we are interested in analyzing temperature changes of the order of 0.01°C. Referring back to Part II, it is now much more obvious why that study had been undertaken. The use of thermocouple sensors requires very sensitive micro-voltmeters, the usual sensitivity of a thermocouple such as copper-constantan is 0.040 mv per degrees Centigrade. The measurement of 0.001°C would require the measurement of $4 \cdot 10^{-5}$ mv, which is outside the realm of normal type instrumentation.

Thermistors exhibit several interesting features, one of which is a very high temperature coefficient of resistance. For example, with the type of bead thermistor that we used, a sensitivity of 10 mv per degree Centigrade is easily obtainable. This means a sensitivity of about 250 times the magnitude that could be obtained with a thermocouple sensor. Embedding the thermistor in a slit made in the rubber with a razor blade, this should have little effect upon the stress distriubution throughout the sample, even though the thermometer bead is finite, approximately 0.03 inches in diameter.

Once the thermistor probe is embedded, it is held in place by a little drop of rubber cement applied to each side of the slit. By operating a Linear Power Activator (POLYNOID), model number 01A, (Skinner Precision Industries, New Britain, Conn.) it is possible to stretch the sample over a distance of about 6 inches in less than 0.1 secs. This is a fast stretch, and below will be referred to as such (fast-stretch tests). As will be seen in a further section, to label these tests as being truly adiabatic requires further discussion.

The increase in length upon extension can be measured with a Linear Motion Potentiometer. Such an instrument was purchased from Bourns, Inc. Riverside, California; model number 156, with a total travel length of 6.5". Knowing the rest length of the sample, the stressed length from which the extension commences, it is possible to calibrate the linear potentiometer directly in centimeters of rubber sample. This was done in Fig. 39. It is therefore easy to read off the stressed length directly from Fig. 39, and to

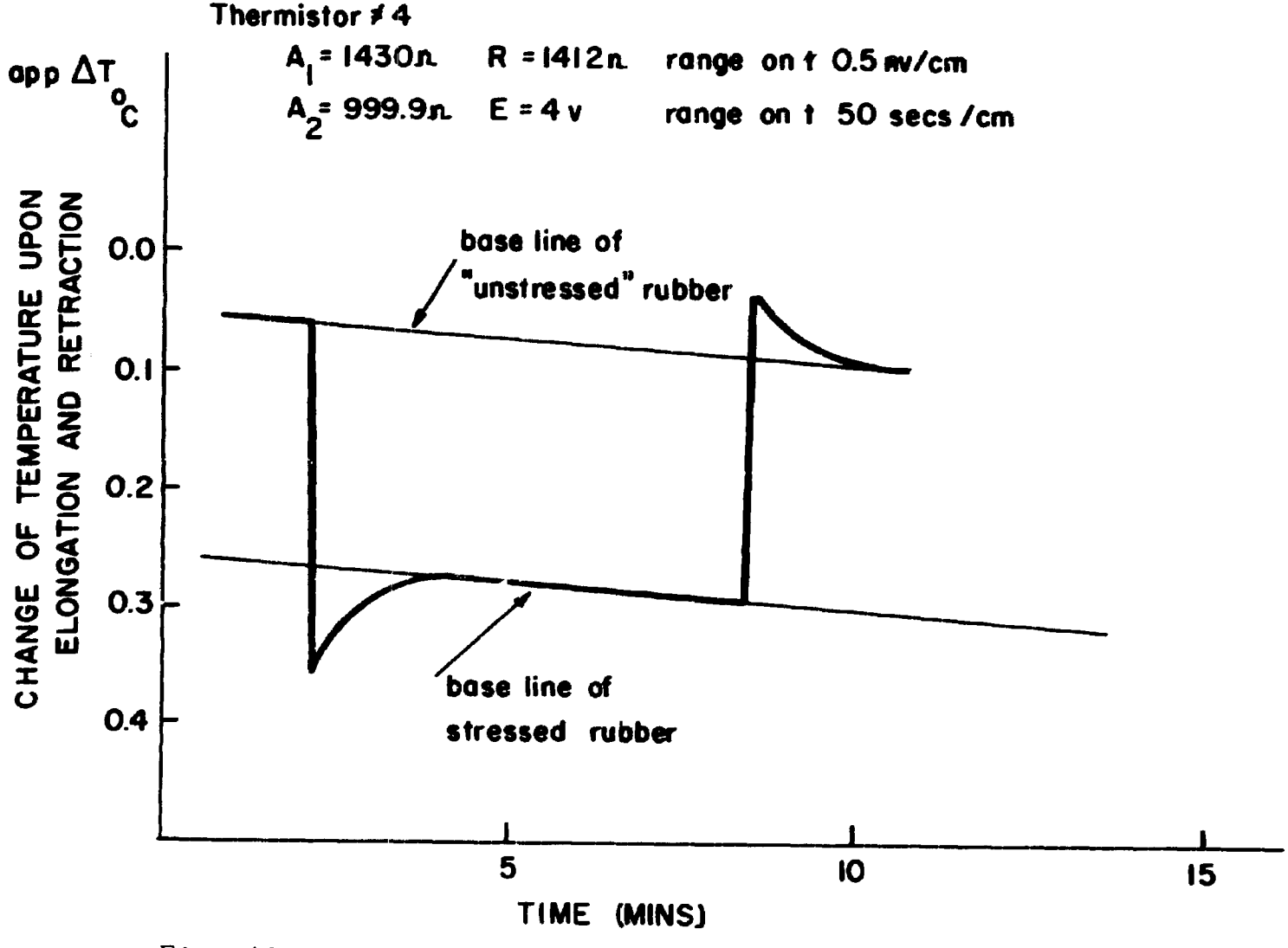

Fig. 40 : Thermistor output as a function of time

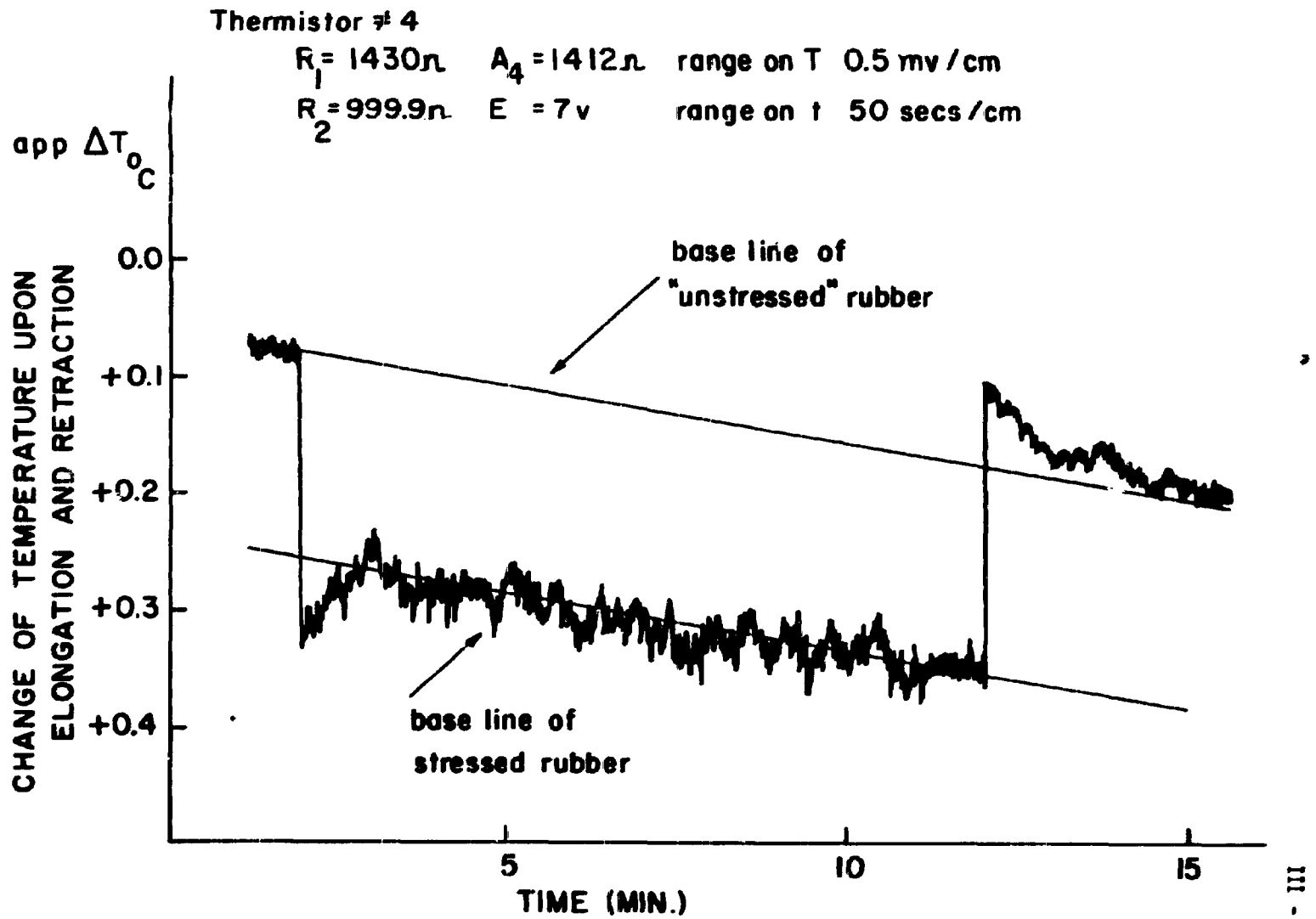

Fig. 41 : Thermistor corrected output as a function of time

calculate the elongation of the sample knowing what its unstressed length is. The final stressed length is determined by the position of the rest against which the Polynoid Activator comes to. Small magnets hold the Activator's core in place and prevent needless bouncing as the sample is stressed or relaxed. The height of the rest is controlled by a lab-jack, which was mounted in such a manner that the platform can move without changing the position of its central torque axis. A hole was drilled through the constant temperature chamber, and the stretching of the sample was controlled from the outside.

All tests were run at constant temperature. It was much easier to analyze the data if the base lines were roughly horizontal. A 25 W white light bulb connected to a small powerstat sufficed to keep the chamber at approximately 30°C. A 15 W fluorescent bulb produced a very noisy interference with the thermistor circuit and had to be eliminated. Figs. 40, 41 show small portions of base lines the differences between them is attributed to the noise emitted by the fluorescent lamp.

In the course of these tests, a study of the time dependency of a stress "spike" was also carried out. This was done by activating the load cell or transducer and measuring the change in force with time.

On the other hand, the progress of relaxation was not followed at the highest temperature. Instead, the sample was stretched a few times to a λ of approximately 2.50, and then hold there for about 12 hours for conditioning. In parallel with the measuring of the thermal effects of "fast-stretching," we will now develop certain relationships that were implied in Part II. There it was shown that:

$$\Delta e_{1i} = \frac{T_i}{\beta_i} + \frac{1}{2}\,\frac{1-a}{1+a} \qquad \text{Part II: Equation}$$

$$\Delta e'_{1i} = \frac{4T_i^2 - \beta_i^2}{4\beta_i T_i^2} \qquad \text{Part II: Equation}$$

$$\Delta e''_{1i} = 0 \qquad \text{Part II: Equation}$$

Thus while the reduced output, Δe_{1i}, at the inflection point is a function of (a), the bridge ratio: the tangent at the inflection point is independent of the (a) ratio. In most cases to obtain any sensitivity at a given point, it is necessary to compensate or buck the output at the given point and just measure the net voltage of the total circuit. This presents several inconveniences, the most important of which is the difficulty to obtain a very stable compensating or bucking source. Looking at Equation II:12, it is obvious that Δe_{1i} is a function of T_i and β_i which are fixed and (a), the bridge ratio, which is variable. Thus by changing the value of (a) (obtained by changing either R_1 or R_2), one can supress the reduced output to any value desired. Over a large range of (a) ($a = 0$ to $a = +\infty$), the value of Δe_{1i} varies from $\frac{T_i}{\beta_i} + 0.5$ to $\frac{T_i}{\beta_i} - 0.5$, and, as in our case $\frac{T_i}{\beta_i} \approx 0.1$, Δe_{1i} varies approximately from 0.6 to - 0.4. There exists therefore a value of (a), such that $\Delta e_{1i} = 0$, and for which the tangent at the inflection point is finite and independent of (a). Experimentally then, it is possible to measure changes of temperature of very small magnitude ($0.001^{\circ}C$).

While carrying out these fast-stretch tests, it was noticed that the thermistor output was not returning to its original base line, even after a relatively long period of time. From a rough calculation of heat dissipation through the sample, it was deduced that all of the heat should have been dissipated within a few minutes of the stretch so that the thermistor could not indicate residual stretching heat. From Fig. 41 it can be seen that at the end of some 3 minutes (x axis: 50 secs/cm) the signals reached a steady value. Even though the base lines are different, they are parallel. Therefore, either the thermistor is responding to some other variable than temperature, or there is some process taking place in the sample which is exothermic. It is also very important that the applied potential across the Wheatstone bridge be a constant. A small drift in E can give a considerable change in base lines.

We examined the latter hypotheses first, but since neither relaxation nor crystallization could be seriously considered (stress relaxation work convinced us that under these conditions the relaxation was minimal, while at small elongations of the order of 100% there could not be any crystallization phenomenon accounting for an exothermic process), we turned our attention to the possible

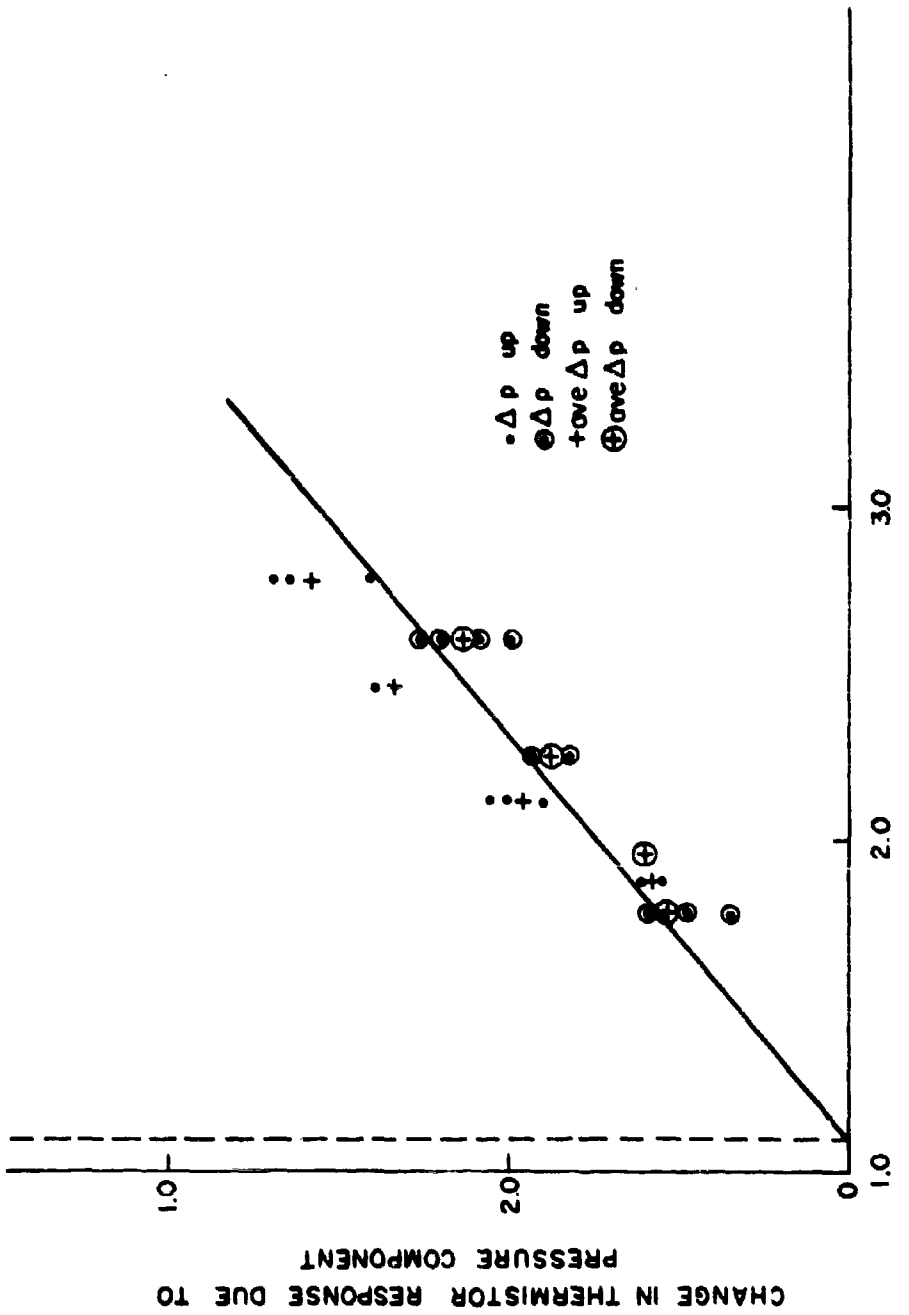

Fig. 42 : Effect of Stress-Thermistor

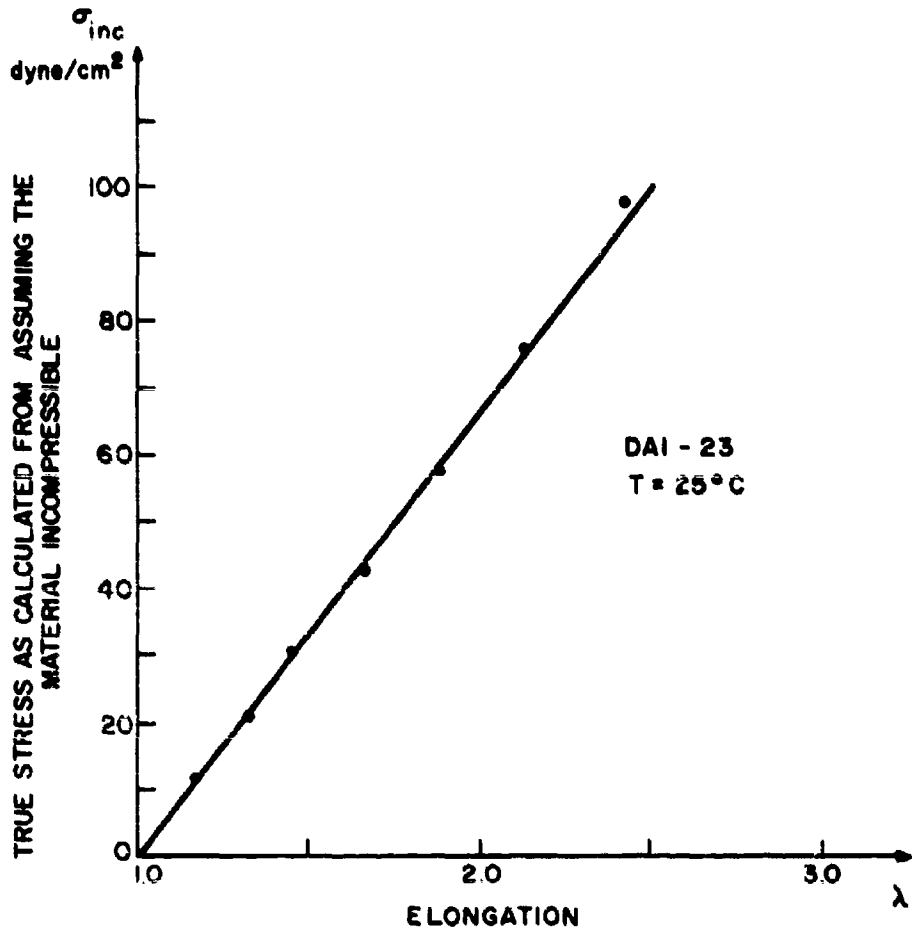

Fig. 43 : True stress as a function of strain

response of the thermistor to some other variable. Plotting the reversible difference in base lines as a function of strain (Fig. 42), we found that, neglecting some scattering, a straight line could be drawn through the point at which we started to stretch. This observation combined with the fact that, if stretching took place slowly, the difference in base lines observed was the same as for a fast stretch, led us to conclude that the thermistor was pressure sensitive and that the plot of (Fig. 42) amounts to a measure of true stress as a function of strain. A careful comparison of the true stress as a function of strain, (Fig. 43) shows a linear relationship between this and the course of the thermistor base line. Thus monitoring the fast stretching experiment by a thermistor leads to the combined measurement of the stress and the temperature rise. Unfortunately, there is too much scatter in the points (Fig. 42) to enable us to use this technique to measure the stress in the rubber directly. However due to the differences in time response of pressure and temperature on the thermistor (temperature time response is practically immediate), the temperature rise upon stretching is given by the total peak, while the incremental pressure is given by the differences in base lines.

A. Calibration of Thermistor 4

Using a LEEDS-NORTHRUP CO., Wheatstone bridge, catalogue number 4760, in conjunction with a large 2 volt WILLARD battery and a Dc millivoltmeter from SENSITIVE RESEARCH Instrument Corp., Mount Vernon, New York, we measured the resistance R of the thermistor at a series of temperatures. Treating the R-T data as shown in Part II, it was readily possible to calibrate the thermistor (Appendix II).

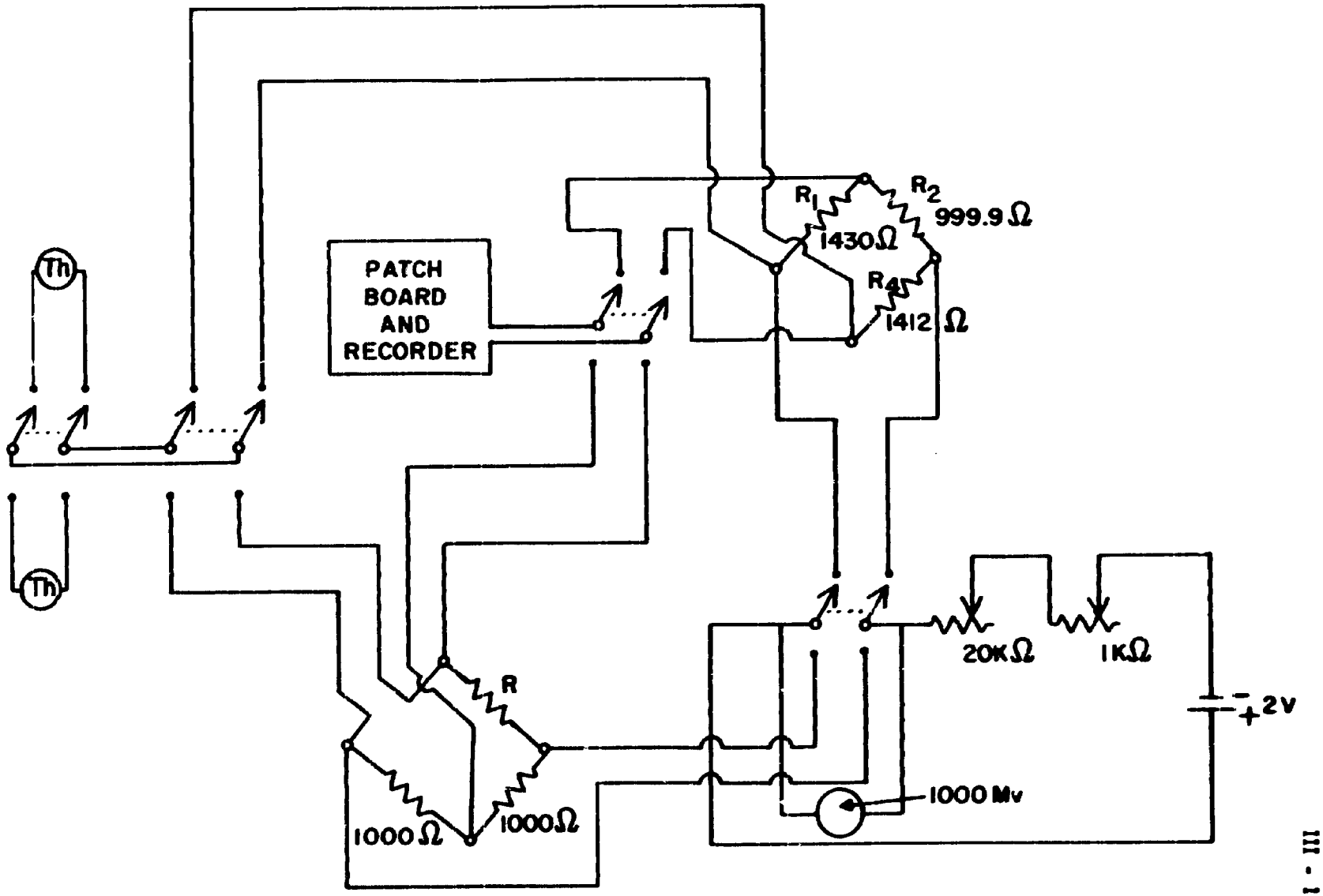
Th
Th
PATCH
BOARD
AND
RECORDER
R1
R2
999.9 Ω
1430 Ω
R4
1412 Ω
R
1000 Ω
1000 Ω
20K Ω
1K Ω
2V
1000 Mv

Run #	L of recorder	L of rubber (cms)	λ_{final}	$\Delta T^{\circ}C$	"Δp" cms
1	30.6	11.8	1.62	0.028	—
1'				0.017	———
2	—	—	—	0.028	———
2'				0.014	———
3	40.2	13.6	1.87	0.073	0.55
3'				0.064	0.60
4	—	—	—	0.065	0.60
4'				0.058	0.60
5	50.0	15.5	2.12	0.105	0.90
5'				0.068	1.00
6	—	—	—	0.105	0.95
6'				0.078	1.00
7	62.2	17.9	2.45	0.170	1.30
7'				0.160	1.30
8	—	—	—	0.162	1.30
8'				0.157	1.40
9	77.8	21.0	2.88	0.232	1.65
9'				0.224	1.70
10	—	—	—	0.226	1.55
10'				0.207	1.40
11	68.0	19.1	2.60	0.168	1.00
11'				0.168	1.20
12	—	—	—	0.170	1.10
12'				0.165	1.25
13	54.5	16.4	2.25	0.129	0.85
13'				0.109	0.85
14	—	—	—	0.126	0.85
14'				0.120	0.90

TABLE V

Summary of fast-stretching experiments

TABLE V Cont'd

Run #	L of recorder	L of rubber (cms)	λ_{final}	ΔT^{e} C	"Δp" cms
15	43.6	14.3	1.96	0.081	0.60
15'				0.078	0.60
16	—	—	—	0.086	0.60
16'				0.073	0.60
17	36.0	12.[illegible]	1.72	0.061	0.50
17'				0.056	0.45
18	—	—	—	0.067	0.60
18'				0.056	2.50

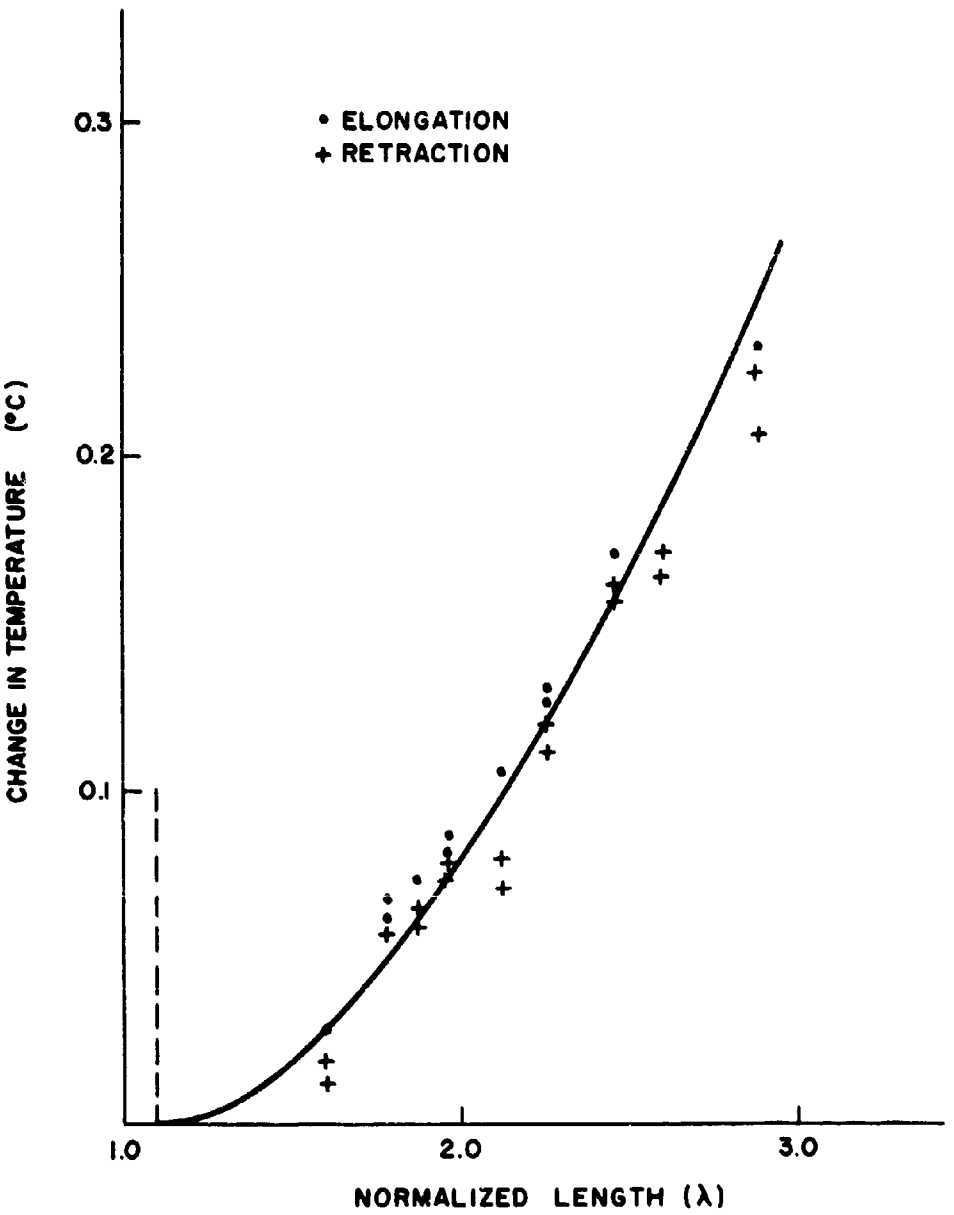

Fig. 45 : Change in Temperature upon elongation and retraction of Rubber

II. RESULTS

A typical sample of natural rubber cut out from the same sheet as those used in other experiments (number DA1-26) was employed in the experiment described in detail below. It had the following dimensions:

Zero length = 80 mm, width = 4.02 mm, thickness = 1.90 mm, length at rest = 73 mm, area = $7.638 \cdot 10^{-2}$ cm^2

The operating temperature was 28.25 °C, and the thermistor circuit set at (Fig. 44):

E = 1 volt, R_1 = 1430 Ω, R_2 = 999.9 Ω, R_4 = 1412 Ω, a = 1000

The stretching of the sample starts from a slightly elongated position (λ = 1.10) so as to minimize errors attending the "rest" state and also to reduce the effect of the relaxation spike. The whole problem will be dwelt upon in detail below in the Discussion section but, briefly, what seems to happen is that when the rubber is rapidly brought back by our sample holder from the stretched to the unstretched condition, its own retraction speed is slower than the movement of the solenoid, and its shape becomes momentarily buckled during the relaxation to zero force. The sample returns then to its original shape and elongation of 1.1 slowly and thus returns to a state of slight stress. This return is better defined than one to complete rest.

Fig. 39 shows the linear calibration used for determining the increase in length of the sample upon stretching. Table V shows the final elongations to which the rubber was stretched, as well as the differences in base lines and changes in temperature.

Figure 45 shows the increase and decrease of temperature as a function of elongation, remembering that the original elongation from which rubber is stretched is 1.10.

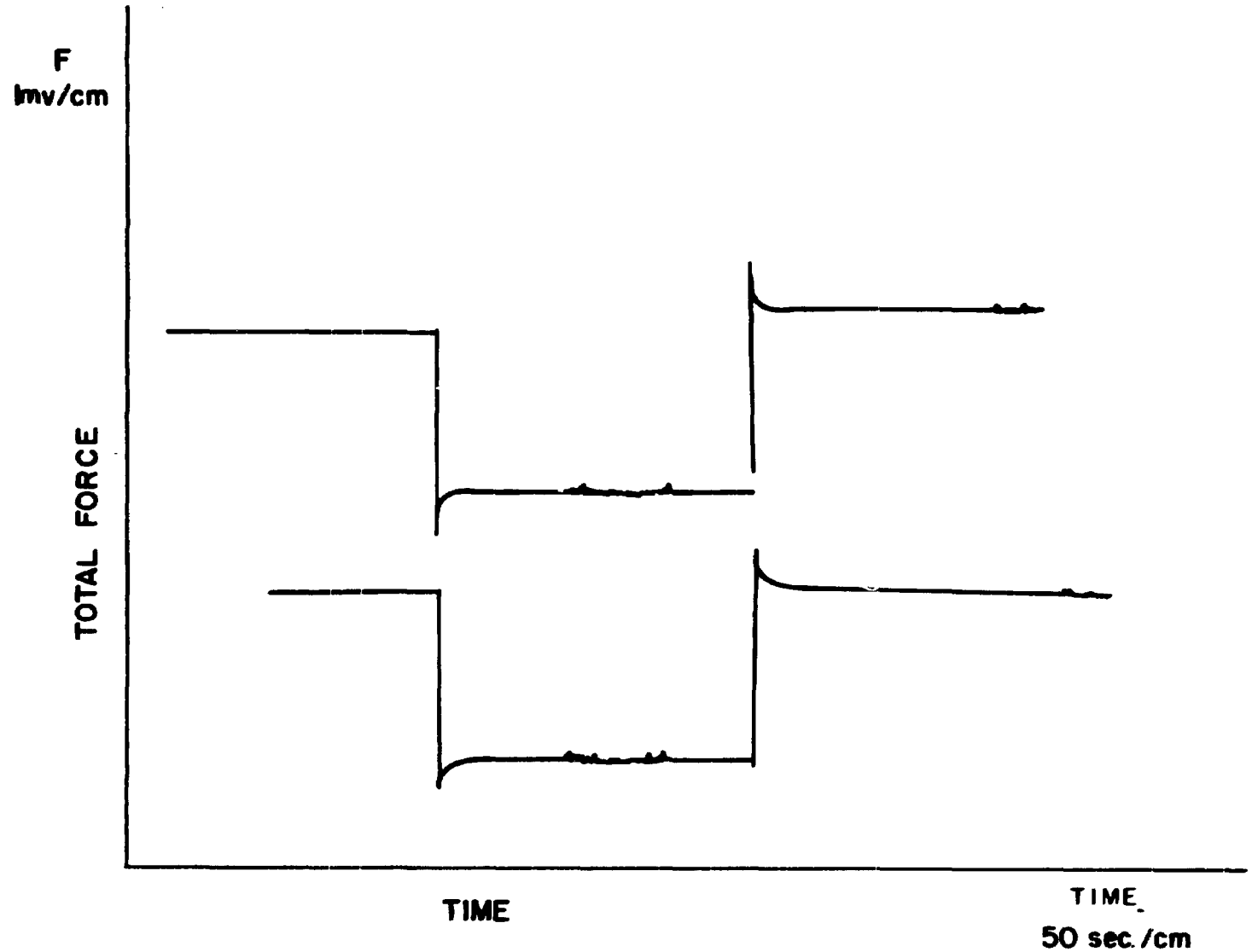

Fig. 46 : Relaxation of "spikes"

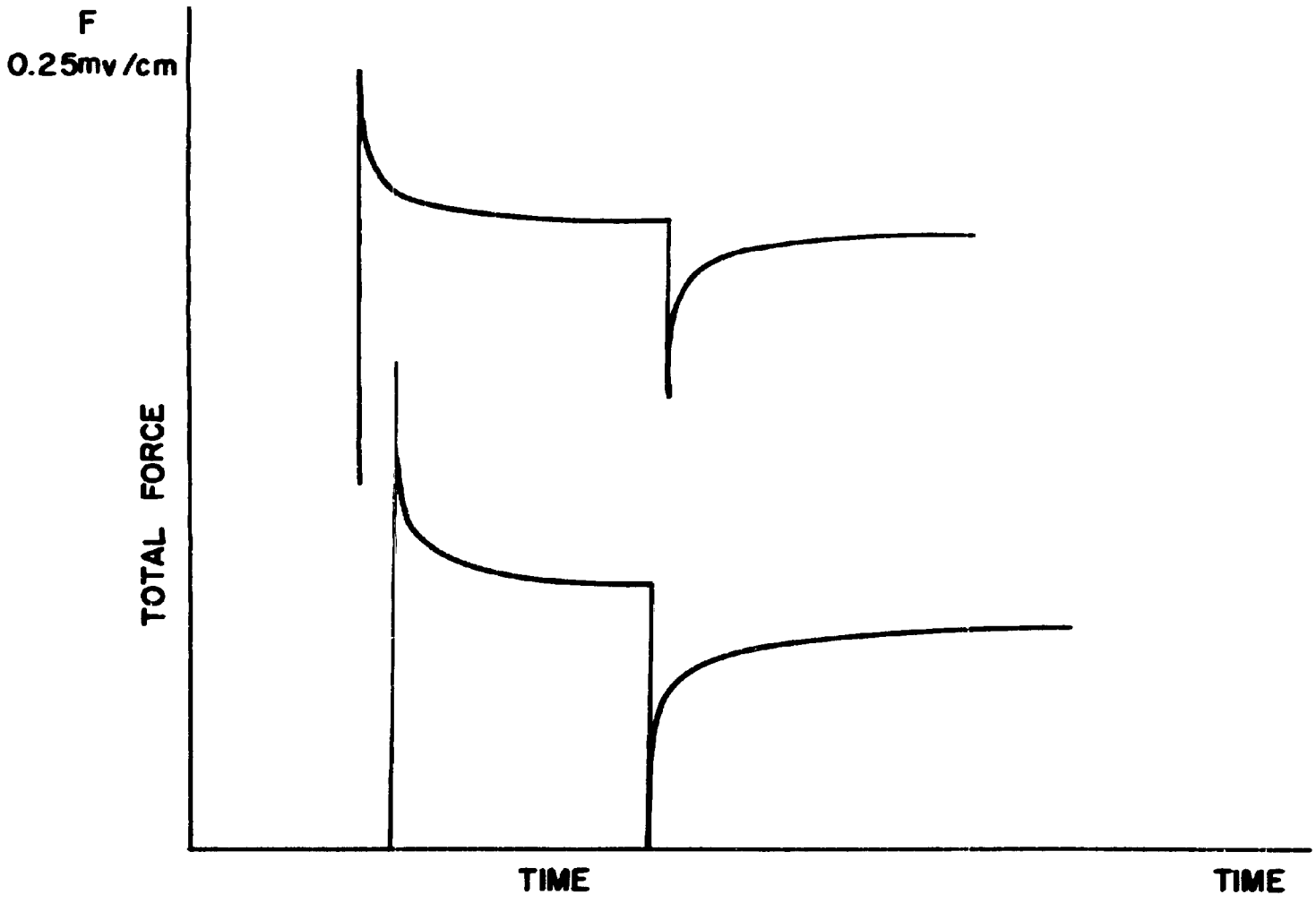

Fig. 47 : Relaxation of spikes at 54° C using bucking potential

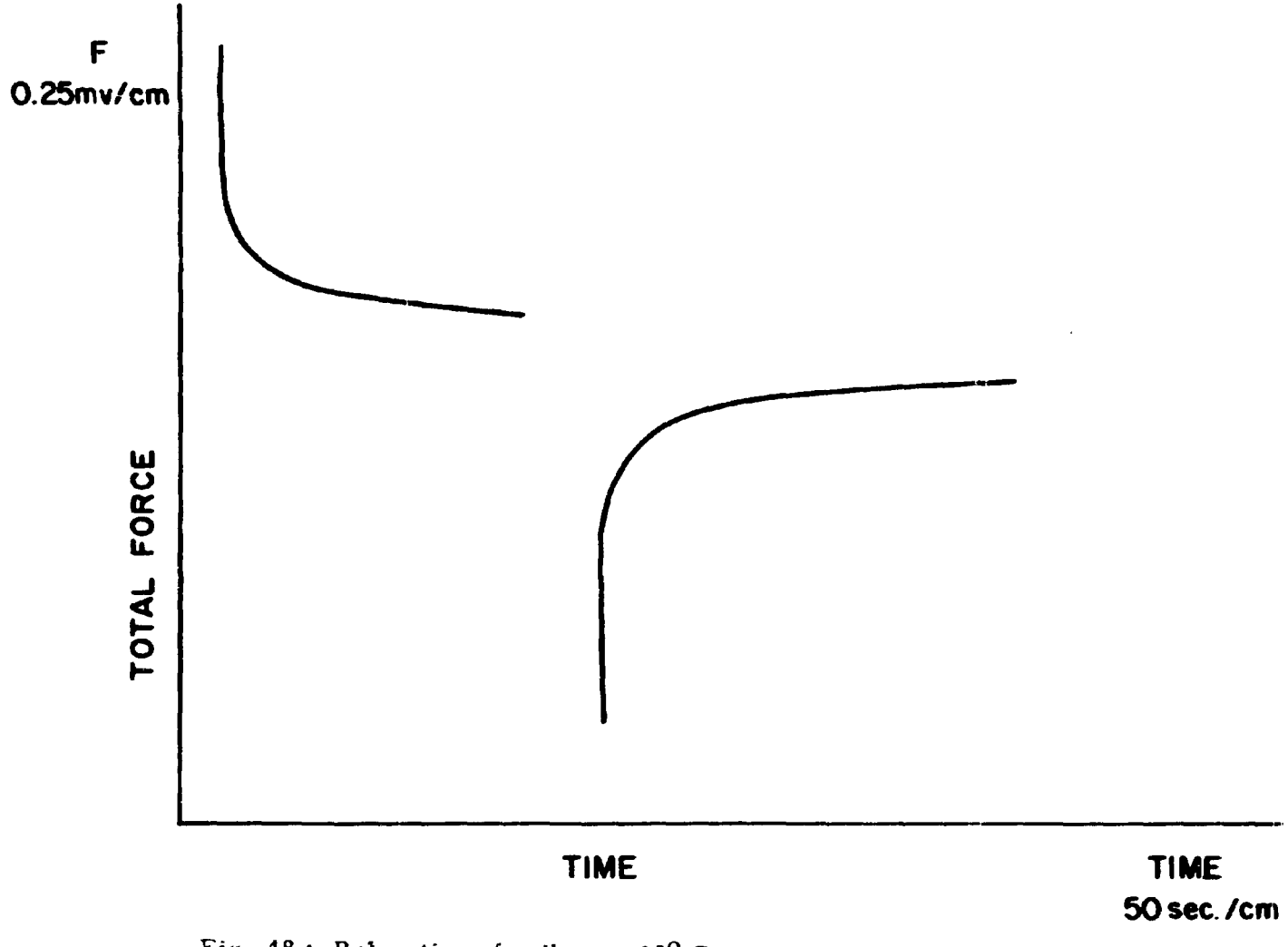

Fig. 48 : Relaxation of spikes at 30° C using bucking potential

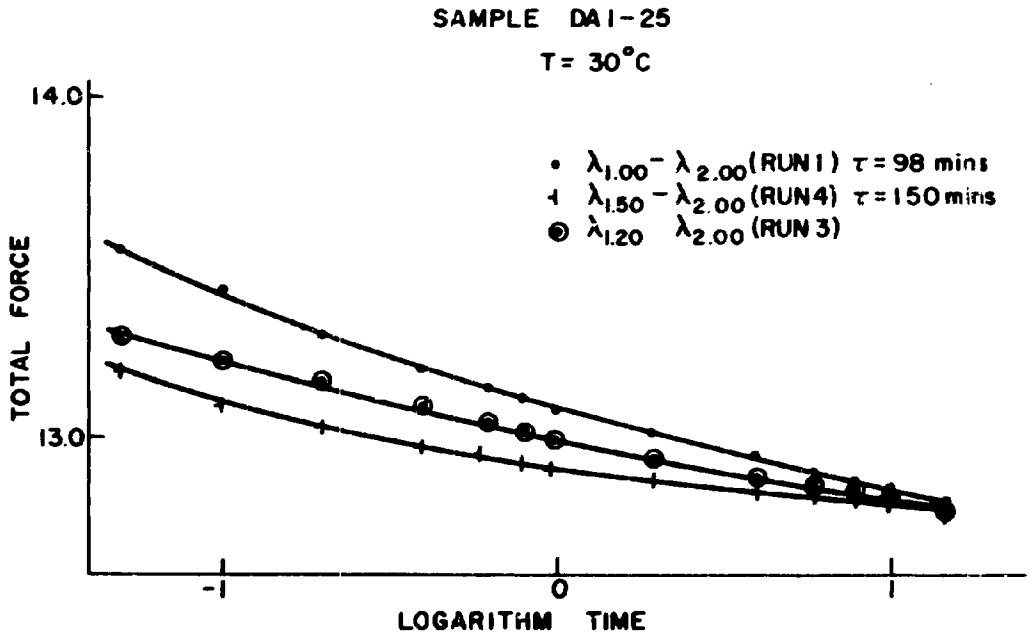

Fig. 49 : Effect of a pre-elongation upon stretching of rubber

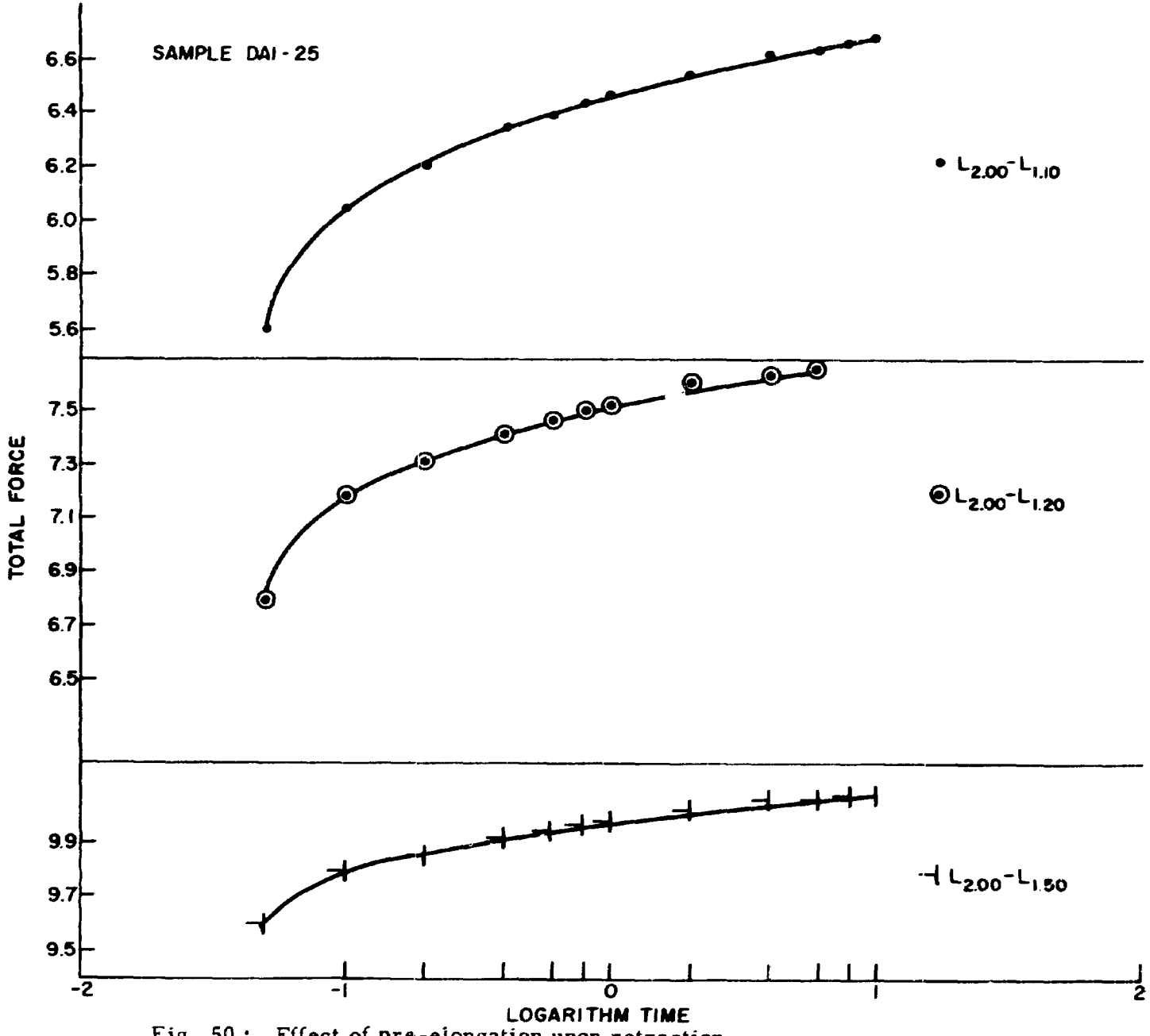

Fig. 50 : Effect of pre-elongation upon retraction

III. DISCUSSION

The experiments of fast-stretching approximate adiabatic conditions. If the stretching of the sample is performed sufficiently fast, then the heat developed on account of the loss of entropy ($dQ_{rev} - TdS$) is measurable as the temperature rise of the sample. Retracting, the sample turns colder, as the entropy returns towards its maximum value at rest. In the process of retraction, in the ideally adiabatic experiment, one should be able to measure a hysterisis in the rate of return of the sample to the unstressed state since ΔS is positive, the reaction endothermic and yet no heat available from the environment. In the case of atomic gases, which would expand in analogy, the increase in entropy would be immediately balanced by corresponding cooling. In the case of rubber the additional number of conformations can be assumed only by drawing on the energy reservoir of rotational and vibrational degrees of freedom which means that while the rubber becomes more random it also becomes less mobile. This is the same process which causes the gas atoms to cool but cooling in the case of rubber means lower mobility and thereby a slower return to its rest length. In other words, for rubber to return to its original shape with the same speed with which it could be extended would require an influx of heat or a not fully adiabatic experiment.

It is then interesting to notice the time effect on the force (Fig. 46) when the sample is being stretched, while all three variables, namely the rise in temperature of the sample, the length to which the sample is being stretched, and the total force applied on the sample, are being plotted simultaneously. There seems to be a relaxation of the force to a reasonably steady value after several minutes after the sample has been stretched fast (1/10 second) to a constant length. This phenomenon was much more clearly established when a counter e. m. f. (bucking force) of approximately 12 mv was used to measure the total e. m. f. of 13 mv. (Figs. 47, 48). In order to elucidate the nature of these force peaks, two functions were examined. Firstly, the effect of the pre-elongation from which the sample is stretched, and secondly the influence of temperature. From Figures 49 and 50 it is clear that for stretches to the same final length, the lower the initial length, the steeper is the relaxation from the maximum height of the spike. Figure 49 shows the relaxation curves for the elongating samples. The equilibrium force attained is the same whatever the initial elongation, as it should be. One

can calculate a relaxation time for the recovery from the overshoot force which turns out to be the shorter the more the sample has been pre-stretched. This difference in stretching distance arises of course from the fact that different elongations were ob ned. We find for the sample stretched from rest length to a $\lambda = 2.00$, a relaxation time of about 150 minutes for the slow relaxation range of the sample stretched from $\lambda = 1.50$ to 2.00. As might be expected from the sharpness of the spike marking the overshooting of force, there is also a very fast relaxation regime which for all the runs is of the order of $\tau = 1.5$ minutes. Interestingly enough the relaxation process for this internal local overextension of the sample has only two relaxation steps. On retraction the samples start from the same strain, arrive at the different elongations so that equilibrium forces at the end of the experiment are correspondingly different. Again an overshooting is observed, now towards the low side of the force. In fact the sample can be observed temporarily to buckle so that it is obvious that it does not retract with its spontaneous speed but is being pushed. The recovery to the equilibrium force again differs for the 3 samples but the relaxation times are difficult to establish because the time when the sample assumes its equilibrium length are hard to ascertain.

To explain these observations it is postulated that the overshooting of the force at the end of the stretching is due to the high speeds of the test, too high for the chains to follow the motions in an affine manner and the net effect is an increase in labile entanglements, that act as temporary additional cross-links and raise the modulus. When the motion stops, the force decreases steadily because of relaxation and disappearance of the network of labile crosslinks. Stating it differently, the chains are impeded in their extension and aligning by preexisting entanglements and internal viscosity. Thus one can understand that the relaxation of the force in the experiments producing the greatest elongation should have the fastest decay since in this case more labile crosslinks (shorter - τ) have been created. Pre-stretching the sample to an appreciable elongation means that the chains are more equilibrated towards the final strain and there is less additional entanglements on further stretching.

During the retraction process complications of molecular motion should be less due to entanglement processes and more to the fact that the internal friction may not allow the chains to return to their random conformations during the

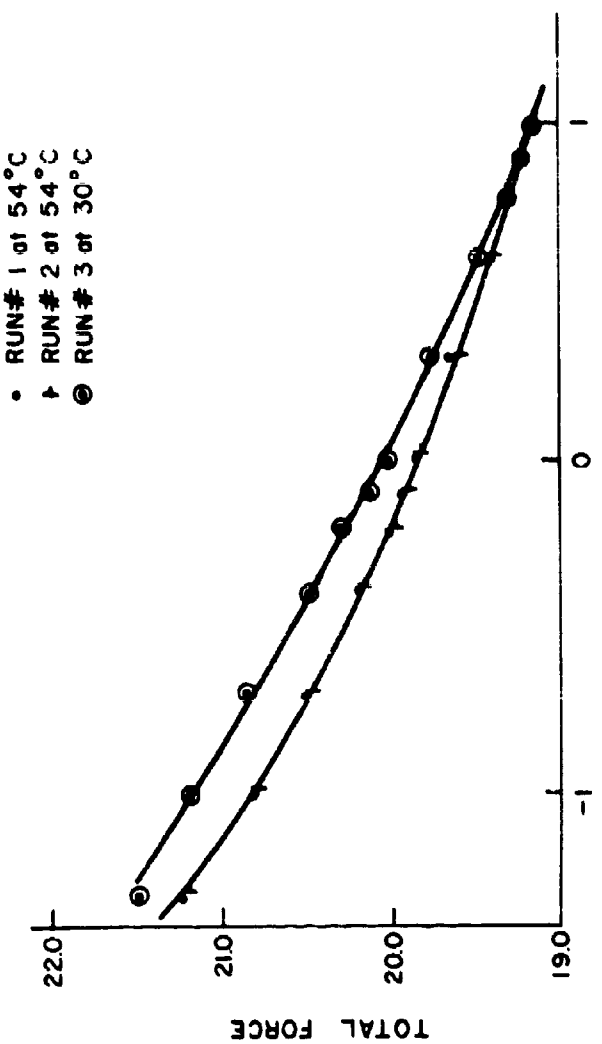

Fig. 51 : Effect of Temperature upon stretching of rubber

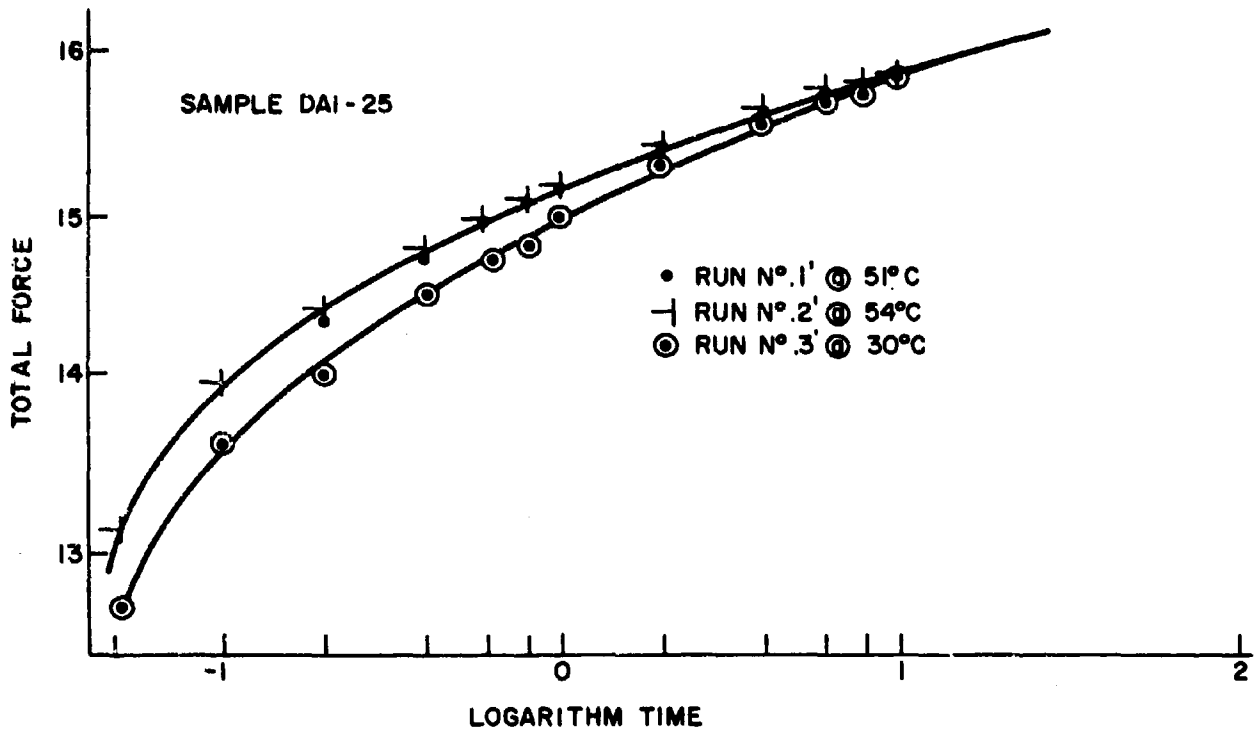

Fig. 52: Effect of Temperature upon retraction of rubber

instrumental time interval. This lag will be enhanced by the largely adiabatic character of the retraction which permits the chains only to a small extent to acquire the necessary influx of enthalpy from the surroundings and has to rely largely on conversions from the internal energy reservoir. The picture is one of a substantial number of molecules not recovering their rest length fast enough, the sample stays longer than if it would contract in less than the instrument time and in fact it can be seen to buckle and bow during the fast push back. In this context, it is interesting to follow the effect of temperature on these phenomena. Figures 51 and 52 show the action of temperature on the relaxation of the force as a function of time. Figure 51 demonstrates that at higher temperature the force relaxes faster. This is to be expected, especially on the basis of our picture of labile entanglements. One can see also on Figure 51 that the results are completely reproducible, (runs 1 and 2) and that the points lie on the same relaxation curve. Figure 52 shows the comparable behavior for the retraction relaxation curves. It would be interesting to examine the phenomenon of time dependent moduli as affected by the speed of stretching more quantitatively. Ordinarily the relaxation times of a well vulcanized rubber are too short to become noticeable during ordinary stretching experiments. In our case we have a rather weakly cross-linked rubber which permits entanglements to become more effective and to form time dependent cross-links which, as the experiments show, exhibit much longer relaxation times.

Finally the specific heat of our rubber at constant length and pressure was calculated using Equation 63 :

$$\int C_{L,p}\, dT = T \int \frac{(\partial f/\partial T)_{p,L}}{V \rho}\, dL$$

and integrating this expression between L_o and L assuming the approximation that $C_{L,p}$ is independent of T, which is acceptable because of the small ΔT we obtain that

$$C = \frac{T \int (\partial f/\partial T)_{p,L}\, dL}{\rho V \quad \Delta T}$$

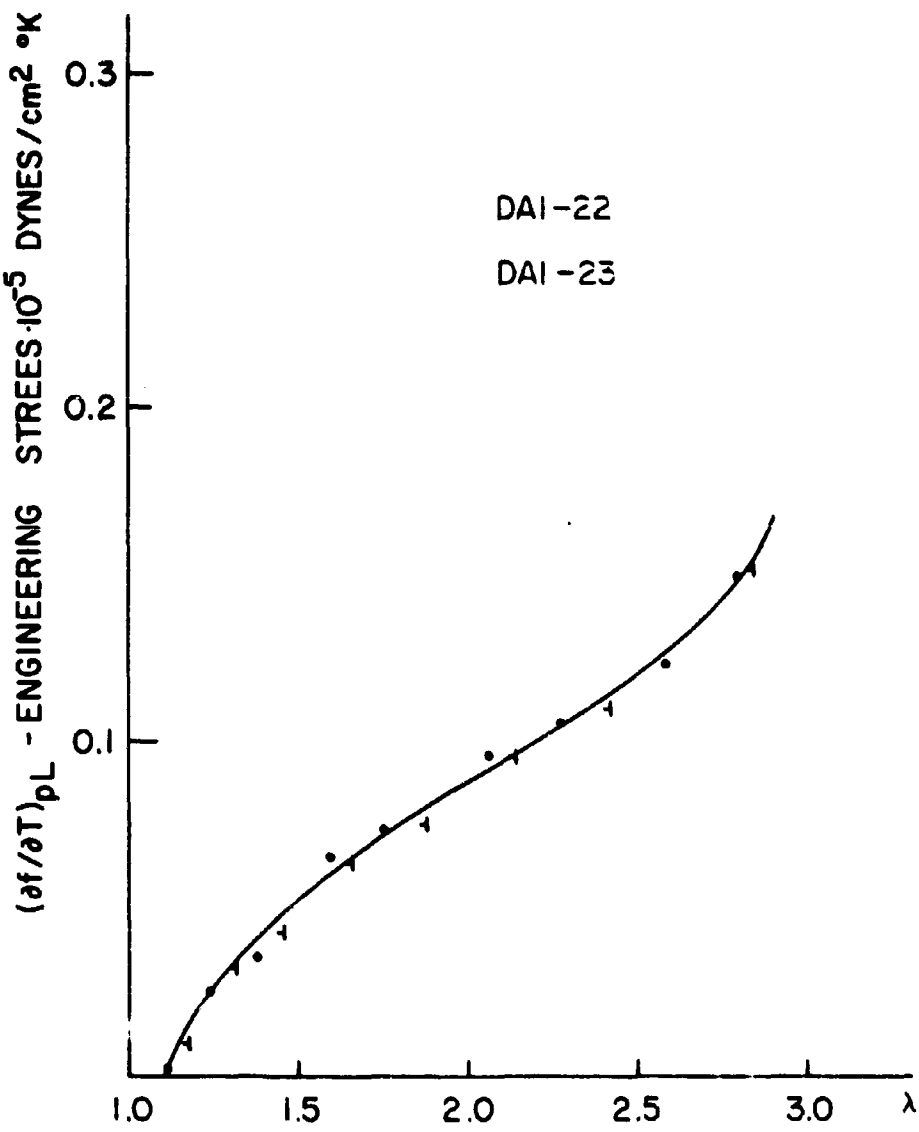

Fig. 53 Engineering Stress-Temperature Coefficient as a function of Uncorrected Normalized Length.

This expression can be further simplified, by setting

$$\lambda = L/L_o$$

or $$d\lambda = dL/L_o$$

and since $V = V_o = L_o A_o$, then

where A_o : initial area

$$C_{L,p} = \frac{\int_{\chi_i}^{T} \lambda f \, (\partial f_{eng}/\partial T)_{p,L} \, d\lambda}{\rho \, \Delta T} \qquad (69)$$

with $f_{eng.}$ as the stress per unit undeformed area.

Calculation of the integral of the force-temperature coefficient is done by the use of a planimeter. Figure 53 shows the plot of $(\partial f_{eng}/\partial T)_{p,L}$ as a function of λ. All elongations start at $\lambda = 1.1$ for reasons that we have already discussed.

λ final	area of $(\partial f/\partial T)_{p,L}$ cm^2	$(\partial f/\partial T)_{p,L}$ 10^{-3}	ρ est.
1.50	0.031	1.225	0.91
1.75	0.072	2.840	0.91
2.00	0.121	4.780	0.92
2.25	0.179	7.060	0.92
2.50	0.247	9.750	0.93
2.80	0.351	13.880	0.93

TABLE VI: Values of $(\partial f/\partial T)_{p,L}$ and ρ estimated

Application of Equation (69) permits one to calculate $C_{L,p}$ as mentioned before. The specific heat at 300 ° K is given below

λ final	$T\int_{\lambda_i}^{\lambda_f}(\partial f/\partial T)_{p,L}\,d\lambda \cdot 10^{-5}$	ΔT	$C_{p,L}$ cal/g°C
1.50	3.675	0.019	0.505
1.75	8.520	0.045	0.495
2.00	14.340	0.080	0.465
2.25	21.180	0.120	0.455
2.50	29.250	0.165	0.452
2.80	41.640	0.225	0.470

TABLE VII : Values of $C_{p,L}$ at different elongations

Thus the specific heats calculated from the adiabatic temperature rise and from the force temperature measurements are quite similar to those of natural rubber measured by calorimetric means [51] i. e. have a value of 0.480 cal/g° C at 300° K. The agreement is deemed good considering the fact that there is appreciable scattering of the measurement of $\Delta T_{adiabatic}$ and also the fact that we were engaged here in an indirect method of measurement.

The specific heat of the rubber as expected, decreases with increasing elongation. Our numbers should be taken as approximate rather than quantitatively. The decrease in specific heat observed is 10% . Bekkedahl and Matheson [51] have shown that there is a decrease of some 8% in the specific heat of partly crystalline rubber versus the amorphous sample. When chains stretch and align, there is a loss of some degrees of freedom. In the random conformation, the molecules have 3 vibrational degrees of freedom, and some of the possible 3 rotational . When they align and or start to crystallize, there is a freezing of vibrational degrees of freedom along the long dimensions of the chains and also of some rotational motions expressing itself as a net decrease in specific heat. It would be very interesting to measure the specific heat of various elastomers at different elongations and temperatures. These results should then be compared to the results obtained from direct calorimetric measurements, and x-ray, I. R. and birefringence data.

IV APPENDIX II

Calibration of Thermistor # 4

A. Resistance as a function of Temperature

Run	T°C	R Ω	T°C	R Ω	T°C	R Ω
1	33.99	1740	29.96	2018	25.91	23.48
2	33.94	1744	29.92	2023	25.90	2350
3	33.91	1744	29.89	2025	25.88	2353
Ave.	33.95	1742	29.91	2022	25.89	2350

TABLE VIII: Resistance as a function of temperature

B. Determination of β 30.00° C

T°C	T°K	1/T 1/°K	R Ω	$\log_{10}$ R	β °K
33.95	307.10	0.0032563	1742	0.2410	3446
29.91	303.06	0.0032996	2022	0.3058	3385
25.89	299.04	0.0033440	2350	0.3211	

TABLE IX: Determination of β 30.00°C

where $$\beta = \frac{2.3026 (\log_{10} R_1 - \log_{10} R_2)}{1/T_1 - 1/T_o}$$

and at 29.91°C, β = 3415° K, R = 2022 Ω

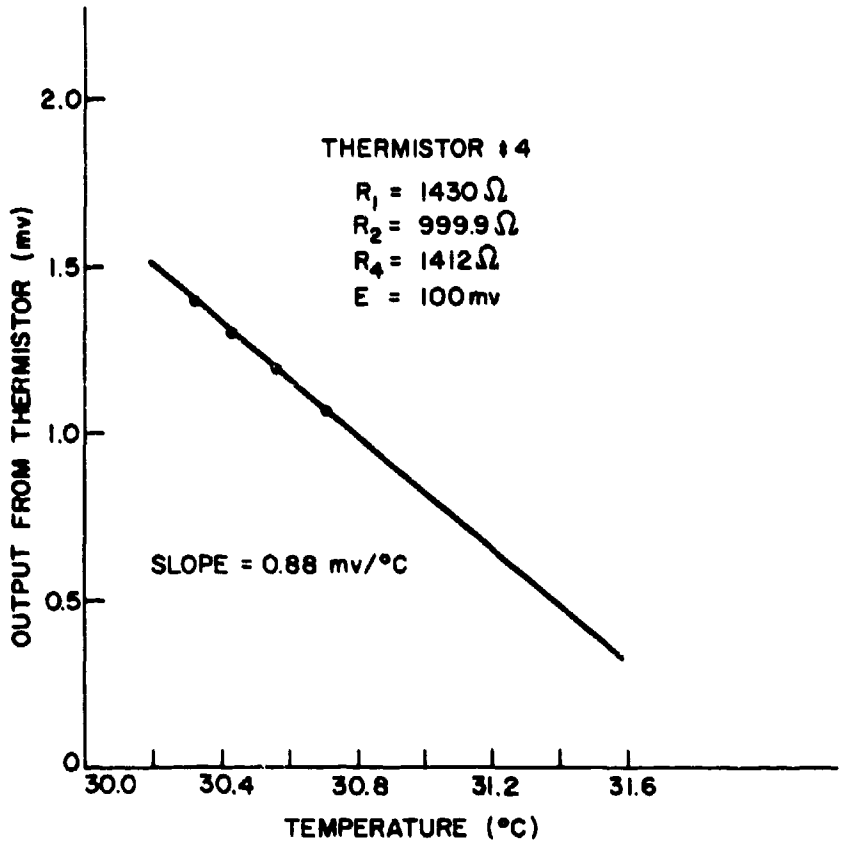

Fig. 54 : Calibration of Thermistor # 4 imbedded in rubber specimen

C. Determination of R_4

$$R_4 = R_{31}\frac{R_1 - 2T_1}{R_1 + 2T_1} = \frac{2022\,(3415 - 606.12)}{(3415 + 606.12)} = 1412\ \Omega$$

D. Checking of Therm stor # 4

$$\Delta e_{1i} = T_1/R_1 - 0.500 \text{ for } a = 1000$$

$$\Delta e_{1i} = -0.4113 \text{ mv/mv}$$

Using E = 100 mv, R_1 = 100 Ω R_2 = 0.1 Ω and R_4 = 1412 Ω.

$$\Delta e_{1i} = -0.4137 \frac{\text{mv}}{\text{mv}}$$

$$\Delta e'_{1i} = \frac{4T_1^2 - R_1^2}{4R_1T_1^2}$$

$$\Delta e'_{1i} = -9.002 \cdot 10^{-3} \frac{\text{mv}}{\text{mv}} /^\circ\text{C}$$

T°C	mv
30.33	1.39
30.44	1.30
30.56	1.19
30.71	1.06

See Figure 54 , which shows the calibration of the thermistor actually imbedded in the sample.

$$\Delta e'_{1i} = -0.88 \cdot 10^{-3} \frac{\text{mv}}{\text{mv}} / ^\circ\text{C}$$

SECTION III

DILATOMETRY OF NATURAL RUBBER

Approximate dimensions: 12" x 12" x 12"

Cavities 1 " deep

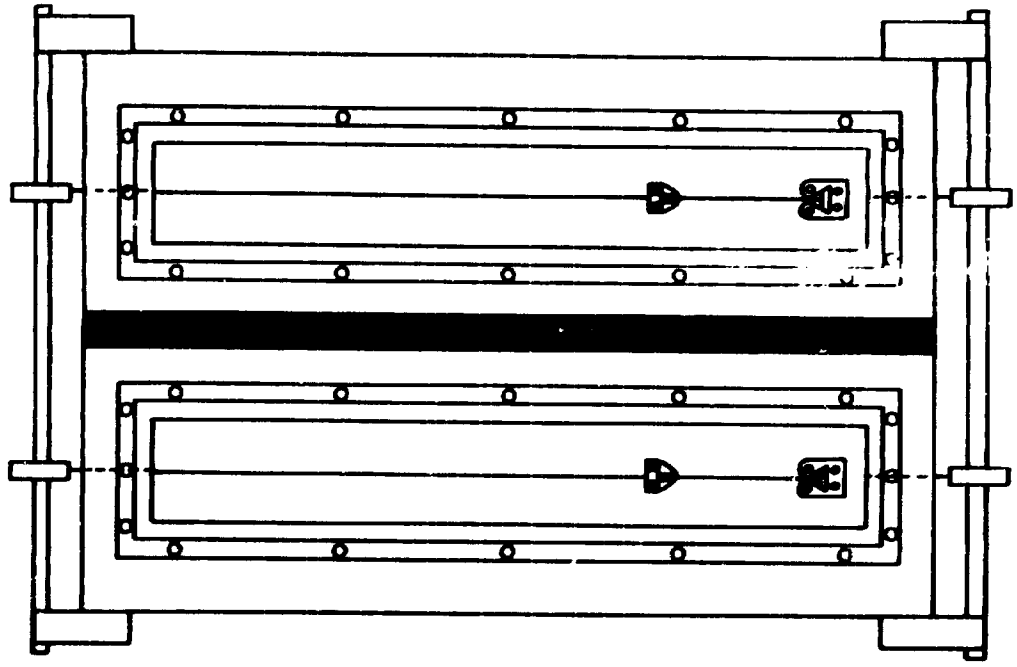

Fig. 55 : Top view of Dilatometer

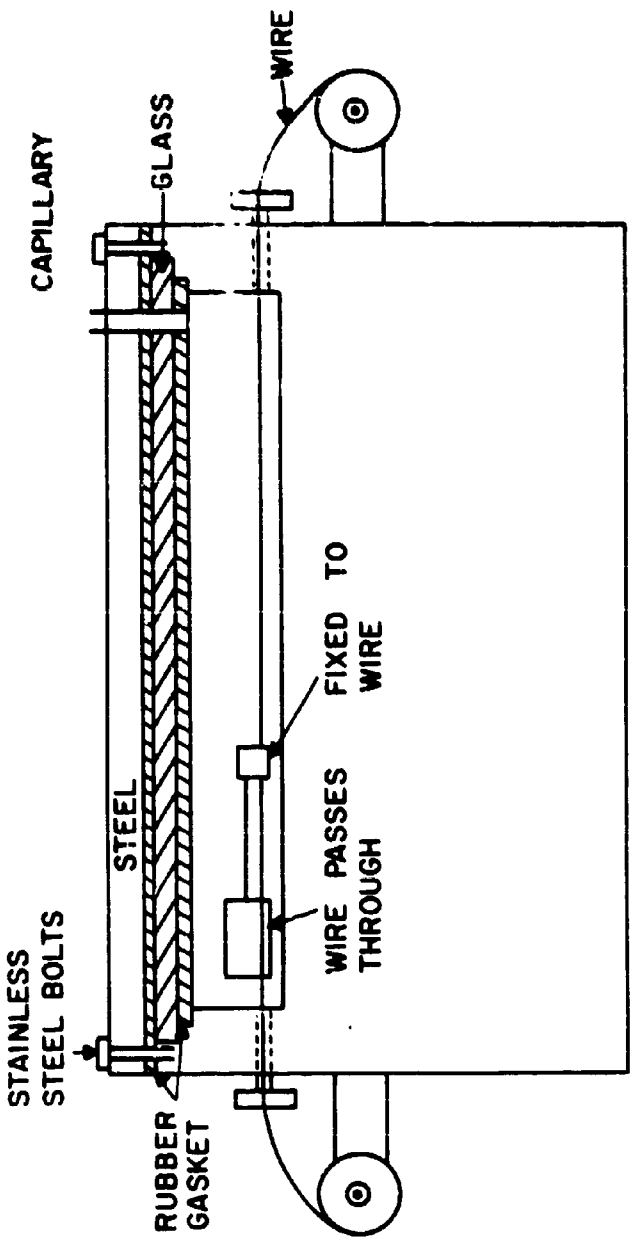

Fig. 56 : Cross sectional view of Dilatometer

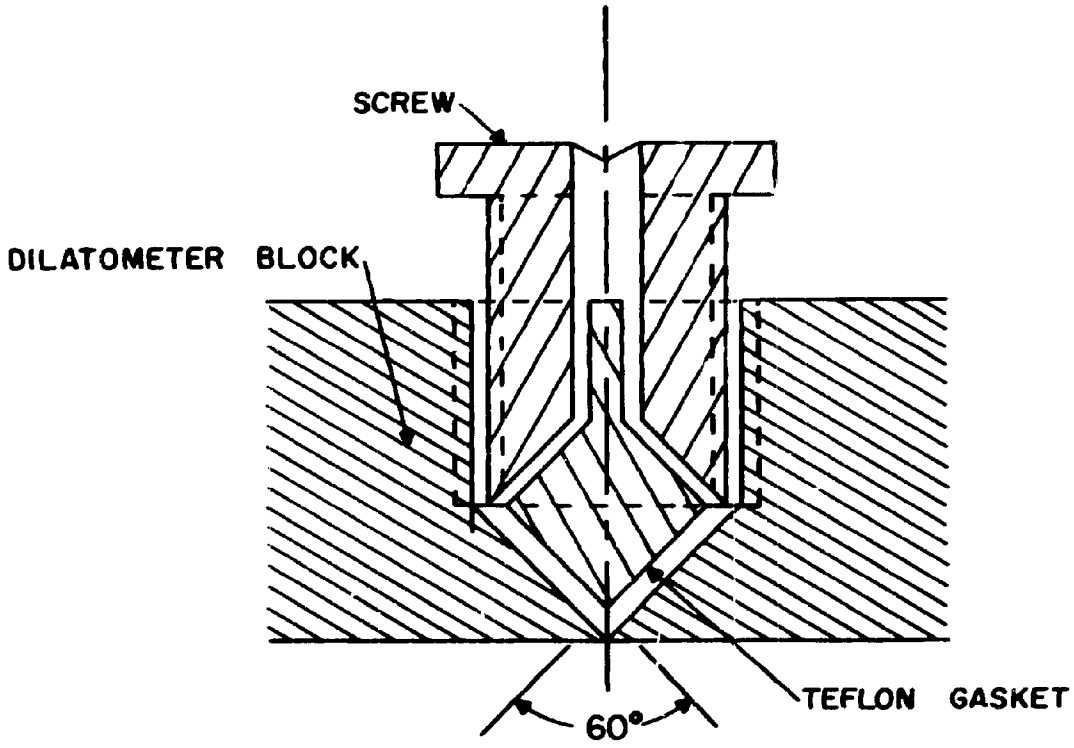

Fig. 57 : Cut through Dilatometer Teflon Gasket

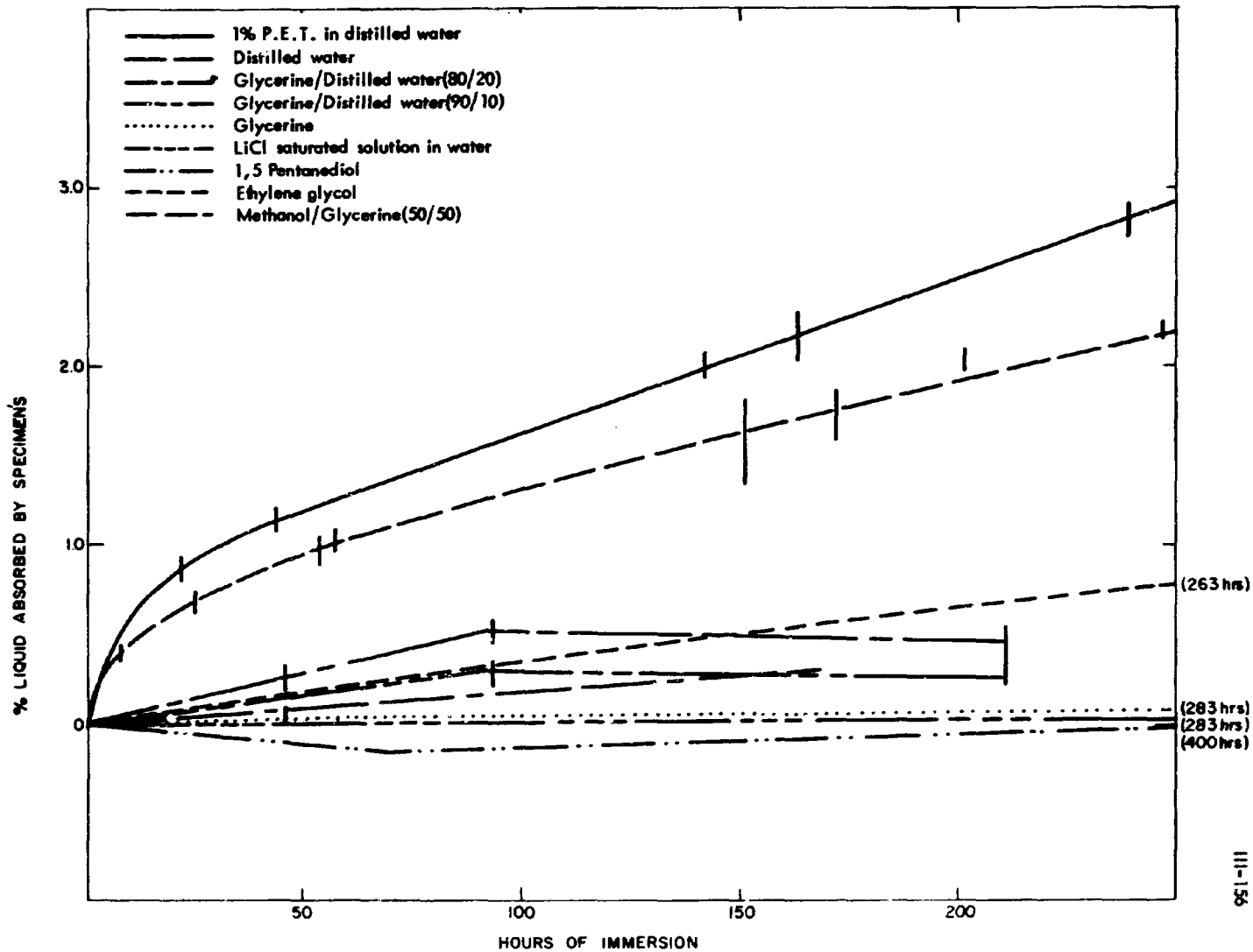

Fig. 58- Swelling of Rubber by various Liquids

I. EXPERIMENTAL

The change in total volume of a typical rubber during stretching as we have seen previously, is very small, of the order of 10^{-4} cc/cc [36, 37 38]. Our basic design of the dilatometer and the method of testing resembles closely the methods used by Dr. Buckely at the Esso Research Laboratories. Figures 55, 56, 57 show sketches of the aluminum dilatometer machined by R. Parla at the Brooklyn Polytechnic Institute. Following Buckely's claims, we planned first to place the dilatometer in an air bath controlled to $\pm$ 0.01°C; it was thought then to be easy to obtain a control of $\pm$ 0.001°C in the dilatometer cavity on account of the large heat sink constituted by the mass of metal. Constancy to 0.001°C was thought necessary to ensure that thermometer effects would be an order of magnitude smaller than the volume changes due to the stretching of the samples. Buckely and his group used Nichrome wire, commercially available, and showed that the variation in thickness of the wire was negligible, so that the construction of the dilatometer could be based on a design with pull from the outside. As will be shown in the Results section, this was proved to be correct. Unfortunately other essential features of the Esso dilatometer proved to be unworkable, and our dilatometric technique had to be extensively changed. In particular, Buckely and co-workers' use of water as the confining liquid like others quoted before, again supported our original idea of working at 3.97°C, at which the coefficient of thermal expansion of water is nil, had to be abandoned, since water was found to swell rubber, even over short periods of time [52].

It was also noticed that our natural rubber became discolored upon long immersions in water and a detailed analysis of the behavior of this elastomer in various liquids was undertaken. Fig. 58 shows the percent weight change as a function of time of natural rubber in various liquids. [52] While no claim is made as to the change in volume upon immersion, these tests do show a distinct and reproducible change in weight. A truly acceptable non-interacting, confining fluid for the dilatometric studies, must not cause any measurable uptake over a substantial period of time. Various salts were added to water. Their effect on the "swelling" is shown in Fig. 58. Many other fluids were tried such as fluorocarbons, other known non-solvents, mono, di-, and trifunctional and alkali salts. Glycerine, pentanediol and Li salts were the only non-swelling agents found for natural rubber. It was rationalized that Li

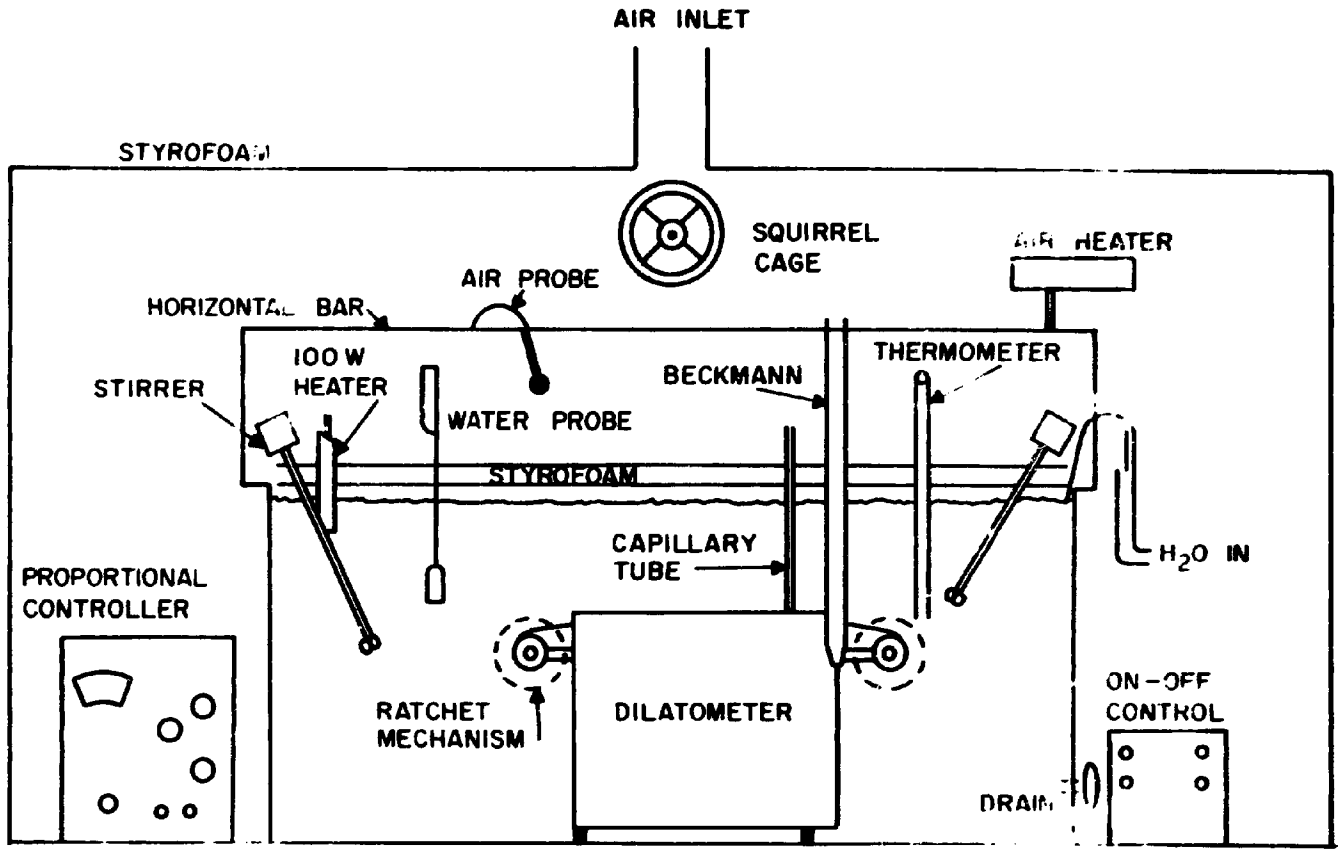

Fig. 59 : Cross-sectional view of constant Temperature bath for Dilatometer

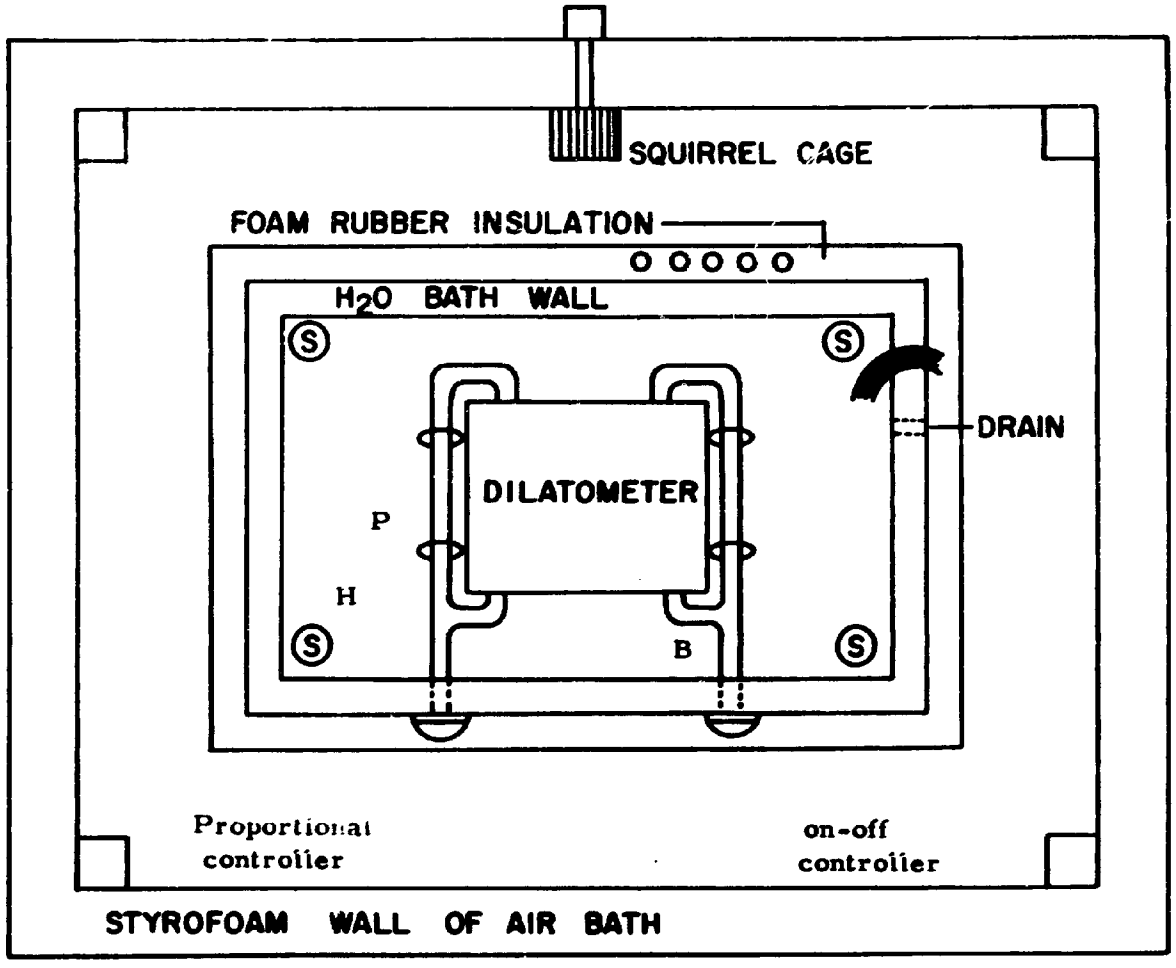

LEGEND

S : Stirrer

H : Heater

P : Probe for Proportional Controller

B : Beckman Thermometer

Fig. 60 : Top view of Constant Temperature bath for Dilatometer

salts were inert because as a result of their large solubility and because of the high charge to volume density of the Li-salts they hold their solvating water most tightly. Li-chlorides as well as nitrates seemed to have no swelling effects. Rather than pentanediol or glycerine, which were too highly viscous and hygroscopic under our conditions it was decided to use the concentrated nitrate solutions because of better metal passivation. For a period of over 200 hours, there was no detectable weight pickup, but unfortunately these salts had a corroding effect on the aluminium block. Various tests were run, and it was shown that a 3 to 5 mil deposit of Nickel metal plated electrolytically on the aluminium seemed to protect the latter from corrosion. All holders, screws and other accessories were also nickel plated or made of stainless steel. A nechrome wire was used to elongate the sample. The sample holder was of the type (self-tightening wedges with rubber pads) as that used in the force-temperature measurements (Fig 13). A detail of the pads is also shown. They were bonded to the wedges with an epoxy resin and, as the sample is stressed, are kept in place by tightening of the wedges. Again, this type holder was found to be very efficient at moderate to high elongations.

The design of the dilatometer is featured further; 2 rubber gaskets form a tight seal with the glass plate (thickness of 5 mm) to which a female joint is attached. A specially constructed doubly inverted teflon seal was designed to allow passage of the nichrome wire through the block, without leakage. Fig. 57 shows a detailed crossectional view of this special gasket. The interchangeable capillaries attached to a fitting male joint can be inserted in the dilatometer fitting. It was found that the thermometer effect of the $LiNO_3$ solution in the cavity required 0.0001°C to ensure base line stability. A constant temperature bath controlling to better than 0.001°C was then designed (Figs 59, 60).

To this end, a few basic principles concerning thermal control had to be observed or elaborated. Firstly all individual factors must be isolated and tested separately. A thermistor bead was used to ascertain the fluctuations in temperature in various areas of the bath. Careful checking with Beckman thermometer in conjunction with the thermistor tested for random departures from the base line of no more than about $5 \cdot 10^{-4}$ °C. It was

essential to hold the temperature within 0.001°C for several days. To this end, a lightening heavy duty stirrer was placed in each corner of the bath. The thermistor control probe was hooked up to a Bayley proportional controller, model 123, Bayley Instrument Company, Danville, California to sense and anticipate the changes in temperature. This unit is guaranteed to ± 0.001° C. In view of the good insulation a glo-quartz immersion 100 W heater was the only heat source for the overall bath.

The evaporation of the water from the bath was the single biggest disturbance. It was found necessary to enclose the water by a surrounding air bath and to heat the air about 3°C above the water temperature which was kept at 34°C and to control the air temperature by a thermistemp on-off contoller, model 171. Slabs of polystyrene foam provided thermal insulation from the room, and a squirrel-cage fan was used to mix the air. Since the lightening stirrers were running quite hot, the air temperature was maintained at approximately 37° C by blowing in cool air with a fan. To maintain a water temperature over a period of days of ± 0.0005°C greatest care must be taken in handling the whole system. Two holes were cut out of the front polystyrene slab and rubber gloves inserted. Further to perform the stretching of the rubber, two axles were guided through the walls of the bath gasketed with 0 ring seals. By turning the shafts, the samples can be stretched without disturbance of the thermal equilibrium.

The solutions of 60 g of $LiNO_3$ /100 cc of H_2O were refluxed for about 24 hours and filtered through milipore filters. The rubber samples were placed into the dilatometer, all gaskets tightened with a torque wrench, and the concentrated $LiNO_3$ solution poured into the dilatometer cavities. The latter were then degassed thoroughly by applying a vacuum: since small bubbles could cause variations in capillary height, due to either atsmospheric and or thermal changes, orders of magnitude larger than the effect we were looking for. For example, a change in pressure of 0.01 atm. on a bubble of .1 cc, would cause the level in the capillary to change by 1 cms while the expected change in volume by stretching the rubber is of the order of 1 mm! Small thermal changes create of course, similar changes in the height of the capillaries.

After the dilatometer is placed into the bath gross thermal control is

obtained by using the thermistemp on-off controller. After a period of approximately 12 hours to ensure thermal equilibrium, the excess $LiNO_3$ solution is wiped off the top of the capillaries, and the bath is allowed to cool a few hundreths of a degree. The proportional controller is then switched on, and the whole thermal system is allowed anew to come to equilibrium. The height in the capillaries is plotted as a function of time to establish the base lines. Generally after a horizontal or a slowly varying base line has been reached, both samples were stretched simultaneously and the changes in volume plotted as a function of time.

In view of the paramount importance of maintaining constant temperature of at least $\pm$ 0.001° C over long periods of time as stressed above the true temperatures of the bath and in the dilatometric cavities were also recorded. To this end, thermistor probe was placed near the Beckman in the bath, and the readings from the Beckman as well as the changes in height of the capillaries followed. The Beckman thermometer showed a stability at 34°C of at least 0.001°C over a span of several hours, while the thermistor probe and the height of the liquid in the capillaries indicate a stability better than $5 \cdot 10^{-4}$°C.

Testing for the degree of leak proofedness of the dilatometer wires, pulling them with no sample present showed no movement in the capillaries. We can thus assume also further that there are no variationss in the diameter of the wires.

The height of the liquid columns in the capillaries (precision bore) was calibrated as a function of degrees Centigrade by plotting the height in the capillaries versus temperature read on the Beckman. We ascertained an average value of 59.5 cm/degree Centigrade for the capillaries of diameter of 0.0383 cm, and a volume calibration of $1.15 \cdot 10^{-3}$ cc/cm.

The samples used were natural rubber cut from the same sheet as used in the other tests.

Sample	length at rest (mm)	Thickness (mm)	Width (mm)	Area 10^2 cm^2
DA1-24	49	1.90	3.96	7.524
DA1-25	49	7.83	4.11	7.521

After the stability of the systems was ascertained both samples (DA1-24 and DA1-25) were stretched by the same amount at the same time. As both samples were from the same sheet, one would have expected the same results from both cavities. Unfortunately, before a sufficient no. could be tested, we ran into some slow leakage problems of the gaskets and were able to get acceptable data for just 2 runs. The trouble is almost certainly due to corrosion of the metal of the gasket grooves. The decision to place the dilatometer in water instead of in an air bath, and the rubber into salt solution instead of into pure water had to be taken long after the dilatometer construction so that aluminium turned out to be the wrong metal to use. For further work the dilatometer should be constructed of a stainless steel resistant to salt corrosion, and the flat gaskets be made out of teflon to minimize their swelling.

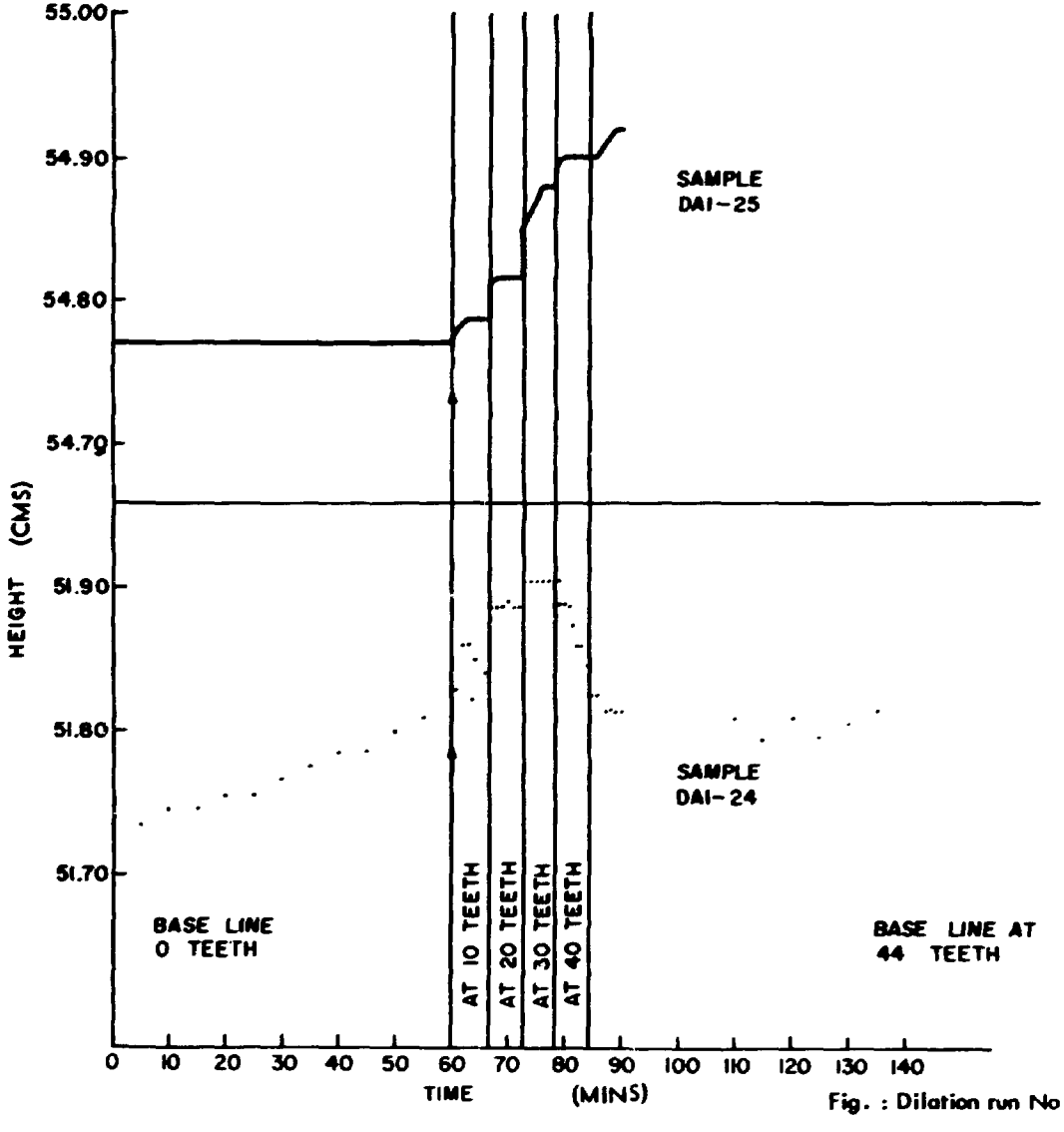

Fig. : Dilation run No. 1

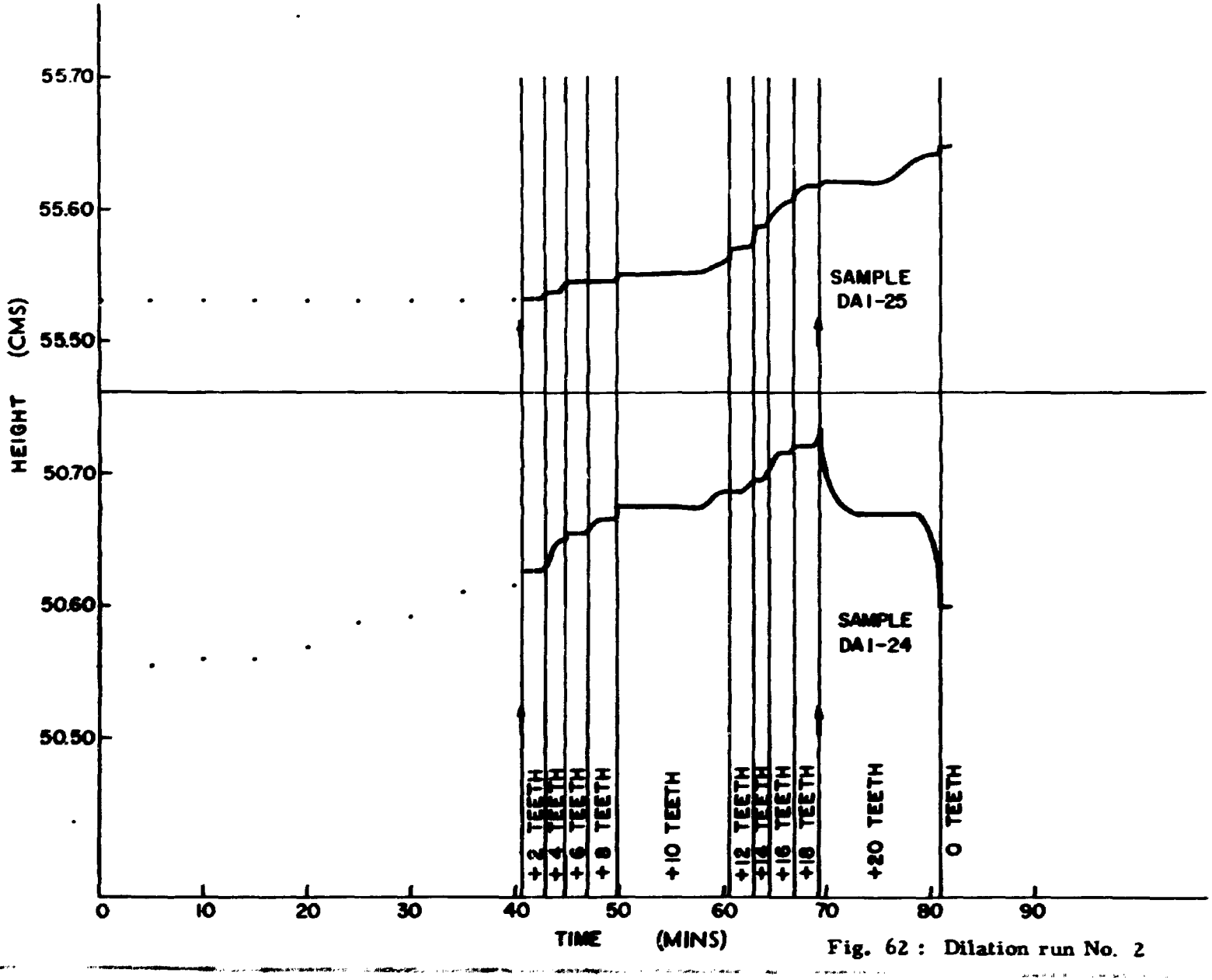

Fig. 62 : Dilation run No. 2

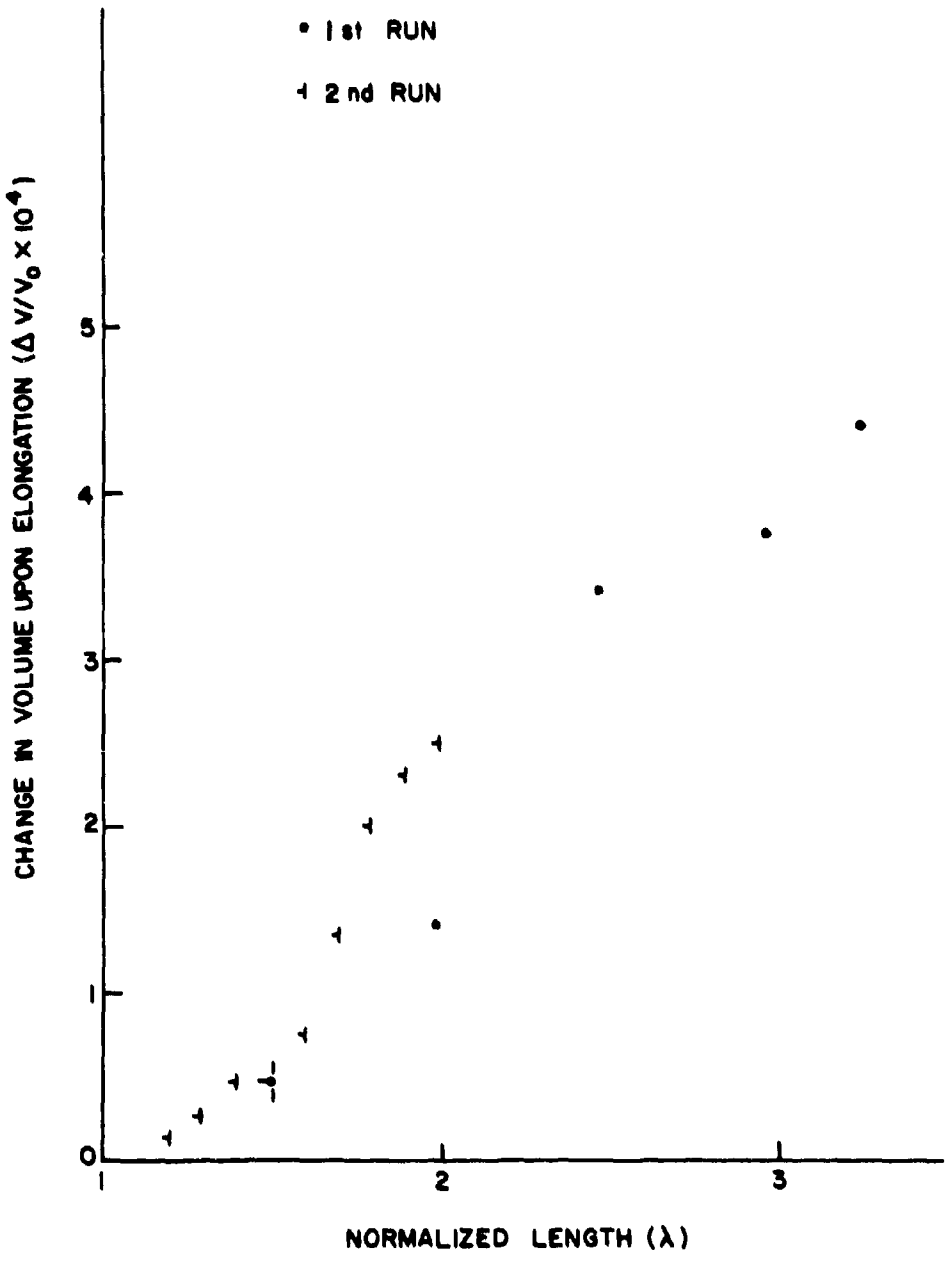

Fig. 63 ; Relative Dilation for sample DA1-24

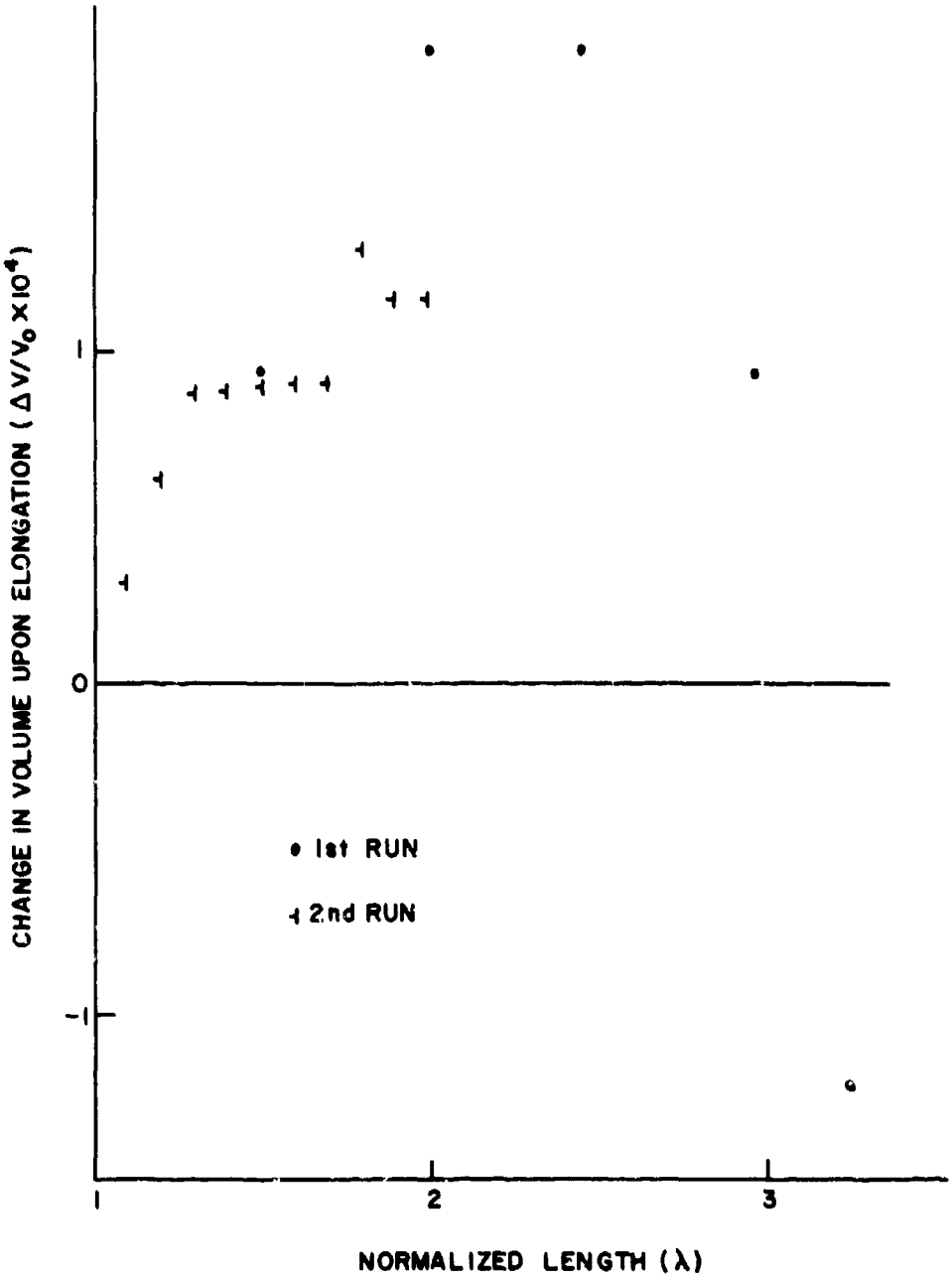

Fig. 64 ; Relative Dilation for sample DA1-25

II. RESULTS

In view of the limitations discussed above, we present the dilatometric data more to show trend and magnitude rather than as a quantitative result. Figures 61 and 62 show the behavior of the capillaries as a function of the elongation of the samples and the time for which they were held at a given elongation. As can be seen, the base line is very stable for the rear cavity (DA1-25) and slightly increasing for the front cavity (DA1-24). Thus it would be difficult to subtract the ill-defined base line to obtain the dilation effect on sample DA1-24. Figures 63 and 64 show the same results expressed in changes of volume ($\Delta V/V_o \cdot 10^{-4}$) as a function of normalized length.

There can be no doubt that the volume of the rubber increases from the very first stretching, but that the amount of increase is very small.

Calibration Wheel = 0.2394 cms/tooth V_o = 0.3700

Sample: DA1-24 Cap. = $1.15 \cdot 10^{-3}$ cc/cm

Length (mm)	λ	ΔV(cm)	ΔV(cc)	ΔV/V_o cc/cc
49	1	0	0	0
49 + 23.94 = 72.94	1.49	0.015	$1.72 \cdot 10^{-5}$	$4.65 \cdot 10^{-5}$
49 + 47.88 = 96.88	1.98	0.045	$5.20 \cdot 10^{-5}$	$1.40 \cdot 10^{-4}$
49 + 71.82 = 120.82	2.46	0.110	$1.26 \quad 10^{-4}$	$3.40 \cdot 10^{-4}$
49 + 95.76 = 144.26	2.96	0.120	$1.38 \cdot 10^{-4}$	$3.74 \cdot 10^{-4}$
49 + 105.33 = 154.33	3.24	0.140	$1.56 \cdot 10^{-4}$	$4.40 \cdot 10^{-4}$

TABLE X: Dilatometry, First run on sample DA1-24

Calibration Wheel = 0.2394 cms/tooth V_o = 0.3700

Sample: DA1-24 Cap. = $1.15 \cdot 10^{-3}$ cc/cm

Length (mm)	λ	ΔV(cm)	ΔV(cc)	ΔV/V_o cc/cc
49	1.00	0	0	0
53.8	1.10	0	0	0
58.6	1.19	0.005	$5.70 \cdot 10^{-6}$	$1.54 \cdot 10^{-5}$
63.4	1.29	0.010	$1.15 \cdot 10^{-5}$	$3.12 \cdot 10^{-5}$
68.2	1.39	0.015	$1.72 \cdot 10^{-5}$	$4.65 \cdot 10^{-5}$
72.94	1.49	0.015	$1.72 \cdot 10^{-5}$	$4.65 \cdot 10^{-5}$
77.74	1.59	0.025	$2.86 \cdot 10^{-5}$	$7.75 \cdot 10^{-5}$
82.54	1.69	0.045	$5.15 \cdot 10^{-5}$	$1.37 \cdot 10^{-4}$

Length (mm)	λ	ΔV(cm)	ΔV(cc)	$\Delta V/V_o$ cc/cc
87.34	1.79	0.065	$7.45 \cdot 10^{-5}$	$2.02 \cdot 10^{-4}$
91.14	1.89	0.075	$8.60 \cdot 10^{-5}$	$2.32 \cdot 10^{-4}$
96.88	1.98	0.080	$9.20 \cdot 10^{-5}$	$2.48 \cdot 10^{-4}$

TABLE XI: Dilatometry, Second run on sample DA1-24

Length (mm)	λ	ΔV(cm)	ΔV(cc)	$\Delta V/V_o$ cc/cc
72.94	1.49	0.030	$3.45 \cdot 10^{-5}$	$9.30 \cdot 10^{-5}$
96.88	1.98	0.060	$6.90 \cdot 10^{-5}$	$1.89 \cdot 10^{-4}$
120.82	2.46	0.060	$6.90 \cdot 10^{-5}$	$1.89 \cdot 10^{-4}$
144.76	2.96	0.030	$3.45 \cdot 10^{-5}$	$9.30 \cdot 10^{-5}$
154.33	3.24	- 0.040	- $4.60 \cdot 10^{-5}$	- $1.22 \cdot 10^{-4}$

TABLE XII: Dilatometry, First run on sample DA1-25

Length (mm)	λ	ΔV(cm)	ΔV(cc)	$\Delta V/V_o$ cc/cc
49	1.00	0	0	0
53.8	1.10	0.010	$1.15 \cdot 10^{-5}$	$3.1 \cdot 10^{-5}$
58.6	1.19	0.020	$2.30 \cdot 10^{-5}$	$6.2 \cdot 10^{-5}$
63.4	1.29	0.030	$3.45 \cdot 10^{-5}$	$8.8 \cdot 10^{-5}$
68.2	1.39	0.030	$3.45 \cdot 10^{-5}$	$8.8 \cdot 10^{-5}$
72.9	1.49	0.030	$3.45 \cdot 10^{-5}$	$8.8 \cdot 10^{-5}$
77.7	1.59	0.030	$3.45 \cdot 10^{-5}$	$8.8 \cdot 10^{-5}$

Length (mm)	λ	Δ V(cm)	ΔV (cc)	$\Delta V/V_o$ cc/cc
82.5	1.69	0.030	$3.45 \cdot 10^{-5}$	$8.8 \cdot 10^{-5}$
87.3	1.79	0.045	$4.80 \cdot 10^{-5}$	$1.30 \cdot 10^{-4}$
91.1	1.89	0.040	$4.25 \cdot 10^{-5}$	$1.15 \cdot 10^{-4}$
96.8	1.98	0.040	$4.25 \cdot 10^{-5}$	$1.15 \cdot 10^{-4}$

TABLE XIII: Dilatometry, Second run on sample DA1-25

III. DISCUSSION

One of the most important aspects of this study of dilation was the swelling of natural rubber in different liquids. Water itself is definately a swelling agent, up to 3% weight change is recorded after an immersion of several days. If this weight uptake were translated entirely into a volume change, this would correspond to a $\Delta V/V_o$ of $3 \cdot 10^{-2}$ which is two orders of magnitude above the expect change from dilation due to the isotropic tension.

Thus one of the first considerations is to question any results in the literature that give the dilation of natural rubber from experiments carried out in water, almost the only kind of experiment used to date. Holt and McPherson [16] and Wolstenholme [35]both measured the dilation in water, although the former do mention that for longer periods of immersion they used mercury. However we found that water uptake was certainly not negligible at even small immersion times. For the results obtained by hydrostatic weightings [36, 38], one should ask oneself how much water is taken up immediately by capillary action into the rubber voids. A fraction of a percent would be still an order of magnitude above the expected mechanical dilation. According to Grove's results [53]; water is not automatically eliminated as dilatometric, fluid because much of the imbibed liquid does not seem to change the overall volume. But even if the overall volume did not change during weight pick-up of liquid, the liquid imbibed must respond to the stretching in several ways:

1. by flowing out of the larger voids and pores, it will make the dilatometric volume of the rubber upon stretching seem larger.

2. parallel to this effect, the liquid that has gone into the molecular interstices will only reappear in the bulk of the liquid very slowly, and hence restricts the motion of the rubber chains and prevent accomodation to the new length. This will tend to decrease the Poisson ratio and make a contribution to the apparent large volume increase upon stretching.

Lowering the activity coefficient of the water by addition of highly soluble salts, we found, as mentioned, gave negligible swelling after several days of

testing. Since K or Na salts were not so effective, one has to deduce that the Li^+ with its stronger capacity to bind water molecules quite strongly, inhibits water swelling of the rubber network at concentrations where there is no free water left [54]. This in itself was a very interesting result.

Before examining and discussing the experimental data, it might be of interest to analyze on the molecular level why an isotropic body expands upon simple tension. In the case of liquids, which relative to the applied stresses are incompressible, all forces immediately cause motion. The packing in a liquid is loose enough (the order is short range) so that the molecules need not penetrate over a geometrical barrier, as there are enough voids to take up any motion and stress relaxation is practically instantaneous. In the case of an elastic solid or a glass, the molecules require more than fluctuation space to move past surrounding denser clusters. During recoverable deformation the molecules need not move from one trough to another, but merely move up the energy quadient and then fallback into the old position on removal of the stress. If the molecules really moved, we would no longer be in the elastic region, but irreversible plastic flow would take place. Hence, as the molecules tend to "rise" on their neighbors, they increase their intermolecular distances and as a result there is a net increase in volume. Further, as the molecule is in a potential energy well increasing its distance to some of its neighbors must increase also its potential energy. But potential energy is free energy, and hence whenever there is a change in stored energy due to distortional stress, there must be a dilation in volume. An interesting corollary is that, when in the case of a swollen network the molecules can move by the way of the voids present in the swelling liquid there can be an elastic storage upon stretching for which one would not expect any change in volume. In general, though, one can say that any isotropic elastic body will undergo dilation due to the negative isotropic stress component in tensile deformation.

The four runs that were carried out (see Tables X, XI, XII and XIII also Figures 61 and 62) even if not quantitatively reliable, show unequivocally that natural rubber exhibits indeed volume dilation upon small elongations. At the higher elongations, the supposedly identical samples begin to differ. We are not in a position at this time to explain the differences, and more work

would have to be carried out with a new dilatometer. A possible explanation might be that the motion of the wires enhance osmotic leakage or promotes gas nucleation following corrosion. As for the observed volume changes, we conclude that the volume expansion is very small, corresponding to a Poisson ratio of 0.499. That is, rubber does indeed behave at first almost like a true liquid, and volume expansion occurs l cally and near cross link points. In our weakly cross-linked rubber this must be expected to be a small disturbance. More tightly vulcanized or partly filled rubbers aught to exhibit more dilation even initially.

Eventually, once the experimental technique is sufficiently reliable, it is planned to measure, amongst others, the volume effects of stress relaxation, the dilational reversibility of the stress-strain cycle, the volume dilation at low to moderate strains to establish the nature of the Poisson coefficient of the rubbers, and finally the kinetics and density changes at higher elongations due to crystallization . It will be particularily worthwhile to study these same parameters in the case of non-crystallizing rubbers.

IV. APPENDIX III

A. Change in volume upon uniaxial tension - Theory

Consider a cylindrical isotropic material, of radius R_o and of length L_o. The initial volume is given by:

$$V_o = \pi R^2_o L_o \qquad \text{(App. II:1)}$$

at a given length L,

$$V = \pi R^2 L \qquad \text{(App. II:2)}$$

where R and L are the radius and the length respectively at any given time.

$$\Delta V = V - V_o \qquad \text{(App. II:3)}$$

where $$V = \pi(R_o + \Delta R)^2 (L_o + \Delta L) \qquad \text{(App. II:4)}$$

and $$V_o = \pi R^2_o L^2_o$$

thus $$\frac{\Delta V}{V_o} = \left[\pi(R_o + \Delta R)^2 (L_o + \Delta L) - \pi R^2_o L_o\right] / \pi R^2_o L_o \qquad \text{(App. II:5)}$$

1. Poisson ratio defined in λ strains

We will define the λ Poisson Ratio, as being:

$$\nu = - \frac{\Delta R / R_o}{\Delta L / L_o} \qquad \text{(App. II:6)}$$

and if furthermore

$$\epsilon = \Delta L/L_o \qquad \text{(App. II:7)}$$

then $$\Delta R/R_o = -\epsilon\nu \qquad \text{(App. II:8)}$$

App. II, Equation (5) can be written as:

$$\begin{aligned}\Delta V/V_o &= (1 + \Delta R/R_o)^2 (1 + \Delta L/L_o) - 1 \\ &= (1 + 2\Delta R/R_o + (\Delta R/R_o)^2)(1 + \Delta L/L_o) - 1 \\ &= 1 + \Delta L/L_o + 2\Delta R/R_o \cdot \Delta L/L_o + (\Delta R/R_o)^2 + \\ &\quad (\Delta R/R_o)^2 \Delta L/L_o - 1 + 2\Delta R/R_o \\ &= \epsilon - 2\epsilon\nu - 2\epsilon\nu \cdot \epsilon + \epsilon^2\nu^2 + \epsilon^3\nu^2 \qquad \text{(App. II:9)}\end{aligned}$$

App. II, Equation (9) can be written in two forms:

$$\Delta V/V_o = \epsilon(1 - 2\nu) + \epsilon^2(\nu^2 - 2\nu) + \epsilon^3\nu^2 \qquad \text{(App. II:10)}$$

$$\Delta V/V_o = \epsilon + \nu(-2\epsilon^2 - 2\epsilon) + \nu^2(\epsilon^2 + \epsilon^3) \qquad \text{(App. II:10')}$$

These equations (10, 10') are exact expressions giving the change of volume of an isotropic sample deformed under simple tension.

a. Case of an incompressible body

If $\Delta V = 0$, then the body by definition is incompressible. Setting ΔV equal to zero in App. II: Equation (10'),

$$\nu_i^2 [\epsilon^2(\epsilon + 1)] - 2\nu_i[\epsilon(\epsilon + 1)] + \epsilon = 0 \qquad \text{(App. II:11)}$$

solving for ν_i:

$$\nu_i = \frac{\epsilon(\epsilon + 1) \quad (\epsilon^2(\epsilon + 1)^2 - \epsilon^2(\epsilon + 1) \cdot \epsilon)^{1/2}}{\epsilon^2(\epsilon + 1)}$$

$$= \frac{\epsilon(\epsilon + 1) \quad \epsilon(\epsilon^2 + 2\epsilon + 1 - \epsilon^2 - \epsilon)^{1/2}}{\epsilon^2(\epsilon + 1)}$$

dividing both the numerator and denominator by ϵ.

$$\nu_i = \frac{\epsilon + (\epsilon + 1)^{1/2}}{\epsilon(\epsilon + 1)} \qquad \text{(App. II:12)}$$

$$\nu_i = \frac{1}{\epsilon}\left[1 \pm (1/\epsilon + 1)^{1/2}\right] \qquad \text{(App. II:12')}$$

For $\epsilon \to \infty$

$$\nu_{i+} = \frac{1 + (1)^{1/2}}{\infty} = 0 \qquad \text{(App. II:13)}$$

$$\nu_{i-} = \frac{1 - (1)^{1/2}}{\infty} = 0 \qquad \text{(App. II:13')}$$

For $\epsilon \to 0$

$$\nu_{i+} = \frac{1 + (\infty)^{1/2}}{0} \quad \text{which is indeterminate}$$

Applying Hospital's rule,

$$(\nu_{i+})_{\epsilon = 0} = \frac{(-\frac{1}{2})(\epsilon + 1)^{-3/2}}{1} = -\frac{1}{2} \qquad \text{(App. II:13'')}$$

$$(\nu_{i-})_{\epsilon = 0} = \frac{(\frac{1}{2})(\epsilon + 1)^{-3/2}}{1} = +\frac{1}{2} \qquad \text{(App. II:13''')}$$

Thus for ϵ approaching to zero, the negative root approaches the value for ν of 0.5. Hence in analogy with the classical development of $\Delta V/V_o = \epsilon(1 - 2\nu)$, and where for a material of $\nu = 0.5$, there is no change in volume whatever the elongation, we choose the negative root of App. II: Equation (12').

$$\nu_i = \frac{1}{\epsilon}\left[1 - (\epsilon + 1)^{-1/2}\right] \qquad \text{(App. II:14)}$$

What are the values of the tangents to this function?

$$\nu_1' = \frac{1}{\epsilon}\left[\frac{1}{2}(\epsilon + 1)^{-3/2}\right] - \left[1 - (\epsilon + 1)^{-1/2}\right]\epsilon^{-2}$$

$$= \frac{\epsilon(\epsilon + 1)^{-3/2} - 2\left[1 - (\epsilon + 1)^{-1/2}\right]}{\epsilon^2} \qquad \text{(App. II:15)}$$

Applying Hospital's rule

At $\epsilon = 0$

$$(\nu'_1)_{\epsilon = 0} = \frac{(\epsilon + 1)^{-3/2} + \epsilon\left(-\frac{3}{2}\right)(\epsilon + 1)^{-5/2} - (\epsilon + 1)^{-3/2}}{2\epsilon}$$

$$= \frac{-\frac{3}{2}(\epsilon + 1)^{-5/2} - \frac{3}{2}(\epsilon + 1)^{-5/2} + \frac{15}{4}\epsilon(\epsilon + 1)^{-7/2} + \frac{3}{2}(\epsilon + 1)^{-5/2}}{2}$$

$$= \frac{-\frac{3}{2} - \frac{3}{2} + \frac{3}{2}}{2}$$

$$(\nu'_1)_{\epsilon = 0} = -\frac{3}{4} \qquad \text{(App. II:16)}$$

at $\epsilon = \infty$, $(\nu'_1)_{\epsilon =} = 0$ (App. II:17)

Thus one conclusion is immediate, and that is that at very small strains, the value of the incompressible Poisson ratio approaches the predicted value of 0.5, but along a non zero tangent. At small strains, the value of Poisson's ratio is not 0.5 for incompressible bodies.

b. Case of a compressible body

Rearranging App. II: Equation (10'),

$$\nu^2[\epsilon^2(\epsilon + 1)] - 2\nu[\epsilon(\epsilon + 1)] + \epsilon - \Delta V/V_o = 0 \quad \text{(App. II:18)}$$

In analogy with the compressible body, we shall choose the negative root.

$$\nu = \frac{\epsilon(\epsilon + 1) - (\epsilon^2(\epsilon + 1)^2 - \epsilon^2(\epsilon + 1)(\epsilon - \Delta V/V_o))^{1/2}}{\epsilon^2(\epsilon + 1)}$$

$$\nu = \frac{(\epsilon + 1) - ((\epsilon + 1)(\epsilon + 1 - \epsilon + \Delta V/V_o))^{1/2}}{\epsilon(\epsilon + 1)}$$

$$\nu = \frac{1}{\epsilon}\left[1 - (V/V_o(\epsilon + 1))^{1/2}\right] \quad \text{(App. II:19)}$$

From App. II: Equation (19) it would be possible to solve for one of the three variables knowing the two others. To enable one to solve this equation easily we will use the reduced variables.

Let us call $V/V_o = d$ (dilation)

$$(\epsilon + 1) - d = S$$

then
$$\epsilon\nu = 1 - \left(\frac{d}{d + S}\right)^{1/2}$$

$$= 1 - \left(\frac{1}{1 + S/d}\right)^{1/2} \quad \text{(App. II:20)}$$

If
$$x = S/d \quad \text{(App. II:21)}$$

$$y = \epsilon\nu \quad \text{(App. II:22)}$$

then
$$y = 1 - (1 + x)^{-1/2} \quad \text{(App. II:23)}$$

A two-dimensional plot of $y = f(x)$ can be drawn up, and the Poisson ratio of a compressible body as a function of the change in volume (d) and a function of the elongation (ϵ) can be calculated.

2. Poisson ratio defined in natural strains

If the Poisson ratio, $\nu_N = - \frac{\ln (1 + \Delta R/R_o)}{\ln (1 + \Delta L/L_o)}$ (App. II:24)

then $$\frac{V}{V_o} = \frac{\pi (R_o + \Delta R)^2 (L_o + \Delta L)}{\pi R_o^2 L_o}$$

$$= (1 + \frac{\Delta R}{R_o})^2 (1 + \frac{\Delta L}{L_o}) \quad \text{(App. II:25)}$$

and if $$(1 + \frac{\Delta R}{R_o}) = (1 + \frac{\Delta L}{L_o})^{-\nu_N} \quad \text{(App. II:24)}$$

then $$\frac{V}{V_o} = (1 + \frac{\Delta L}{L_o})^{1-2\nu_N} \quad \text{(App. II:26)}$$

and $$\frac{\Delta V}{V_o} = \frac{V}{V_o} - 1 = (1 + \epsilon)^{1-2\nu_N} - 1 \quad \text{(App. II:27)}$$

Contrary to the expression for $\Delta V/V_o$ obtained by using the Poisson ratio as defined in λ strains, this expression for $\Delta V/V_o$ is always zero for a Poisson ratio of 0.5.

Thus an isotropic incompressible body has a Poisson ratio as defined by natural strains, always equal to 0.5 and this value of ν_N is independent of the elongation ϵ.

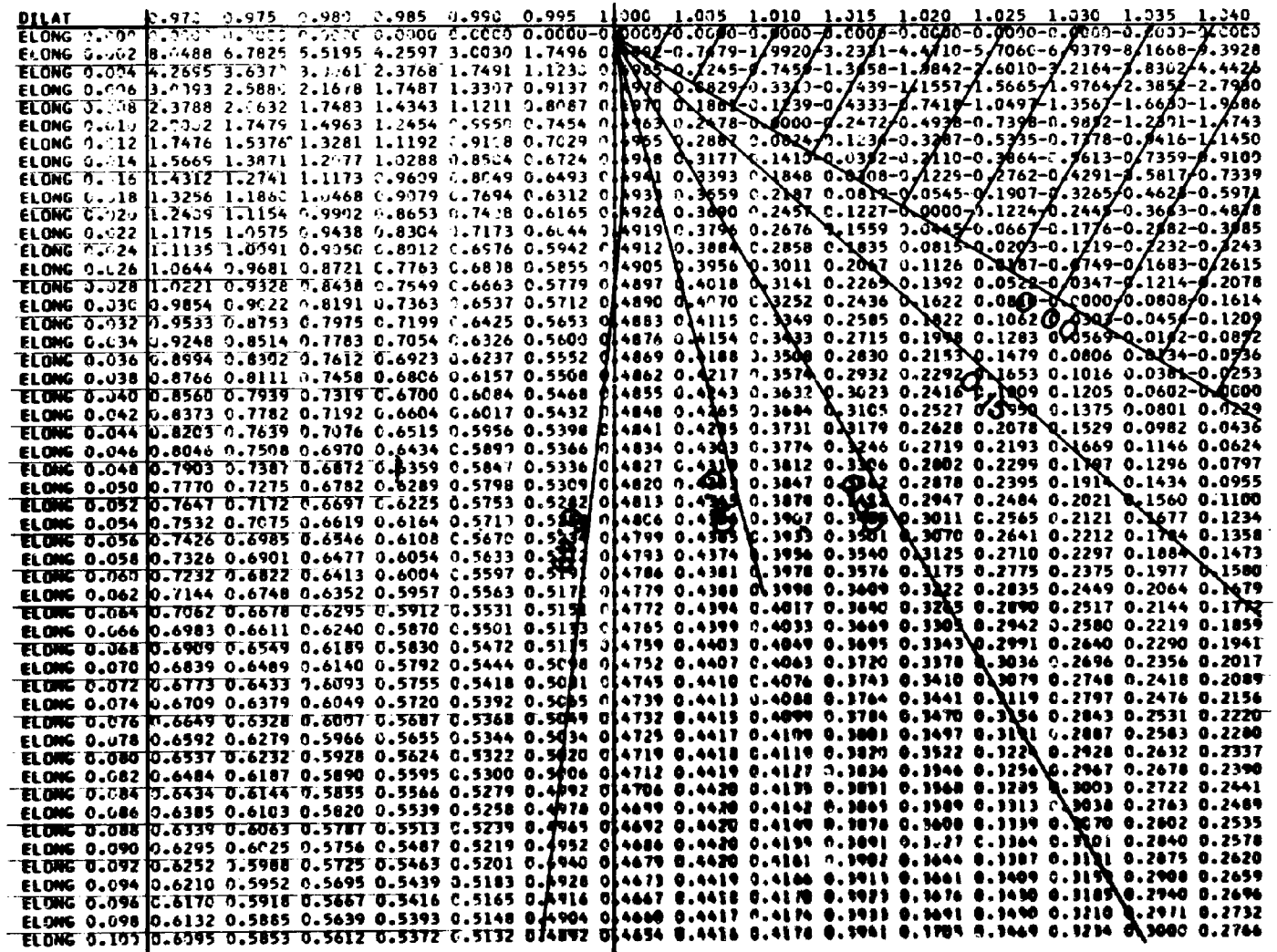

FIG.65 Poisson ratio (λ strains) as a function of Dilation and Elongation (small elongations and small dilations)

DILAT	0.86	0.88	0.90	0.92	0.94	0.96	0.98	1.00	1.02	1.04	1.06	1.08	1.10	1.12	1.14
ELONG 0.00	0.000	0.000	0.000	0.000	0.000	0.000	0.000	0.000	-0.000	-0.000	-0.000	-0.000	-0.000	-0.000	-0.000
ELONG 0.02	4.089	3.558	3.033	2.514	2.001	1.493	0.990	0.492	0.000	-0.488	-0.971	-1.450	-1.924	-2.394	-2.859
ELONG 0.04	2.266	2.003	1.743	1.487	1.232	0.981	0.732	0.485	0.242	0.000	-0.239	-0.476	-0.711	-0.944	-1.174
ELONG 0.06	1.654	1.481	1.309	1.140	0.972	0.806	0.641	0.479	0.317	0.158	0.000	-0.156	-0.312	-0.465	-0.617
ELONG 0.08	1.346	1.217	1.089	0.963	0.838	0.715	0.593	0.472	0.352	0.234	0.116	0.000	-0.115	-0.229	-0.343
ELONG 0.10	1.158	1.056	0.955	0.855	0.756	0.658	0.561	0.465	0.370	0.277	0.184	0.091	0.000	-0.090	-0.180
ELONG 0.12	1.031	0.947	0.863	0.781	0.699	0.618	0.538	0.459	0.381	0.303	0.226	0.150	0.075	0.000	-0.074
ELONG 0.14	0.939	0.867	0.796	0.726	0.657	0.588	0.520	0.453	0.386	0.320	0.255	0.191	0.126	0.063	0.000
ELONG 0.16	0.869	0.806	0.745	0.684	0.624	0.564	0.505	0.447	0.389	0.332	0.275	0.219	0.164	0.109	0.054
ELONG 0.18	0.813	0.758	0.704	0.650	0.597	0.545	0.493	0.441	0.390	0.340	0.290	0.241	0.192	0.143	0.095
ELONG 0.20	0.767	0.718	0.670	0.622	0.575	0.528	0.482	0.436	0.390	0.345	0.301	0.257	0.213	0.170	0.127
ELONG 0.22	0.729	0.685	0.641	0.598	0.556	0.513	0.472	0.430	0.389	0.349	0.309	0.269	0.229	0.190	0.152
ELONG 0.24	0.697	0.657	0.617	0.578	0.539	0.500	0.462	0.425	0.388	0.351	0.314	0.278	0.242	0.207	0.172
ELONG 0.26	0.669	0.632	0.596	0.560	0.524	0.489	0.454	0.420	0.386	0.352	0.318	0.285	0.252	0.220	0.188
ELONG 0.28	0.644	0.610	0.577	0.544	0.511	0.478	0.446	0.415	0.383	0.352	0.321	0.291	0.261	0.231	0.201
ELONG 0.30	0.622	0.591	0.560	0.529	0.499	0.469	0.439	0.410	0.381	0.352	0.323	0.295	0.267	0.239	0.212
ELONG 0.32	0.603	0.573	0.545	0.516	0.488	0.460	0.432	0.405	0.378	0.351	0.325	0.298	0.272	0.246	0.221
ELONG 0.34	0.585	0.558	0.531	0.504	0.478	0.452	0.426	0.400	0.375	0.350	0.325	0.301	0.276	0.252	0.228
ELONG 0.36	0.569	0.543	0.518	0.493	0.468	0.444	0.420	0.396	0.372	0.349	0.325	0.302	0.280	0.257	0.235
ELONG 0.38	0.554	0.530	0.506	0.483	0.460	0.437	0.414	0.391	0.369	0.347	0.325	0.304	0.282	0.261	0.240
ELONG 0.40	0.541	0.518	0.496	0.473	0.451	0.430	0.408	0.387	0.366	0.345	0.325	0.304	0.284	0.264	0.244
ELONG 0.42	0.528	0.507	0.485	0.464	0.444	0.423	0.403	0.383	0.363	0.343	0.324	0.305	0.285	0.266	0.248
ELONG 0.44	0.516	0.496	0.476	0.456	0.436	0.417	0.398	0.379	0.360	0.341	0.323	0.305	0.286	0.268	0.251
ELONG 0.46	0.505	0.486	0.467	0.448	0.430	0.411	0.393	0.375	0.357	0.339	0.322	0.304	0.287	0.270	0.253
ELONG 0.48	0.495	0.477	0.459	0.441	0.423	0.405	0.388	0.371	0.354	0.337	0.320	0.304	0.287	0.271	0.255
ELONG 0.50	0.486	0.468	0.451	0.434	0.417	0.400	0.383	0.367	0.351	0.335	0.319	0.303	0.287	0.272	0.256
ELONG 0.52	0.477	0.460	0.443	0.427	0.411	0.395	0.379	0.363	0.348	0.332	0.317	0.302	0.287	0.272	0.258
ELONG 0.54	0.468	0.452	0.436	0.420	0.405	0.390	0.375	0.360	0.345	0.330	0.315	0.301	0.287	0.273	0.259
ELONG 0.56	0.460	0.445	0.429	0.414	0.400	0.385	0.370	0.356	0.342	0.328	0.314	0.300	0.286	0.273	0.259
ELONG 0.58	0.452	0.437	0.423	0.408	0.394	0.380	0.366	0.352	0.339	0.325	0.312	0.299	0.286	0.273	0.260
ELONG 0.60	0.445	0.431	0.417	0.403	0.389	0.376	0.362	0.349	0.336	0.323	0.310	0.297	0.285	0.272	0.260
ELONG 0.62	0.438	0.424	0.411	0.397	0.384	0.371	0.358	0.346	0.333	0.321	0.308	0.296	0.284	0.272	0.260
ELONG 0.64	0.431	0.418	0.405	0.392	0.380	0.367	0.355	0.342	0.330	0.318	0.306	0.295	0.283	0.271	0.260
ELONG 0.66	0.425	0.412	0.400	0.387	0.375	0.363	0.351	0.339	0.327	0.316	0.304	0.293	0.282	0.271	0.260
ELONG 0.68	0.418	0.406	0.394	0.382	0.371	0.359	0.347	0.336	0.325	0.314	0.303	0.291	0.281	0.270	0.259
ELONG 0.70	0.412	0.401	0.389	0.378	0.366	0.355	0.344	0.333	0.322	0.311	0.301	0.290	0.279	0.269	0.259
ELONG 0.72	0.407	0.395	0.384	0.373	0.362	0.351	0.341	0.330	0.319	0.309	0.299	0.288	0.278	0.268	0.258
ELONG 0.74	0.401	0.390	0.379	0.369	0.358	0.348	0.337	0.327	0.317	0.307	0.297	0.287	0.277	0.267	0.258
ELONG 0.76	0.396	0.385	0.375	0.364	0.354	0.344	0.334	0.324	0.314	0.304	0.295	0.285	0.276	0.266	0.257
ELONG 0.78	0.391	0.381	0.370	0.360	0.350	0.341	0.331	0.321	0.312	0.302	0.293	0.283	0.274	0.265	0.256
ELONG 0.80	0.386	0.376	0.366	0.356	0.347	0.337	0.328	0.318	0.309	0.300	0.291	0.282	0.273	0.264	0.255
ELONG 0.82	0.381	0.372	0.362	0.352	0.343	0.334	0.325	0.316	0.307	0.298	0.289	0.280	0.271	0.263	0.254
ELONG 0.84	0.377	0.367	0.358	0.349	0.340	0.331	0.322	0.313	0.304	0.295	0.287	0.278	0.270	0.262	0.253
ELONG 0.86	0.372	0.363	0.354	0.345	0.336	0.327	0.319	0.310	0.302	0.293	0.285	0.277	0.269	0.260	0.252
ELONG 0.88	0.368	0.359	0.350	0.341	0.333	0.324	0.316	0.308	0.299	0.291	0.283	0.275	0.267	0.259	0.251
ELONG 0.90	0.364	0.355	0.346	0.338	0.330	0.321	0.313	0.305	0.297	0.289	0.281	0.273	0.266	0.258	0.250
ELONG 0.92	0.359	0.351	0.343	0.335	0.326	0.318	0.310	0.303	0.295	0.287	0.279	0.272	0.264	0.257	0.249
ELONG 0.94	0.356	0.347	0.339	0.331	0.323	0.315	0.308	0.300	0.292	0.285	0.277	0.270	0.263	0.256	0.248
ELONG 0.96	0.352	0.344	0.336	0.328	0.320	0.313	0.305	0.298	0.290	0.283	0.276	0.268	0.261	0.254	0.247
ELONG 0.98	0.348	0.340	0.332	0.325	0.317	0.310	0.303	0.295	0.288	0.281	0.274	0.267	0.260	0.253	0.246
ELONG 1.00	0.344	0.337	0.329	0.322	0.314	0.307	0.300	0.293	0.286	0.279	0.272	0.265	0.258	0.252	0.245

FIG. 66 Poisson ratio (λ strains) as a function of Dilation and Elongation (moderate elongations and moderate dilations)

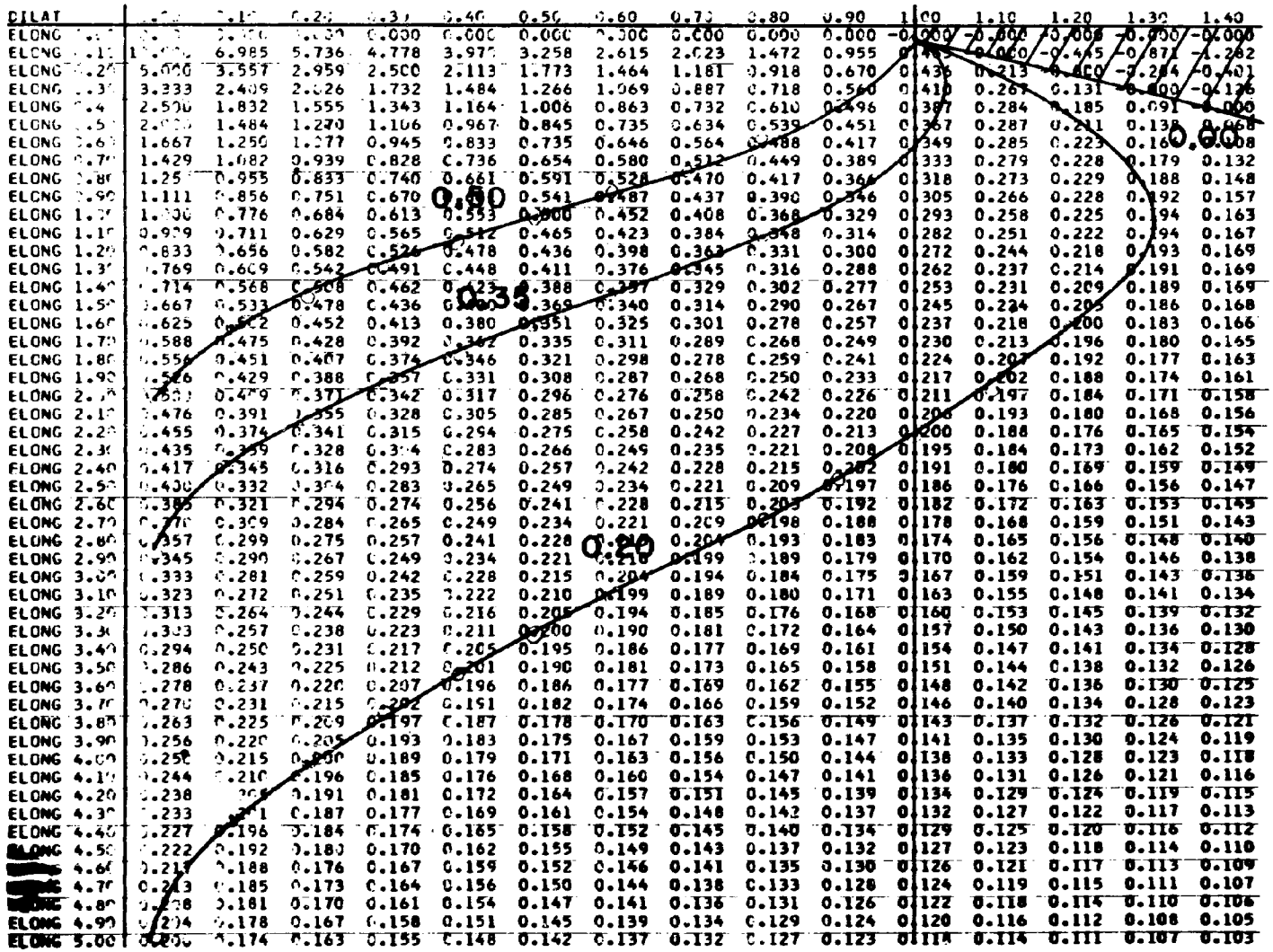

DILAT	0.00	0.10	0.20	0.30	0.40	0.50	0.60	0.70	0.80	0.90	1.00	1.10	1.20	1.30	1.40
ELONG 0.00	[illegible]	[illegible]	[illegible]	0.000	0.000	0.000	0.000	0.000	0.000	0.000	-0.000	-0.000	-0.000	-0.000	-0.000
ELONG 0.10	10.000	6.985	5.736	4.778	3.977	3.258	2.615	2.023	1.472	0.955	0.465	0.000	-0.445	-0.871	-1.282
ELONG 0.20	5.000	3.557	2.959	2.500	2.113	1.773	1.464	1.181	0.918	0.670	0.436	0.213	0.000	-0.204	-0.401
ELONG 0.30	3.333	2.409	2.026	1.732	1.484	1.266	1.069	0.887	0.718	0.560	0.410	0.267	0.131	0.000	-0.126
ELONG 0.40	2.500	1.832	1.555	1.343	1.164	1.006	0.863	0.732	0.610	0.496	0.387	0.284	0.185	0.091	0.000
ELONG 0.50	2.000	1.484	1.270	1.106	0.967	0.845	0.735	0.634	0.539	0.451	0.367	0.287	0.211	0.138	0.068
ELONG 0.60	1.667	1.250	1.077	0.945	0.833	0.735	0.646	0.564	0.488	0.417	0.349	0.285	0.223	0.166	0.108
ELONG 0.70	1.429	1.082	0.939	0.828	0.736	0.654	0.580	0.512	0.449	0.389	0.333	0.279	0.228	0.179	0.132
ELONG 0.80	1.25	0.955	0.833	0.740	0.661	0.591	0.528	0.470	0.417	0.366	0.318	0.273	0.229	0.188	0.148
ELONG 0.90	1.111	0.856	0.751	0.670	0.600	0.541	0.487	0.437	0.390	0.346	0.305	0.266	0.228	0.192	0.157
ELONG 1.00	1.000	0.776	0.684	0.613	0.553	0.500	0.452	0.408	0.368	0.329	0.293	0.258	0.225	0.194	0.163
ELONG 1.10	0.909	0.711	0.629	0.565	0.512	0.465	0.423	0.384	0.348	0.314	0.282	0.251	0.222	0.194	0.167
ELONG 1.20	0.833	0.656	0.582	0.526	0.478	0.436	0.398	0.363	0.331	0.300	0.272	0.244	0.218	0.193	0.169
ELONG 1.30	0.769	0.609	0.542	0.491	0.448	0.411	0.376	0.345	0.316	0.288	0.262	0.237	0.214	0.191	0.169
ELONG 1.40	0.714	0.568	0.508	0.462	0.423	0.388	0.357	0.329	0.302	0.277	0.253	0.231	0.209	0.189	0.169
ELONG 1.50	0.667	0.533	0.478	0.436	0.400	0.369	0.340	0.314	0.290	0.267	0.245	0.224	0.205	0.186	0.168
ELONG 1.60	0.625	0.502	0.452	0.413	0.380	0.351	0.325	0.301	0.278	0.257	0.237	0.218	0.200	0.183	0.166
ELONG 1.70	0.588	0.475	0.428	0.392	0.362	0.335	0.311	0.289	0.268	0.249	0.230	0.213	0.196	0.180	0.165
ELONG 1.80	0.556	0.451	0.407	0.374	0.346	0.321	0.298	0.278	0.259	0.241	0.224	0.207	0.192	0.177	0.163
ELONG 1.90	0.526	0.429	0.388	0.357	0.331	0.308	0.287	0.268	0.250	0.233	0.217	0.202	0.188	0.174	0.161
ELONG 2.00	0.500	0.409	0.371	0.342	0.317	0.296	0.276	0.258	0.242	0.226	0.211	0.197	0.184	0.171	0.158
ELONG 2.10	0.476	0.391	0.355	0.328	0.305	0.285	0.267	0.250	0.234	0.220	0.206	0.193	0.180	0.168	0.156
ELONG 2.20	0.455	0.374	0.341	0.315	0.294	0.275	0.258	0.242	0.227	0.213	0.200	0.188	0.176	0.165	0.154
ELONG 2.30	0.435	0.359	0.328	0.304	0.283	0.266	0.249	0.235	0.221	0.208	0.195	0.184	0.173	0.162	0.152
ELONG 2.40	0.417	0.345	0.316	0.293	0.274	0.257	0.242	0.228	0.215	0.202	0.191	0.180	0.169	0.159	0.149
ELONG 2.50	0.400	0.332	0.304	0.283	0.265	0.249	0.234	0.221	0.209	0.197	0.186	0.176	0.166	0.156	0.147
ELONG 2.60	0.385	0.321	0.294	0.274	0.256	0.241	0.228	0.215	0.203	0.192	0.182	0.172	0.163	0.153	0.145
ELONG 2.70	0.370	0.309	0.284	0.265	0.249	0.234	0.221	0.209	0.198	0.188	0.178	0.168	0.159	0.151	0.143
ELONG 2.80	0.357	0.299	0.275	0.257	0.241	0.228	0.216	0.204	0.193	0.183	0.174	0.165	0.156	0.148	0.140
ELONG 2.90	0.345	0.290	0.267	0.249	0.234	0.221	0.210	0.199	0.189	0.179	0.170	0.162	0.154	0.146	0.138
ELONG 3.00	0.333	0.281	0.259	0.242	0.228	0.215	0.204	0.194	0.184	0.175	0.167	0.159	0.151	0.143	0.136
ELONG 3.10	0.323	0.272	0.251	0.235	0.222	0.210	0.199	0.189	0.180	0.171	0.163	0.155	0.148	0.141	0.134
ELONG 3.20	0.313	0.264	0.244	0.229	0.216	0.205	0.194	0.185	0.176	0.168	0.160	0.153	0.145	0.139	0.132
ELONG 3.30	0.303	0.257	0.238	0.223	0.211	0.200	0.190	0.181	0.172	0.164	0.157	0.150	0.143	0.136	0.130
ELONG 3.40	0.294	0.250	0.231	0.217	0.205	0.195	0.186	0.177	0.169	0.161	0.154	0.147	0.141	0.134	0.128
ELONG 3.50	0.286	0.243	0.225	0.212	0.201	0.190	0.181	0.173	0.165	0.158	0.151	0.144	0.138	0.132	0.126
ELONG 3.60	0.278	0.237	0.220	0.207	0.196	0.186	0.177	0.169	0.162	0.155	0.148	0.142	0.136	0.130	0.125
ELONG 3.70	0.270	0.231	0.215	0.202	0.191	0.182	0.174	0.166	0.159	0.152	0.146	0.140	0.134	0.128	0.123
ELONG 3.80	0.263	0.225	0.209	0.197	0.187	0.178	0.170	0.163	0.156	0.149	0.143	0.137	0.132	0.126	0.121
ELONG 3.90	0.256	0.220	0.205	0.193	0.183	0.175	0.167	0.159	0.153	0.147	0.141	0.135	0.130	0.124	0.119
ELONG 4.00	0.250	0.215	0.200	0.189	0.179	0.171	0.163	0.156	0.150	0.144	0.138	0.133	0.128	0.123	0.118
ELONG 4.10	0.244	0.210	0.196	0.185	0.176	0.168	0.160	0.154	0.147	0.141	0.136	0.131	0.126	0.121	0.116
ELONG 4.20	0.238	0.206	0.191	0.181	0.172	0.164	0.157	0.151	0.145	0.139	0.134	0.129	0.124	0.119	0.115
ELONG 4.30	0.233	0.201	0.187	0.177	0.169	0.161	0.154	0.148	0.142	0.137	0.132	0.127	0.122	0.117	0.113
ELONG 4.40	0.227	0.196	0.184	0.174	0.165	0.158	0.152	0.145	0.140	0.134	0.129	0.125	0.120	0.116	0.112
ELONG 4.50	0.222	0.192	0.180	0.170	0.162	0.155	0.149	0.143	0.137	0.132	0.127	0.123	0.118	0.114	0.110
ELONG 4.60	0.217	0.188	0.176	0.167	0.159	0.152	0.146	0.141	0.135	0.130	0.126	0.121	0.117	0.113	0.109
ELONG 4.70	0.213	0.185	0.173	0.164	0.156	0.150	0.144	0.138	0.133	0.128	0.124	0.119	0.115	0.111	0.107
ELONG 4.80	0.208	0.181	0.170	0.161	0.154	0.147	0.141	0.136	0.131	0.126	0.122	0.118	0.114	0.110	0.106
ELONG 4.90	0.204	0.178	0.167	0.158	0.151	0.145	0.139	0.134	0.129	0.124	0.120	0.116	0.112	0.108	0.105
ELONG 5.00	0.200	0.174	0.163	0.155	0.148	0.142	0.137	0.132	0.127	0.123	0.118	0.114	0.111	0.107	0.103

Fig. 67 Poisson ratio (λ strains) as a function of Dilation and Elongation
(large elongations and large dilations)

DILAT	0.970	0.975	0.980	0.985	0.990	0.995	1.000	1.005	1.010	1.015	1.020	1.025	1.030	1.035	1.040
ELONG 0.000	0.5000	0.5000	0.5000	0.5000	0.5000	0.5000	0.5000	0.5000	0.5000	0.5000	0.5000	0.5000	0.5000	0.5000	0.5000
ELONG 0.002	8.1225	6.8358	5.5558	4.2822	3.0151	1.7544	0.5000	-0.7481	-1.9901	-3.2259	-4.4556	-5.6794	-6.8971	-8.1090	-9.3150
ELONG 0.004	4.3156	3.6711	3.0304	2.3930	1.7588	1.1278	0.5000	-0.1241	-0.7463	-1.3647	-1.9803	-2.5927	-3.2022	-3.8088	-4.4124
ELONG 0.006	3.0459	2.6161	2.1886	1.7632	1.3400	0.9190	0.5000	0.0831	-0.3317	-0.7444	-1.1552	-1.5639	-1.9706	-2.3754	-2.7782
ELONG 0.008	2.4113	2.0887	1.7677	1.4484	1.1307	0.8145	0.5000	0.1874	-0.1244	-0.4343	-0.7426	-1.0493	-1.3548	-1.6587	-1.9611
ELONG 0.010	2.0306	1.7722	1.5152	1.2595	1.0050	0.7519	0.5000	0.2494	0.0000	-0.2481	-0.4951	-0.7408	-0.9858	-1.2287	-1.4700
ELONG 0.012	1.7767	1.5612	1.3468	1.1335	0.9213	0.7101	0.5000	0.2909	0.0828	-0.1241	-0.3301	-0.5350	-0.7390	-0.9420	-1.1440
ELONG 0.014	1.5954	1.4105	1.2266	1.0435	0.8614	0.6803	0.5000	0.3206	0.1421	-0.0364	-0.2122	-0.3880	-0.5630	-0.7372	-0.9105
ELONG 0.016	1.4594	1.2975	1.1364	0.9761	0.8166	0.6579	0.5000	0.3429	0.1866	0.0310	-0.1238	-0.2778	-0.4311	-0.5836	-0.7354
ELONG 0.018	1.3537	1.2096	1.0662	0.9236	0.7817	0.6405	0.5000	0.3602	0.2211	0.0827	-0.0950	-0.1921	-0.3284	-0.4642	-0.5992
ELONG 0.020	1.2691	1.1393	1.0101	0.8816	0.7538	0.6266	0.5000	0.3741	0.2488	0.1241	0.0000	-0.1235	-0.2463	-0.3686	-0.4903
ELONG 0.022	1.1998	1.0817	0.9642	0.8473	0.7309	0.6152	0.5000	0.3854	0.2714	0.1579	0.0440	-0.0677	-0.1792	-0.2904	-0.4011
ELONG 0.024	1.1422	1.0338	0.9259	0.8186	0.7119	0.6057	0.5000	0.3949	0.2902	0.1861	0.0825	-0.0206	-0.1232	-0.2253	-0.3269
ELONG 0.026	1.0933	0.9932	0.8935	0.7944	0.6958	0.5976	0.5000	0.4028	0.3062	0.2100	0.1143	0.0190	-0.0758	-0.1701	-0.2640
ELONG 0.028	1.0515	0.9584	0.8658	0.7736	0.6820	0.5908	0.5000	0.4097	0.3198	0.2304	0.1415	0.0529	-0.0352	-0.1229	-0.2101
ELONG 0.030	1.0152	0.9283	0.8417	0.7557	0.6700	0.5848	0.5000	0.4156	0.3317	0.2482	0.1650	0.0823	0.0000	-0.0819	-0.1634
ELONG 0.032	0.9835	0.9019	0.8207	0.7399	0.6595	0.5796	0.5000	0.4208	0.3421	0.2637	0.1857	0.1080	0.0308	-0.0461	-0.1228
ELONG 0.034	0.9555	0.8786	0.8021	0.7260	0.6503	0.5750	0.5000	0.4254	0.3512	0.2773	0.2039	0.1307	0.0580	-0.0145	-0.0865
ELONG 0.036	0.9306	0.8579	0.7856	0.7137	0.6421	0.5709	0.5000	0.4295	0.3593	0.2895	0.2200	0.1509	0.0822	0.0137	-0.0545
ELONG 0.038	0.9083	0.8394	0.7708	0.7026	0.6347	0.5672	0.5000	0.4331	0.3666	0.3004	0.2346	0.1690	0.1037	0.0388	-0.0258
ELONG 0.040	0.8883	0.8228	0.7576	0.6927	0.6281	0.5639	0.5000	0.4364	0.3731	0.3102	0.2475	0.1852	0.1232	0.0614	0.0000
ELONG 0.042	0.8702	0.8077	0.7455	0.6837	0.6221	0.5609	0.5000	0.4394	0.3791	0.3191	0.2593	0.1999	0.1408	0.0819	0.0233
ELONG 0.044	0.8537	0.7940	0.7346	0.6755	0.6167	0.5582	0.5000	0.4421	0.3845	0.3271	0.2701	0.2133	0.1568	0.1005	0.0446
ELONG 0.046	0.8386	0.7815	0.7246	0.6680	0.6117	0.5557	0.5000	0.4446	0.3894	0.3345	0.2798	0.2255	0.1714	0.1175	0.0640
ELONG 0.048	0.8248	0.7700	0.7155	0.6612	0.6072	0.5535	0.5000	0.4468	0.3939	0.3412	0.2888	0.2367	0.1848	0.1331	0.0817
ELONG 0.050	0.8121	0.7595	0.7070	0.6549	0.6030	0.5514	0.5000	0.4489	0.3980	0.3474	0.2971	0.2470	0.1971	0.1475	0.0981
ELONG 0.052	0.8004	0.7497	0.6993	0.6491	0.5991	0.5494	0.5000	0.4508	0.4019	0.3531	0.3047	0.2566	0.2085	0.1607	0.1132
ELONG 0.054	0.7896	0.7407	0.6921	0.6437	0.5955	0.5477	0.5000	0.4526	0.4054	0.3585	0.3117	0.2652	0.2190	0.1729	0.1271
ELONG 0.056	0.7795	0.7323	0.6854	0.6387	0.5922	0.5460	0.5000	0.4542	0.4087	0.3634	0.3183	0.2734	0.2288	0.1843	0.1401
ELONG 0.058	0.7701	0.7245	0.6792	0.6340	0.5891	0.5445	0.5000	0.4558	0.4118	0.3680	0.3244	0.2810	0.2379	0.1949	0.1522
ELONG 0.060	0.7614	0.7172	0.6734	0.6297	0.5862	0.5430	0.5000	0.4572	0.4146	0.3722	0.3301	0.2881	0.2464	0.2048	0.1635
ELONG 0.062	0.7532	0.7104	0.6679	0.6256	0.5835	0.5417	0.5000	0.4585	0.4173	0.3762	0.3354	0.2948	0.2543	0.2141	0.1740
ELONG 0.064	0.7455	0.7041	0.6628	0.6218	0.5810	0.5404	0.5000	0.4598	0.4198	0.3800	0.3404	0.3010	0.2618	0.2227	0.1839
ELONG 0.066	0.7383	0.6981	0.6580	0.6182	0.5786	0.5392	0.5000	0.4610	0.4222	0.3835	0.3451	0.3068	0.2688	0.2309	0.1932
ELONG 0.068	0.7315	0.6924	0.6535	0.6149	0.5764	0.5381	0.5000	0.4621	0.4244	0.3868	0.3495	0.3123	0.2753	0.2385	0.2019
ELONG 0.070	0.7251	0.6871	0.6493	0.6117	0.5743	0.5370	0.5000	0.4631	0.4265	0.3900	0.3537	0.3176	0.2816	0.2458	0.2102
ELONG 0.072	0.7190	0.6821	0.6453	0.6087	0.5723	0.5360	0.5000	0.4641	0.4284	0.3929	0.3576	0.3224	0.2874	0.2526	0.2179
ELONG 0.074	0.7133	0.6773	0.6415	0.6059	0.5704	0.5351	0.5000	0.4651	0.4303	0.3957	0.3613	0.3271	0.2930	0.2591	0.2253
ELONG 0.076	0.7079	0.6728	0.6379	0.6032	0.5686	0.5342	0.5000	0.4660	0.4321	0.3984	0.3648	0.3315	0.2982	0.2652	0.2323
ELONG 0.078	0.7028	0.6685	0.6345	0.6006	0.5669	0.5334	0.5000	0.4668	0.4338	0.4009	0.3682	0.3356	0.3032	0.2710	0.2389
ELONG 0.080	0.6979	0.6645	0.6313	0.5982	0.5653	0.5326	0.5000	0.4676	0.4354	0.4033	0.3713	0.3396	0.3080	0.2765	0.2452
ELONG 0.082	0.6932	0.6606	0.6282	0.5959	0.5638	0.5318	0.5000	0.4684	0.4369	0.4055	0.3744	0.3433	0.3125	0.2817	0.2512
ELONG 0.084	0.6888	0.6569	0.6252	0.5937	0.5623	0.5311	0.5000	0.4691	0.4383	0.4077	0.3772	0.3469	0.3168	0.2867	0.2569
ELONG 0.086	0.6846	0.6534	0.6224	0.5916	0.5609	0.5304	0.5000	0.4698	0.4397	0.4098	0.3800	0.3504	0.3209	0.2915	0.2623
ELONG 0.088	0.6806	0.6501	0.6198	0.5896	0.5596	0.5297	0.5000	0.4704	0.4410	0.4117	0.3826	0.3536	0.3248	0.2961	0.2675
ELONG 0.090	0.6767	0.6469	0.6172	0.5877	0.5583	0.5291	0.5000	0.4711	0.4423	0.4136	0.3851	0.3567	0.3285	0.3004	0.2724
ELONG 0.092	0.6730	0.6438	0.6148	0.5859	0.5571	0.5285	0.5000	0.4717	0.4435	0.4154	0.3875	0.3597	0.3321	0.3046	0.2772
ELONG 0.094	0.6695	0.6409	0.6124	0.5841	0.5559	0.5279	0.5000	0.4722	0.4446	0.4171	0.3898	0.3626	0.3355	0.3085	0.2817
ELONG 0.096	0.6661	0.6381	0.6102	0.5824	0.5548	0.5273	0.5000	0.4728	0.4457	0.4188	0.3920	0.3653	0.3388	0.3124	0.2861
ELONG 0.098	0.6629	0.6354	0.6080	0.5808	0.5538	0.5268	0.5000	0.4733	0.4468	0.4204	0.3941	0.3679	0.3419	0.3160	0.2902
ELONG 0.100	0.6598	0.6328	0.6060	0.5793	0.5527	0.5263	0.5000	0.4738	0.4478	0.4219	0.3961	0.3705	0.3449	0.3195	0.2942

FIG.68 Poisson ratio (natural strains) as a function of Dilation and Elongation (small elongations and small dilations)

DILAT	0.86	0.88	0.90	0.92	0.94	0.96	0.98	1.00	1.02	1.04	1.06	1.08	1.10	1.12	1.14
ELONG	[illegible]	[illegible]	[illegible]	[illegible]	0.500	0.500	0.500	0.500	0.500	0.500	0.500	0.500	0.500	0.500	0.500
ELONG	4.72	4.308	3.728	3.160	2.605	2.062	1.531	1.010	0.500	0.000	-0.490	-0.971	-1.443	-1.907	-2.361	-2.808
ELONG	2.34	2.423	2.133	1.843	1.563	1.289	1.020	0.758	0.500	0.248	0.000	-0.243	-0.481	-0.715	-0.945	-1.170
ELONG	1.66	1.794	1.597	1.404	1.215	1.031	0.850	0.673	0.500	0.330	0.163	0.000	-0.160	-0.318	-0.472	-0.624
ELONG	1.28	1.480	1.331	1.185	1.042	0.902	0.765	0.631	0.500	0.371	0.245	0.121	0.000	-0.119	-0.236	-0.351
ELONG	1.10	1.291	1.171	1.053	0.937	0.825	0.714	0.606	0.500	0.396	0.294	0.194	0.096	0.000	-0.095	-0.187
ELONG	1.12	1.165	1.064	0.965	0.868	0.773	0.680	0.589	0.500	0.413	0.327	0.243	0.160	0.079	0.000	-0.078
ELONG	1.14	1.076	0.98[illegible]	0.902	0.818	0.736	0.656	0.577	0.500	0.424	0.350	0.278	0.206	0.136	0.068	0.000
ELONG	1.16	1.008	0.931	0.855	0.781	0.708	0.638	0.568	0.500	0.433	0.368	0.304	0.241	0.179	0.118	0.059
ELONG	1.18	0.956	0.886	0.818	0.752	0.687	0.623	0.561	0.500	0.440	0.382	0.324	0.268	0.212	0.158	0.104
ELONG	1.20	0.914	0.851	0.789	0.729	0.670	0.612	0.555	0.500	0.446	0.392	0.340	0.289	0.239	0.189	0.141
ELONG	1.22	0.879	0.821	0.765	0.710	0.656	0.603	0.551	0.500	0.450	0.401	0.353	0.306	0.260	0.215	0.171
ELONG	1.24	0.851	0.797	0.745	0.694	0.644	0.595	0.547	0.500	0.454	0.409	0.365	0.321	0.278	0.237	0.195
ELONG	1.26	0.826	0.777	0.728	0.680	0.634	0.588	0.544	0.500	0.457	0.415	0.374	0.333	0.294	0.255	0.217
ELONG	1.28	0.805	0.759	0.713	0.669	0.625	0.583	0.541	0.500	0.460	0.421	0.382	0.344	0.307	0.270	0.235
ELONG	1.30	0.787	0.744	0.701	0.659	0.618	0.578	0.539	0.500	0.462	0.425	0.389	0.353	0.318	0.284	0.250
ELONG	1.32	0.772	0.730	0.690	0.650	0.611	0.574	0.536	0.500	0.464	0.429	0.395	0.361	0.328	0.296	0.264
ELONG	1.34	0.758	0.718	0.680	0.642	0.606	0.570	0.535	0.500	0.466	0.433	0.400	0.369	0.337	0.306	0.276
ELONG	1.36	0.745	0.708	0.671	0.636	0.601	0.566	0.533	0.500	0.468	0.436	0.405	0.375	0.345	0.316	0.287
ELONG	1.38	0.734	0.698	0.664	0.629	0.596	0.563	0.531	0.500	0.469	0.439	0.410	0.381	0.352	0.324	0.297
ELONG	1.40	0.724	0.690	0.657	0.624	0.592	0.561	0.530	0.500	0.471	0.442	0.413	0.386	0.358	0.332	0.305
ELONG	1.42	0.715	0.682	0.650	0.619	0.588	0.558	0.529	0.500	0.472	0.444	0.417	0.390	0.364	0.338	0.313
ELONG	1.44	0.707	0.675	0.644	0.614	0.585	0.556	0.528	0.500	0.473	0.446	0.420	0.394	0.369	0.345	0.320
ELONG	1.46	0.699	0.669	0.639	0.610	0.582	0.554	0.527	0.500	0.474	0.448	0.423	0.398	0.374	0.350	0.327
ELONG	1.48	0.692	0.663	0.634	0.606	0.579	0.552	0.526	0.500	0.475	0.450	0.426	0.402	0.378	0.355	0.333
ELONG	1.50	0.686	0.658	0.630	0.603	0.576	0.550	0.525	0.500	0.476	0.452	0.428	0.405	0.382	0.360	0.338
ELONG	1.52	0.680	0.653	0.626	0.600	0.574	0.549	0.524	0.500	0.476	0.453	0.430	0.408	0.386	0.365	0.344
ELONG	1.54	0.675	0.648	0.622	0.597	0.572	0.547	0.523	0.500	0.477	0.455	0.433	0.411	0.390	0.369	0.348
ELONG	1.56	0.670	0.644	0.618	0.594	0.570	0.546	0.523	0.500	0.478	0.456	0.434	0.413	0.393	0.373	0.353
ELONG	1.58	0.665	0.640	0.615	0.591	0.568	0.545	0.522	0.500	0.478	0.457	0.436	0.416	0.396	0.376	0.357
ELONG	1.60	0.660	0.636	0.612	0.589	0.566	0.543	0.521	0.500	0.479	0.458	0.438	0.418	0.399	0.379	0.361
ELONG	1.62	0.656	0.632	0.609	0.586	0.564	0.542	0.521	0.500	0.479	0.459	0.440	0.420	0.401	0.383	0.364
ELONG	1.64	0.652	0.629	0.606	0.584	0.563	0.541	0.520	0.500	0.480	0.460	0.441	0.422	0.404	0.385	0.368
ELONG	1.66	0.649	0.626	0.604	0.582	0.561	0.540	0.520	0.500	0.480	0.461	0.443	0.424	0.406	0.388	0.371
ELONG	1.68	0.645	0.623	0.602	0.580	0.560	0.539	0.519	0.500	0.481	0.462	0.444	0.426	0.408	0.391	0.374
ELONG	1.70	0.642	0.620	0.599	0.579	0.558	0.538	0.519	0.500	0.481	0.463	0.445	0.427	0.410	0.393	0.377
ELONG	1.72	0.639	0.618	0.597	0.577	0.557	0.538	0.519	0.500	0.482	0.464	0.446	0.429	0.412	0.396	0.379
ELONG	1.74	0.636	0.615	0.595	0.575	0.556	0.537	0.518	0.500	0.482	0.465	0.447	0.431	0.414	0.398	0.382
ELONG	1.76	0.633	0.613	0.593	0.574	0.555	0.536	0.518	0.500	0.482	0.465	0.448	0.432	0.416	0.400	0.384
ELONG	1.78	0.631	0.611	0.591	0.572	0.554	0.535	0.518	0.500	0.483	0.466	0.449	0.433	0.417	0.402	0.386
ELONG	1.80	0.628	0.609	0.590	0.571	0.553	0.535	0.517	0.500	0.483	0.467	0.450	0.435	0.419	0.404	0.389
ELONG	1.82	0.626	0.607	0.588	0.570	0.552	0.534	0.517	0.500	0.483	0.467	0.451	0.436	0.420	0.405	0.391
ELONG	1.84	0.624	0.605	0.586	0.568	0.551	0.533	0.517	0.500	0.484	0.468	0.452	0.437	0.422	0.407	0.393
ELONG	1.86	0.622	0.603	0.585	0.567	0.550	0.533	0.516	0.500	0.484	0.468	0.453	0.438	0.423	0.409	0.394
ELONG	1.88	0.619	0.601	0.583	0.566	0.549	0.532	0.516	0.500	0.484	0.469	0.454	0.439	0.425	0.410	0.396
ELONG	1.90	0.617	0.600	0.582	0.565	0.548	0.532	0.516	0.500	0.485	0.469	0.455	0.440	0.426	0.412	0.398
ELONG	1.92	0.616	0.598	0.581	0.564	0.547	0.531	0.515	0.500	0.485	0.470	0.455	0.441	0.427	0.413	0.400
ELONG	1.94	0.614	0.596	0.579	0.563	0.547	0.531	0.515	0.500	0.485	0.470	0.456	0.442	0.428	0.414	0.401
ELONG	1.96	0.612	0.595	0.578	0.562	0.546	0.530	0.515	0.500	0.485	0.471	0.457	0.443	0.429	0.416	0.403
ELONG	1.98	0.610	0.594	0.577	0.561	0.545	0.530	0.515	0.500	0.486	0.471	0.457	0.444	0.430	0.417	0.404
ELONG	2.00	0.609	0.592	0.576	0.560	0.545	0.529	0.515	0.500	0.486	0.472	0.458	0.444	0.431	0.418	0.405

FIG. 69 Poisson ratio (natural strains) as a function of Dilation and Elongation (moderate elongations and moderate dilations)

B. Plots of Poisson ratios as a function of dilation and elongation

From App. II: Equation (19) it is possible to calculate the Poisson ratio for any given dilation and any given elongation. This equation has been set up on the computer, and Figures (65, 66, 67) show the Poisson ratio for various ranges of elongation and dilation .

Figure (67) shows the figures for both large elongations and large dilations. Here it is quite apparent that in the case of Poisson ratio defined from λ strains, a material of such a constant equal to 0.5, would show a strong contraction in volume upon elongation. Also at $\epsilon = 200\%$, one would actually have no volume left at all! Figure (66) shows intermediate Poisson ratio as defined by λ strains as a function of small values of elongation and dilation. There it can be clearly seen that the tangent at the origin ($\epsilon = 0$) for $\nu_i = 0.5$ is not equal to zero. Thus even at infinitesimal strains, for a Poisson ratio as defined here equal to 0.5, the dilation (actually a contraction) is finite.

Figures (68, 69) show the Poisson ratio, as defined for various natural strains, as a function of elongation and dilation. In this case, negative values of dilation (or contraction of volume) are not possible for $\nu_N \leq 0.5$. Also if the material is truly incompressible, then the Poisson ratio is 0.5 for all elongations.

CONCLUSION

Of the three different experiments carried out on Natural Rubber, the force versus temperature measurement have verified that the decay of stress in stretched elastomers is approximately linear with logarithm of time for a considerable period, as was found by Kraus and Moczygemba [26], Gent [27], and Smith [28]. A viscoelastic mechanism for this decay according to a spectrum of Maxwell terms, can be ruled out as the basis for this form of relaxation because of the nature of the time dependence. As a further difficulty small local defects leading to crack propagation by stress concentration and crystallization of the sample complicate this relatively simple but unexplained form of relaxation. Thus, there is a natural difficulty in the way of determining when the criterion of equilibrium has been adequately fulfilled. In our experiments, the sample was considered fully relaxed when the increment of relaxation over the total span of testing was less than one percent. Other authors simply indicate without further elucidation that they waited for the decay of stresses to be "negligible".

Over the ranges of temperature (30° C - 60° C) and elongations λ = (1.00 - 3.00) studied, the force temperature curves were reproducible, reversible and linear. A series of computer programs were written in order to correct the raw data for the thermal expansion of the rubber. (Before correction, the slope of the force temperature data is negative at low values of strain, and becomes positive at higher values; this phenomena is known as the thermo-elastic inversion, first pointed out by Meyer and Ferri [55] and corrected for by Anthony, Caston and Guth [46]. This thermo-elastic inversion simply shows that at the lower elongations the thermal expansion of the rubber by increasing its length at constant stress, reduces the tension at constant length. In other words at very low strains the reduction of tension by thermal expansion exceeds the increase of tension with temperature to be expected from the kinetic theory of elasticity. The thermo-elastic inversion point is the strain at which these two effects balance exactly. The thermo-elastic inversion influences also of course, the adiabatic temperature change in elastomers, which if $(\partial f/\partial T)_{p,L}$ remains uncorrected will be calculated to have a negative sign at very low strains (Fig. 23). Unfortunately, our experiments were not sufficiently accurate at these low strains to observe this inversion.

The Mooney-Rivlin parametric equation as was stressed in the Introduction has no molecular basis, and really describes a purely hypothetical body. It was also shown that, even though several authors [22, 50] have done extensive work on the dependency of both, C_2 of the Mooney-Rivlin equation and of f_e/f (the internal energy contribution to the total retractive force) upon the elongations at low values of strain, Roe and Krigbaum [18] feel that precise data gathered from the low strain values would cast additional light upon the validity of the Gaussian approximation, which should be valid as long as the chains are only slightly stretched. Unfortunately, the behavior of the samples at these low strains might well suffer from a lack of well defined response to a stress. At moderate elongations the network is deformed as a whole, and we are truly seeing average properties taken over a large population, but at very small strains, many fewer chains, or small sections of the network, may participate in the deformation, and the averages become accidental functions of minor disturbances.

Moreover as shown in the Appendices, it is mathematically obvious that at very low strains the errors of the measurements, be they on the Mooney-Rivlin strain ($\lambda - \lambda^2$) or the internal energy contribution ($\lambda^3 - 1)^{-1}$, must become very large i. e. a small uncertainty on λ is greatly magnified as λ approaches unity. The available data at low strains, particularily that obtained from Anthony, Caston and Guth [46] show in all cases that, if the actual stress is plotted as a function of strain, a straight line is obtained that does not pass through the origin. This we have attributed to a type of superstructure, that first must be broken up (requiring energy to do so), before the material exhibits truly rubber elastic response. This fact would tend to negate Van der Hoff's [22] ascertion that for very low values of strain, the C_2 term of the Mooney-Rivlin equation is nil. Van der Hoff defines his rest length (critical because of the sensitivity of both C_2 and f_e/f to its value at low strains) by assuming Hookeian behavior and placing the origin into the straight extension of the line of his points. We do not dispute a linear type of response at moderate strains (from $\lambda = 1.2$ to 1.3) but we do question that this linearity can be presumed to extend into the region of still lower strains.

With the aid of a weighting factor it was possible to calculate the values of the Mooney-Rivlin parameters ($2C_1$ and $2C_2$) for the combined data of the

two samples. C_1 depends linearly on T as predicted by the simple kinetic theory, while C_2 was found to be relatively insensitive to changes in T. Again, it is difficult to read the data pertaining to C_2. In our analysis, all data at values of λ smaller than 1.25 were discarded as being error prone.

It can similarily be deduced that f_e/f must depend strongly upon the rest length at low elongations and that, in fact, Shen's data tend to show a rapidly increasing value of C_2 in agreement with others in the literature and in contrast to Van der Hoff's data. Small changes in rest length indeed changes the aspect of f_e/f, drastically from an increasing contribution of internal energy at the low strains, to a decreasing one, depending on the chosen value of the rest length. One might sum up the outcome of this study with respect to C_1 and C_2 into the following way with reference to the idealized diagram where the stress is directly proportional to the Mooney-Rivlin strain $(\lambda - 1/\lambda^2)$. Referring to this linear extension graph the Gaussian line represents the final approximation with all of its well known oversimplifying assumptions. The Mooney-Rivlin curve, cutting off after the second term, is a good second order approximation. According to this investigation C_2 is not zero, probably not even in the limit of $\lambda \to 1$. Thus linear back extrapolation to the origin are not justified, though an experimental verification is extremely difficult because of the indetermination of the magnitude of deformation (zero length) at small elongations and possibly also because of the fluctuations of structures in undeformed rubbers themselves, and because as soon as these fluctuations became less important on account of larger deformations, the rubber has become anisotropic and ordinary continuum theories can no longer apply. To judge, by the thermal inversion point, this may become true at much smaller elongations than hitherto thought. The first deviations from Gaussian behavior, as encompassed by the Mooney-Rivlin theory and indirectly by experiment, are, similar to many other cases, probably best understood in terms of Van der Waals type attraction or repulsion forces, and here also as anisotropic volume terms. There may be also, but not decisively contributions from non-equilibrium states. While none of these suggestions is entirely new, it is believed that as matter of their emphasis, confirmation of certain previous information, and interelation of these and previous findings, the present is a new aspect of rubberlike behavior at low and moderate elongations.

The results obtained from dilatometry are encouraging. Preliminary tests show that the samples do dilate upon elongation, and that the dilation is of the expected magnitude, of 10^{-4} cc/cc. The Poisson ratio, defined in terms of natural strains, turns out to be approximately 0.499 which is very close to showing that our rubber is incompressible. Experimentally the difficulties so far could not yet be overcome. The water bath in which the dilatometer is immersed must be controlled to better than 0.001°C over relatively long periods of time. Secondly the dilatometer must be leakproof better than one part in a million and stay quite uncorroded. Thirdly, the swelling of the rubber upon immersion of the sample must be less than 1 part in 1000 and change little with temperature or state of strain. We could fulfill the first, and practically also the third condition, but failed so far in the second.

Before investigating the thermal effects of fast stretching, it was necessary to derive a linearized output of the Thermistor as the fourth leg of a Wheatstone Bridge as a function of temperature. The reduced open-circuit output potential was found to be an inflected function of temperature; knowing the resistance and the temperature coefficient of the resistance at a specified point allowed one to choose the position of the Thermistor Function at inflexion. The slope of the tangent as well as the value of the inflection point were accessible to theroretical calculations.

The use of a thermistor bead as a temperature measuring device presents many advantages (its size, its sensitivity, and its fast response to thermal changes). Unfortunately, in this particular case it is also pressure sensitive and this effect must be corrected for in the total response. Since the pressure response appears to be much slower than the thermal response, the original peak may be taken to be wholly due to thermal changes in the rubber. With the help of the temperature changes during elongation and retraction thus measured and of the previously determined force-temperature curves, it was possible to calculate the specific heats of the stretched elastomer, independent of temperature and at various stages of strain. It was found that the specific heat is a decreasing function with increasing elongation. A result not unexpected in view of the effective aligning of chains and therefore loss of entropy. Compared with the literature these results are found to agree quite closely with the few available other data.

Stress-strain data from isothermal stepwise stretching experiments are usually difficult to evaluate because it is so hard to ascertain whether one deals truly with equilibrium data. Therefore, not withstanding the slow relaxation encountered by us and other authors during $(\partial f / \partial T)_{L,P}$ measurements, stress-strain relaxations derived from force-temperature data should in general be closer to mechanical equilibrium, especially when the data have been derived after some temperature cycling at constant strain. This should be true for the data on which we based the previous discussion of C_2 values.

In contrast to this, the "adiabatic" stress-strain data should be extensively of non-equilibrium nature. The rapidly relaxing stress peak must then be due to the presence of relaxation mechanisms which are slower than our fast-stretching experiments. While the data are too few to allow any other conclusions, the principle, if established, should offer one important approach to the so elusive problem of chain entanglement . In a slighty different way, the force tracings during retraction can throw light on the mechanism of internal viscosity and, thermal extension and the re-partition of energetic degrees of freedom.

Finally some suggestions for further work in the investigation of Rubber-like elasticity may be permissible. The nature of C_2 of the Mooney-Rivlin equation has been puzzling for a long time. It would be valuable to study the internal energy contribution to C_2 and to the total retractive force by employing systematically a number of well defined elastomers of various different types. To learn more of the effect of conformational changes as related to bond angles and rotational energics upon the sign and magnitude of f_e/f would be of major interest. The same is true for extensive work in dilatometry and further studies of adiabatic stretching. The experimental system developed here would appear to have many advantages over others. For adiabatic work, since no direct measurements of specific heat as a function of strain have been reported, and it would be most worthwhile to compare the values of $C_{p,L}$ obtained from the measurement of force temperature and elongation curves with those values obtained directly from calorimetry.

25. CIFERRI, A., and FLORY, P. J., J. Appl. Physics, 30, 1498(1959).
26. KRAUS, G., and MOCZVGEMBA, G. A., J. Pol. Sci., A2, 277(1964).
27. GENT, A. N., Proc. Fourth Rubber Tech. Conf., London (1962).
28. SMITH, T. L., J. Pol. Sci. (in press).
29. BLATZ, P. J., and KO, W. L., Trans. Soc. Rheol., 6, 223(1962).
30. ROE, R. J., and KRIGBAUM, W. R., J. Pol. Sci., A1, 2049(1963).
31. MARK, J. E., and FLORY, P. J., J. Am. Chem. Soc., 86, 138(1964).
32. CIFERRI, A., Trans. Faraday Soc., 57, 846(1961).
33. WOOD, L. A., and BEKKEDAHL, A., Journal of Appl. Phys., 17, 362(1946).
34. GENT, A. N., Trans. Far. Soc., 50, 521(1954).
35. WOLSTENHOLME, W. E., Contribution No. 248 from the research center of the U. S. Rubber Company, Wayne, New Jersey.
36. GEE, G., STERN, J., and TRELOAR, L. R. G., Trans. of the Faraday Soc., 46, 1101(1950).
37. GEE, G., Trans. Faraday Soc., 42, 585(1946).
38. HEWITT, F. G., and ANTHONY, R. L., J. of Appl. Physics, 29, 1411(1958).
39. DART, S. L., ANTHONY, R. L., and GUTH, E., Ind. and Eng. Chem., 34, 11, 1340(1942).
40. LEADERMAN, H., Unpublished notes from Fulbright Visiting Lecturer, Tokyo(1957).
41. CAULFIELD, D., and IMMERGUT, B., ONR, PIBAL report No. 661.
42. CIFERRI, A., HOEVE, C. A. J., and FLORY, P. J., J. Am. Chem. Soc., 83, 5, 1015(1961).
43. JOSEPH KAYE & CO., INC., private communication.
44. THIRION, P., et CHASSET, R., Revue Gen. du Caoutchouc et des Plastiques, 41, 271(1964).
45. RIVLIN, R. S., Phil. Trans. Roy. Soc. (London), A 241, 379(1948).
46. ANTHONY, R. L. CASTON, R. H., and GUTH, E., J. Phys. Chem., 46, 826(1942).
47. BLATZ, P. J., Private communication.
48. DEMING, W. E., "Statistical adjustment of Data", Dover Publ., Inc. New York, (1964).
49. NATTA, G., CRESPI, G., and FLISI, V., J. Pol. Sci., A1, 3569(1963).
50. SHEN, M. C., McQUARRIE, D. A., and JACKSON, J. L., private communication.
51. BEKKEDAHL, N., and MATHESON, H. J., J. Res. Natl. Bur. Standards, 15, 503(1935).

52. GROVE, R., unpublished work, 1964.

53. GROVE, R., Master of Science Thesis, Chemistry, Brooklyn Polyt. Inst., 1966.

54. CHOPPIN, A. R., and BUIJS, K., J. Chem. Phys., 39, 2042(1963).

55. MEYER, and FERRI, Helv. Chim. Acta., 18, 570 (1935).

Unclassified
Security Classification

DOCUMENT CONTROL DATA - R & D

(Security classification of title, body of abstract and indexing annotation must be entered when the overall report is classified)

1. ORIGINATING ACTIVITY (Corporate author)
Polytechnic Institute of Brooklyn

2a. REPORT SECURITY CLASSIFICATION
Unclassified

2b. GROUP

3. REPORT TITLE
Thermodynamics, Thermal Effects and Dilatation of Natural Rubber

4. DESCRIPTIVE NOTES (Type of report and inclusive dates)
Research Report

5. AUTHOR(S) (First name, middle initial, last name)
Michel Bo8l and Frederick Eirich

6. REPORT DATE	7a. TOTAL NO. OF PAGES	7b. NO. OF REFS
October 1966	195	55

8a. CONTRACT OR GRANT NO	9a. ORIGINATOR'S REPORT NUMBER(S)
Nonr 839(32)FBM b. PROJECT NO NR 064-457 c. d.	Pibal Report No. 931 9b. OTHER REPORT NO(S) (Any other numbers that may be assigned this report)

10. DISTRIBUTION STATEMENT
ONR and DDC
Distribution of this document is unlimited

11. SUPPLEMENTARY NOTES	12. SPONSORING MILITARY ACTIVITY
	Office of Naval Research Washington, D. C.

13. ABSTRACT

Force-temperature experiments at constant length, corrected for thermal expansion, allow to re-evaluate and re-interpret the thermoelastic inversion point. The extent of the temperature dependence of the Mooney-Rivlin constants C_1 and C_2 could be derived and their values be discussed in terms of the internal energy contribution.

Stress-strain data from fast (near adiabatic) rubber stretching show the process to be non-equilibrium in nature, and rate dependent force peaks develop. The calculated values of $C_{p.L}$ thus are found to differ from theoretical expectations.

A new dilatometer was constructed which allows to follow volume changes with stretching. For the first time complications due to swelling could be overcome. Extremely small volume increases were determined during the early exploratory runs, but the dilatometer has to be reconstructed to eliminate metal corrosion.

DD FORM 1 NOV 65 1473

Unclassified
Security Classification

Unclassifled
Security Classification

14 KEY WORDS	LINK A		LINK B		LINK C	
	ROLE	WT	ROLE	WT	ROLE	WT
Force - temperature rubber studies Thermoelastic inversion point Mooney-Riviin constants Internal energy in rubber elasticity heat capacities from adiabatic stretching Dilatometer Small volume increases						

Unclassifled
Security Classification